Human antigen R (HuR) in the lung: Friend or foe?

Noof Aloufi

Department of Pathology, Meakins-Christie Laboratories
McGill University, Montreal

May 2022

Thesis submitted to McGill University in partial fulfillment of the requirements of the degree of Doctor of Philosophy (PhD)

TABLE OF CONTENTS

LIST OF FIGURES v
LIST OF TABLES vii
LIST OF ABBREVIATIONS viii
ABSTRACT xiii
RÉSUMÉ xvi
ACKNOWLEDGEMENTS xix
CONTRIBUTIONS TO ORIGINAL KNOWLEDGE xx
CONTRIBUTIONS OF AUTHORS xxi
CHAPTER I 1
1. LITERATURE REVIEW 1
1.1. INTRODUCTION 1
1.2. CHRONIC OBSTRUCTIVE PULMONARY DISEASE (COPD) 2
1.2.1. Risk factors 3
1.2.1.1. Exposure to cigarette smoke (CS) 3
1.2.1.2. Exposure to air pollution 3
1.2.1.3. Exposure to e-cigarettes 4
1.2.1.4. Exposure to cannabis smoke 5
1.2.2. COPD Pathogenesis 6
1.2.2.1. Structural and immune cell crosstalk in COPD 7
1.2.3. Exacerbations in COPD 9
1.2.4. Disease Management 10
1.3. RNA BINDING PROTEINs (RBPs) 11
1.3.1. Biological functions of RBPs 12
1.3.1.1. Polyadenylation 13
1.3.1.2. pre-mRNA splicing 14
1.3.1.3. mRNA editing 15
1.3.1.4. mRNA turnover 15
1.3.1.5. mRNA subcellular localization 16
1.3.1.6. mRNA translation 16
1.3.2. Interplay of RBPs 17

1.3.3. The regulation of RBPs in COPD 17
1.3.3.1. RBPs in inflammation 18
1.3.3.2. RBPs in apoptosis and protease expression 19
1.3.3.3. The response of RBPs to CS 20
1.4. Hu/ELAV FAMILY: HuR 21
1.4.1. The control of HuR function 23
1.4.1.1. HuR expression and abundance 23
1.4.1.1.1. HuR ubiquitination 23
1.4.1.1.2. HuR cleavage 24
1.4.1.2. HuR phosphorylation 25
1.4.1.3. HuR methylation 26
1.4.2. HuR function 26
1.4.2.1. HuR function in lung diseases 30
1.4.2.1.1. Lung cancer 31
1.4.2.1.2. Idiopathic pulmonary fibrosis (IPF) 32
1.4.2.1.3. Asthma 32
1.4.2.1.4. COPD 33
1.5. PROJECT INTRODUCTION 35
CHAPTER II 36
2. Angiotensin-converting enzyme 2 expression in COPD and IPF fibroblasts: the forgotten cell in COVID-19 36
2.1. ABSTRACT 37
2.2. INTRODUCTION 38
2.3. METHODS 40
2.4. RESULTS 43
2.5. DISCUSSION 48
2.6. REFERENCES 51
PREFACE: CHAPTER III 54
CHAPTER III 55
3. Role of human antigen R (HuR) in the regulation of pulmonary ACE2 expression 55
3.1. ABSTRACT 56
3.2. INTRODUCTION 57
3.3. METHODS 60

3.4. RESULTS ... 69
3.5. DISCUSSION ... 87
3.6. REFERENCES ... 94
PREFACE: CHAPTER IV ... 99
CHAPTER IV ... 100
4. A multi-omics approach reveals fundamental roles for human antigen R in lung fibroblasts ... 100
4.1. ABSTRACT ... 101
4.2. INTRODUCTION ... 102
4.3. METHODS ... 105
4.4. RESULTS ... 113
4.5. DISCUSSION ... 139
4.6. SUPPLEMENTARY TABLES ... 147
4.7. REFERENCES ... 148
PREFACE: CHAPTER V ... 156
CHAPTER V ... 157
5. Standardized cannabis smoke extract induces inflammation in human lung fibroblasts 157
5.1. ABSTRACT ... 158
5.2. INTRODUCTION ... 159
5.3. MATERIALS AND METHODS ... 162
5.4. RESULTS ... 169
5.5. DISCUSSION ... 183
5.6. REFERENCES ... 190
6. GENERAL DISCUSSION ... 197
6.1. Where does HuR bind? ... 198
6.2. What are the possible protein partners of HuR that control target mRNA stability? ... 199
6.3. Are there miRNA partners of HuR that control target mRNA in response to CSE? ... 200
6.4. Does HuR regulate miRNA expression in lung fibroblasts? ... 201
6.5. Is HuR involved in SGs assembly caused by CS? ... 201
6.6. How does CS control HuR function? ... 202
6.7. Does HuR regulate cannabis smoke-induced inflammation? ... 204
6.8. Is HuR a friend or foe? ... 205

6.9. Future Directions and Conclusion 207
7. APPENDIX 212
8. REFERENCES 219

LIST OF FIGURES

Figure 1.1. Etiology and pathogenesis of COPD. 9
Figure 1.2. Cellular functions of RBPs. 13
Figure 1.3. Structure of HuR. 22
Figure 1.4. HuR cleavage. 24
Figure 1.5. HuR function. 30
Figure 2.1. Cell-specific *ACE2* expression in COPD and IPF lungs 44
Figure 2.2. ACE2 protein is higher in COPD- and IPF-derived lung fibroblasts. 45
Figure 2.3. Chronic cigarette smoke exposure increases pulmonary ACE2 protein expression. 47
Figure 3.1. *ELAVL1* single-cell level expression in nasopharyngeal and bronchial cells. 70
Figure 3.2. *ELAVL1* single-cell level expression in COPD. 72
Figure 3.3. Correlation between *ELAVL1* and *ACE2* in COPD. 73
Figure 3.4. Cytoplasmic expression of HuR increased in lung tissue and macrophages from smoker and COPD subjects. 75
Figure 3.5. HuR expression in non-smoker, smoker, and COPD HLFs. 77
Figure 3.6. *ACE2* mRNA expression and binding to HuR. 79
Figure 3.7. *ACE2* mRNA and protein stability are not controlled by HuR. 81
Figure 3.8. Cytoplasmic HuR is increased by cigarette smoke. 84
Figure 3.9. HuR silencing does not affect protein and mRNA expression of ACE2. 86
Figure 4.1. Identification of mRNAs in HLFs. 115
Figure 4.2. HuR regulates different genes involved in inflammation and oxidative stress in HLFs. 120
Figure 4.3. KEGG pathway analysis of upregulated mRNA. 121
Figure 4.4. HuR induces the expression of mRNA involved in the regulation of cytosolic calcium and inflammatory response. 124
Figure 4.5. KEGG pathway analysis of the downregulated mRNA. 125
Figure 4.6. HuR binds to hundreds of genes in HLFs. 127
Figure 4.7. GO and KEGG pathway analysis of HuR-associated genes. 129
Figure 4.8. Protein-protein interaction network and MCODE components. 131
Figure 4.9. HuR silencing increases COX-2 and IL-8 expression in CSE-exposed HLFs. 134
Figure 4.10. Validation of HuR suppression to CSE-induced COX-2 and IL-8 in HLFs. . 135
Figure 4.11. HuR binds to PTGS2 and CXCL8 mRNA in response to CSE. 137
Figure 4.12. Knockdown of HuR stabilizes PTGS2 and CXCL8 mRNA in response to CSE. 138
Figure 4.13. HuR function in lung fibroblasts exposed to CS. 146
Figure 5.1. The standard curve for Δ^9-THC. 170
Figure 5.2. Validation of CB1-mediated Rho activation. 175
Figure 5.3. CaSE promotes Rho activation in CB1 expressing cells. 177
Figure 5.4. CaSE promotes Rho activation in CB1 expressing cells in comparison to Δ^9-THC. 179

Figure 5.5. CaSE-induced Rho activation is mediated by CB1. 180
Figure 5.6. CaSE induces COX-2 and IL-8 expression in human lung fibroblasts. 182
Figure 6.1. Mechanisms regulated by HuR in lung cells exposed to external stimuli. 211

LIST OF TABLES

Table 1.1. Influence of HuR on target mRNA that involved in cellular processes. 29
Table 3.1. Primer sequences used for RT-qPCR analysis. 64
Table 4.1. Primer sequences used for qRT-PCR analysis. 111
Table 4.2. Top genes differentially expressed by HuR silencing. 116
Table 4.3. GO enrichment analysis and MCODE network components. 132
Tables S4.: Supplementary tables from the RNA-seq data. 147
Table 5.1. Primer sequences used for qRT-PCR analysis. 167
Table 5.2. Estimated concentration of Δ^9-THC and CBD in CaSE. 172
Table 5.3. Δ^9-THC absorbance (OD_{320}) and estimated concentration by ELISA. 173
Table 5.4. Estimation of THC concentrations in 100% CaSE. THC concentrations in CaSE were estimated from interpolation of standard THC concentration response curve in Figure 5.3. 178
Table 5.5. Estimation of THC concentration in 100% CaSE. THC concentrations in CaSE were estimated from interpolation of standard THC concentration response curve in Figure 5.4. 179
Table A1. Proteins associated with HuR in lung fibroblasts at the basal level (ΔIP-HuR). LFQ (label-free quantification) ratios. 212
Table A2. Proteins associated with HuR in lung fibroblasts exposed to CSE (ΔIP-HuR-CSE). 213
Table A3. miRNA associated with HuR in lung fibroblasts at the basal level (ΔIP-HuR). 215
Table A4. miRNAs associated with HuR in lung fibroblasts exposed to CSE (ΔIP-HuR-CSE). 216
Table A5. miRNA differentially expressed with HuR silencing in lung fibroblasts at the basal level (ΔsiH). 217
Table A6. miRNAs differentially expressed with HuR silencing in lung fibroblasts exposed to CSE (ΔsiH-CSE). 218

LIST OF ABBREVIATIONS

α1AT	Alpha 1-anti-trypsin
2-AG	2-arachidonoylglycerol
ACE2	Angiotensin-converting enzyme 2
ACEA	Arachidonyl-2′-chloroethylamide
ActD	Actinomycin D
ADAR	Adenosine deaminases acting on RNA
AhR	Aryl hydrocarbon receptor
ANOVA	Analysis of variance
AP-1	Activator protein-1
AQG	Air quality guideline
ARE	Adenylate-uridylate (AU)-rich elements
AS	Alternative splicing
α-SMA	Alpha-smooth muscle actin
AT1R	Angiotensin II type 1 receptor
ATII	Alveolar type II
ATP	Adenosine triphosphate
AUF1	AU-binding factor 1
BAL	Bronchoalveolar lavage
BAX	Bcl-2-associated X protein
BMDMs	Bone-marrow-derived-macrophages
BRET	Bioluminescence Resonance Energy Transfer
β-TrCP	β-transducin repeat-containing protein
CARM1	Coactivator-associated arginine methyltransferase 1
CaSE	Cannabis smoke extract
cAMP	cyclic adenosine monophosphate
CBC	Cannabichromene
CBD	Cannabidiol
CBG	Cannabigerol
CBR	Cannabinoids receptors
CCL	C-C motif ligand
CCSA	Canadian Centre on Substance Use and Addiction
CDK1	Cyclin-dependent kinase 1
CFIIm	Mammalian cleavage factors II
CFIm	Mammalian cleavage factors I
CHX-1	Cycloheximide
CNBP	Cellular nucleic acid-binding protein
CNR1/CB1	Cannabinoid-1 receptor
CNR2/CB2	Cannabinoid-2 receptor
CNS	Central nervous system

CO	Carbon monoxide
CoCl2	Cobalt chloride
COL	Collagens
COPD	Chronic Obstructive Pulmonary Disease
COVID-19	Coronavirus disease 2019
COX-2	Cyclooxygenase-2
CP-1	HuR cleavage product-1
CP-2	HuR cleavage product-2
cPLA2α	Cytosolic phospholipase A2α
CPSF	Cleavage and polyadenylation specificity factor
CRM1	Chromosome region maintenance 1
CS	Cigarette smoke
CSE	Cigarette smoke extract
CSF-1	Colony-stimulating factor-1
CstF	Cleavage stimulation factor
CTSS	Cathepsin S
CXCL	C-X-C motif ligand
DEG	Differentially expressed gene
DMEM	Dulbecco's modified Eagle's medium
dsRBD	Double-stranded RBD
ECL	Enhanced chemiluminescence
ECM	Extracellular matrix
ECS	Endocannabinoid system
eIF4E	Eukaryotic initiation factors 4E
ELAVL1	Embryonic lethal abnormal vision-like protein 1
ELISA	Enzyme-Linked Immunosorbent Assay
EMT	Epithelial-to-mesenchymal transition
ENDS	electronic nicotine delivery systems
esiRNA	Endoribonuclease prepared siRNA
EtOH	Ethanol
FADD	Fas associated via death domain
FBS	Fetal bovine serum
FGF10	Fibroblast growth factor 10
FMRP	Fragile X mental retardation protein
FMRP	Fragile X mental retardation protein
FN	Fibronectin
FXS	Fragile X syndrome of mental retardation
G3BP	G3BP stress granule assembly factor 1
GM-CSF	Granulocyte-macrophage colony-stimulating factor
GO	Gene Ontology
GOLD	Global Initiative for Chronic Obstructive Lung Disease

GPCRs	G protein coupled receptors
GR	Glucocorticoid receptors
GWAS	Genome-wide association study
HCV	Hepatitis C virus
HDM	House dust mite
HEK	Human embryonic kidney
HIF-1α	Hypoxia-Inducible Factor 1α
HLFs	Human lung fibroblasts
hnRNP	Heterogeneous nuclear ribonucleoprotein
HNS	HuR nuclear shuttling domain
HPV16	Human papillomaviruse 16
HRP	Horseradish peroxidase
HRV	Human rhinovirus
HuR	Human antigen R
ICOS	Inducible co-stimulator
ICS	Inhaled corticosteroids
IgE	Immunoglobulin E
IgG	Immunoglobulin G
IKKα	IkB kinase α
IL	Interleukin
IPF	Idiopathic pulmonary fibrosis
IR	Ionizing radiation
IRP2 or IREB2	Iron-responsive element binding protein 2
KEGG	Kyoto Encyclopedia of Genes and Genomes
KH	K-homology domain
KSRP	KH-type splicing regulatory protein
LABA	Long-acting β-agonists
LARP1	la-related protein 1
LC-MS/MS	Liquid Chromatography with Tandem Mass Spectrometry
lncRNA	long non-coding RNA
LPS	Lipopolysaccharide
LRE	Late regulatory element
LTB4	Leukotriene B4
MCC	Mucociliary clearance
MCODE	Molecular complex detection
MeOH	Methanol
mIHC	Multiplex immunohistochemistry
MiRNA	Micro-RNA
MMP	Matrix metalloproteinase
mRNA	messenger RNA
Mxi1	MAX Interactor 1

NE	Neutrophil Elastase
NF-κB	Nuclear Factor Kappa B
NK	Natural killer
NNK	4-(methylnitrosamino)-1-(3-pyridyl)-1-butanone
NO2	Nitrogen oxides
NPM	Nucleophosmin
OA	Osteoarthritis
p38 MAPK	p38 Mitogen-activated protein kinase
PABP	Poly(A)-binding protein
PABPN1	Nuclear poly(A) binding protein
PAHs	Polycyclic aromatic hydrocarbons
PAP	Poly (A) polymerase
P-bodies	Processing bodies
PDCD4	Programmed cell death 4
PG	Prostaglandin
PKA	Protein kinase A
PKC	Protein kinase C
PM	Particulate matter
PNEC	Pulmonary neuroendocrine cell
PRMTs	Protein arginine methyltransferases
ProTα	Prothymosin α
RAS	Renin-angiotensin-system
RBD	RNA-binding domain
RBM3	RNA binding motif protein 3
RBM5	RNA-binding motif protein 5
RBP	RNA-binding protein
RIP	RNA Immunoprecipitation
RIP-qPCR	RNA Immunoprecipitation-quantitative PCR
RISC	RNA-induced silencing complex
RNA-Seq	RNA sequencing
RNP	Ribonucleoprotein
ROS	Reactive oxygen species
RRM	RNA recognition motifs
RT-qPCR	Quantitative RT-PCR
SARS-CoV-2	Severe acute respiratory syndrome coronavirus 2
scRNA-seq	Single-cell RNA sequencing
SD	Standard deviation
SEM	Standard error of the mean
SGs	Stress granules
siC	Control siRNA
siH	HuR-specific siRNA

siRNA	Small interfering RNA
SMADs	SMAD mothers against decapentaplegic homolog
snRNAs	Small nuclear RNAs
SO2	sulfur dioxide
sp-hCB1	Signal peptide human CB1
SR	Serine-Arginine rich
SVL	Simian virus 40 late
TGF-β	Transforming growth factor beta
TIA-1	T-cell Intracellular Antigen 1
TLRs	toll-like receptors
TM	Thrombomodulin
TNF-α	Tumor necrosis factor α
TTP	Tristetraprolin
U2AF	U2 auxiliary factor
U2AF65	U2 auxiliary factor 65 kDa
UFPM	ultra-fine particulate matter
UTR	Untranslated region
VE	Vascular endothelial
VEGF	Vascular endothelial growth factor
WHO	World Health Organization
ZFP36	Zinc finger protein 36
Znf	Zinc fingers
Δ^9-THC or THC	Delta-9-tetrahydrocannabinol

ABSTRACT

The lungs, the main organs of the respiratory system, are constantly exposed to the external environment. Exposure to noxious agents in inhaled air can include inhaled pathogens as well as air pollution that is caused by different factors such as cigarette smoke. Cigarette Smoke (CS) exposure has been linked to numerous diseases with no cure and limited therapeutic options; this includes chronic obstructive pulmonary disease (COPD) and more recently coronavirus-induced disease (COVID)-19. Persistent exposure to CS induces inflammation in several cell types found in the lung, such as epithelial cells, fibroblasts and alveolar macrophages. This inflammation is characterized by secretion of inflammatory mediators (*e.g.,* interleukin-8 [IL-8] and cyclooxygenase-2 [COX-2]), recruitment of immune cells (mainly neutrophils, lymphocytes and monocytes) and release of proteases (*e.g.,* matrix metalloproteinases [MMPs]). Uncontrolled, this inflammation leads to the obstruction of small airways and destruction of lung parenchyma. Cannabis is the most smoked plant after tobacco but there is equivocal evidence for its involvement in the development of lung diseases. CS and cannabis smoke may cause lung inflammation via activation of human antigen R (HuR). HuR is a ubiquitously-expressed RNA-binding protein (RBP) that regulates the stability, localization and/or translation of inflammatory-associated mRNAs. To stabilize target mRNA, HuR translocates from the nucleus (where it normally resides) to the cytoplasm. CS may increase HuR translocation to the cytoplasm, thus indirectly augmenting cellular protein levels. Patients with COPD, primarily caused by CS, face an increased risk for severe illness from COVID-19 because of angiotensin-converting enzyme 2 (ACE2) upregulation, the entry receptor for severe acute respiratory syndrome coronavirus 2 (SARS-CoV-2). However, how ACE2 expression is controlled in the lungs is not well understood.

Given the broad spectrum of mRNA regulated by HuR, and the well documented overexpression of this protein in cancer development, we aimed to characterize the role of HuR in pathological features associated with exposure to CS and its implication in COPD. We found that COPD-derived lung fibroblasts express higher level of ACE2, and chronic CS exposure significantly increases pulmonary ACE2 protein. We also found that cytoplasmic localization of HuR (indicative of activation) is higher in lung tissue from Smoker and COPD subjects compared to Non-smoker subjects. Further, there was an increase in cytoplasmic HuR in human lung fibroblasts (HLFs) exposed to cigarette smoke extract (CSE), an *in vitro* surrogate for CS exposure. HuR also binds to *ACE2* mRNA; however, knockdown of HuR does not change ACE2 protein levels. Moreover, we revealed that HuR controls numerous biological pathways in HLFs. Contrary to what was expected, we found that the protein and mRNA levels of *PTGS2*/COX-2 and *CXCL8*/IL-8 were significantly higher in siHuR-transfected HLFs in response to CSE. Interestingly, opposite to what known about HuR stabilizing targets mRNA, we found that HuR destabilizes *PTGS2* and *CXCL8* mRNA in response CSE. This suggests that HuR attenuates CSE-induced COX-2 and IL-8 expression by promoting the degradation of their mRNA. Finally, we have optimized the preparation of a standardized cannabis smoke extract (CaSE) in cell culture media, and we found that cannabis smoke induces COX-2 and IL-8 in HLFs. This standardized preparation can now be used to evaluate if HuR is involved in the inflammatory response to CaSE.

To date, the specific mechanisms of how smoke exposure causes the development of chronic diseases is not completely understood. This thesis is the first that investigate the role of HuR in regulating smoke-induced inflammation; this includes both tobacco and cannabis smoke. Further, the experimental design in this study will allow the identification of smoking-related alterations in primary lung cells. Accordingly, this innovative mechanism could be therapeutically

targeted to develop a novel therapy for smoke-related diseases such as COPD. In turn, this research evokes new hope for thousands of Canadians living with this fatal disease.

RÉSUMÉ

Les poumons, principaux organes du système respiratoire, sont constamment exposés au milieu extérieur. L'exposition à des agents nocifs dans l'air inhalé peut inclure des agents pathogènes inhalés ainsi que la pollution de l'air causée par différents facteurs ; tels que la fumée de cigarette. L'exposition à la fumée de cigarette (CS) a été associée à de nombreuses maladies incurables dont les options thérapeutiques sont limitées ; cela inclut la maladie pulmonaire obstructive chronique (MPOC) et plus récemment la maladie induite par le coronavirus (COVID)-19. Une exposition persistante au CS induit une inflammation dans plusieurs types de cellules pulmonaires, telles que les cellules épithéliales, les fibroblastes et les macrophages alvéolaires. Cette inflammation est caractérisée par la sécrétion de médiateurs inflammatoires (ex : interleukine-8 [IL-8] et cyclooxygénase-2 [COX-2]), le recrutement de cellules immunitaires (principalement des neutrophiles, des lymphocytes et des monocytes) et la libération de protéases (ex : les métalloprotéinases matricielles [MMPs]). Si cette inflammation n'est pas contrôlée, elle entraîne l'obstruction des petites voies respiratoires et la destruction du parenchyme pulmonaire. Le cannabis est la substance la plus consommée après le tabac, mais il existe des preuves équivoques de son implication dans le développement des maladies pulmonaires. Le tabac et le cannabis peuvent provoquer une inflammation pulmonaire via l'activation de l'antigène humain R (HuR). HuR est une protéine de liaison à l'ARN exprimée de manière omniprésente ; elle régule la stabilité, la localisation et/ou la traduction des ARNm associés à l'inflammation. Pour stabiliser l'ARNm cible, HuR effectue une translocation du noyau (où elle réside normalement) vers le cytoplasme. CS peut induire la translocation de HuR vers le cytoplasme, augmentant ainsi indirectement ses niveaux de protéines cellulaires. Les patients atteints de MPOC, principalement causée par le CS, font face à un risque accru de maladie grave due au COVID-19 en raison de la

régulation à la hausse de l'enzyme de conversion de l'angiotensine 2 (ACE2), un récepteur d'entrée du SRAS-CoV-2. Cependant, la façon dont l'expression de l'ACE2 est contrôlée dans les poumons n'est pas bien comprise.

Compte tenu du large spectre d'ARNm régulés par HuR et de la surexpression bien documentée de cette protéine dans le développement du cancer, nous avons cherché à caractériser le rôle de HuR dans les caractéristiques pathologiques associées à l'exposition au CS et son implication dans la MPOC. Nous avons constaté que les fibroblastes pulmonaires dérivés des patients atteints de MPOC expriment un niveau plus élevé d'ACE2 et que l'exposition chronique au CS augmente de manière significative les niveaux d'expression de la protéine pulmonaire ACE2. Nous avons également constaté que la localisation cytoplasmique de HuR (indiquant l'activation) est plus élevée dans le tissu pulmonaire des sujets fumeurs et des sujets atteints de MPOC par rapport aux sujets non-fumeurs. De plus, il y a eu une augmentation du HuR dans le cytoplasme des fibroblastes pulmonaires humains (HLFs) exposés au CSE, un substitut *in vitro* de l'exposition à la fumée de cigarette. HuR se lie également à l'ARNm ACE2 ; cependant, la suppression de HuR ne modifie pas les niveaux de la protéine ACE2. De plus, nous avons révélé que HuR contrôle plusieurs voies biologiques dans les HLFs. Contrairement à ce qui était attendu, nous avons constaté que les niveaux de protéines et d'ARNm de PTGS2/COX-2 étaient significativement plus élevés dans les HLFs transfectées par siHuR en réponse au CS. Fait intéressant, contrairement à ce que l'on savait sur les effets de HuR sur la stabilisation de l'ARNm de g***è***enes cibles, nous avons constaté que HuR déstabilise l'ARNm de *PTGS2* et *CXCL8* en réponse au CS. Cela suggère que HuR atténue l'expression de COX-2 et IL-8 induite par CS en favorisant la dégradation de leur ARNm. Enfin, nous avons optimisé la préparation d'un extrait de

fumée de cannabis standardisé dans des milieux de culture cellulaire, et nous avons découvert que la fumée de cannabis induisait COX-2 et IL-8 dans les HLFs.

À ce jour, les mécanismes spécifiques de la façon dont l'exposition à la fumée du tabac provoque le développement de maladies chroniques ne sont pas complètement compris. Cette thèse est la première à étudier le rôle de HuR dans la régulation de l'inflammation induite par la fumée ; cela comprend à la fois la fumée du tabac et du cannabis. De plus, la conception expérimentale de cette étude permettra d'identifier les altérations liées au tabagisme dans les cellules pulmonaires primaires. En conséquence, ce mécanisme innovant pourrait être ciblé pour développer une nouvelle thérapie pour les maladies liées à la fumée ; telles que la MPOC. À son tour, cette recherche évoque un nouvel espoir pour des milliers de Canadiens vivant avec cette maladie mortelle.

ACKNOWLEDGEMENTS

I would like to express my deepest gratitude to my supervisor, Dr. Carolyn Baglole, for her guidance and encouragement. Her continuous belief in my abilities helped me to be more confident and to pursue research projects that I have found challenging and exciting. My deepest thanks to Dr. Edith Zorychta for being caring and helpful during this journey. I am also grateful to my committee members: Dr. Sabah Hussain and Dr. Imed Gallouzi for their encouragement and their insightful comments. I would like to thank my current and previous colleagues in the Baglole lab for contributing to a stimulating work environment especially Dr. Hussein Traboulsi and Dr. Aicha Melouane (Rym). Each in their own way has inspired me with their dedication and hard work, to say nothing of their collegiality and kindness. I would also like to acknowledge the faculty members of the Meakins-Christie Laboratories, particularly Dr. David Eidelman, for their invaluable scientific advice. I sincerely thank Taibah University for their supporting and sponsoring my studies. Finally, deep thanks to my family, particularly to my parents, as well as my friends for their love and support during this journey. It would have been impossible to complete it without them.

CONTRIBUTIONS TO ORIGINAL KNOWLEDGE

The studies included in this thesis have identified, for the first time, the importance of HuR in primary HLFs and its implication in COPD. This work has collectively characterized the regulation of HuR function by CS. In doing so, we have shown that lung fibroblasts from Smokers and COPD have high expression of ACE2, a receptor for SARS-CoV-2 that causes COVID-19. Then, we assessed the role of HuR in the regulation of this receptor. We also demonstrated that cytoplasmic HuR level was higher in lung tissue, including epithelial cells and fibroblasts, from Smokers and COPD subjects. Moreover, we found that HuR cleavage product (CP-1) elevated in lung fibroblasts from Smoker and COPD, and that CS induces its cleavage. Most importantly, we revealed fundamental roles for HuR in the regulation of numerous biological processes, such as inflammation, in primary HLFs at the basal level and in response to CS. Collectively, these findings highlight an important role for HuR in the regulation of CS-induced lung damage. To then identify the function of HuR in response to another inhaled stimuli, we standardized a protocol for aqueous CaSE preparation. This protocol can be used for further molecular investigations of cannabis smoke that will improve our understanding about the impact of cannabis smoke on lung pathology features.

CONTRIBUTIONS OF AUTHORS

This doctoral thesis is based on my original work and includes the text and figures from one published review, three published research articles and one manuscript currently in progress for submission, all of which I am first author.

The published and in progress works have been re-formatted in accordance with manuscript-based style outlined by the McGill University Graduate and Postdoctoral studies thesis preparation guidelines. The references of all Chapters have been combined into one reference section at the end of the thesis except references of Chapter II, III, IV and V, which have been combined into reference section at the end of each manuscript.

CHAPTER I:

Some sections, including Figure 1.1 and Figure 1.2, were reproduced/modified with permission from: **Aloufi, N.**, Alluli, A., Eidelman, D. H., & Baglole, C. J. (2021). Aberrant Post-Transcriptional Regulation of Protein Expression in the Development of Chronic Obstructive Pulmonary Disease. *International Journal of Molecular Sciences*, 22(21), 11963 [1].

The work presented in this Chapter is my own and was done in consultation with Dr. Baglole with the following exceptions:

1- Alluli, A.: Provided assistance with the writing for the "Biological Function of lncRNA" subsection.

2- Eidelman, D. H.: Provided assistance with manuscript editing.

CHAPTER II:

Aloufi, N., Traboulsi, H., Ding, J., Fonseca, G. J., Nair, P., Huang, S. K., Hussain, S., Eidelman, D. H., & Baglole, C. J. (2021). Angiotensin-converting enzyme 2 expression in COPD and IPF

fibroblasts: the forgotten cell in COVID-19. *American Journal of Physiology: Lung Cellular and Molecular Physiology*, 320(1), L152–L157 [2].

The work presented in this Chapter is my own in which planned the experiments and analyzed the data; preparation of the manuscript and figures were done in consultation with Dr. Baglole with the following exceptions:

1- Traboulsi, H.: Performed mice exposure and western blot for Figure 2.3D and E.

2- Ding, J.: Prepared Figure 2.1 and aided in the interpretation of the results.

3- Fonseca, G. J.: Interpreted results of experiments.

4- Nair, P.: Provided samples from Non-smoker, Smoker and COPD subjects that were used in this project.

5- Huang, S. K.: Provided samples of Control and IPF lung fibroblasts that were used in this project.

6- Hussain, S., and Eidelman, D. H.: Provided assistance with experimental design and manuscript editing.

CHAPTER III:

Aloufi, N., Haidar, Z., Ding, J., Nair, P., Benedetti, A., Eidelman, D. H., Gallouzi, I. E., Di Marco, S., Hussain, S. N., & Baglole, C. J. (2021). Role of Human Antigen R (HuR) in the Regulation of Pulmonary ACE2 Expression. *Cells*, 11(1), 22 [3].

The work presented in this Chapter is my own, including planning and analysis of experiments; preparation of the manuscript and figures were done in consultation with Dr. Baglole with the following exceptions:

1- Haidar, Z.: Performed replicates for Figure 3.6C and D and Figure 3.7E.

2- Ding, J.: Prepared scRNA-seq data in Figure 3.1, Figure 3.2 and Figure 3.3, and interpreted the results.

3- Nair, P.: Provided samples from Non-smoker, Smoker and COPD subjects that were used in this project.

4- Benedetti, A.: Assisted with statistical analysis.

5- Eidelman, D. H., Gallouzi, I. E., Di Marco, S., and Hussain, S. N.: Provided assistance with experimental design and with manuscript editing.

CHAPTER IV:

Aloufi, N., Hajjar, M., Fonseca, G. J., Nair, P., Eidelman, D. H., & Baglole, C. J. A multi-omics approach reveals fundamental roles for human antigen R in lung fibroblasts. *In Progress*.
The work presented in this Chapter is my own where I planned the experiments and analyzed the data; preparation of the manuscript and figures were done in consultation with Dr. Baglole with the following exceptions:

1- Hajjar, M., and Fonseca, G. J.: Provided assistance with Fastq files and fpkm normalized counts for the RNA-seq data.

2- Nair, P.: Provided human samples that were used in this project.

3- Eidelman, D. H.: Provided assistance with experimental design and with manuscript editing.

CHAPTER V:

Aloufi, N., Namkung, Y., Traboulsi, H., Wilson, E. T., Laporte, S. A., Kaplan, B. L. F., Ross, M. K., Nair, P., Eidelman, D. H., & Baglole, C. J. (2022). Standardized Cannabis Smoke Extract Induces Inflammation in Human Lung Fibroblasts. *Front. Pharmacol.*, 13 [4].

The work presented in this Chapter is my own as well where I planned the experiments and analyzed the data; preparation of the manuscript and figures were done in consultation with Dr. Baglole with the following exceptions:

1- Namkung, Y.: Provided assistance with experimental design, Rho BRET Assay and manuscript editing.

2- Traboulsi, H., Wilson, E. T.: Provided assistance with cannabis smoke extract preparation.

3- Kaplan, B. L. F., and Ross, M. K.: Performed the Mass Spectrometry.

4- Nair, P.: Provided human samples that were used in this project.

5- Laporte, S. A. and Eidelman, D. H.: Provided assistance with experimental design and with manuscript editing.

APPENDIX:

- HuR IP-Mass Spectrometry: Andrew Bayne and Jean-Francois Trempe provided assistance with the analysis of the mass spectrometry data.

CHAPTER I

1. LITERATURE REVIEW

1.1. INTRODUCTION

Human organ systems rely on the dynamics of gene expression to regulate homeostasis, cell survival, fate and differentiation, as well as responses to stress and environmental signals [5]. Eukaryotic cells have developed sophisticated mechanisms to produce and use the transcripts with optimum efficacy through their life cycle. When RNA is synthesized in the nucleus, its biogenesis, translocation to the cytosol and interaction with proteins and other components are necessary to achieve their encoded function. All these steps undergo post-transcriptional regulation of that initial messenger RNA (mRNA), and these steps comprise an important part of overall gene and protein expression. Post-transcriptional regulation is a coordinated process that takes place when the RNA is transcribed but before it is translated into protein. Factors that associate with and regulate target mRNAs at the post-transcriptional level are RNA-binding proteins (RBPs), microRNA (miRNA) and long non-coding RNA (lncRNA) [6, 7]. In mammalian cells, the fate of mRNA is controlled by almost 2000 RBPs [8]. This factor dynamically modulates mRNAs during biological processes [8] and its dysregulation is likely to be involved in pathological processes, including those caused by environmental exposures.

Cigarette smoke (CS) exposure remains a major cause of morbidity and mortality worldwide and causes a variety of chronic lung disorders, including chronic obstructive pulmonary disease (COPD). CS is responsible for approximately 70% of COPD cases [9]. Other inhalation exposures of concern include air pollution, e-cigarettes, and cannabis. In fact, cannabis (marijuana) is the second most-smoked plant after tobacco and the third most prevalent psychoactive substance used worldwide after alcohol and tobacco [10-13], but the impact of cannabis smoke inhalation on

respiratory health is largely unknown. However, it has been established that the pathogenesis of diseases associated with cigarette smoking involves the dysregulation of numerous cellular and physiological pathways such as proliferation, apoptosis and inflammation [14-19]. These processes are controlled at both the transcriptional and post-transcriptional level via the regulation of mRNAs. In this writing, will discuss RBPs that regulate the post-transcriptional modifications of mRNA and their involvement in normal physiology. We will then highlight RBP regulatory mechanisms that are dysregulated in response to smoke and thus may be implicated in the pathogenesis of COPD. Finally, we will address the current knowledge about one of the best characterized RBPs called human antigen R (HuR), the central focus of this thesis.

1.2. CHRONIC OBSTRUCTIVE PULMONARY DISEASE (COPD)

COPD is a leading cause of chronic morbidity and mortality worldwide [20]. The World Health Organization (WHO) lists COPD as the third leading cause of death [21], with its prevalence expected to increase by more than 30% in the coming decade. The Global Initiative for Chronic Obstructive Lung Disease (GOLD) defines COPD as a lung disease characterized by progressive and irreversible airflow limitation which is usually associated with an abnormal inflammatory response in the airways and lungs to noxious particles or gases. The clinical presentation in COPD patients include cough, sputum production, and/or dyspnea [22]. Chronic airflow limitation is due to both emphysema, which is the irreversible destruction of the gas-exchanging alveoli, and chronic bronchitis, a clinical entity characterized by the presence of productive cough for at least three consecutive months during the last two consecutive years [23]. Small airway disease is also a recognized feature of COPD characterized by the presence of inflammation, fibrosis, and mucous plugging, all of which correlated with the severity of airflow obstruction [24].

1.2.1. Risk factors

The risk factors for the development of COPD include a combination of genetic susceptibility and exposure to environmental toxicants [25]. Genetic factors are associated with the development of COPD. The most notable of these is deficiency of alpha-1 antitrypsin (α1AT), which accounts for approximately 1- 2% of COPD cases [25, 26]. Additional risk factors for COPD include respiratory infections, age, and childhood asthma [9, 25].

1.2.1.1. Exposure to cigarette smoke (CS)

The main cause of COPD is CS [25]. Globally, there are around 1.3 billion tobacco smokers [27]. CS is a complex combination of thousands of chemicals (approximately 7000 individual components) of which at least 158 have known toxicological properties [28, 29]. The components with the strongest correlations to disease development are polycyclic aromatic hydrocarbons (PAHs) and N-nitrosamines. Other components that are associated with pulmonary toxicity include free radicals, catechols, and aldehydes [17]. Clinical symptoms can develop in patients many years after starting to smoke, with COPD commonly diagnosed in people over the age of 50 years, with the highest incidence at the age of 75 to 79 years [30, 31].

1.2.1.2. Exposure to air pollution

Beyond CS, additional risk factors for COPD include exposure to ambient and biomass air pollution [9, 23, 25, 26, 32]. Air pollution is an alteration of the natural characteristics of the atmosphere by any chemical, physical, or biological contamination. Air pollution consists of particulate matter (PM), ozone, carbon monoxide (CO), sulfur dioxide (SO_2) and nitrogen oxides (NO_2) [33, 34]. PM is a mixture of small solid and liquid particles which is divided, depending on the particle size (in μm), into fractions including ultra-fine particulate matter (UFPM), $PM_{2.5}$ and PM_{10} [35]. According to the WHO, air pollution accounts for around 7 million deaths worldwide

per year due to diseases including chronic respiratory diseases [33]. Therefore, the WHO developed air quality guideline (AQG) levels for major health-damaging air pollutants. The recommended annual AQG level for $PM_{2.5}$ and PM_{10} is 5 $\mu g/m^3$ and 15 $\mu g/m^3$, respectively. Additionally, the recommended 24 hour AQG level for CO, SO_2 and NO_2 is 4 mg/m^3, 40 $\mu g/m^3$ and 25 $\mu g/m^3$, respectively [36]. However, around 99% of the world's population live in areas where the air quality levels exceed WHO limits [33]. The inhaled air pollution constituents induce inflammatory responses in several cell types, including epithelial cells and macrophages. The constituents of air pollution trigger cellular signalling pathways such as toll-like receptors (TLRs) and PAH sensing pathways, which in turn induce pro-inflammatory cytokine production [35]. Subsequently, long time exposure to the pollutants could produce irreversible loss of pulmonary function and the development of COPD.

1.2.1.3. Exposure to e-cigarettes

E-cigarettes, which are also called vape devices or electronic nicotine delivery systems (ENDS), have become widely popular in the last decade [37]. The components of e-cigarette are a battery, atomizer, and e-liquid-containing reservoir, which holds the e-liquid that contains humectants (glycerin and/or propylene glycol), nicotine, and often flavors. Chemicals, including formaldehyde, acetaldehyde, acrolein and benzaldehyde, are detected in the aerosol generated from e-cigarette solutions [38]. In 2020, there were approximately 68 million of e-cigarette users worldwide [39]. The association between e-cigarette exposure and development of COPD is yet to be established. However, there is experimental evidence suggesting a link between e-cigarettes and COPD [40]. A preclinical study has shown that chronic exposure of mice to e-cigarettes induces distal airspace enlargement, airway hyper-reactivity, and the expression of cytokine and proteases [41]. Furthermore, e-cigarette aerosol induces an inflammatory response in the

respiratory system by increasing neutrophil and macrophage infiltration as well as increasing the production of pro-inflammatory mediators [37, 42]. These studies suggest that exposure to e-cigarette may be involved in the development of COPD, although additional studies are needed.

1.2.1.4. Exposure to cannabis smoke

Cannabis sativa- commonly referred to as marijuana, is an erect annual, dioecious, flowering herb. Belonging to the family of *Cannabaceae*, there are three genera- *C. sativa*, *C. indica* and *C. ruderalis*- which are differentiated from each other by key physical characteristics [43-45]. Cannabis contains more than 100 chemicals called cannabinoids, as well as other compounds such as terpenes and flavonoids [10]. Among the cannabinoids, delta-9-tetrahydrocannabinol (Δ^9-THC or THC) is the one which is psychoactive [46]. According to the WHO, around 150 million people (3% of world population) consume cannabis each year, making this the most widely-used illicit drug in the world [47]. Cannabis smoke contains complex mixture of chemicals qualitatively similar to tobacco smoke, except for nicotine which is a unique component in tobacco products. Chemicals in cannabis smoke including carcinogens (*e.g.,* PAHs) and other toxicants (*e.g.,* CO). The concentration of other chemicals such as aromatic amines, hydrogen cyanide and nitrogen oxides are three to five times higher in cannabis smoke than tobacco smoke [48]. A recent study revealed that cannabis smoke contains chemicals with known health risks through carcinogenic, mutagenic, or other toxic mechanisms [49]. These studies suggest that cannabis smoke shares similar compounds with tobacco smoke.

The increase in usage of cannabis smoke raises concerns about the short and the long-term impacts on respiratory system. The consequence of cannabis smoke on the function of respiratory system and the development of COPD remains unclear. However, cannabis smoking is related to a greater incidence of respiratory symptoms including sore throat, productive cough and shortness

of breath [50]. These symptoms may be due to harmful impacts of cannabis smoke on the respiratory system, including goblet cell hyperplasia, squamous metaplasia and inflammation, as observed in tracheobronchial specimens of cannabis smokers [51]. Consistently, airway inflammatory changes are observed even in asymptomatic cannabis smokers [52]. Furthermore, *in vitro* studies on the molecular pathways affected by cannabis smoke in comparison with tobacco smoke highlight that in epithelial cells exposed to cannabis smoke condensate or tobacco smoke condensate, the genes involved in inflammation, oxidative stress and DNA damage response are significantly altered. Although the effects of the condensates are largely similar, cannabis smoke condensate is noticeably more potent than tobacco smoke condensate. Interestingly, apoptotic and inflammatory pathways are significantly more affected in cells exposed to cannabis smoke condensate [53]. Independent study also showed that exposure to cannabis smoke induces pro-inflammatory mediators [54]. These studies indicate that cannabis smoke may increase the risk factor for the development of lung diseases such as COPD. Nevertheless, the pathogenetic mechanisms of the noxious effects of cannabis smoke is equivocal and warrants additional investigations.

1.2.2. COPD Pathogenesis

The main risk factor for COPD is CS [25]. Mechanistically, the development of COPD is initiated by inflammation caused by repeated exposure to CS, which induces a pulmonary inflammatory response in several cell types, including epithelial cells, fibroblasts, and macrophages [14-16]. Repeated exposure to CS leads to the additional recruitment of innate and adaptive immune cells including neutrophils, macrophages, and lymphocytes. This, in turn, amplifies the production of inflammatory mediators such as tumor necrosis factor alpha (TNF-α), interleukin (IL)-6, C-C motif ligand 2 (CCL2), CCL7, C-X-C motif ligand 1 (CXCL1), CXCL5,

CXCL8 (IL-8), leukotriene (LT) B4 and cyclooxygenase-2 (COX-2/ PTGS2) [15, 55-60]. In addition to inflammation, other pathogenic mechanisms involved in COPD include an imbalance between proteases and antiproteases as well as heightened oxidative stress in the lungs [61]. Mechanistically, repeated exposure to CS causes the release of proteases, such as neutrophil elastase (NE) and matrix metalloproteinases (MMPs), can result in apoptosis of alveolar septal cells, ultimately leading to the destruction of alveolar walls seen in emphysema [56, 62-64]. Moreover, proteases, such as NE, cathepsin G and proteinase-3 promote mucus secretion by increasing the number of goblet cells, stimulating degranulation in these cells, and cause the enlargement of submucosal glands. The combination of mucus hypersecretion, inflammation in the airways, fibrosis formation around the small airways and loss of lung elastic recoil leads to the narrowing of small airways, and subsequently airflow obstruction [56, 62, 63] (Figure 1.1).

1.2.2.1. Structural and immune cell crosstalk in COPD

The lungs are made up of over 40 different cell types, with many believed to contribute to disease pathogenesis [65]. Cells which contribute to COPD pathogenesis include both lung structural cells, such as epithelial cells, fibroblasts and endothelial cells, and inflammatory cells, such as macrophages, neutrophils, lymphocytes and dendritic cells [66]. Epithelial cells, lining the airways and the lungs, are a 'front line' of defence and are susceptible to direct damage caused by CS [66, 67]. Consequently, exposure to CS releases inflammatory mediators, impairs the defense response mechanisms of the airway epithelium and increases the susceptibility to infection [66, 67]. Pulmonary fibroblasts directly connect type II pneumocytes to endothelial cells, which provide a bridge for leukocyte migration [68, 69]. Further, cell adhesion molecules are activated in endothelial cells from COPD patients [70]. Thus, the inflammatory mediators secreted by these structural cells activate and attract immune cells to the lung. Indeed, it is now recognized that these

structural cells can regulate immune responses and educate local immune cells within the lung, which are functions classically attributed to immune cells [66, 67]. As a consequence, activated alveolar macrophages, for example, produce additional inflammatory mediators, thereby recruiting immune cells to the site of injury [71, 72]. Included among the recruited immune cells are neutrophils, coming to both the airways and parenchyma, that are facilitated by their initial adhesion to endothelial cells via adhesion molecules including E-selectin. E-selectin is upregulated on endothelial cells from COPD patients [70, 73]. The number of neutrophils is increased in response to CS and in COPD, which is associated with the severity of the disease [64, 74]. Activated neutrophils and macrophages are sources of proteases that contribute to the destruction of alveolar walls as well as mucus secretion [64, 72, 74]. Furthermore, abnormalities in the number and the function of T lymphocytes are observed in COPD, which is correlated with the chronic inflammation and the amount of alveolar destruction [75]. Another type of immune cell involved in COPD pathogenesis are dendritic cells, which in turn communicate and activate other immune cells [76]. Altogether, the perpetual crosstalk between structural and immune cells in the lungs may contribute to COPD pathogenesis in a susceptible individual.

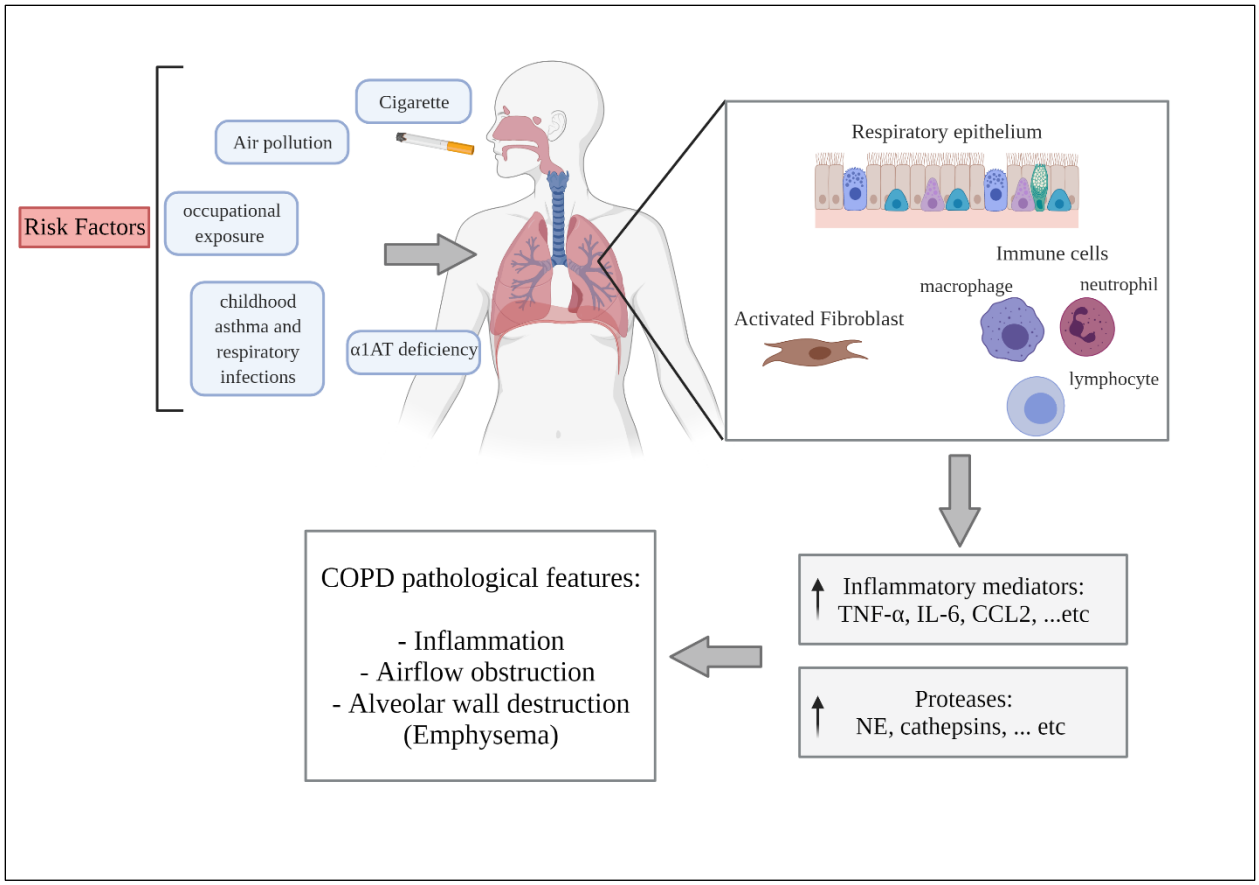

Figure 1.1. Etiology and pathogenesis of COPD.

The risk factors for the development of COPD include CS, air pollution and occupational exposures; childhood asthma; respiratory infections; and α1AT deficiency. Upon exposure to CS, lung structural cells, including epithelial cells and fibroblasts, as well as alveolar macrophages, are activated. These cells produce inflammatory mediators to recruit additional inflammatory cells as neutrophils, macrophages, and lymphocytes to the site of exposure. This augments the production of inflammatory mediators such as TNF-α, IL-6, CCL2, CCL7, CXCL1, CXCL5, CXCL8 (IL-8), LTB4 and COX-2 as well as boosts the releases proteases such as NE, cathepsins and MMPs. This dysregulation leads to chronic pulmonary inflammation, airflow obstruction and alveolar wall destruction (emphysema) in susceptible individuals [1].

1.2.3. Exacerbations in COPD

The inflammation in COPD further increases during acute exacerbations, which are defined as a worsening of day-to-day symptoms, and are predominantly caused by bacterial or viral infection [55]. Exacerbations in COPD are strongly correlated with an increase in hospitalization

and mortality, and a decrease in lung function [30]. Additionally, COPD is associated with increased severity of coronavirus disease 2019 (COVID-19) [77], which is caused by severe acute respiratory syndrome coronavirus 2 (SARS-CoV-2), a novel β-coronavirus [78, 79]. Structurally, SARS-CoV-2 has main structural proteins including spike (S), envelope (E), membrane (M), and nucleocapsid (N) as well as several accessory proteins. The entry of SARS-CoV-2 into host cells depends on the binding of surface S1 of the S proteins to the cellular receptor angiotensin-converting enzyme 2 (ACE2) [79]. In COPD, ACE2 is overexpressed in alveolar and bronchial epithelium [80, 81]. Thus, patients with COPD may be at heightened risk for severe COVID-19. The mechanism(s) accounting for the increased ACE2 expression in the lungs is currently not known.

1.2.4. Disease Management

Upon diagnosis of COPD, effective strategies to reduce symptoms and limit the severity of exacerbations should be provided according to individualized evaluations. As COPD is characterized by airflow limitation, the first line treatments are short-acting and long-acting bronchodilators, such as long-acting β-agonists (LABA) [82]. β2-agonists bind to β2-adrenoceptors on the cell membrane and activate the Gs protein [83], which in turn activates intracellular adenyl cyclase. Then, adenyl cyclase converts adenosine triphosphate (ATP) to cyclic adenosine monophosphate (cAMP), a second messenger that activates protein kinase A (PKA). This leads to myosin dephosphorylation and smooth muscle relaxation [83, 84]. A second line treatment for COPD patients is the prescription of inhaled corticosteroids (ICS) to reduce inflammation [82]. ICS cross the plasma membrane and activate glucocorticoid receptors (GR) in the cytoplasm, which either decreases pro-inflammatory gene expression or activates the transcription of anti-inflammatory genes. However, corticosteroids have limited effectiveness in

COPD [85]. When symptoms persist or worsen, ICS are combined with LABA. It is also recommended that the patient stops smoking, reduces exposure to environmental and occupational risk factors, and get an influenza vaccine annually [25].

However, no disease modifying therapies exist for COPD. After smoke exposure and in COPD, transcriptional regulation alters the expression of inflammatory mediators, such as IL-6, COX-2, TNF-α, IL-1β and IL-8 [86]. It is well-studied that in response to smoke and in COPD, the expression of these inflammatory mediators is regulated by the transcription factor nuclear factor-κB (NF-κB) [86, 87]. Inhibitors targeting NF-κB activity have been developed as a potential therapy for COPD, but these have not been approved for clinical use [88, 89]. However, targeting NF-κB in COPD may not be sufficient, because inflammation in COPD is also regulated by other transcription factors, such as activator protein-1 (AP-1) [90, 91]. Furthermore, immunosuppression and infection susceptibility caused by the inhibition of NF-κB must be considered as a confounding factor. In this regard, the post-transcriptional regulation of mRNA by RBPs has emerged an important mechanism in the overall control of gene and protein expression under both normal and pathological conditions. Post-transcriptional regulation includes the regulation of mRNA maturation, stability, and translation [92]. Therefore, a better understanding of the mechanistic underpinnings of post-transcriptional regulation of mRNA by RBPs could lead to the development of new targeted therapies for COPD. Here, we summarize the current state-of-knowledge of post-transcriptional regulation by RBPs that is applicable to pathogenic mechanisms implicated in the response to CS and in the development of COPD.

1.3. RNA BINDING PROTEINs (RBPs)

RBPs are a group of over 2000 proteins, each possessing multiple RNA binding domains, and which are known to be involved in RNA decay [8]. RBPs associate with RNA transcripts and

form ribonucleoprotein (RNP) complexes after transcription. Some RBPs bind early during RNA synthesis to precursor mRNA (pre-mRNA) and remain bound to the pre-mRNA until its degradation or translation, while other RBPs recognize and bind to pre-mRNA for specific processes such as splicing, stability, transport, and cellular localization [93]. The diversity of RBP functions suggest that several RNA-binding domains (RBD) are responsible for RNA recognition and for recruitment to specific RNA targets [94, 95]. RBPs contain one or multiple RBDs, such as the RNA-recognition motif (RRM), K-homology domain (KH), double-stranded RBD (dsRBD), zinc fingers (Znf), DEAD box helicase domain, among others. There is also diversity in the specificity and affinity of RBD interaction with RNA [8, 96, 97]. Some RBPs with dsRBD interact with the phosphate-sugar backbone of their RNA targets [8, 96]. Other RBPs, such as those with RRMs, interact in a sequence-specific manner with the nucleotide base and shape complementarity of the RNA [8, 96-98]. In this section, we will explore the role of RBPs in different aspects of RNA biology.

1.3.1. Biological functions of RBPs

RBP-mediated post-transcriptional regulation is essential for proper cellular function and as such, its perturbation can lead to the development of disease. For example, the fragile X syndrome of mental retardation (FXS) is caused by a defect in the RBP fragile X mental retardation protein (FMRP), which is important for normal brain development [99]. The fate of RNA, from transcription to translation, is highly dependent on RBP-mediated polyadenylation, pre-mRNA splicing, as well as mRNA editing, turnover, subcellular localization, and translation (Figure 1.2).

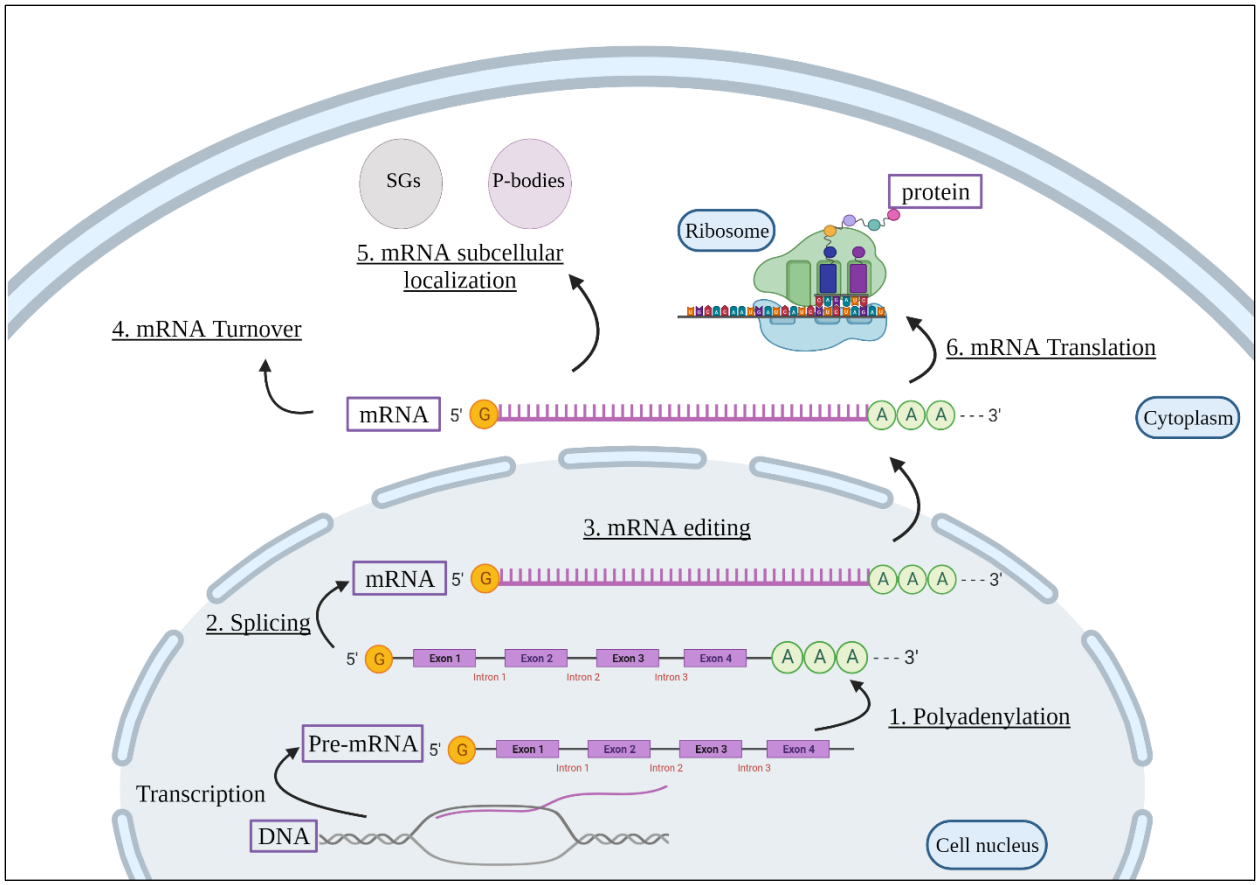

Figure 1.2. Cellular functions of RBPs.

RBPs are involved in post-transcriptional regulation of target mRNA. pre-mRNA is first transcribed from the DNA. Then, RBPs regulate the production of mature mRNA via polyadenylation (1), splicing (2) and mRNA editing (3). RBPs can also regulate mRNA stability (4) and mRNA subcellular localization (5) within the cell in SGs or P-bodies; RBPs are also involved in mRNA translation into proteins (6). SGs, stress granules; P-bodies, Processing-bodies [1].

1.3.1.1. Polyadenylation

Polyadenylation of pre-mRNA is an essential processing event for RNA nuclear export, stability, and translation. Polyadenylation is a 3′ end maturation step which all pre-mRNAs in eukaryotic cells, except histones, receive poly(A) tails of around 200 adenine (A) nucleotides to their 3' end by a multiprotein machinery complex [100, 101]. This occurs in a coupled cleavage reaction whereby the pre-mRNA is first cleaved between AAUAAA sequences upstream and

U/GU rich sequences downstream of the cleavage site followed by addition of a polyadenosine tail. The cleavage and polyadenylation machinery consists of four multi-subunit protein complexes: the cleavage and polyadenylation specificity factor (CPSF), the cleavage stimulation factor (CstF), and mammalian cleavage factors I and II (CFIm and CFIIm) [102]. The CPSF protein complex consists of six protein subunits that are vital for cleavage of pre-mRNA and interaction with AAUAAA sequences [101, 102]. CstF consists of three subunits that interacts with the downstream element and upstream site of the pre-mRNA [100, 102, 103]. CFIm and CFIIm are required for the cleavage step [103, 104]. Then, poly (A) polymerase (PAP), stimulated by CPSF and the RBP nuclear poly(A) binding protein (PABPN1), adds the poly(A) tail to the cleavage product of the synthesized pre-mRNA molecule to produce mature mRNA [105, 106].

1.3.1.2. pre-mRNA splicing

Splicing of pre-mRNA is a step of gene expression in which introns (noncoding sequences) are removed and exons (coding sequences) are assembled by the spliceosome. The spliceosome is a ribonucleoprotein complex composed of five small nuclear RNAs (snRNAs)- U1, U2, U4, U5 and U6- and more than 50 protein factors such as U2 auxiliary factor (U2AF) and SR (Serine-Arginine rich) proteins [107, 108]. Some exons are constitutively spliced [109]. However, many exons are alternatively spliced, in which more than one mRNA can be generated from a single pre-mRNA. At least 74% of human multi-exon genes express several mRNAs through alternative splicing (AS) [110]. Studies using high-throughput sequencing showed that ~95% of multi-exon genes undergo AS [111, 112]. RBPs also regulate this process, including SR proteins and heterogeneous nuclear ribonucleoproteins (hnRNPs) [113]. In human cells, hnRNPs are the most abundant RBPs that regulate AS of pre-mRNA. Genome-wide analysis showed that more than half of all AS events are regulated by six major hnRNP proteins: A1, A2/B1, H1, F, M, and U [114].

1.3.1.3. mRNA editing

RNA editing is a type of RNA modification characterized by alteration of site-specific RNA sequence from that encoded in DNA [115]. The RNA codon and protein sequence are changed if the editing occurs in the coding region [116]. When editing occurs in the noncoding regions, it may affect splicing, stability, or translation of the mRNA [117, 118]. RNA editing, mediated by adenosine deaminases acting on RNA (ADAR) proteins, involves adenosine (A) deamination to inosine (I) that is then recognized as guanosine by the translational apparatus [115, 117, 119, 120]. ADARs contain two or three RBDs and a highly conserved deaminase domain [121]. Three ADAR proteins, ADAR1, ADAR2 and ADAR3, are present in humans [120-123]. A-to-I editing can occur in noncoding regions of the RNA, such as in Alu repeats which are good substrates for ADAR proteins [118, 124, 125].

1.3.1.4. mRNA turnover

The translation of mRNA is coupled with its stability and decay. RBPs that regulate mRNA stability are either mRNA decay activators or mRNA stabilizers. Activators of mRNA decay recognize the constitutive decay AU- and GU-rich elements of their target mRNA and affect its cellular levels by several mechanisms [126]. For example, tristetraprolin (TTP), also known as zinc finger protein 36 (ZFP36), is an RBP that promotes mRNA decay [127]. TTP promotes deadenylation of *TNF-α* mRNA and its degradation upon exposure to lipopolysaccharide (LPS) [128-130]. TTP also downregulates numerous inflammatory mRNA, such as IL-6, IL-2 and COX-2 [131-133]. Other RNA-binding proteins implicated in mRNA decay include KH-type splicing regulatory protein (KSRP) [134], Roquin [135], and ARE/poly(U)-binding/degradation factor 1 (AUF1) [136-138]. Conversely, other RBPs act as mRNA stabilizers and impede mRNA degradation. One of the best known RBPs with a regulatory influence on mRNA stability is HuR.

HuR targets mRNAs which have uridylate (U)- or adenylate-uridylate (AU)-rich elements (AREs) in the 3'-untranslated region (UTR); these mRNA typically encode proteins involved in cell proliferation, differentiation, migration, apoptosis, inflammation, and fibrosis [139-146].

1.3.1.5. mRNA subcellular localization

Localization of mRNA is critical for protein synthesis. Stress granules (SGs) and Processing (P) bodies are cytoplasmic RNA granules consisting of aggregates of ribonucleoprotein complexes. SGs and P-bodies are assembled in stressed and in unstressed cells, respectively [147]. SGs sequester mRNA for storage and translational silencing [148]. In human osteoarthritis (OA) chondrocytes, for example, in response to IL-1β, *PTGS2* mRNA is sequestered in SGs by HuR, thereby decreasing protein levels due to a delay in the translation of the mRNA [149]. SGs also contain other RPBs involved in RNA metabolism including poly(A)-binding protein (PABP), T-cell intracellular antigen 1 (TIA-1) and TTP [150]. In contrast, P-bodies contain mRNA targeted for degradation and the RBPs that are involved in this process [151]. For instance, roquin suppresses inducible co-stimulator (ICOS) expression, which prevents autoimmunity through its association with P-bodies in T-helper cells [152].

1.3.1.6. mRNA translation

The regulation of mRNA translation controls gene expression in the cytoplasm. Numerous proteins, including RBPs, regulate mRNA location and assembly into ribosomes for protein synthesis. For example, the RBP PABP that binds to stable mRNA also interacts with eukaryotic initiation factors 4E (eIF4E) whereby the 48S and 80S ribosome initiation complex are assembled and translation is initiated [153]. Another example is the RBP TIA-1 which represses translation of various mRNA, including *PTGS2* mRNA [154].

1.3.2. Interplay of RBPs

Dynamic interactions between RBPs may fine-tune post-transcriptional modifications of common mRNAs. RBPs can either cooperate or compete to bind target mRNAs. For example, ADAR1 cooperates with HuR and forms an RNA-dependent complex, which regulates the stability of ADAR1 targets in human B cells [155]. ADAR1 mediates A-to-I editing of cathepsin S (*CTSS*) [156], a cysteine protease associated with remodeling/degradation of connective tissue and basement membrane [157]. HuR also binds to the 3′ UTR of *CTSS* mRNA and controls its stability and expression [156]. HuR and TIA-1 can also interact to impact mRNA encoding programmed cell death 4 (PDCD4), a tumor suppressor that induces apoptosis. Here, increasing TIA-1 prevents HuR from binding to *PDCD4* mRNA, while decreasing TIA-1 induces HuR binding to *PDCD4* mRNA [158]. Furthermore, TTP interacts with PABP1 in activated primary mouse bone-marrow-derived-macrophages (BMDMs) to represses the translation of TTP target mRNA involved in inflammatory response [159]. Together, these few studies illustrate the interplay of RBPs in the regulation of various post-transcriptional processes involved in physiological and pathological mechanisms.

1.3.3. The regulation of RBPs in COPD

Elucidation of changes in the expression and the function of RBPs may suggest putative pathogenetic roles for them. Targeting RBPs could also be a novel therapeutic strategy. However, only a handful of studies have directly investigated RBPs in COPD. One such study was a genome-wide association study (GWAS) which identified iron-responsive element binding protein 2 (IRP2 or IREB2), an RNA-binding protein that regulate cellular iron homeostasis, as a COPD susceptibility gene. *IRP2* mRNA and protein levels are elevated in lungs from COPD subjects [160-163], and IRP2 expression is increased in the lungs of mice chronically exposed to CS.

Furthermore, knockout of IRP2 protected mice from CS-induced pulmonary inflammation and impairment of airway mucociliary clearance (MCC). Mechanistically, IRP2 in the lungs induces mitochondrial dysfunction by promoting mitochondrial iron loading and cytochrome c oxidase [164]. Previous observations have shown that iron deposition is increased in lungs from severe COPD patients as well as in response to CS [165, 166], which may be regulated by the elevation of IRP2.

Another RBP studied in the context of COPD is AUF1, which participates in mRNA decay. AUF1 is decreased in the bronchial epithelium from COPD subjects compared to smokers without COPD. Analysis of a microarray from primary airway epithelium of COPD subjects revealed that AUF1 target genes are upregulated, including those associated with inflammation [167]. Although this suggests that AUF1 may regulate the expression of inflammatory genes involved in COPD, direct regulation by AUF1 of these downstream mRNA and its implications for the pathogenesis of COPD remain to be investigated. Overall, these studies raise the possibility that RBPs may be involved in the development of COPD. As little is known about the direct role of RBPs in COPD per se, below we summarize studies which have examined related mechanisms associated with the development of this disease.

1.3.3.1. RBPs in inflammation

CS causes direct damage to airway and alveolar epithelial cells, which leads to the recruitment of inflammatory cells and the release of numerous inflammatory mediators including TNF-α [15, 17, 55-59, 168], the overexpression of which induces pulmonary inflammation and airspace enlargement [169]. An RBP known to regulate TNF-α expression is TTP. TTP is generally an anti-inflammatory RBP, as TTP knockout mice have a proinflammatory phenotype [170]. TTP promotes mRNA decay of *TNF-α* by binding to AREs present within the 3'UTR [128]. TTP also

destabilizes other mRNA associated with inflammation including *PTGS2*, *IL-6*, *CXCL8* and *CCL2* [171, 172]. Glucocorticoids, which are used clinically in COPD, elevate mRNA and protein levels of TTP, that are crucial for glucocorticoid-mediated inhibition of *TNF-α* mRNA [173]. Glucocorticoid inhibition of other inflammatory genes including *CCL2*, *CCL7*, *CXCL1* and *CXCL5* is also abrogated in TTP-knockout cells [174]. Overall, these studies suggest that TTP target mRNA encoding proteins that are responsible for the inflammatory response associated with COPD pathogenesis.

AUF1 is another RBP that induces the decay of target mRNA, including TNF-α. AUF1 knockout mice are susceptible to endotoxin challenge due to TNF-α and IL-1β overproduction [175]; these mice also exhibit chronic dermatitis with age, concomitant with TNF-α and IL-1β overexpression [176]. Given that AUF1 expression is decreased in COPD [167] and that many inflammatory mediators regulated by AUF1 are also upregulated in COPD, it is possible that dysregulation of AUF1 may contribute to the inflammatory response associated with this disease.

1.3.3.2. RBPs in apoptosis and protease expression

Emphysema is characterized by the loss of lung structural cells, including alveolar epithelial cells and fibroblasts [22, 177]. Mechanistically, emphysema is thought to develop because of CS-induced apoptotic cell death [18, 19]. Evidence for this comes from studies where intra-tracheal administration of active caspase-3 induces epithelial cell apoptosis, elastolytic activity in bronchoalveolar lavage (BAL) and airspace enlargement in mouse lungs [178]. Other proteins, such as vascular endothelial growth factor (VEGF), help alveolar cells withstand damage by CS. Experimentally, blocking of VEGF receptors stimulates apoptosis of alveolar cells and induces an emphysema-like pathology [179, 180]. In COPD, the level of VEGF is decreased, which may be a contributing factor to the development of emphysema in people [181]. Many of

the RPBs mentioned above that regulate inflammation also have roles in apoptosis. For example, TTP destabilizes *VEGF* mRNA [182]. In contrast, hnRNP L stabilizes *VEGF* expression [183]. hnRNP L is a multifunctional splicing factor that involved in the regulation of AS and mRNA stability [183, 184]. Interestingly, knockout of hnRNP L in hematopoietic stem cells causes cell death through caspase-dependent pathways [185], raising the possibility that the downregulation of VEGF and upregulation of cell death in COPD could be regulated by hnRNP L. In addition to aberrant cell death, lung tissue destruction in COPD is mediated by proteases. As for apoptosis, RBPs implicated in the regulation of proteases include TTP, which destabilizes *MMP-9* and *MMP-2* mRNA [186].

1.3.3.3. The response of RBPs to CS

One of the RBPs that has been studied in the context of smoking is RNA-binding motif protein 5 (RBM5). The gene of RBM5, also known as H37 or Luca15 located in chromosomal region 3p21.3, is frequently deleted in heavy smokers and lung cancer patients [187, 188]. *Rbm5* loss-of-function (heterozygous) mice exposed to the tobacco carcinogen 4-(methylnitrosamino)-1-(3-pyridyl)-1-butanone (NNK) develop more aggressive lung cancer [189]. In cells exposed to CSE, *RBM5* mRNA and protein levels are decreased whereas β-catenin is increased. β-catenin is a key player in canonical Wnt signaling, whose activation induces genes involved in cell differentiation [190]. β-catenin is increased in proximal airway epithelium in COPD, with activation of Wnt/β-catenin signaling increasing epithelial-to-mesenchymal transition (EMT) [191]. EMT is a process where epithelial cells gradually lose cellular polarity and adhesiveness and acquire migratory capacity and invasiveness like that in a mesenchymal phenotype. EMT is increased in bronchial epithelial cells from COPD patients, which contributes to fibrosis formation around the small airways leading to airflow obstruction [192]. Although the evidence is indirect,

these studies raise the prospect that RBM5 could regulate EMT in COPD through β-catenin pathway. At this writing, the expression and function of RBM5 in COPD is unknown.

Collectively, RBPs are examples of post-transcriptional regulons that may be involved in the pathogenesis of COPD and in the pathological changes caused by tobacco smoke. To date, many studies have largely focused on transcriptional regulatory pathways implicated in the development of COPD and in response to toxicants such as tobacco and cannabis smoke. However, it is increasingly apparent that post-transcriptional regulation of gene expression adds a dynamic layer of complexity to chronic diseases, as RBPs regulate polyadenylation, pre-mRNA splicing, RNA modification, nuclear export, localization, and turnover of target mRNA. Altered function of RBPs may contribute to the development of chronic diseases, particularly those caused by environmental exposures, such as COPD, and future work should address these mechanisms. In this regard, RBPs such as HuR represent potential therapeutic targets. For instance, MS-444 is a small molecule inhibitor that interferes with the RNA binding activity of HuR [193] which has been shown to exhibit antitumor activity *in vitro* and *in vivo* [194]. Therefore, post-transcriptional regulation of protein expression by HuR deserves serious consideration in therapeutic strategies for smoke related diseases such as COPD.

1.4. Hu/ELAV FAMILY: HuR

One of the best known RBPs with a regulatory influence on mRNA is hu antigen R (HuR). HuR, also known as HuA or embryonic lethal abnormal vision-like protein 1 (ELAVL1), belongs to the embryonic lethal abnormal vision (ELAV) family of RBPs. Other members include HuB, HuC and HuD, which are neural-specific proteins [195]. Hu/elav proteins were discovered in the early 1990s as tumor antigens, with a molecular mass of 35- 40 kDa, that are expressed in small cell lung cancer and in neurons [196, 197]. HuR was identified in 1996 as a ubiquitously-expressed

member of ELAV family of proteins [198], and its gene is localized on chromosome 19p13.2 in human [199].

HuR has a predicted molecular mass of 36 kDa and contains a short N-terminal domain followed by two RNA-binding domains called RRM1 and RRM2, a basic linker domain in the hinge region (HuR nuclear shuttling domain; HNS) and a third RRM, RRM3, in the C-terminal domain [198, 200, 201] (Figure 1.3).

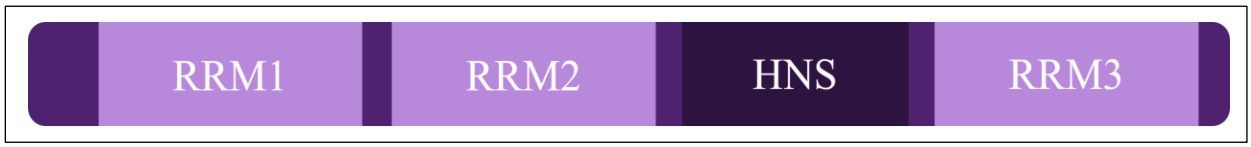

Figure 1.3. Structure of HuR.
This illustrating the three RNA recognition motifs (RRMs) and the hinge region of HuR.

RRM1 and RRM2 bind to AREs, while RRM3 binds to the poly (A) sequence of target mRNAs [198, 202]. However, a recent study revealed that RRM3 binds to the ARE of target mRNA and has low affinity to poly (A) sequence [201]. RRM3 is also involved in the HuR-RNA complex stabilization as well as in protein-protein interactions [203, 204]. The HNS is localized in the hinge region between RRM2 and RRM3 and is important for the shuttling of HuR out of and back into the nucleus [200]. Besides the HNS region, the mobilization of HuR is regulated by transportins 1 and 2, the chromosome region maintenance 1 (CRM1) and importin-1α, which are components of nuclear transport machinery [205-207]. Further, posttranslational modifications of HuR impact its subcellular localization as well as its RNA-binding activity, which will be discussed below.

1.4.1. The control of HuR function

1.4.1.1. HuR expression and abundance

HuR abundance controls, in part, the function of HuR, with the cellular abundance of *ELAVL1* mRNA and protein being regulated by multiple mechanisms. First, the expression of HuR is regulated at the transcriptional level by the NF-κB and SMAD mothers against decapentaplegic homolog (SMADs) [208, 209]. HuR expression is also controlled by a positive feedback loop via HuR binding to and stabilizing its own mRNA, thus inducing its protein level [210-212]. On the other hand, HuR protein levels are reduced by miRNAs such as miR-125a, miRNA-519, miR-291b-3p and miR-570-3p [213-216]. Finally, HuR abundance is affected by mechanisms that operate at the posttranslational level such as ubiquitination and cleavage.

1.4.1.1.1. HuR ubiquitination

Ubiquitination, also referred to as ubiquitylation, is a cellular process by which the protein is recognized by proteasome for degradation. Ubiquitination occurs through consecutive steps that requires three enzymes. First, the activating (E1) enzyme transfers the ubiquitin to the active cysteine (Cys) residue of the conjugating (E2) enzyme. Sequentially, E2 interacts with the ligase (E3) enzyme that mediates ubiquitin attachment to an internal lysine (Lys) residue of a substrate protein [217]. In certain instances, such as heat shock, HuR is ubiquitinated at residue Lys-182 and degraded by proteasome, thus HuR protein levels are decreased [218-220]. Additionally, glycolytic stress induces HuR translocation to the cytoplasm, where it is targeted for ubiquitination by β-transducin repeat-containing protein (β-TrCP), an E3 ubiquitin ligase [221]. Interestingly, HuR ubiquitination can also influence its binding to mRNA. For instance, ubiquitination of HuR with a short K29-linked polyubiquitin chain interferes with HuR from binding to target mRNA

such as *p21* [222]. These studies suggest that HuR ubiquitination alters its protein stability and abundance, as well as its RNA-binding activity in cells under conditions of stress.

1.4.1.1.2. HuR cleavage

Under lethal condition such as treatment with staurosporine, HuR is translocated to the cytoplasm and cleaved at aspartate 226 (A226) in the HNS by caspase-3 and caspase-7 into two cleavage products designated as CP-1 (24 kDa) and CP-2 (~ 8 kDa) (Figure 1.4).

Figure 1.4. HuR cleavage.

HuR undergoes cleavage at A226 by caspases and produces two cleavage products: CP-1 and CP-2.

HuR cleavage is also dependent on the Fas associated via death domain (FADD)/caspase-8 pathway. The products of this cleavage promote apoptosis [223], and mutation of the cleavage site A226 delays apoptotic cell death [224]. Additionally, ionizing radiation (IR) activates caspase-3 which induces HuR cleavage. The cleaved product CP-1 binds to and stabilizes the pro-apoptotic factor *BAX* (Bcl-2-associated X protein) mRNA and activates the apoptotic pathway. Inhibition of caspase-3 activation, following IR, reduces HuR cleavage and decreases the rate of apoptosis *in vitro* and *in vivo* [225]. CP-1 is also associated with other target mRNA encoding proteins that are involved in cell death pathways [226]. An independent study also showed that both CP-1 and CP-2 associate with and stabilize caspase-9 which promotes caspase-mediated apoptosis [227]. Furthermore, HuR is cleaved by activated caspase-3 during myogenesis, a physiological muscle

fiber formation. Consequently, CP-1 prevents nuclear import of HuR which causes accumulation of HuR in the cytoplasm. Here, HuR stabilizes pro-myogenic mRNAs, including *myogenin* mRNA, to promote myogenesis [228]. These studies revealed that caspase-induced HuR cleavage regulates apoptosis as well as myogenesis.

1.4.1.2. HuR phosphorylation

Phosphorylation is a reversible posttranslational modification of proteins, whereby a phosphate group is attached to an amino acid residue by protein kinases, such as cyclin-dependent kinase 1(CDK1), protein kinase C (PKC)α, PKCδ, p38 mitogen-activated protein kinase (MAPK) and IkB kinase α (IKKα) [144, 221, 229-232]. HuR phosphorylation influences its function by affecting subcellular localization, RNA-binding affinity, and protein stability. For example, HuR phosphorylation at the serine 202 (S202) residue in the HNS region by CDK1, a G2-phase kinase, retains HuR in the nucleus during G2 /M phase [230]. However, HuR phosphorylation at the S221 residue in the HNS region by PKCα or PKCδ, in response to a stable ATP analog or angiotensin II, respectively, induces HuR translocation to the cytoplasm [144, 231]. p38 MAPK also induces HuR translocation to the cytoplasm in cells exposed to γ-irradiation by phosphorylating HuR at the threonine 118 (T118) residue in the RRM2 [232]. Furthermore, in response to IL-1β, activated p38 phosphorylates HuR at T118 and induces its binding to and stabilizing *PTGS2/COX-2* mRNA and cytosolic phospholipase A2α (*cPLA2α*) mRNA [233]. cPLA2α is involved in inflammation by breaking down phospholipids from the plasma membrane to produce arachidonic acid which in turn metabolized by COX-2 to synthesize prostaglandins [234, 235]. Finally, HuR phosphorylation by PKCα at S318 and by IKKα at the S304 residues in the RRM3 induces HuR degradation, by which PKCα and IKKα regulates cytoplasmic translocation of HuR. Subsequently, HuR is targeted for ubiquitination by β-TrCP1 [221]. Overall, phosphorylation of HuR at different residues affects

HuR function by regulating its subcellular localization, RNA-binding activity, and protein stability.

1.4.1.3. HuR methylation

Protein methylation is another posttranslational modification of proteins, whereby a methyl group is added to arginine residues. Protein methylation is catalyzed by protein arginine methyltransferases (PRMTs) such as PRMT4, also known as coactivator-associated arginine methyltransferase 1 (CARM1) [236]. Under certain conditions, HuR methylation influences its function by affecting the decay of target mRNA. For example, in macrophages exposed to LPS, CARM1 methylates HuR at arginine 217 (R217) in the HNS [237], which may be involved in HuR stabilization of *TNF-α* mRNA [238]. Further, mutation of R217 or knockdown of CARM1 reduces the ability of HuR to stabilize target mRNAs including cyclin A [239], a protein that regulates cell cycle progression [139]. These studies suggest that HuR methylation may involve in HuR regulation of target mRNAs.

1.4.2. HuR function

The abundance and posttranslational modifications of HuR impact its function by controlling its subcellular localization as well as its ability to control target genes. HuR participates in polyadenylation and pre-mRNA splicing as well as controls mRNA stability, translocation and/or translation (Figure 1.5) [240-243]. HuR blocks polyadenylation of the simian virus 40 late (SVL) poly(A) site that has U-rich sequences both upstream and downstream of the cleavage site, which leads to a decrease of SVL poly(A) site-containing mRNA [240]. HuR is also involved in pre-mRNA splicing process, which can promote exon 6 skipping of the apoptosis receptor Fas pre-mRNA through the inhibition of U2 auxiliary factor 65 kDa (U2AF65) association with the

upstream 3' splice site. This leads to the production of the soluble isoform of Fas that prevents apoptosis [241].

Perhaps the best known function of HuR is its ability to stabilize or destabilize mRNA bearing AREs in the 3′UTR, depending on cell type and/or stimuli [243]. HuR is well-described to associate with the 3′UTR of mRNA and stabilize these mRNA, such as cyclin A2, B1, D1 and E1, p21, myogenin, MyoD, COX-2, TNF-α, IL-6, IL-8, VEGF and transforming growth factor beta (TGF-β). These mRNA are involved in cell proliferation, survival, and differentiation as well as inflammation, angiogenesis and fibrosis [139, 140, 146, 238, 244-252]. Furthermore, HuR destabilizes target mRNA and downregulates its expression by cooperating with miRNA or RBP. An example of this is the ability of HuR to promote the interaction of the miRNA let-7- loaded RNA-induced silencing complex (RISC) with the 3′UTR of the proto-oncogene *MYC* mRNA to destabilize it and repress its expression [253]. HuR also cooperates with the RBP KSRP and form a complex that binds to the 3′UTR of nucleophosmin (NPM) and destabilizes it, and consequently promotes myogenesis [254]. HuR has also the ability to regulate the translation of target mRNA when it associates with the 3′UTR of mRNA. For instance, HuR binds to 3′UTR of prothymosin α (ProTα), an enhancer of cell survival, and induces its translation [255]. These studies suggest that HuR binding to 3′UTR controls the stability or the translation of target mRNA, thus affecting their expression.

HuR can also bind to the coding region of target mRNA to regulate their localization within the cells. For instance, HuR binds to the coding region of *CD83* mRNA, a marker for mature dendritic cells. During the stimulation of cytokine production, HuR binds to and induces the cytoplasmic accumulation of *CD83* mRNA and induces its expression [256]. Hence, HuR binding to the coding region of target mRNA controls its localization and expression.

Finally, besides HuR binding to the 3′UTR and coding region of target mRNA, HuR associates with the 5′UTR of target mRNA and regulates their translation. For example, HuR associates with the 5′UTR of thrombomodulin (TM), a transmembrane endothelial protein that binds thrombin and thus activates protein C, which has anti-coagulation and anti-inflammation effects. In inflammation, the expression of TM is reduced. Mechanistically, HuR binds to the 5′UTR of TM and prevents its translation in response to IL-1β [257]. On the other hand, HuR binds to 5′UTR of hypoxia-Inducible Factor 1α (*HIF1α*) mRNA and induces its translation in response to hypoxia mimetic cobalt chloride ($CoCl_2$) [258]. These studies suggest that HuR binding to 5′UTR regulates the translation of target mRNA. Table 1.1 contains well-known mRNAs with their biological processes that regulated by HuR.

Table 1.1. Influence of HuR on target mRNA that involved in cellular processes.

Cellular process	HuR target mRNAs	HuR function	Reference
Angiogenesis	VEGF	↑ Stability	[259]
	HIF1α	↑ Translation	[258]
Fibrosis	TGF-β1	↑ Stability	[146, 251]
	ACTA/α-SMA	↑ Stability	[260]
	COL1	?	[260, 261]
	FN	?	[260, 261]
Immunity/Inflammation	PTGS2/COX2	↑ Stability	[233]
	cPLA2α	↑ Stability	[233]
	CXCL8/IL-8	↑ Stability	[248, 252]
	TNF-α	↑ Stability	[145, 238, 248]
	CCL2	↑ Stability	[145, 262]
	CCL11	↑ Stability	[263]
	IL4	↑ Stability	[264]
	IL13	↑ Stability	[265]
	CD83	localization	[256]
	TM	↓ Translation	[257]
Proteases/Invasion	MMP9	↑ Stability	[266]
	CTSS	↑ Stability	[156]
Myogenesis	Myogenin	↑ Stability	[140]
	MyoD	↑ Stability	[140]
	NPM	↓ Stability	[254]
Proliferation/Survival	Cyclin A2	↑ Stability	[139]
	Cyclin B1	↑ Stability	[139]
	Cyclin D1	↑ Stability	[244]
	Cyclin E1	↑ Stability	[245]
	P21	↑ Stability	[244]
	MYC	↓ Translation	[253]
	ProTα	↑ Translation	[255]

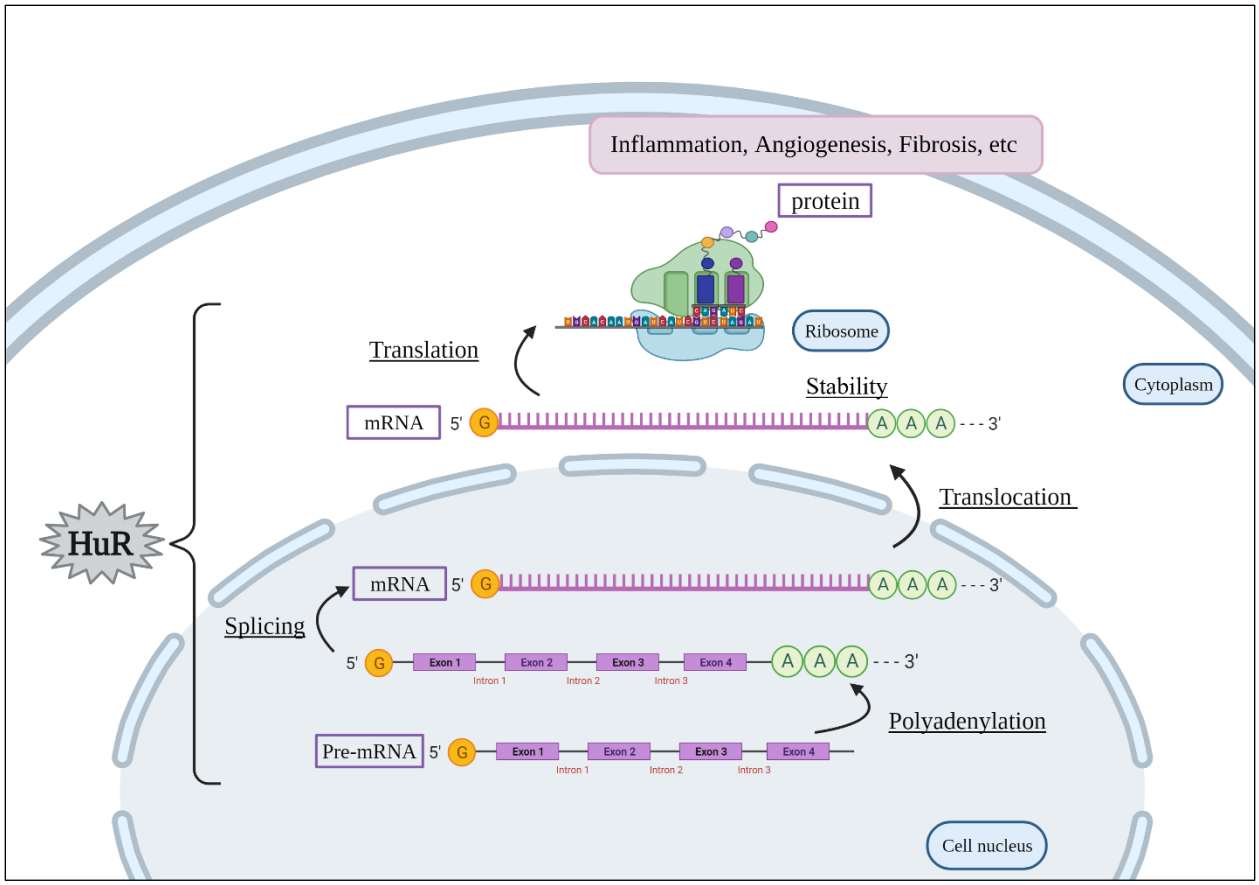

Figure 1.5. HuR function.

HuR participates in polyadenylation and splicing of target genes. HuR also controls the stability, localization, and translation of target mRNA (Table 1.1) encoding protein involved in many cellular processes as inflammation, angiogenesis, fibrosis, etc. Created with BioRender.com.

1.4.2.1. HuR function in lung diseases

HuR has been studied in the context of many diseases, particularly cancer, where HuR has bene shown to regulate the expression of mRNA that are involved in disease pathogenesis. In addition, the expression of HuR is higher in many types of cancer, including colon cancer, pancreatic cancer, breast cancer and ovarian cancer [249, 267-270]. HuR expression and its cytoplasmic localization are increased during cancer development and has been shown to be a prognostic factor in colon cancer and ovarian cancer [270-272]. Moreover, changes in the expression and the function of HuR may also occur in respiratory diseases including lung cancer,

asthma, pulmonary fibrosis, and COPD; these are all lung diseases with an environmental etiology. Here, the current state-of-knowledge of HuR in pulmonary disease will be highlighted.

1.4.2.1.1. Lung cancer

Globally, lung cancer remains as the most common cause of cancer death. In 2020, approximately 2.2 million people were diagnosed with lung cancer and there were 1.79 million fatalities, accounting for 18% of total cancer deaths [273]. CS accounts for about 80% of lung cancer cases [274]; other risk factors include radon and air pollution [274, 275]. Lung carcinogenesis is a series of complex molecular events involving abnormal DNA repair and genetic predisposition which cause aberrant cell proliferation along with evasion of apoptosis. Subsequently, normal cells transform into malignant cells that lead to cell invasion and metastasis [276]. HuR is implicated in the pathogenesis of lung cancer, and high levels of HuR in lung cancer tissue is associated with metastasis and poor survival [277]. HuR cytoplasmic localization is elevated in lung cancer tissue, which is associated with the high level of VEGF-C, a member of VEGF family. A causal relationship between HuR and VEGF-C was experimentally shown via knockdown of HuR in lung cancer cells, which reduced the expression of VEGF-C as well as COX-2 [278]. Owing to the association between HuR and lung cancer, it has been suggested that targeting HuR by siRNA-based nanoparticles could inhibit lung cancer cell proliferation, migration, and invasion [279]. Further support for the utility of targeting HuR as a therapy comes from the discovery of CMLD-2, a small molecule inhibitor that disrupts the interaction between HuR protein and ARE of target mRNAs; CMLD-2 exhibits antitumor activity in lung cancer cells [280].

1.4.2.1.2. Idiopathic pulmonary fibrosis (IPF)

IPF is a chronic progressive lung disease characterized by irreversible loss of lung function due to abnormal accumulation of fibrotic tissue [281, 282]. While the cause of IPF is not known, IPF risk factors including CS, metal/wood dust inhalation and genetic factors [281]. Mechanistically, IPF is driven by the accumulation of fibrotic tissue caused by the activation of alpha-actin (α-SMA)-expressing myofibroblasts and excessive extracellular matrix (ECM) protein production, including collagens (COL) and fibronectin (FN) [282]. The process of lung fibroblast differentiation to myofibroblasts occurs under the direction of cytokines and growth factors, particularly TGF-β [282]. We have recently shown that cytoplasmic HuR is increased in the lungs of IPF patients and mice exposed to bleomycin and thoracic radiation, two well characterized lung fibrosis models. We also showed the importance of HuR in driving myofibroblast differentiation, with HuR stabilizing *ACTA/α-SMA* mRNA to increase its protein expression in primary human lung fibroblasts exposed to TGF-β. HuR also increased ECM production, including COL1 and FN protein under fibrotic conditions [260, 261]. These data suggest that HuR controls myofibroblast differentiation and ECM production that is key to the development of fibrotic lung disease. Thus, HuR could be a promising therapeutic target for IPF, a disease with no current medications that can halt the fibrotic progression or improve patient survival.

1.4.2.1.3. Asthma

Asthma is a serious global health problem that affects more than 339 million individuals [283]. Asthma is a common respiratory disease characterized by reversible airflow obstruction and chronic inflammation of the airways [284-286] that is associated with airway hyperresponsiveness. This nature of asthmatic inflammation encompasses both the activation of airway and lung structural cells as well as the activation and/or recruitment of inflammatory cells including

eosinophils and Th2 lymphocytes. These cells release chemokines and cytokines such as CCL11 (eotaxin), IL-4, IL-5 and IL-13 that contribute to many pathogenic features of the disease (*e.g.,* mucus production, immunoglobulin E (IgE) production by B lymphocytes *etc.*,). [91, 287]. IgE activates mast cells by crosslinking of the high affinity receptor for IgE with allergens to produce mediators, such as histamine, which are capable of inducing bronchoconstriction, mucus secretion, microvascular permeability, and inflammation [285, 287]. Several studies have shown that HuR upregulates mRNA of cytokines and chemokines that are involved in asthma, such as CCL11, IL-4 and IL-13, in various cell types including airway epithelial cells, Th2 cells, and airway smooth muscle cell [263-265, 288]. Furthermore, airway epithelium-specific HuR deletion reduced allergen house dust mite (HDM)-induced lung inflammation, including eosinophil infiltration, and chemokines production, such as CCL11 [288]. These data emphasize the role of HuR at post-transcriptional level of gene expression which could be a promising therapeutic strategy to treat asthma.

1.4.2.1.4. COPD

Investigation of a role for HuR and COPD is still in its infancy. However, HuR expression is increased in the airway epithelium from smokers with and without COPD [289], suggesting that the increase in HuR expression is likely due to smoking and not COPD itself. This notion was further supported by a separate study showing that HuR expression is similar in the bronchial epithelium from both COPD subjects and smokers without COPD [167]. While these studies support that HuR may be dysregulated by smoking, there are a few studies exploring HuR in the context of COPD itself. Below, we summarize studies that have investigated HuR in mechanisms associated with the pathogenesis of this disease, thereby highlighting the potential of HuR driving this obstructive lung disease.

Several studies have shown that HuR upregulates mRNA of inflammatory mediators (Table 1.1) which are involved in COPD pathogenesis [15, 55-60], in various cell types including bronchial epithelial cells and macrophages exposed to different stimuli such as CS and TNF-α [145, 238, 248, 252, 263, 290, 291]. Thus, HuR may be involved in the early pathogenic events, such as inflammation, that are associated with the development of COPD. Furthermore, emphysema is another condition involved in COPD pathogenesis that characterized by the loss of lung structural cells which is mediated by increase in cell death and proteases activity [18, 19, 22, 177, 178]. Activated neutrophils and macrophages are sources of proteases, such as MMP-9 and cathepsins, all of which can contribute to the destruction of alveolar walls [64, 72, 74]. HuR can greatly impact the expression of proteases. For example, HuR binds to *MMP9* and *CTSS* mRNAs to stabilize their expression [156, 266, 292, 293]. Taken together, these data show that HuR regulate the expression of proteases, leading to the notion of their importance in COPD pathogenesis.

To sum, the post-transcriptional regulation of mRNA is an important part of gene expression. HuR is one of the post-transcriptional regulators of target mRNA expression. HuR abundance and its posttranslational modifications affect HuR binding to target mRNA, all effectively impacting HuR function. HuR associates with target mRNA and controls its stability, translation and/or nucleocytoplasmic translocation (Figure 1.5). These target mRNA (Table 1.1) encode proteins involved in inflammation [243]. However, nothing is known about the post-transcriptional regulation of mRNA by HuR in the pathogenic events of COPD, including inflammation, and future work should address these mechanisms. Thus, elucidation of the mechanisms that regulated by HuR could lead to the development of therapeutic strategies for COPD.

1.5. PROJECT INTRODUCTION

HuR targets mRNA that encode proteins involved in different pathological processes [243]. It is well-studied that in response to CS, the expression of inflammatory mediators, as COX-2 and IL-8, are upregulated [15, 16]. Persistent exposure to CS induces inflammation in different lung cells including fibroblasts [14-16]. This inflammation leads to obstruction of the small airways and destruction of lung parenchyma, which involved in the development of COPD [55]. CS is a risk factor for numerous diseases with no cure and limited therapeutic options, including COPD and COVID-19 [25, 294, 295]. Indeed, COPD patients may have an increased risk for severe illness of COVID-19 because of the higher expression of ACE2, the entry receptor for SARS-CoV-2 [77]. Further, there is equivocal evidence that other inhalational toxicants may be involved in the development of COPD; this includes cannabis smoke [296]. To our knowledge, the involvement of HuR in COPD pathogenesis, including the association with COVID-19, and in response to cigarette and cannabis smoke, are currently unknown. Therefore, we hypothesis that HuR controls the pathological features associated with cigarette smoke exposure that may be involved in the development COPD.

CHAPTER II

2. Angiotensin-converting enzyme 2 expression in COPD and IPF fibroblasts: the forgotten cell in COVID-19

Noof Aloufi[1,2], Hussein Traboulsi[1], Jun Ding[1,5], Gregory J. Fonseca[1,3], Parameswaran Nair[6], Steven K. Huang[7], Sabah N. A. Hussein[1,2], David H. Eidelman[3] and Carolyn J. Baglole[1,2,3,4]

[1]Research Institute of the McGill University Health Centre, Departments of [2]Pathology, [3]Medicine, [4]Pharmacology and Therapeutics, McGill University; [5]Computational Biology Department, Carnegie Mellon University; [6]Department of Medicine, McMaster University & St Joseph's Healthcare, Hamilton, Ontario, Canada; [7]Department of Internal Medicine, University of Michigan USA;

Correspondence and requests for materials should be addressed to:
*Carolyn J. Baglole
1001 Decarie Blvd (EM22248)
Montreal, Quebec H4A3J1
Telephone: (514) 934-1934 ext. 76109
E-mail: Carolyn.baglole@mcgill.ca

(This research was originally published in **American journal of physiology. Lung cellular and molecular physiology** "Aloufi, N., Traboulsi, H., Ding, J., Fonseca, G. J., Nair, P., Huang, S. K., Hussain, S., Eidelman, D. H., & Baglole, C. J. (2021). Angiotensin-converting enzyme 2 expression in COPD and IPF fibroblasts: the forgotten cell in COVID-19. *American Journal of Physiology. Lung Cellular and Molecular Physiology*, 320(1), L152–L157 [2].")

Keywords: ACE2; SARS-Cov-2; fibroblast; COVID-19; pulmonary fibrosis; chronic obstructive pulmonary disease

Acknowledgement: This work was supported by the Canada Foundation for Innovation (CFI) and the Canadian Institutes for Health Research (CIHR). C.J.B. was supported by a salary award from the Fonds de recherche du Quebec-Sante (FRQ-S). N.A was supported by a scholarship from Taibah University, Saudi Arabia.

2.1. ABSTRACT

The COVID-19 pandemic is associated with severe pneumonia and acute respiratory distress syndrome leading to death in susceptible individuals. For those who recover, post-COVID-19 complications may include development of pulmonary fibrosis. Factors contributing to disease severity or development of complications is not known. Using computational analysis with experimental data, we report that IPF and COPD-derived lung fibroblasts express higher levels of ACE2, the receptor for SARS-CoV-2 entry and part of the renin-angiotensin system that is anti-fibrotic and anti-inflammatory. In preclinical models, we found that chronic exposure to cigarette smoke, a risk factor for both COPD and IPF and potentially for SARS-CoV-2 infection, significantly increased pulmonary ACE2 protein expression. Further studies are needed to understand the functional implications of ACE2 on lung fibroblasts, a cell type that thus far as received relatively little attention in the context of COVID-19.

2.2. INTRODUCTION

In December 2019, a newly-identified novel coronavirus called SARS-CoV-2 spread rapidly through the world, causing an outbreak of coronavirus disease-2019 (COVID-19) (28). COVID-19 is associated with a myriad of symptoms ranging from asymptomatic to severe pneumonia and acute respiratory distress syndrome leading to death (16). There are at least 20 million COVID-19 cases worldwide and hundreds of thousands of deaths. SARS-CoV-2 infects humans by binding to the human angiotensin-converting enzyme 2 (ACE2). Pulmonary ACE2 is concentrated in type II alveolar cells and bronchial and tracheal epithelial cells, which serve as an entry point for viral infection (12). Changes in the expression of ACE2 may contribute to susceptibility of SARS-Cov-2. Environmental factors such as smoking are linked to an increase in ACE2 expression. Although controversial, high ACE2 expression may explain the risk of severe COVID-19 in certain populations, including those with underlying health conditions linked to smoking, such as chronic obstructive pulmonary disease (COPD) (23, 24). Even among COVID-19 patients who recover, there is the potential for post-COVID-19 complications, particularly the development of pulmonary fibrosis (7, 11).

Although most studies have focused on epithelial expression, ACE2 in other cell types within the lung may also be important. Fibroblasts have been shown to harbor viral particles from SARS-CoV-2 in patients with COVID-19 (10). It is well-accepted that fibroblasts provide structure to the lungs and other organs by synthesizing extracellular matrix (ECM) proteins, and are increasingly recognized to play key roles in innate immunity (17). In pulmonary fibrosis, fibroblasts are the key cell type involved in excessive ECM deposition that stiffens the lungs. In COPD, loss of lung fibroblast repair function may contribute to the emphysema component of this

disease and cause small airway fibrosis that limits airflow (22). When we also consider that ACE2 is part of the renin-angiotensin-system (RAS) branch that is anti-fibrotic and anti-inflammatory (18), knowledge regarding the expression of ACE2 in lung fibroblasts is highly relevant. Here, we sought to determine the expression of ACE on COPD- and IPF-derived lung fibroblasts and provide direct evidence on whether cigarette smoke changes pulmonary ACE levels.

2.3. METHODS

Computational analysis of single cell ACE2 expression

The single-cell data used for the analyses was downloaded from https://advances.sciencemag.org/content/6/28/eaba1983, which profiled 32 IPF lungs, 18 COPD lungs and 28 control donor lungs (1). The dataset was further processed using the scanpy (25) and scdiff (9) software. Cells expressing less than 200 genes or with more than 40% of mitochondrial reads were filtered. The expression was transformed into the log space (log1p). After the processing, we got 312922 cells in total, including 147167 IPF cells, 69452 COPD cells, and 96303 Control cells.

Derivation and culture of lung fibroblasts

For COPD, fibroblasts were derived from lung tissues of subjects undergoing lung resection surgery at McMaster University as previously described (20). Patient characteristics are in (20) and a subset of these cells were utilized in this study which included never-smokers (Control; Male [M]/Female [F] = 1/3; age 71 ± 7 years) as well as current smokers with (COPD; M/F = 2/2; age 61 ± 5.4 years) and without COPD (Smoker; M/F = 1/3; age 61.3 ± 4.8 years). For IPF fibroblasts, Control (M/F = 2/2; age 35 ± 11.05 years) and IPF (3M [1 unknown]); age 58.7 ± 6.8 years)-derived primary normal lung fibroblasts were cultured from the outgrowths of histologically normal regions of lungs that were provided for organ donation but were later deemed unsuitable for transplantation (Gift of Life, Michigan). Cells were isolated and cultured as previously described (13).

Western blot

Total cellular protein was extracted using RIPA lysis buffer (Thermo Scientific, Rockford) and Protease Inhibitor Cocktail (PIC, Roche, US). Ten to twenty μg of protein lysate were subjected to 10% SDS-PAGE gels and transferred onto Immuno-blot PVDF membranes (Bio-Rad Laboratories, Hercules, CA). Then, membrane was blocked for one hour at room temperature in blocking solution (5% w/v of non-fat dry milk in 1x PBS/0.1% Tween-20). Antibodies against ACE2 (SN0754; 1:500-1:1000; Invitrogen, CA), actin (1:10000; Millipore, MA) and tubulin (1:50000; Sigma, CA) and the secondary antibodies goat anti-rabbit IgG HRP-linked (1:10000, Cell Signaling Technologies, CA) and HRP-conjugated horse anti-mouse IgG (1:10000, Cell Signaling) were used. Protein bands were visualized using a ChemiDoc™ MP Imaging System (Bio-Rad). Densitometric analysis was performed using Image Lab™ Software Version 5 (Bio-Rad). Protein expression was normalized to tubulin or actin and the data presented as the fold-change. All antibodies detected the target protein at the predicted molecular weight. As an additional control, ACE2 siRNA was used to reduce ACE2 protein levels (data not shown).

Preparation of Cigarette Smoke Extract (CSE)

Research grade cigarettes (3R4F) with a filter were obtained from the Kentucky Tobacco Research Council (Lexington, KT) and CSE was generated as previously described (2-5). Briefly, smoke from one cigarette was bubbled into 10 ml of serum free-media and subsequently passed through a 0.45 μm sterile filter (25-mm Acrodisc; Pall Corp., Ann Arbor, MI). An optical density of 0.65 (320 nm) was considered to represent 100% CSE. This CSE preparation was diluted to 2% in serum-free media.

Preclinical Cigarette Smoke exposure

Mice (Jackson Laboratory; C57/BL6; age 8-12 weeks; male mice) were exposed to cigarette smoke using a whole-body exposure system as we have described (InExpose; SCIREQ Inc., Montreal, Canada) (8, 21, 26). Briefly, mice were exposed to research cigarettes (3R4F; University of Kentucky, Lexington, KY) for two, 1-hr smoke exposures per day for 3 days or for 5 days/week for 2 or 4 weeks. All animal procedures were approved by the McGill University Animal Care Committee (Protocol Number 5933) and were carried out in accordance with the Canadian Council on Animal Care. Lung tissue was collected for protein/western blot analysis as described above.

Statistical Analysis

Statistical analysis was performed using Prism 6-1 (La Jolla, CA). Statistical differences between group mean values were determined by ANOVA followed by a Newman-Keuls multiple comparisons test. A t-test was used to determine significance between two groups. P-value < 0.05 was considered significant.

2.4. RESULTS

To first address the extent to which *ACE2* gene expression differed between COPD and IPF in pulmonary cell populations, we used single-cell data profiled from 32 idiopathic pulmonary fibrosis (IPF) lungs, 18 COPD lungs and 28 control lungs (1). The dataset was further processed using scanpy and scdiff software (9, 25) and the expression was transformed into the log space (log1p). *ACE2* expressions in *ACE2*+ COPD cells (mean value=1.08) are significantly higher than the *ACE2* expressions in *ACE2*+ IPF cells (mean value=0.85) as well as Control cells (mean value=0.96) with one-sided Mann-Whitney U test (p-values 5.16e-49 and 3.53e-11, respectively) (Figure 2.1A). We also found that *ACE2*+ cells account for 2.94% (4321/147167) of the IPF cells, 2.40% (1667/69452) of the COPD cells, and 2.30% (2211/96393) of Control cells (Figure 2.1B). We further examined the percentage of *ACE2*+ cells amongst the different cell types in the lungs (1). *ACE2*+ cells are mostly enriched in lung epithelial cells (goblet cells 6.6%; basal cells 5.6%). Fibroblasts (4.0%) are also enriched with *ACE2*, ranking 9th of all 38 cell types (Figure 2.1C).

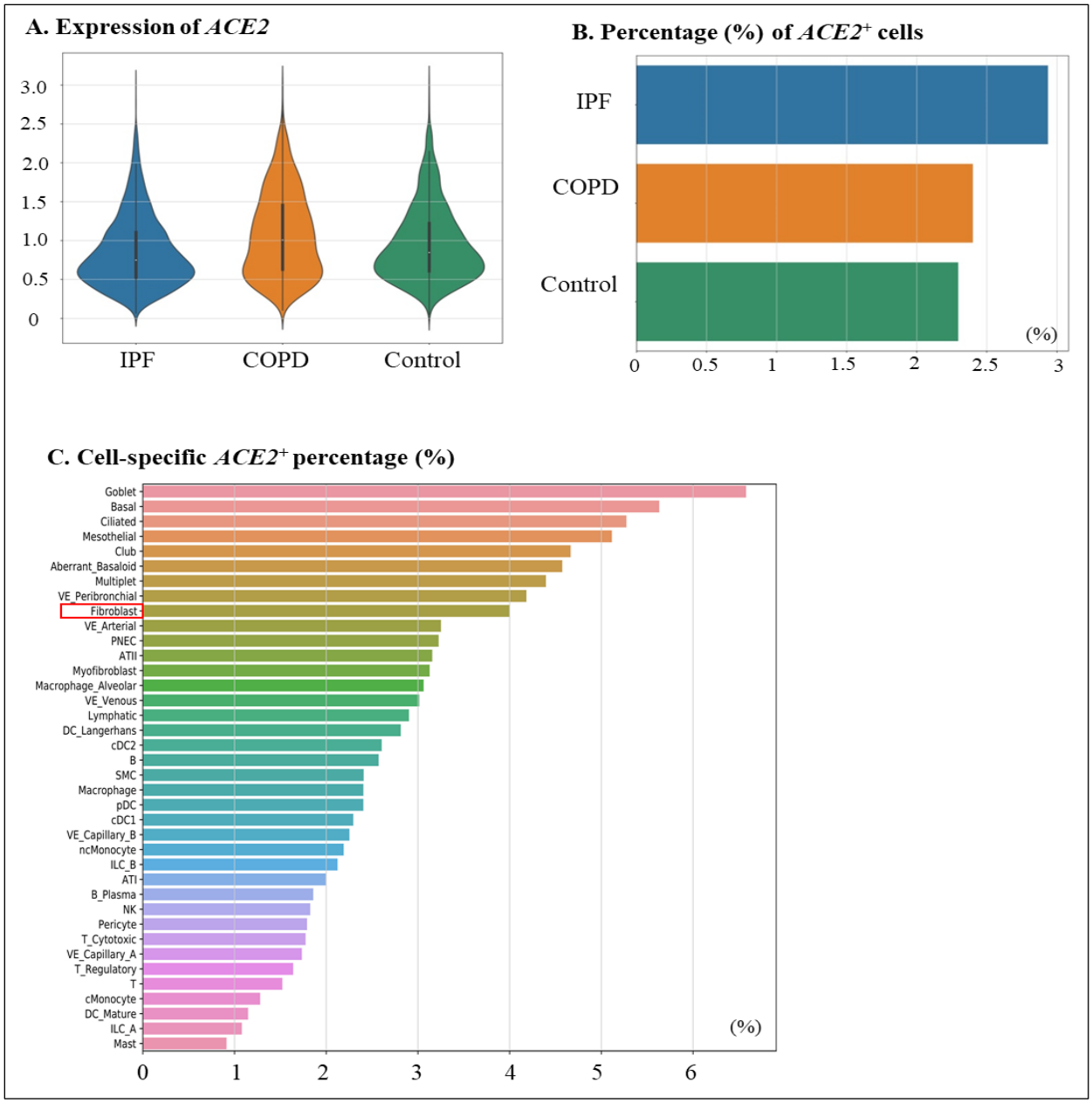

Figure 2.1. Cell-specific *ACE2* expression in COPD and IPF lungs.

A. Expression of *ACE2*: Data analysis of scRNA-seq of COPD, IPF and control lungs revealed that there were more ACE2+ cells in COPD. **B.** Percentage (%) of *ACE2*+ cells: *ACE2*+ cells accounted for 2.94% of the IPF cells, 2.40% of the COPD cells, and 2.30% of Control cells. **C.** Cell-specific *ACE2*+ percentage (%): *ACE2*+ cells are mostly enriched in lung epithelial cells (goblet cells 6.6%; basal cells 5.6%). Fibroblasts (4.0%) are also enriched with *ACE2*, ranking 9th of all 38 cell types. Results were analysed with a one-sided Mann-Whitney U test. *ACE2*, angiotensin-converting enzyme 2; COPD, chronic obstructive pulmonary disease; IPF, idiopathic pulmonary fibrosis.

Next, we examined ACE2 protein expression by western blot in COPD and IPF fibroblasts. COPD fibroblasts were derived as described previously (20) and included never-smokers and smokers with and without COPD. In COPD-derived fibroblasts, ACE2 protein was significantly higher compared to control (never-smokers) fibroblasts (Figure 2.2A and 2.2B). There was a trend towards increase ACE2 in smoker-derived cells, but this did not reach statistical significance. In IPF lung fibroblasts, protein levels of ACE2 were also significantly increased compared to control lung fibroblasts (Figure 2.2C and 2.2D).

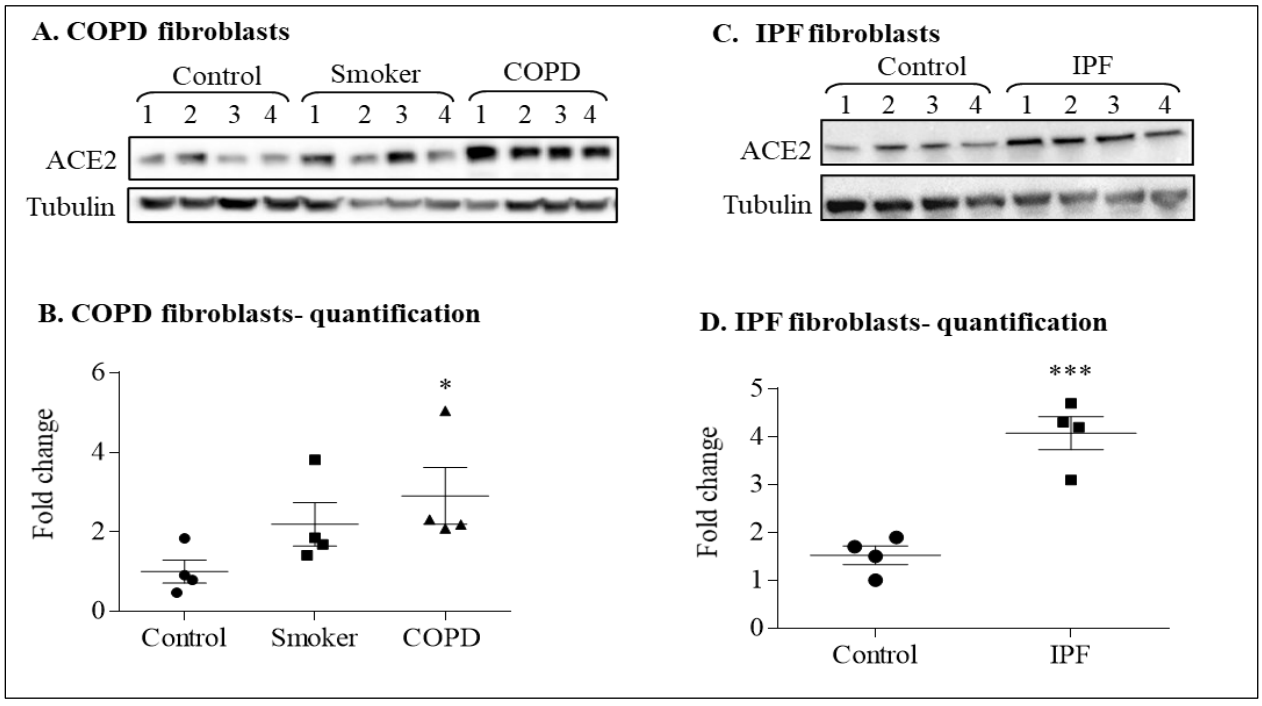

Figure 2.2. ACE2 protein is higher in COPD- and IPF-derived lung fibroblasts.

A. and **B.** COPD fibroblasts: Lung fibroblasts derived from COPD subjects had significantly higher ACE2 protein expression compared to lung fibroblasts from never-smokers (*$p<0.05$). There was a trend towards higher ACE2 in smoker-derived fibroblasts. Smoker and COPD-derived lung fibroblasts were from current smokers. Data were analyzed by a one-way ANOVA followed by Dunn's test. **C.** and **D.** IPF fibroblasts: Lung fibroblasts derived from IPF subjects had significantly higher ACE2 protein compared to control cells. Data were analyzed by a 2-tailed t-test. Results are expressed as the mean ± SEM (***$p< 0.001$ compared to control cells) N = 4/group. ACE2, angiotensin-converting enzyme 2; COPD, chronic obstructive pulmonary disease; IPF, idiopathic pulmonary fibrosis.

Cigarette smoke remains a prevalent environmental toxicant and leading risk factor for both COPD and pulmonary fibrosis. This led us to wonder if exposure to cigarette smoke could directly increase ACE2 protein expression, as suggested by recent data from smoker lungs (15). First, we evaluated whether ACE2 was affected by exposure of lung fibroblasts to CSE, an in vitro surrogate for cigarette smoke (19). For these studies, lung fibroblasts from a never-smoker were exposed to 2% CSE for up to 48 hours; this concentration of CSE induces an overall inflammatory and oxidative stress response in lung structural cells (3, 4). However, there was no difference in ACE2 protein in response to CSE (Figure 2.3A). We next used our preclinical model of cigarette smoke exposure to mimic acute and chronic exposure scenarios (8, 21). In lungs from mice exposed to a 3-day (acute) cigarette smoke, ACE2 protein expression was not significantly altered (Figure 2.3B and 2.3C). However, ACE2 protein expression was significantly increased in lungs from mice chronically exposed to cigarette smoke (Figure 2.3D and 2.3E). Exposure to cigarette smoke for 4 weeks significantly increased ACE2 protein compared to air-exposed controls as well as those exposed for 2 weeks (normalized to actin). Thus, chronic exposure to cigarette smoke is necessary to increase ACE2 expression in the lungs.

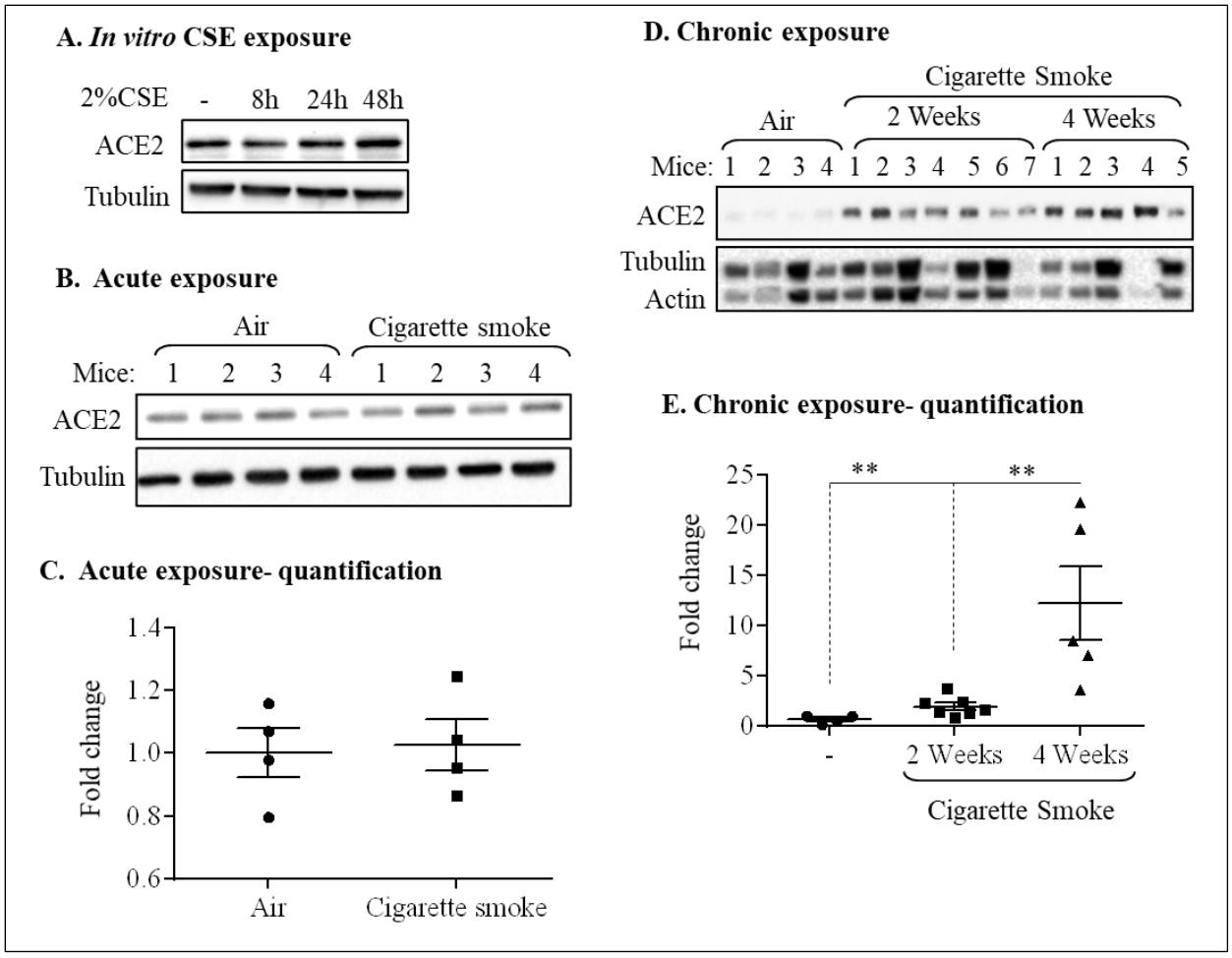

Figure 2.3. Chronic cigarette smoke exposure increases pulmonary ACE2 protein expression.

A. in vitro CSE exposure: Primary human lung fibroblasts from a never smoker were exposed to 2% CSE for 8-48 hours and ACE2 protein evaluated by western blot; normalization was done to tubulin. There was no change in total ACE2 expression upon exposure to CSE. **B.** and **C.** Acute exposure: Mice were exposed to cigarette smoke using the SCIREQ inExpose whole body exposure system twice per days for 3 days. Control mice were exposed to room air. Mice were sacrificed and the lungs processed for western blot analysis. There was no change in the total levels of ACE2 in the CS-exposed mice compared to the control mice. Number of mice in each group is indicated Data were analyzed by a 2-tailed t-test. **D.** and **E.** Chronic exposure: Mice were exposed to cigarette smoke for 5 days/week for 2 or 4 weeks and the lungs processed for western blot; tubulin and actin were used as loading controls; data were normalized using actin. Control mice were exposed to only room air. There was a noticeable increase in ACE2 protein expression after 2 weeks of smoke exposure; this increase in ACE2 reached statistical significance by 4 weeks of cigarette smoke exposure compared to both air control mice (**$p<0.01$) as well as mice exposed to CS for 2 weeks (**$p< 0.05$). Number of mice in each group is indicated. Data were analyzed by a one- way ANOVA followed by Holm-Sidak post hoc test. ACE2, angiotensin-converting enzyme 2; CSE, cigarette smoke extract.

2.5. DISCUSSION

COVID-19 is a pandemic disease and people with pre-existing conditions may be at a higher risk. Potential post-COVID-19 complications include the development of pulmonary fibrosis, which may be an emerging health threat for the millions who recover. Although epithelial cells are considered the primary cells for SARS-CoV-2 infection, lung fibroblasts also express ACE2 and may be an important cell type responsible for the persistence of infection, disease severity and recovery from COVID-19. Lung fibroblasts not only respond directly to inciting agents like cigarette smoke, but also to cues provided by adjacent cells, including leukocytes and epithelial cells. In the context of SARS-Cov-2 infection, their release of pro-fibrotic/inflammatory mediators such as TGF-β could drive myofibroblast differentiation and consequent ECM deposition. Characterization of ACE2 in lung fibroblasts is also particularly relevant as activation of the ACE2-Ang-(1–7)-Mas axis protects against fibrosis (27) and smoke-induced lung inflammation (14).

Our findings are also the first direct evidence that chronic (but not acute) cigarette smoke exposure increases ACE2. Although a limitation of this study is that we did not determine the specific cell type(s) in which ACE2 expression increased after smoke exposure, we would anticipate increased levels in multiple cell types, including epithelial cells and fibroblasts. Part of the reason for this is that our data also show there is an increase in ACE2 expression in COPD- and IPF-derived lung fibroblasts, a finding that may initially seem contradictory given the protective role of ACE2. It is possible that this increase reflects a compensatory response to the disease phenotype and/or the inciting agent (*i.e.*, smoke). Whether ACE2 in fibroblasts reduces features of inflammation (*i.e.*, cytokine expression) and fibrosis (*e.g.,* ECM protein expression) in

the context of COVID-19 is not known. It could also be that there is dysregulation of other components of the ACE2-Ang-(1–7)-Mas axis not examined in this study, particularly Mas receptor which is down-regulated by TGF-β in fibroblasts (6). One might speculate that although ACE2 could have anti-fibrotic properties, lower levels of the Mas receptor may abrogate these protective effects, with increased ACE2 not only augmenting susceptibility to SARS-CoV-2 infection, but also post-COVID complications.

There were some additional limitations of this study, including the evaluation of a relatively small number of lung fibroblasts and that the cross-sectional nature of these data does not allow us to show causation. Nevertheless, our work is the first to evaluate ACE2 expression in human lung fibroblasts, a cell type that has been overlooked in COVID-19 but whose dysfunction may contribute significantly to disease burden. More research is needed to understand the functional significance of higher ACE2 in lung fibroblasts and the potential consequence towards COVID-19 and its clinical outcomes.

Disclosures

No conflicts of interest, financial or otherwise, are declared by the authors.

Author contributions

S.N.A.H. and C.J.B. conceived and designed research; N.A. and H.T. performed experiments; N.A., H.T., and J.D. analyzed data; H.T., J.D., G.J.F., S.K.H., D.H.E., and C.J.B. interpreted results of experiments; J.D. and C.J.B. prepared figures; N.A. and C.J.B. drafted manuscript; N.A., H.T., G.J.F., P.N., S.K.H., S.N.A.H., D.H.E., and C.J.B. edited and revised manuscript; N.A., H.T., J.D., G.J.F., P.N., S.K.H., S.N.A.H., D.H.E., and C.J.B. approved final version of manuscript.

2.6. REFERENCES

1. Adams TS, Schupp JC, Poli S, Ayaub EA, Neumark N, Ahangari F, Chu SG, Raby BA, DeIuliis G, Januszyk M, Duan Q, Arnett HA, Siddiqui A, Washko GR, Homer R, Yan X, Rosas IO, and Kaminski N. Single-cell RNA-seq reveals ectopic and aberrant lung-resident cell populations in idiopathic pulmonary fibrosis. Science Advances 6: eaba1983, 2020.

2. Baglole CJ, Bushinsky SM, Garcia TM, Kode A, Rahman I, Sime PJ, and Phipps RP. Differential induction of apoptosis by cigarette smoke extract in primary human lung fibroblast strains: implications for emphysema. Am J Physiol Lung Cell Mol Physiol 291: L19-29, 2006.

3. Baglole CJ, Maggirwar SB, Gasiewicz TA, Thatcher TH, Phipps RP, and Sime PJ. The aryl hydrocarbon receptor attenuates tobacco smoke-induced cyclooxygenase-2 and prostaglandin production in lung fibroblasts through regulation of the NF-kappaB family member RelB. J Biol Chem 283: 28944-28957, 2008.

4. Baglole CJ, Sime PJ, and Phipps RP. Cigarette smoke-induced expression of heme oxygenase-1 in human lung fibroblasts is regulated by intracellular glutathione. Am J Physiol Lung Cell Mol Physiol 295: L624-636, 2008.

5. Carp H, and Janoff A. Possible mechanisms of emphysema in smokers. In vitro suppression of serum elastase-inhibitory capacity by fresh cigarette smoke and its prevention by antioxidants. Am Rev Respir Dis 118: 617-621, 1978.

6. Cofre C, Acuna MJ, Contreras O, Morales MG, Riquelme C, Cabello-Verrugio C, and Brandan E. Transforming growth factor type-beta inhibits Mas receptor expression in fibroblasts but not in myoblasts or differentiated myotubes; Relevance to fibrosis associated to muscular dystrophies. Biofactors 41: 111-120, 2015.

7. Dalan R, Bornstein SR, El-Armouche A, Rodionov RN, Markov A, Wielockx B, Beuschlein F, and Boehm BO. The ACE-2 in COVID-19: Foe or Friend? Horm Metab Res 52: 257-263, 2020.

8. de Souza AR, Zago M, Eidelman DH, Hamid Q, and Baglole CJ. Aryl hydrocarbon receptor (AhR) attenuation of subchronic cigarette smoke-induced pulmonary neutrophilia is associated with retention of nuclear RelB and suppression of intercellular adhesion molecule-1 (ICAM-1). Toxicol Sci 140: 204-223, 2014.

9. Ding J, Aronow BJ, Kaminski N, Kitzmiller J, Whitsett JA, and Bar-Joseph Z. Reconstructing differentiation networks and their regulation from time series single-cell expression data. Genome Research 28: 383-395, 2018.

10. Facchetti F, Bugatti M, Drera E, Tripodo C, Sartori E, Cancila V, Papaccio M, Castellani R, Casola S, Boniotti MB, Cavadini P, and Lavazza A. SARS-CoV2 vertical transmission with adverse effects on the newborn revealed through integrated immunohistochemical, electron microscopy and molecular analyses of Placenta. EBioMedicine 59: 102951, 2020.

11. Grillo F, Barisione E, Ball L, Mastracci L, and Fiocca R. Lung fibrosis: an undervalued finding in COVID-19 pathological series. Lancet Infect Dis 2020.

12. Hamming I, Timens W, Bulthuis ML, Lely AT, Navis G, and van Goor H. Tissue distribution of ACE2 protein, the functional receptor for SARS coronavirus. A first step in understanding SARS pathogenesis. J Pathol 203: 631-637, 2004.

13. Huang SK, Scruggs AM, McEachin RC, White ES, and Peters-Golden M. Lung fibroblasts from patients with idiopathic pulmonary fibrosis exhibit genome-wide differences in DNA methylation compared to fibroblasts from nonfibrotic lung. PLoS One 9: e107055, 2014.

14. Hung YH, Hsieh WY, Hsieh JS, Liu FC, Tsai CH, Lu LC, Huang CY, Wu CL, and Lin CS. Alternative Roles of STAT3 and MAPK Signaling Pathways in the MMPs Activation and Progression of Lung Injury Induced by Cigarette Smoke Exposure in ACE2 Knockout Mice. Int J Biol Sci 12: 454-465, 2016.

15. Jacobs M, Van Eeckhoutte HP, Wijnant SRA, Janssens W, Joos GF, Brusselle GG, and Bracke KR. Increased expression of ACE2, the SARS-CoV-2 entry receptor, in alveolar and bronchial epithelium of smokers and COPD subjects. Eur Respir J 2020.

16. Kai H, and Kai M. Interactions of coronaviruses with ACE2, angiotensin II, and RAS inhibitors-lessons from available evidence and insights into COVID-19. Hypertens Res 2020.

17. Krausgruber T, Fortelny N, Fife-Gernedl V, Senekowitsch M, Schuster LC, Lercher A, Nemc A, Schmidl C, Rendeiro AF, Bergthaler A, and Bock C. Structural cells are key regulators of organ-specific immune responses. Nature 583: 296-302, 2020.

18. Lumbers ER, Delforce SJ, Pringle KG, and Smith GR. The Lung, the Heart, the Novel Coronavirus, and the Renin-Angiotensin System; The Need for Clinical Trials. Front Med (Lausanne) 7: 248, 2020.

19. Sarill M, Zago M, Sheridan JA, Nair P, Matthews J, Gomez A, Roussel L, Rousseau S, Hamid Q, Eidelman DH, and Baglole CJ. The aryl hydrocarbon receptor suppresses cigarette-smoke-induced oxidative stress in association with dioxin response element (DRE)-independent regulation of sulfiredoxin 1. Free Radic Biol Med 89: 342-357, 2015.

20. Sheridan JA, Zago M, Nair P, Li PZ, Bourbeau J, Tan WC, Hamid Q, Eidelman DH, Benedetti AL, and Baglole CJ. Decreased expression of the NF-kappaB family member RelB in lung fibroblasts from Smokers with and without COPD potentiates cigarette smoke-induced COX-2 expression. Respir Res 16: 54, 2015.

21. Thatcher TH, Maggirwar SB, Baglole CJ, Lakatos HF, Gasiewicz TA, Phipps RP, and Sime PJ. Aryl hydrocarbon receptor-deficient mice develop heightened inflammatory responses to cigarette smoke and endotoxin associated with rapid loss of the nuclear factor-kappaB component RelB. Am J Pathol 170: 855-864, 2007.

22. Togo S, Holz O, Liu X, Sugiura H, Kamio K, Wang X, Kawasaki S, Ahn Y, Fredriksson K, Skold CM, Mueller KC, Branscheid D, Welker L, Watz H, Magnussen H, and Rennard SI. Lung fibroblast repair functions in patients with chronic obstructive pulmonary disease are altered by multiple mechanisms. Am J Respir Crit Care Med 178: 248-260, 2008.

23. Vardavas CI, and Nikitara K. COVID-19 and smoking: A systematic review of the evidence. Tob Induc Dis 18: 20, 2020.

24. Wang D, Hu B, Hu C, Zhu F, Liu X, Zhang J, Wang B, Xiang H, Cheng Z, Xiong Y, Zhao Y, Li Y, Wang X, and Peng Z. Clinical Characteristics of 138 Hospitalized Patients With 2019 Novel Coronavirus-Infected Pneumonia in Wuhan, China. JAMA 2020.

25. Wolf FA, Angerer P, and Theis FJ. SCANPY: large-scale single-cell gene expression data analysis. Genome Biology 19: 15, 2018.

26. Zago M, Sheridan JA, Nair P, Rico de Souza A, Gallouzi IE, Rousseau S, Di Marco S, Hamid Q, Eidelman DH, and Baglole CJ. Aryl Hydrocarbon Receptor-Dependent Retention of Nuclear HuR Suppresses Cigarette Smoke-Induced Cyclooxygenase-2 Expression Independent of DNA-Binding. PLoS One 8: e74953, 2013.

27. Zhang BN, Xu H, Gao XM, Zhang GZ, Zhang X, and Yang F. Protective Effect of Angiotensin (1-7) on Silicotic Fibrosis in Rats. Biomed Environ Sci 32: 419-426, 2019.

28. Zhou P, Yang XL, Wang XG, Hu B, Zhang L, Zhang W, Si HR, Zhu Y, Li B, Huang CL, Chen HD, Chen J, Luo Y, Guo H, Jiang RD, Liu MQ, Chen Y, Shen XR, Wang X, Zheng XS, Zhao K, Chen QJ, Deng F, Liu LL, Yan B, Zhan FX, Wang YY, Xiao GF, and Shi ZL. A pneumonia outbreak associated with a new coronavirus of probable bat origin. Nature 579: 270-273, 2020.

PREFACE: CHAPTER III

In Chapter II, we demonstrated that the expression of ACE2, the receptor for SARS-CoV-2, is elevated in lung fibroblasts from COPD patients. Moreover, we found that chronic CS exposure significantly increases pulmonary ACE2 protein. However, mechanisms controlling ACE2 expression is poorly understood, a limitation in our understanding that precludes the development of drugs targeting this protein.

Therefore, in Chapter III, we investigated the involvement of HuR in regulating ACE2 expression. ACE2 expression may be controlled at multiple levels (*e.g.,* transcriptional, post-transcriptional and/or translational) [297]. However, there is no information on HuR involvement in the regulation of ACE2. Thus, in this next study, we evaluated HuR expression in lungs from COPD and COVID-19 subjects and mechanistically interrogated whether HuR controls ACE2 expression in response to CS.

CHAPTER III

3. Role of human antigen R (HuR) in the regulation of pulmonary ACE2 expression

Noof Aloufi[1,2,3,4], Zahraa Haidar[1,2,5], Jun Ding[1,2,5], Parameswaran Nair[10], Andrea Benedetti[2,5,7], David H. Eidelman[1,2,5], Imed Gallouzi[8,9], Sergio di Marco[8], Sabah N. Hussain[1,2,3,5] and Carolyn J. Baglole[1,2,3,5,6*]

[1]Meakins-Christie Laboratories and [2]Translational Research in Respiratory Diseases Program at the Research Institute of the McGill University Health Centre; Department of [3]Pathology, McGill University; [4]Department of Medical Laboratory Technology, Taibah University, Saudi Arabia; Departments of [5]Medicine and [6]Pharmacology and Therapeutics, [7]Epidemiology, Biostatistics & Occupational Health and [8]Biochemistry, McGill University; [9] Smart-Health Initiative and Biological and Environmental Science and Engineering (BESE) Division, King Abdullah University of Science and Technology (KAUST), Thuwal, Saudi Arabia; [10]Department of Medicine, McMaster University & St Joseph's Healthcare, Hamilton, Ontario, Canada.

Correspondence and requests for materials should be addressed to:
*Carolyn J. Baglole
1001 Decarie Blvd (EM22248)
Montreal, Quebec H4A3J1
Telephone: (514) 934-1934 ext. 76109
E-mail: Carolyn.baglole@mcgill.ca

(This research was originally published in **Cells, MDPI** Aloufi, N., Haidar, Z., Ding, J., Nair, P., Benedetti, A., Eidelman, D. H., Gallouzi, I. E., Di Marco, S., Hussain, S. N., & Baglole, C. J. (2021). Role of Human Antigen R (HuR) in the Regulation of Pulmonary ACE2 Expression. *Cells*, 11(1), 22 [3].)

Keywords: HuR; ACE2; fibroblast; COVID-19; chronic obstructive pulmonary disease; ELAVL1.

Acknowledgement: This work was supported by the CIHR (168836 and 162273) and NSERC. CJB was supported by a salary award from the Fonds de recherche du Quebec-Sante (FRQ-S). N.A was supported by a scholarship from Taibah University, Saudi Arabia. I.G. was supported by a Canadian Institutes of Health Research Operating Grant (MOP-142399). The multiplex immunohistochemistry (mIHC) images were acquired through the Histopathology Platform of the RI-MUHC.

3.1. ABSTRACT

Patients with COPD may be at an increased risk for severe illness from COVID-19 because of ACE2 upregulation, the entry receptor for SARS-CoV-2. Chronic exposure to cigarette smoke, the main risk factor for COPD, increases pulmonary ACE2. How ACE2 expression is controlled is not known but may involve HuR, an RNA binding protein that increases protein expression by stabilizing mRNA. We hypothesized that HuR would increase ACE2 protein expression. We analyzed scRNA-seq data to profile *ELAVL1* expression in distinct respiratory cell populations in COVID-19 and COPD patients. HuR expression and cellular localization was evaluated in COPD lung tissue by multiplex immunohistochemistry and in human lung cells by imaging flow cytometry. The regulation of ACE2 expression was evaluated using siRNA-mediated knockdown of HuR. There is a significant positive correlation between *ELAVL1* and *ACE2* in COPD cells. HuR cytoplasmic localization is higher in smoker and COPD lung tissue; there were also higher levels of cleaved HuR (CP-1). HuR binds to ACE2 mRNA but knockdown of HuR does not change ACE2 protein levels in primary human lung fibroblasts (HLFs). Our work is the first to investigate the association between ACE2 and HuR. Further investigation is needed to understand the mechanistic underpinning behind the regulation of ACE2 expression.

3.2. INTRODUCTION

Chronic obstructive pulmonary disease (COPD) is a leading cause of morbidity and mortality worldwide [1]. COPD is now the third leading cause of death [2], which is expected to further increase in the coming decades. COPD is an umbrella term encompassing emphysema, which is the irreversible destruction of alveolar sacs, and chronic bronchitis that is characterized by a productive cough accompanied by an abnormal inflammatory response in the airways and lungs [3]. Smoking is the main risk factor for developing COPD [4], and people with COPD may also face an increased risk for severe illness from coronavirus disease (COVID-19) with increased hospitalization and intensive care unit (ICU) admission [5]. COVID-19 has rapidly spread through the world and is caused by severe acute respiratory syndrome coronavirus 2 (SARS-CoV-2), a novel β-coronavirus [6].

One reason that individuals with COPD may be at heightened risk for severe COVID-19 is the increased expression of the angiotensin-converting enzyme 2 (ACE2), the entry receptor for SARS-CoV-2 [6,7]. ACE2 is expressed in many organs, including the kidney, heart, and lungs [8]. Pulmonary ACE2 is concentrated mainly in type II alveolar cells and macrophages but is also present in bronchial and tracheal epithelial cells and lung fibroblasts [8,9,10,11,12]. Although ACE2 is the primary means for SARS-CoV-2 entry, maintenance of ACE2 levels is essential for combatting inflammatory and fibrotic lung disease [13]. ACE2 is part of the renin–angiotensin system (RAS) that cleaves angiotensin II to Ang-(1-7) [14]. Ang-(1-7) then activates the Mas receptor, leading to release of nitric oxide, prostaglandin E2, and bradykinin [15], resulting in vasodilation, natriuresis and a decrease in inflammation [16,17].

Therefore, changes in the expression of ACE2 may contribute to susceptibility to COVID-19 or predispose to post-COVID-19 complications. Environmental factors, such as smoking, increase ACE2 expression [18,19]. In COPD, ACE2 is overexpressed in alveolar and bronchial epithelium [20], and our group recently showed that COPD-derived lung fibroblasts express higher levels of ACE2; chronic cigarette smoke also increased ACE2 protein in mouse lungs [9]. Although ACE2 expression may be controlled at multiple levels (e.g., transcriptional, post-transcriptional and/or translational) [21], with the stability of mRNA factoring predominantly in the overall regulation of gene expression in response to changing environmental conditions (e.g., oxidative stress, hypoxia) [22], ACE2 expression may be controlled by alterations in mRNA stability [23]. However, it is not well understood how ACE2 expression is regulated.

mRNA stability can be controlled by RNA-binding proteins (RBPs), such as human antigen R (HuR). HuR, encoded by the *ELAVL1* gene, belongs to the embryonic lethal abnormal vision (ELAV) family of RBPs [24,25]. HuR binds to mRNAs to control stability and/or translation of target mRNAs, and participates in pre-mRNA splicing and the nucleocytoplasmic translocation of target mRNAs [24,25,26]. These target mRNAs encode proteins involved in cellular processes, such as proliferation, differentiation, apoptosis, and inflammation [24,25]. HuR is mainly located in the nucleus in resting cells and translocates to the cytoplasm along with bound mRNA in response to stimuli, such as UVB, radiation, and cigarette smoke [24,25,27,28]. Although HuR is expressed in several lung cell types, including epithelial cells and fibroblasts [28], little is known about its expression in other lung cells. It is also not known whether HuR/ELAVL1 expression changes in the context of lung disease, including COVID-19 and COPD, or whether the

upregulation of ACE2 in smokers and COPD is regulated by HuR. Therefore, we hypothesis that HuR controls the expression of pulmonary ACE2.

Using scRNA-seq datasets, we first profiled the differential expression of *ELAVL1* in cells of the upper and lower respiratory system in COPD and COVID-19 subjects. We found a significant positive correlation between *ELAVL1* and *ACE2* in COPD cells, and that there is elevated cytoplasmic HuR protein in cells within smoker and COPD lungs. Mechanistically though, HuR does not control the upregulation of ACE2 in smoker and COPD cells despite HuR binding to the *ACE2* transcript. These data highlight the need for more mechanistic research into factors controlling pulmonary ACE2 expression. Identification of these mechanisms could lead to new therapeutic targets for both inflammatory and fibrotic stimuli as well as for SARS-CoV-2 entry into the respiratory system.

3.3. METHODS

Chemicals

All chemicals were obtained from Sigma (St. Louis, MO, USA) unless otherwise indicated. Actinomycin D (ActD) was from Enzo Life Sciences.

Single Cell RNA-Sequencing Analysis

Raw single-cell RNA-seq expression matrices for lung cells [29] or nasopharyngeal/bronchial cells [30] were filtered using SCANPY software [31]. Cells with less than 200 expressing genes or more than 40% of mitochondrial reads were filtered. Genes that were only expressed in less than three cells were also removed. Genes were further filtered if they exhibited low dispersion (<0.15) or very low-level expression (<0.0125). The filtered gene expression matrix was then converted to log2 space (log2 expression+1) for the following analysis. We then cluster cells from the obtained cell-by-gene expression matrices (by rows). The cell type annotations for the resulting clusters were directly downloaded from the original studies [29,30], which were based on known cell type markers. We further explored the expression of *ELAVL1* gene in various cell populations. Mann–Whitney U tests were used to quantify the difference in *ELAVL1* gene expression between different cell populations. The *ELAVL1* positive cells in each cell population (cluster) are also counted, and we sort all the cell types based on the percentage of *ELAVL1* positive cells. By comparing the difference in the percentage of *ELAVL1* positive cells, we can also identify a list of cell types with the most differential *ELAVL1* gene expression between conditions (e.g., COPD vs. control).

COPD Subjects

The study population included current smokers with COPD (COPD), smokers without COPD (smoker) and non-smokers without COPD (non-smoker; normal). Subject characteristics are as we have published [32]. Lung tissue was obtained from subjects undergoing lung resection surgery at McMaster University.

Multiplex Immunohistochemistry (mIHC)

mIHC was performed on lung tissues from non-smokers (control; M/F = 1/3; age 64.75 ± 6.1 years), current smokers with COPD (COPD; M/F = 1/3; age 54.5 ± 3.4 years) and without COPD (smoker; M/F = 0/3; age 67.3 ± 4.98 years) by the Discovery Ultra Ventana automated slide preparation system (Roche, Laval, QC, Canada). Briefly, formalin-fixed paraffin-embedded blocks were cut to a one 4-µm-thick section. Slides were deparaffinized at 69 °C and pretreated with CC1 (EDTA) for 24 min at 95 °C. Then, Discovery Inhibitor was added for 4 min. The slides were incubated with primary anti-HuR antibody (1:100; Santa Cruz, Dallas, TX, USA) for 15 min at 37 °C. Secondary antibody conjugated to horseradish peroxidase (HRP) (OMap anti-mouse HRP, Roche, Laval, QC, Canada) was incubated for 16 min. Immunodetection was performed with 3,3′-diaminobenzidine (DAB, Roche, Laval, QC, Canada). Then, primary anti-vimentin antibody (1:50; Cell Signaling Technologies, Whitby, ON, Canada) was incubated for 16 min at 37 °C followed by the secondary antibody UltraMap (anti- rabbit alkaline phosphatase) and incubated for 16 min at 37 °C. Immunodetection was performed with DISCOVERY Yellow kit. Next, the slides were incubated with the triple stain using the primary antibody for cytokeratin 19 (Roche, Laval, QC, Canada) for 16 min at 37 °C. The secondary antibody was multimer HRP (OMap anti-

mouse HRP, Roche, Laval, QC, Canada) and was incubated for 16 min. Immunodetection was performed with DISCOVERY Purple detection. Finally, nuclei were subsequently visualized with hematoxylin. The images were taken with Aperio ImageScope. We semi-quantitively scored the slides based on the intensity of the brown color (HuR): weak, moderate, and strong. The intensity of the HuR was also analyzed by the Aperio Positive Pixel Count Algorithm v9.

Cell Culture

Primary human lung fibroblasts (HLFs) were isolated from lung tissue by explant procedure [33]. Cells utilized in this study were derived from non-smokers (control; M/F = 1/3; age 71 ± 7 years), current smokers with COPD (M/F = 2/2; age 61 ± 5.4 years) and without COPD (smoker; M/F = 1/3; age 61.3 ± 4.8 years). Experiments were conducted with fibroblasts from 3–4 different individuals of each patient group unless otherwise indicated and were between passages five to eight. All fibroblast strains were cultured and analyzed at the same time and were within one passage to assess the basal expression levels of HuR.

Western Blot

HLFs were grown to approximately 70–80% confluence and cultured with serum-free MEM for 18 h before the treatment. Total cellular protein was extracted using RIPA lysis buffer (ThermoFisher Scientific, Waltham, MA, USA) and Protease Inhibitor Cocktail (PIC, Roche, Laval, QC, Canada). Nuclear and cytoplasmic fractions were extracted using a nuclear extract kit (Active Motif, Carlsbad, CA, USA). Ten to twenty μg (for ACE2 and COX-2 detection) or 60 μg (for cleaved HuR detection) of protein lysate were subjected to 10% SDS-PAGE gels and

transferred onto Immuno-blot PVDF membranes (Bio-Rad Laboratories, Mississauga, ON, Canada), as previously described [34]. Then, the membrane was blocked for one hour at room temperature in blocking solution (5% w/v of non-fat dry milk in 1× PBS/0.1% Tween-20). Antibodies against HuR (1:2000; Santa Cruz, Dallas, TX, USA), ACE2 (SN0754; 1:500–1:1000; Invitrogen, Waltham, MA, USA), COX-2 (1:1000; Cell Signaling Technologies, Whitby, ON, Canada), Laminin A/C (1:1000; Cell Signaling Technologies, Whitby, ON, Canada) and β-Tubulin (1:50,000; Sigma, St. Louis, MO, USA) were used. Secondary antibodies goat anti-rabbit IgG HRP-linked (1:10,000, Cell Signaling Technologies) and HRP-conjugated horse anti-mouse IgG (1:10,000, Cell Signaling Technologies, Whitby, ON, Canada) were used. Detection of protein was catalyzed by enhanced chemiluminescence (ECL) and visualized using a ChemiDoc™ MP Imaging System (Bio-Rad Laboratories, Mississauga, ON, Canada). Densitometric analysis was performed using Image Lab™ Software Version 5 (Bio-Rad, Mississauga, ON, Canada). Protein expression was normalized to β-Tubulin and the data presented as the fold-change relative to the untreated condition.

Quantitative RT-PCR (RT-qPCR)

Total RNA was isolated using miRNeasy Kits (QIAzol based RNA purification, Qiagen) according to the manufacturer's instructions. Quantification was conducted on a Nanodrop 1000 spectrophotometer (infinite M200 pro, TECAN, San Jose, CA, USA). Reverse transcription of RNA was carried out using iScript™ Reverse Transcription Supermix (Bio-Rad Laboratories, Mississauga, ON, Canada). Then, mRNA levels of *ELAVL1*, *ACE2* and *S9* were analyzed using this cDNA template and gene-specific primers (Table 3.1). Quantitative PCR (qPCR) was performed by addition of 1 μL cDNA and 0.5 μM primers with SsoFast™ EvaGreen® (Bio-Rad

Laboratories, Mississauga, ON, Canada), and PCR amplification was performed using a CFX96 Real-Time PCR Detection System (Bio-Rad Laboratories, Mississauga, ON, Canada). Thermal cycling was initiated at 95 °C for 3 min and followed by 39 cycles denaturation at 95 °C for 10 s and annealing at 59 °C for 5 s. Gene expression was analyzed using the ΔΔCT method, and results are presented as fold-change normalized to the housekeeping gene (*S9*).

Table 3.1. Primer sequences used for RT-qPCR analysis.

Gene	Forward Primer Sequence	Reverse Primer Sequence
ELALV1	AAC GCC TCC TCC GGC TGG TGC	GCG GTA GCC GTT CAG GCT GGC
ACE2-201-202	AAC TGC TGC TCA GTC CAC CA	GAC CAT TTG TCC CCA GCA TT
ACE2-202	CCC AGA GCA TGC CTG ATA GA	CCC ACT TCA GAG GGT GAA CA
S9	CAG CTT CAT CTT GCC CTC A	CTG CTG ACG CTT GAT GAG AA

RNA Immunoprecipitation-qPCR (RIP-qPCR)

HLFs were grown to approximately 70–80% confluence and cultured with serum-free MEM for 18 h before collection. Cells were collected in PBS and centrifuged at 1500 rpm at 4 °C for 5 min. The cell pellets were lysed (50 mM Tris PH 8; 0.5% Triton X100; 450 mM NaCl; Protease Inhibitor Cocktail; Phosphatase Inhibitor (Roche, Laval, QC, Canada), incubated for 15 min on ice, and then centrifuged at 10,000 rpm, 4 °C for 15 min. The extracts were transferred into as new tube and a buffer containing 50 mM Tris pH 8; 0.5% Triton X100; 10% glycerol; Protease Inhibitor Cocktail; Phosphatase Inhibitor (Roche, Laval, QC, Canada) [35,36] was added. Protein concentration was measured by the BCA Protein Assay Kit. Thirty-five µL of protein G SepharoseTM 4 fast glow beads (GE Healthcare, Mississauga, ON, Canada) were pre-coated with 3 µg of IgG (Cell Signaling Technologies, Whitby, ON, Canada) or 3 µg of anti-HuR (Santa Cruz Biotechnology, Dallas, TX, USA) antibodies overnight on a rotator at 4 °C. Beads were washed

three times with buffer (50 mM Tris PH 8; 0.5% Triton X100; 150 mM NaCl) and incubated with cell extracts for 2 h a 4 °C. Beads were washed three times to wash out unbound materials. RNA was then extracted, reverse transcribed and analyzed by qPCR (RT-qPCR), as described above. RNA expression was normalized to S9 mRNA bound in a non-specific manner to IgG.

HuR-esiRNA Knockdown in Human Lung Fibroblasts

HLFs were seeded at 10 × 104 cells/cm2 and transfected with 60 pmol of endoribonuclease prepared siRNA (esiRNA) against ELAVL1 (MISSION® esiRNA, Sigma, St. Louis, MO, USA) or non-targeting control esiRNA (MISSION® esiRNA, Sigma) with Lipofectamine RNAiMAX transfection reagent (ThermoFisher Scientific, Waltham, MA, USA) in accordance with the manufacturer's instructions. One hour after the transfection, 10% MEM medium was added on the cells. After 24 h, the cells were switched to serum-free MEM for 44 h, after which cellular proteins were collected. Confirmation of HuR knockdown was done by Western blot within 68 h after transfection.

Determination of mRNA Stability

HLFs were serum-starved for 18 h followed by treatment of Actinomycin D (ActD-1 µg/mL) (Enzo Life Sciences, Toronto, ON, Canada), an inhibitor of RNA synthesis [28,37], for 0, 3, 6, and 9 h, after which RNA was collected; qPCR was performed as described above to determine the remaining levels of *ACE2* mRNA. The concentration of ActD used in this experiment did not affect cell viability (data not shown) but blocked transcription [38].

Determination of Protein Stability

HLFs were serum-starved for 18 h followed by the protein collection for the 0-h time point. The remaining cells were treated with cycloheximide (CHX-1 μg/mL)—an inhibitor of protein synthesis [39]—for 4, 8, 24, and 48 h. Total protein was harvested, and Western blot was performed to determine the remaining levels of ACE2 protein. CHX concentration used in this experiment did not affect cell viability (data not shown).

Preparation of Cigarette Smoke Extract (CSE)

Research grade cigarettes (3R4F) with a filter were acquired from the Kentucky Tobacco Research Council (Lexington, KT, USA). Each cigarette contains 0.73 mg of nicotine, 9.4 mg of tar, and 12.0 mg of CO, as described by the manufacturer. CSE was produced as previously described [28,32,38,40,41].

Imaging Flow Cytometry

HLFs were grown to approximately 70–80% confluence and cultured with serum-free MEM for 18 h before the treatment. Cells were exposed to 2% CSE for 4 h. Then, cells were trypsinized, collected, and prepared according to the manufacturer's instructions. Briefly, after washing cells with PBS-0.2% BSA, cells were fixed with 4% paraformaldehyde (PFA) for 20 min at room temperature. After incubation, PBS-0.2% BSA was added, spun down at 400× g at 4 °C for 5 min, and the supernatant was discarded. The pellet was resuspended in 400 μL PBS-0.2%

BSA, spun down at 400× g at 4 °C for 5 min, and again the supernatant was discarded. Then, the pellet was resuspended in 100 µL of permeabilization buffer (BD Perm/WashTM Buffer, eBioscience™), and was incubated for 15 min at room temperature. After incubation, 1 µL of PE mouse anti-HuR (1:100, BD Pharmingen™) was added and incubated for 30 min at 4 °C in the dark, and then 1 mL of permeabilization buffer was added. The samples were centrifuged, and the pellet was resuspended in 75 µL of 1× PBS-0.2% BSA. The samples were filtered and kept in the dark. Before acquiring the samples, 5 µL Hoechst (1: 20,000, Hoechst 3342, ThermoFisher Scientific, Waltham, MA, USA) was added. In each experiment 20,000 events for each sample were acquired using a 12 channel Amnis® ImageStream®X Mark II (EMD Millipore, Oakville, ON, Canada) imaging flow cytometer equipped with the 405 nm and 488 nm lasers. Samples were gated to remove debris, and 20,000 event/sample were analyzed using IDEAS®. After gating the cytoplasmic fraction, intensity was used to evaluate HuR expression.

Statistical Analysis

Using GraphPad Prism 6 (v. 6.02; La Jolla, CA, USA), statistical analysis was performed using a non-parametric one-way analysis of variance (ANOVA) followed by Dunn's multiple comparisons test to assess the differences between the non-smoker, smoker, and COPD subjects as well as between treatments of more than two. Groups of two were analyzed by the one- or two-tailed unpaired t-test, as described below. A two-way analysis of variance (ANOVA), followed by Sidak's multiple comparisons test was used to evaluate differences between groups and conditions of more than two. Results are presented as means ±standard error of the means (SEM) of the fold-changes relative to control cells. In all cases, p values < 0.05 were considered statistically

significant. Mann–Whitney U tests were also used in single-cell RNA-seq to quantify the difference in *ELAVL1* gene expression between different cell populations.

3.4. RESULTS

Expression of *ELAVL1* and *ACE2* in Cells of the Upper and Lower Respiratory System

Comprehensive expression analysis of *ELAVL1* in pulmonary cell populations has not been done. Therefore, we first analyzed existing single-cell RNA-seq datasets to comprehensively profile *ELAVL1* in cells along the respiratory tract. The first dataset utilized nasopharyngeal/bronchial cells from 19 SARS-CoV-2-positive patients and five SARS-CoV-2-negative donors [30]. Conducting airway epithelial cells, (basal, secretory, ciliated, FOXN4+ cells, and ionocytes) and immune cells (macrophages, dendritic cells, and natural killer (NK) cells) were among the cells detected (Figure 3.1A). Comparing *ELAVL1* expression in these different cell populations in COVID-19 patients revealed that the expression of *ELAVL1* is significantly higher (Mann–Whitney U test, p-value = 0) in ciliated, FOXN4+, and secretory cells (Figure 3.1B) and that there was differential *ELAVL1* expression based on COVID-19 severity (Figure 3.1C).

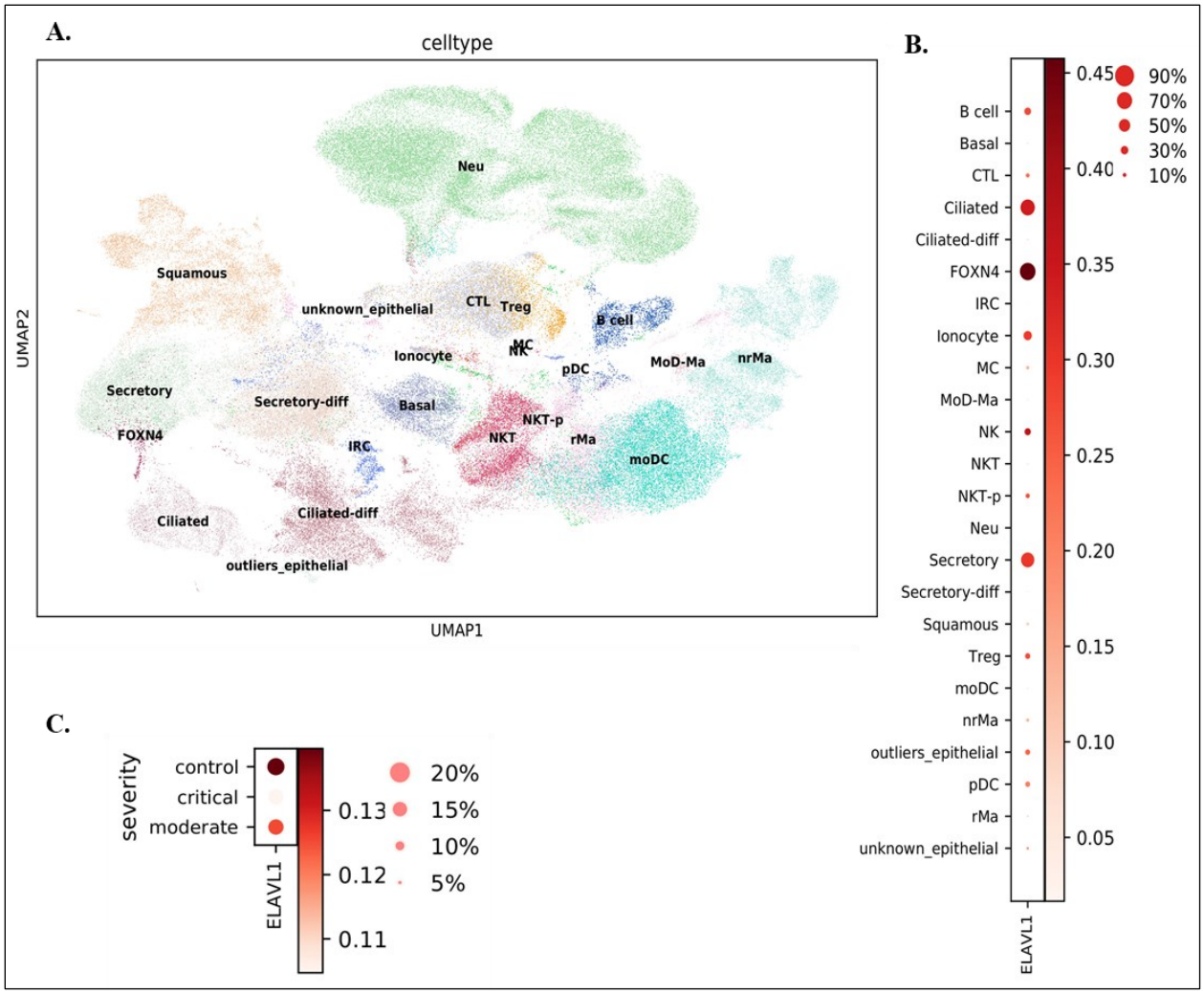

Figure 3.1. *ELAVL1* single-cell level expression in nasopharyngeal and bronchial cells.

A. Different cell populations in an existing single-cell RNA-seq data [30] were analyzed as described in the Materials and Methods. **B.** Dotplot representing the expression of *ELAVL1* in different cell populations. The size of the circle denotes the % of cells expressing the *ELAVL1* gene. The darkness of the circle shows the expression level. The expression of *ELAVL1* is significantly higher (Mann–Whitney U test, p-value = 0) in ciliated, FOXN4, secretory cells than that in any other cells. **C.** The expression of *ELAVL1* is significantly lower (Mann–Whitney U test, p-value = 4.41×10^{-23}) in critical COVID-19 patients than in moderate and control patients.

It is also unknown whether *ELAVL1* expression changes with COPD. Therefore, we also assessed *ELAVL1* expression in lung cells from COPD patients using existing single-cell RNA-seq expression data on samples obtained from 28 control donor lungs and 18 COPD lungs [29]. The cell populations identified are in Figure 3.2A. In COPD, *ELAVL1* expression is higher in

aberrant basaloid, mesothelial, peribronchial vascular endothelial (VE), pulmonary neuroendocrine cell (PNEC), ciliated, and club cells, relative to other cell types (Figure 3.2B). Further, we found that mesothelial, PNEC, and myofibroblasts have relatively high *ELAVL1* expression in COPD, whereas alveolar type II (ATII), fibroblasts, and macrophages are among the cell types with relatively high % of *ELAVL1*+ cells in control (Figure 3.2C).

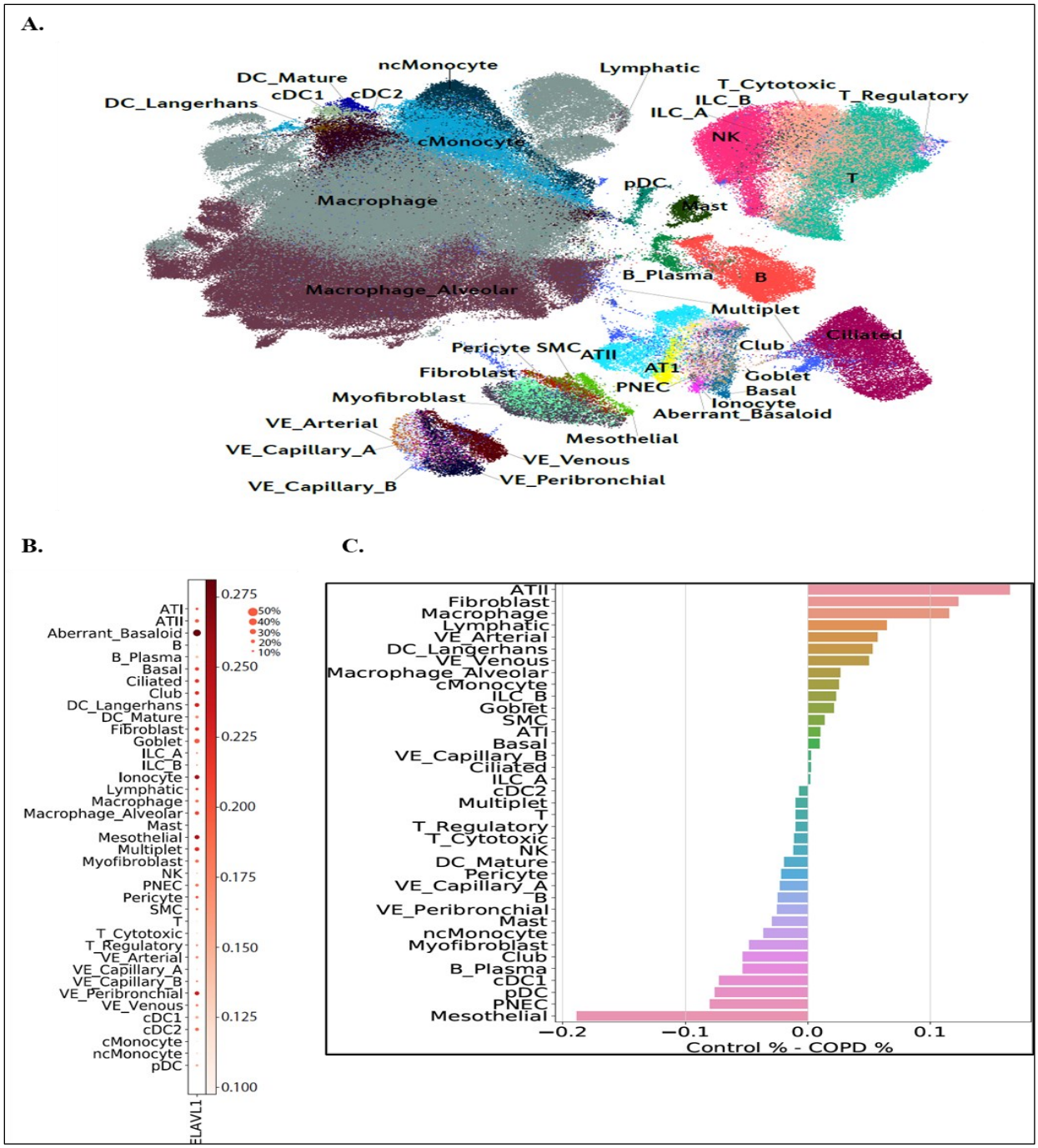

Figure 3.2. *ELAVL1* single-cell level expression in COPD.

A. Different cell populations in the COPD single-cell RNA-seq data [29]. **B.** Dotplot shows the expression of *ELAVL1* in different cell populations. The size of the circle denotes the % of cells expressing *ELAVL1*. The darkness of the circle shows the expression level. Aberrant_basaloid, mesothelial, VE_peribronchial, PNEC, ciliated, and club cells are among the cell types with the highest expression of *ELAVL1*. **C.** Percentage of *ELAVL1*+ cells: on the right side (positive % difference) is the cell types with higher % of *ELAVL1*+ cells in control. On the left side are the cell types with higher % of *ELAVL1*+ cells in COPD (0.1 denotes 10%).

Finally, we explored whether there was a correlation between *ELAVL1* and *ACE2* expressions in COPD cells that express both genes. We found a significant positive correlation (Pearson correlation coefficient = 0.631; p-value < 0.01) between *ELAVL1* and *ACE2* expression (Figure 3.3). In summary, *ELAVL1* expression varies amongst various pulmonary cell types and disease phenotypes but there is a positive correlation between *ELAVL1* and *ACE2* expression in COPD.

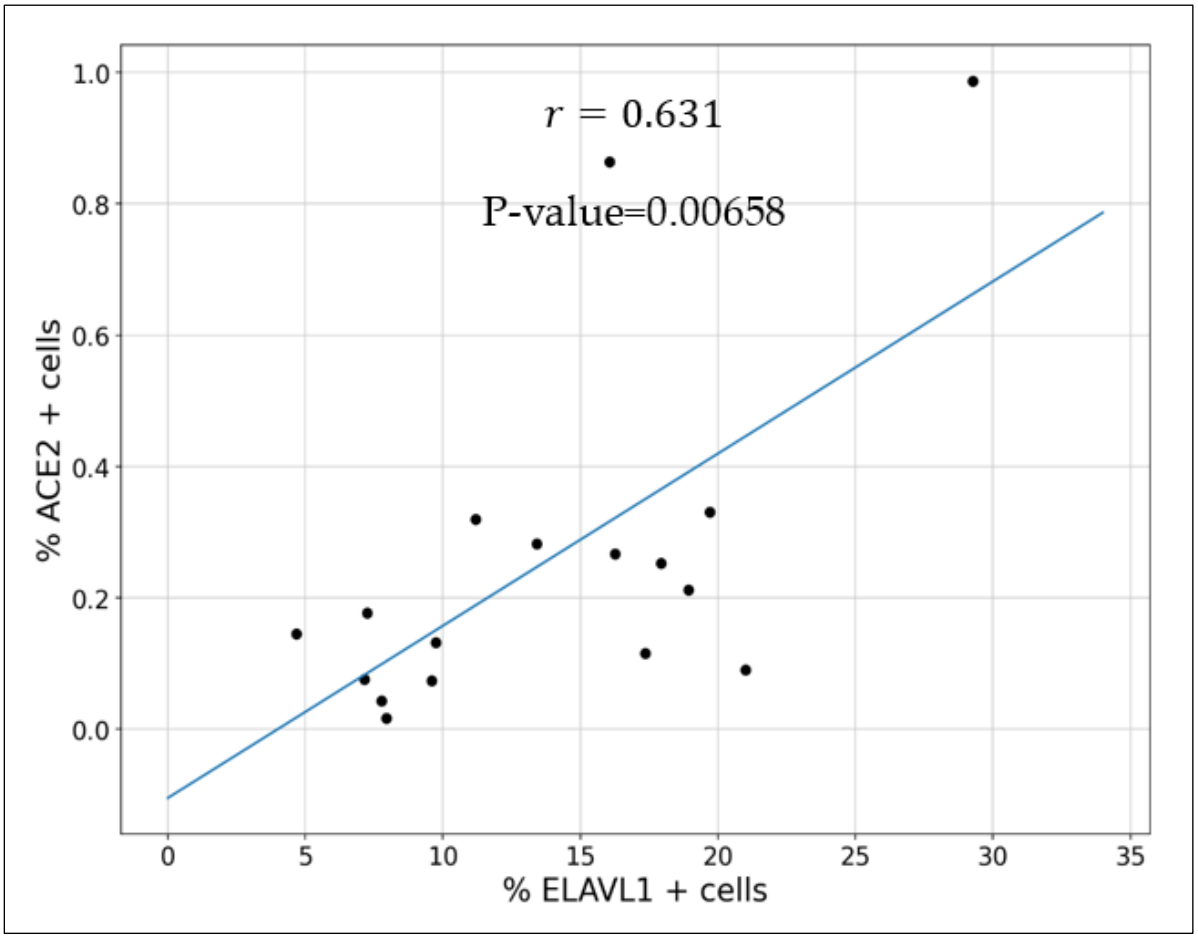

Figure 3.3. Correlation between *ELAVL1* and *ACE2* in COPD.

The percentage of *ELAVL1* and *ACE2* positive cells in all cell types of the COPD samples were analyzed. There was a significant (p-value < 0.01) correlation (Pearson correlation coefficient = 0.631) between *ELAVL1* and *ACE2*. Only cell types expressing both *ELAVL1* and *ACE2* were included in the analysis.

Cytoplasmic Localization of HuR Is Increased in Smoker and COPD Lung Cells

We next used mIHC to detect HuR (brown) in epithelial cells (purple) and fibroblasts (yellow) (Figure 3.4A and B). In lungs of non-smokers, HuR was localized predominantly in the nucleus of epithelial cells and fibroblasts while only weak cytoplasmic HuR expression was detected in both cell types (Figure 3.4A–left panel). Prominent HuR expression was detected in lung cells of smokers with and without COPD (Figure 3.4A–middle and right panels). We also found that cytoplasmic HuR expression was relatively high in pulmonary macrophages of smokers and COPD subjects (Figure 3.4B). These data indicate differential localization of HuR in the lungs in response to cigarette smoke, with there being prominent cytoplasmic levels.

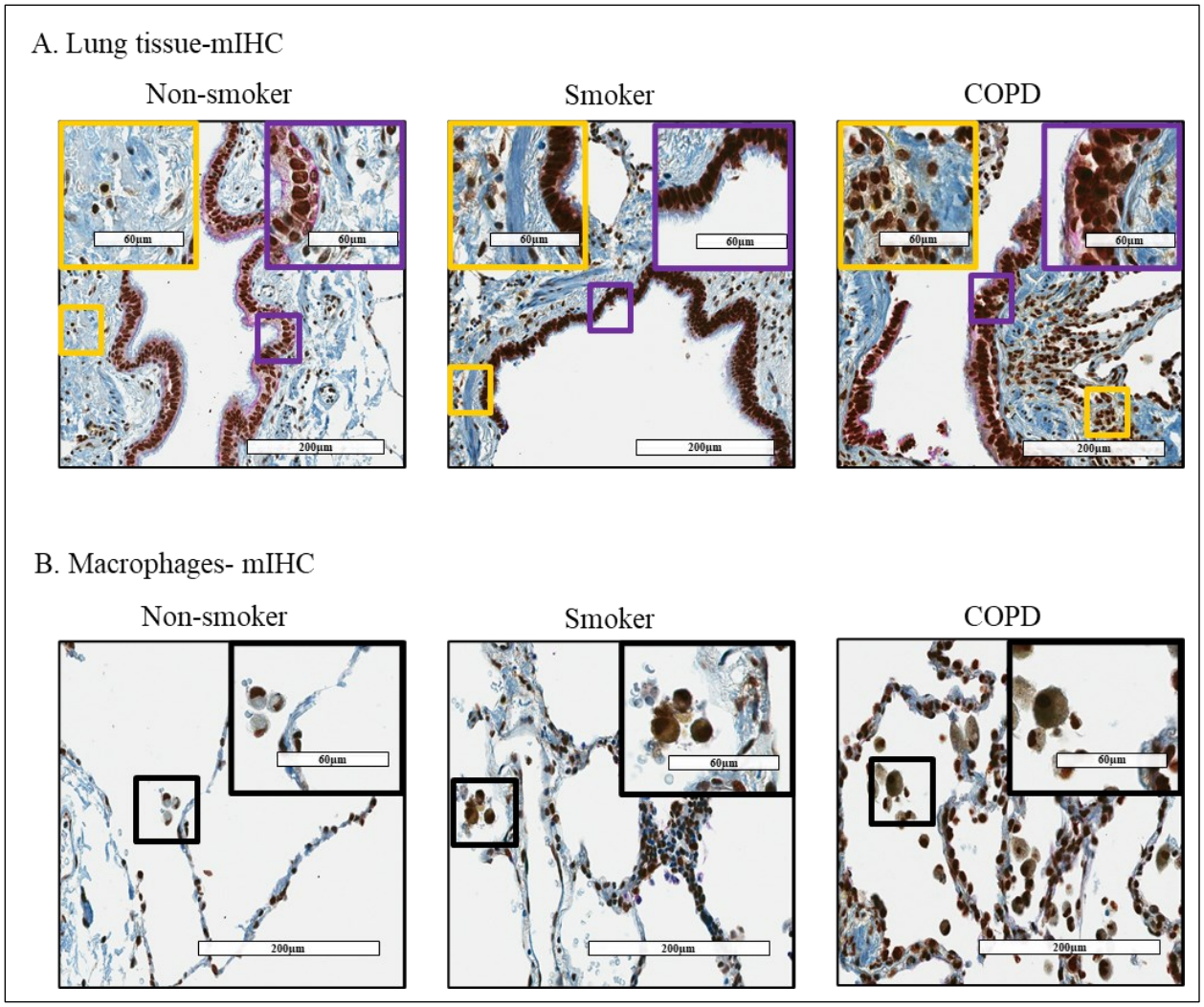

Figure 3.4. Cytoplasmic expression of HuR increased in lung tissue and macrophages from smoker and COPD subjects.

A. Lung tissue—mIHC: lung tissue was stained with mIHC: HuR was stained with brown color, Cytokeratin 19 expression (a marker of epithelial cells) was stained with purple color, and vimentin (a marker for fibroblasts) was stained yellow. There was more HuR in the cytoplasm of epithelial cells and fibroblasts from smoker and COPD subjects comparing to these cells from non-smoker individuals. **B.** Macrophages—mIHC: there was an increase in cytoplasmic HuR in macrophages from smoker and COPD subjects. The pictures were taken by Aperio ImageScope with 20×, and 40× for higher magnification. Images are representative for 3 to 4 subjects/group.

Protein Expression of HuR Is Similar between Non-Smoker, Smoker, and COPD-Derived Lung Fibroblasts

We used HLFs to mechanistically evaluate the involvement of HuR in controlling ACE2 expression, as we have previously shown that HuR protein is constitutively expressed in these cells [28] and that there is more ACE2 protein in COPD-derived lung fibroblasts [9]. *ELAVL1* mRNA levels were significantly higher in COPD-derived HLFs relative to the smoker-derived cells (Figure 3.5A). In the non-smoker, smoker, and COPD-derived HLFs, HuR protein was detected at its predicted molecular weight (MW) of ~34 kDa (Figure 3.5B). There was no significant difference in HuR protein expression between the three groups (Figure 3.5C). Interestingly, another ~27 kDa protein band was detected only in the smoker and COPD-derived cells (Figure 3.5B) that likely reflects cleaved HuR (CP-1) [42]; CP-1 expression is significantly higher in smoker comparing to non-smoker HLFs (Figure 3.5D). Then, we evaluated the effect of cigarette smoke extract (CSE) on the expression of HuR in non-smoker-derived HLFs by treating cells with 2% CSE for 6 h, 8 h, and 24 h. There was no difference in total HuR protein expression in response to 2% CSE (Figure 3.5E). However, there was a significant increase in cleaved HuR (CP-1) in response to 2% CSE for 24 h in non-smoker-derived HLFs (Figure 3.5E). Together, these data indicate that cigarette smoke does not change the total HuR protein in HLFs but induces its cleavage.

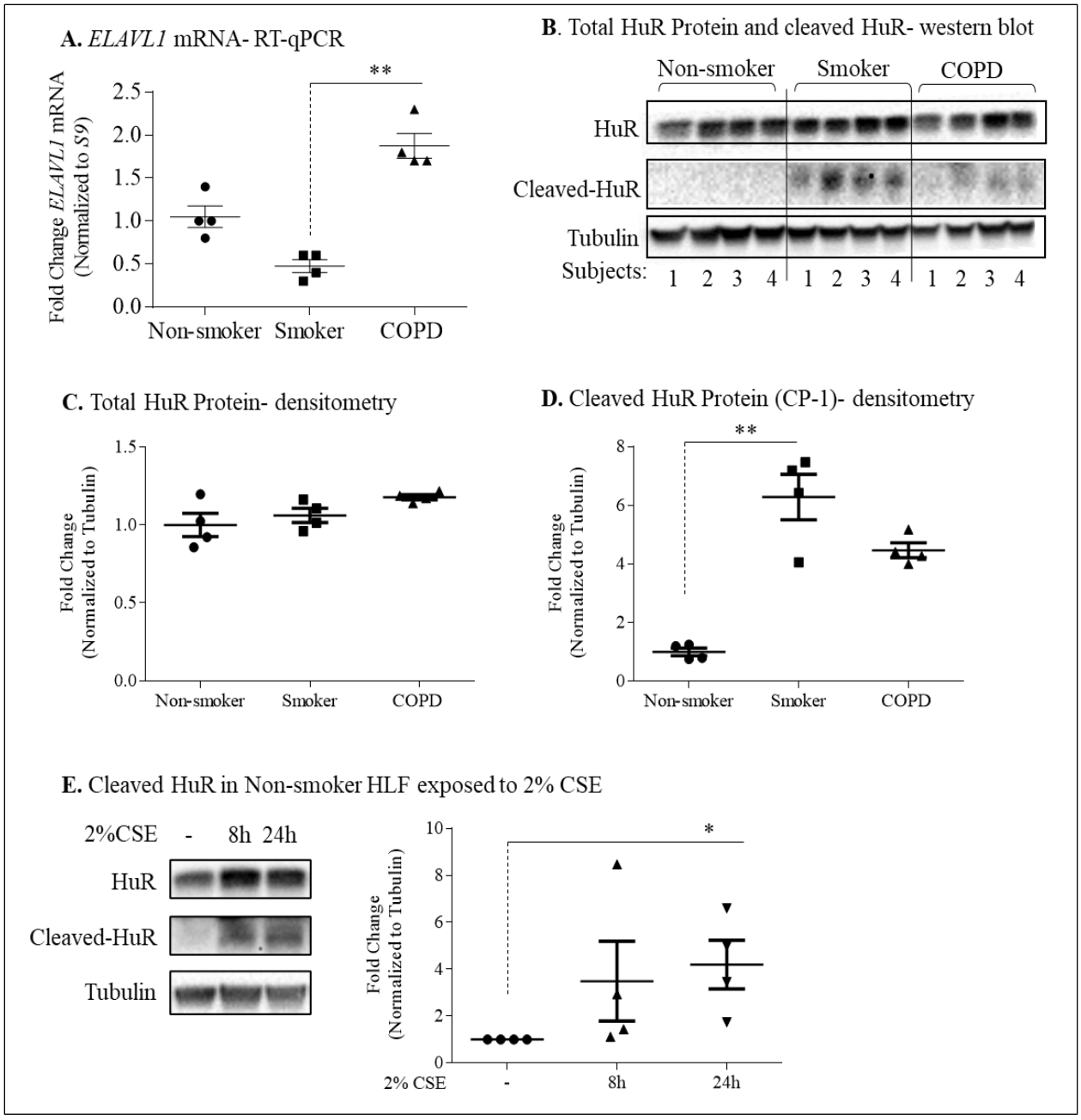

Figure 3.5. HuR expression in non-smoker, smoker, and COPD HLFs.

A. *ELAVL1* mRNA-RT-qPCR: HLFs from 4 non-smoker (circle), 4 smoker (square), and 4 COPD (triangle) subjects were harvested for RT-qPCR. There was a significant difference between smoker and COPD-derived HLFs (** $p < 0.01$). Results are expressed as the mean ± SEM. **B.** Total HuR Protein—Western blot- densitometry: HLFs from 4 non-smoker, 4 smoker, and 4 COPD subjects were harvested for Western blot. HuR protein expression was detected at the predicted MW of 34 kDa. The cleaved HuR product (CP-1, 27 kDa) was detected in HLFs from smoker and COPD subjects. β-Tubulin was used as loading control. **C.** Total HuR Protein—densitometry: there was no significant difference in total expression of HuR between non-smoker (circle), smoker (square), and COPD (triangle) HLFs. Results are expressed as the mean ± SEM.

D. Cleaved HuR Protein (CP-1)—densitometry: there was significant increase in the cleaved HuR (CP-1) in smoker (square) HLFs comparing to non-smoker (circle) HLFs (** p = 0.009). Results are expressed as the mean ± SEM. **E.** Cleaved HuR in non-smoker HLFs exposed to 2% CSE: there was an increase in the cleaved HuR product (CP-1) in HLFs from non-smokers exposed to 2% CSE for 8 h and 24 h (* p = 0.01). Results are expressed as the mean ± SEM of 4 independent experiments.

Increased ACE2 Protein in COPD-Derived Lung Fibroblasts Is Not Associated with Changes at the mRNA Level or Increased Binding to HuR

We next examined if there was differential expression of *ACE2* at the mRNA level. Using two different primers sets for human *ACE2* (*ACE2-201-202* and *ACE2-202*), we found that there was a significant difference in *ACE2* mRNA levels between quiescent HLFs derived from non-smoker and smoker lungs for *ACE2-201-202* (Figure 3.6A) but not for *ACE2-202* (Figure 3.6B). Overall, this suggests that changes at the transcriptome level are unlikely to account for higher ACE2 protein in COPD-derived HLFs.

HuR binds to target mRNA, thereby increasing stability of the transcript [25]. It is not known whether HuR associates with *ACE2* mRNA. To address this, we assessed HuR association with *ACE2* mRNA by immunoprecipitation of HuR followed by RT-qPCR analysis of *ACE2* mRNA. Western blot analysis showed that HuR immunoprecipitated from HLF cell extracts similarly between non-smoker, smoker, and COPD (Figure 3.6C). Note the specificity of the IP, as the immunoglobulin G (IgG) antibody did not immunoprecipitate HuR, as indicated by the absence of a band on the Western blot. Furthermore, HuR strongly bound *ACE2-201-202* mRNA in smoker-derived HLFs (Figure 3.6D). HuR did not associated with *ACE2-202* mRNA (data not shown). Thus, HuR can bind *ACE2* mRNA in HLFs.

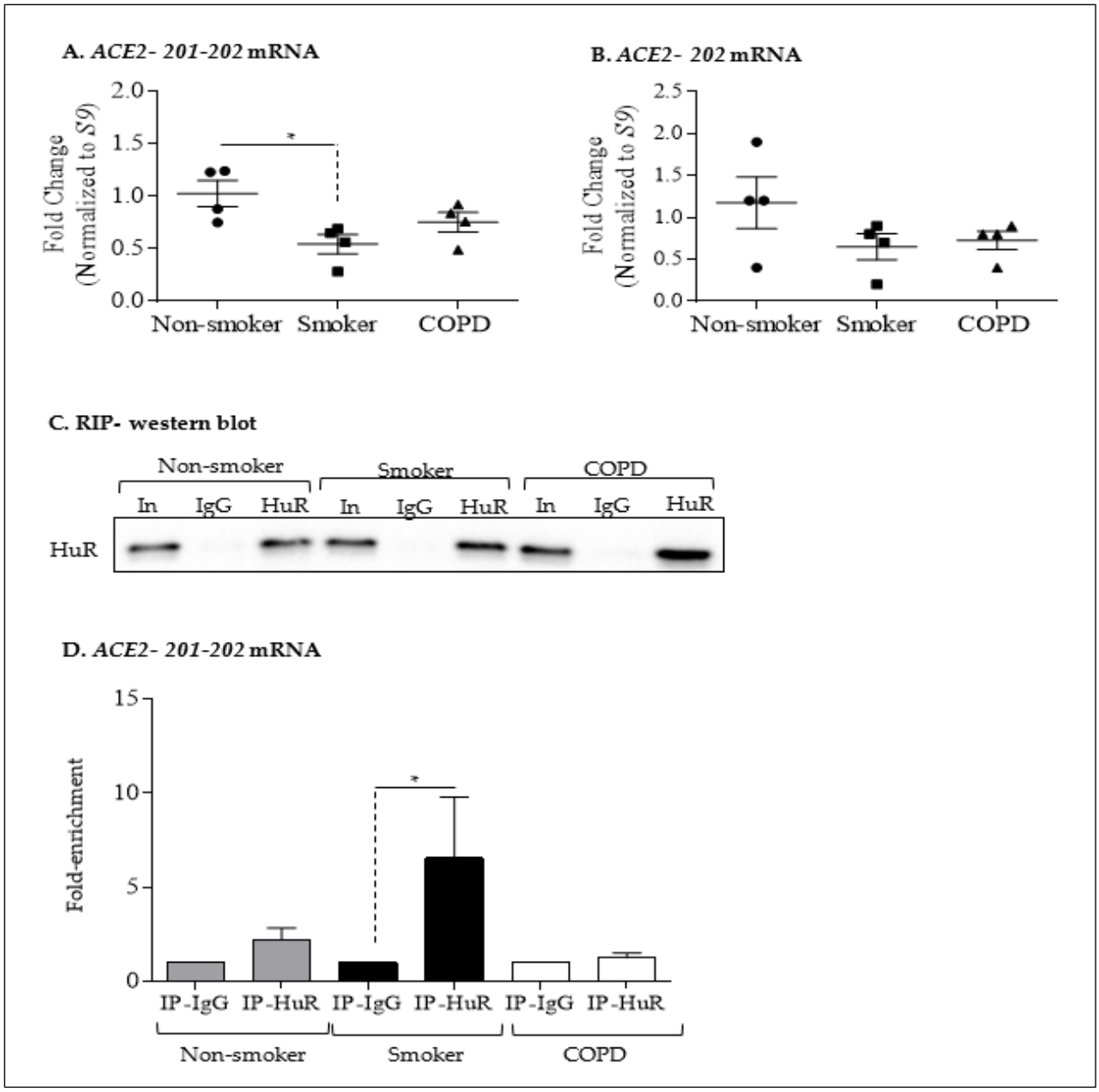

Figure 3.6. *ACE2* mRNA expression and binding to HuR.

A. *ACE2-201-202* mRNA: there was significantly less mRNA in smoker (triangle) compared to non-smoker (circle) HLFs (* $p < 0.05$) **B.** *ACE2-202* mRNA: there was no significant difference between the three groups of HLFs. **C.** RIP—Western blot: representative Western blot of HuR IP is shown. Input (In) refers to cell lysates. IP-IgG refers to immunoprecipitation (IP) with control IgG antibody while IP-HuR refers to the IP with anti-HuR IgG antibody. Note the presence of HuR protein in IP-HuR but not in IP-IgG. **D.** *ACE2-201-202* mRNA: detection of *ACE2-201-202* mRNA in IP-IgG and IP-HuR was done using qPCR. Values are expressed as fold enrichment to values measured in IP-IgG. The enrichment of *ACE2-201-202* in IP-HuR of HLFs from non-smoker and smoker but not in COPD. Results are presented as the mean ± SEM) (* $p < 0.05$ compared to IP-IgG).

HuR Does Not Control *ACE2* mRNA or Protein Stability

To evaluate stability of the *ACE2* transcript between non-smoker, smoker, and COPD-derived HLFs, we treated these cells with actinomycin D (ActD 1 μg/mL), an inhibitor of RNA synthesis [28,37], for 3, 6, and 9 h, followed by an analysis of *ACE2* mRNA. There was no significant difference in the rate of *ACE2* mRNA decay between cells from the three subject groups (Figure 3.7A). There was also no change in the rate of *ACE2* mRNA decay within cells from subjects within a group. This indicates that *ACE2* mRNA expression is unlikely to be controlled at the level of mRNA stability in HLFs.

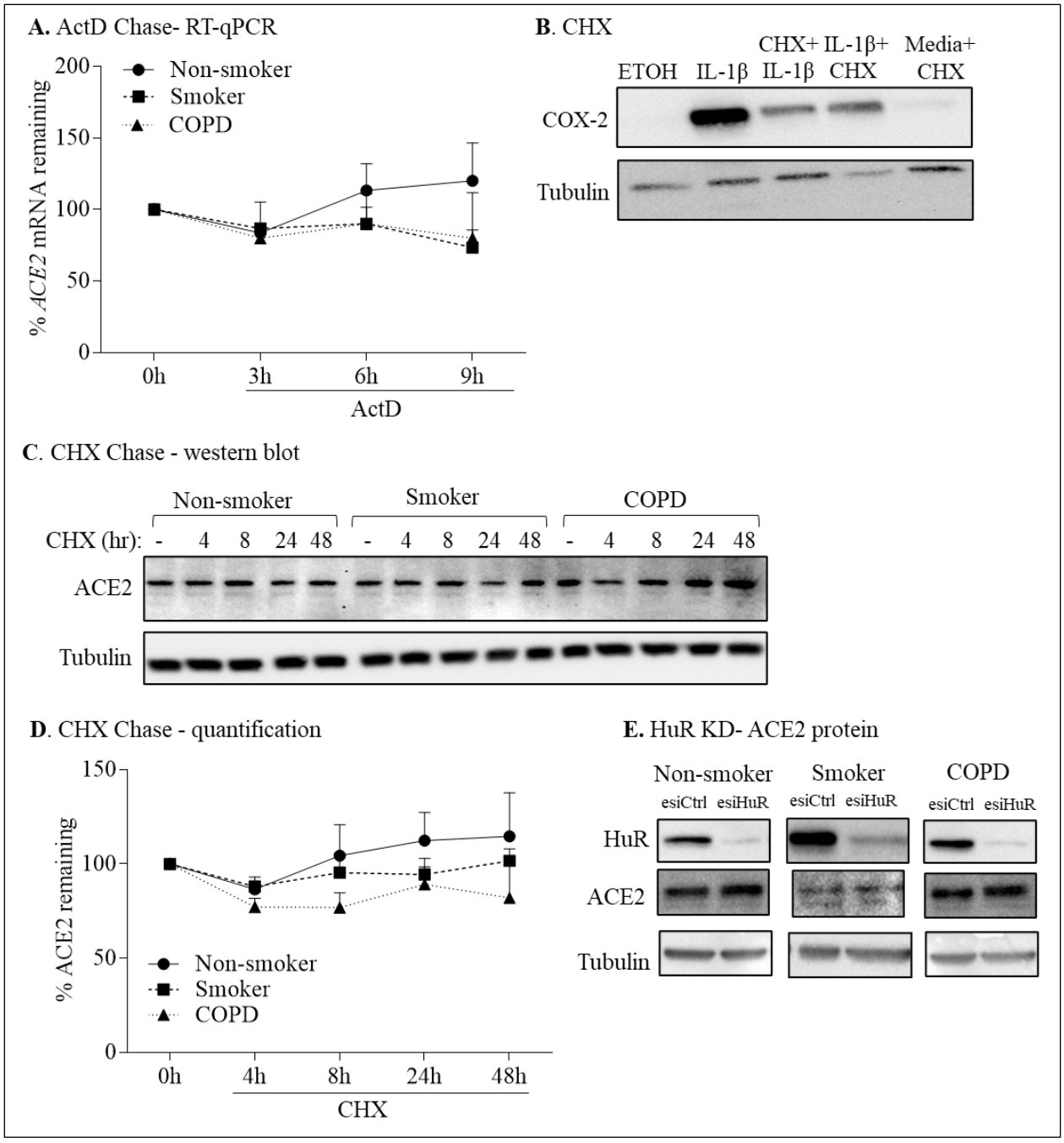

Figure 3.7. *ACE2* mRNA and protein stability are not controlled by HuR.

A. ActD Chase—RT-qPCR: HLFs from 3 non-smoker, 3 smoker, and 3 COPD subjects were exposed to ActD (1 µg/mL) for the indicated time point. *ACE2* levels were set to equal 100% after starvation for 18 h (0 h) and are expressed as percentage (%) of *ACE2* mRNA remaining. In non-smoker, smoker, and COPD HLFs, *ACE2* mRNA was similar after exposure to ActD for 3 h, 6 h, and 9 h compared to time 0. **B.** CHX: HLFs were exposed to ethanol (control), IL-1β (1 ng/mL) alone for 24 h, pretreated with CHX (1 µg/mL) for 1 h followed by IL-1β for 24 h, or pretreated with IL-1β for 24 h followed by CHX for 24 h. COX-2 protein expression was reduced by CHX. Representative Western blot is shown. **C.** CHX Chase—Western blot: HLFs from 3 non-smoker,

3 smoker, and 3 COPD subjects were exposed to CHX (1 μg/mL) for the indicated time point. Note that there is no change in ACE2 upon CHX treatment. **D.** CHX chase—quantification: ACE2 levels were set to equal 100% after starvation for 18 h (0 h) and are expressed as percentage (%) of ACE2 remaining. In non-smoker, smoker, and COPD HLFs, ACE2 protein was similar after exposure to CHX for 4 h, 8 h, 24 h, and 48 h compared to time 0. Results are expressed as the mean ± SEM. **E.** HuR KD-ACE2 protein: HuR knockdown had minimal effect on basal ACE2 protein levels in lung fibroblasts. Representative Western blots are shown.

To evaluate ACE2 protein stability, we exposed HLFs from non-smoker, smoker, and COPD subjects to cycloheximide (CHX 1 μg/mL), an inhibitor of protein synthesis [39], for up to 48 h, and assessed ACE2 protein expression by Western blot. To ensure that protein synthesis was indeed blocked by CHX, we include data demonstrating that both pre-and post-treatment with CHX attenuated IL-1β-induced COX-2 expression (Figure 3.7B). CHX did not significantly change ACE2 protein levels in HLFs. In addition, no significant difference in ACE2 protein stability between non-smoker, smoker, and COPD-derived lung fibroblasts were observed (Figure 3.7C and D). These results indicate that increased ACE2 expression in COPD-derived HLFs is not due to alterations in mRNA or protein stability.

To confirm HuR involvement in basal ACE2 expression, we transiently transfected HLFs derived from non-smoker, smoker, and COPD with control esiRNA (esiCtrl) or HuR-specific esiRNA (esiHuR). Basal HuR expression declined by ~80% in cells transfected with esiHuR-relative to esiCtrl-transfected cells (Figure 3.7E) but there was no significant difference in ACE2 protein levels in esiHuR-transfected cells relative to those transfected with esiCtrl in the three groups, suggesting that HuR does not play a dominant role in regulating ACE2 protein expression in quiescent HLFs (Figure 3.7E).

Non-Smoker and COPD-Derived Lung Fibroblasts Exposed to CSE Exhibit Increased Cytoplasmic HuR

Finally, to directly assess whether HuR regulates ACE2 expression in response to cigarette smoking, we used CSE, an in vitro surrogate of cigarette smoke exposure. Cytoplasmic HuR protein levels detected by Western blotting significantly increased in response to acute 2% CSE exposure (Figure 3.8A and B); ActD was used as a positive control. To confirm the effect of CSE on HuR localization, we used imaging flow cytometry (ImageStream®). There was a noticeable increase in cytoplasmic HuR levels in response to 2% CSE (4 h) in HLFs derived from non-smoker (Figure 3.8C) and COPD (Figure 3.8D), suggesting that acute cigarette smoke exposure induces translocation of HuR to the cytoplasm of primary HLFs.

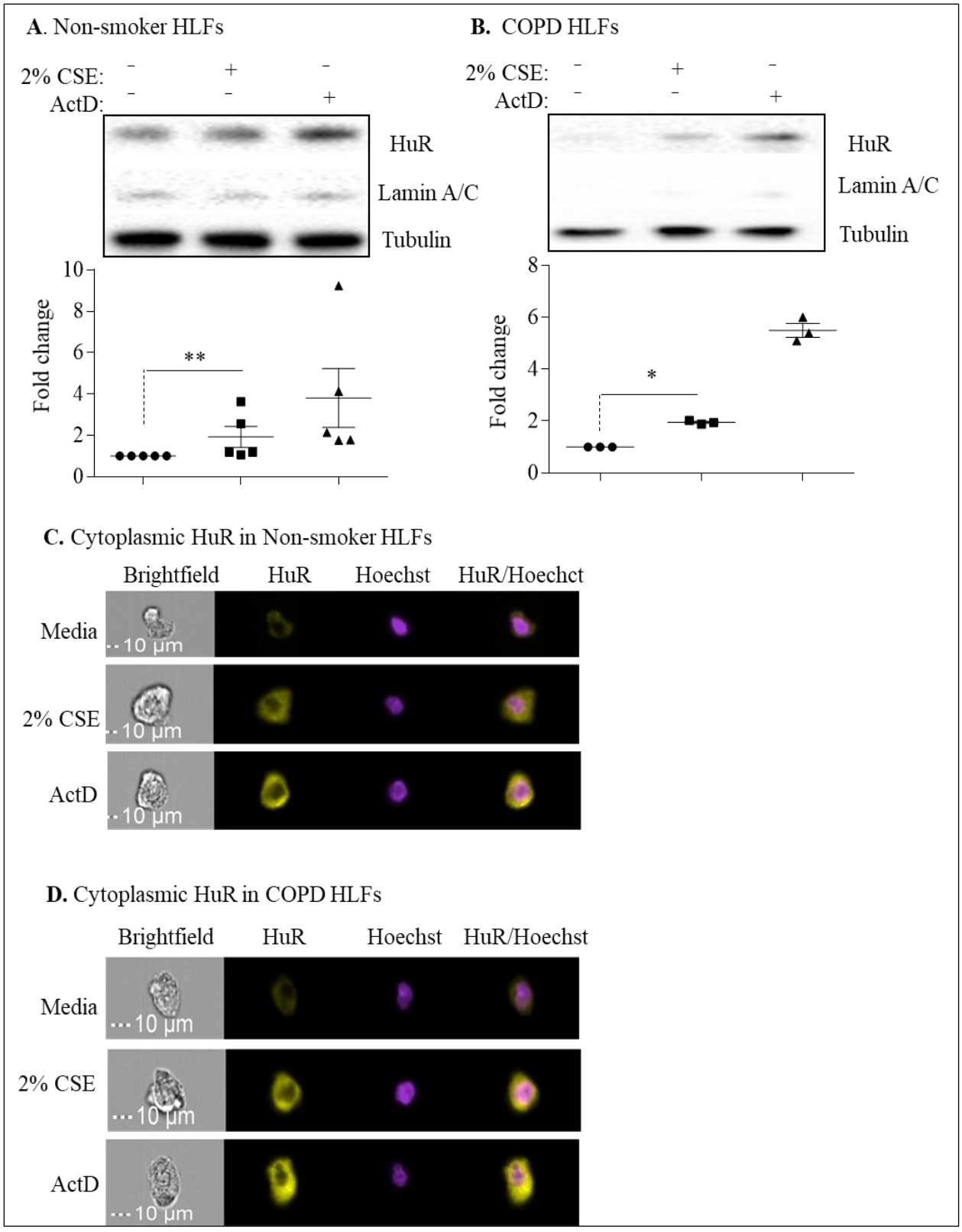

Figure 3.8. Cytoplasmic HuR is increased by cigarette smoke.

A. Cytoplasmic HuR in non-smoker HLFs: there was an increase in HuR cytoplasmic localization in response to 2% CSE for 4 h (** $p = 0.004$). Actinomycin D (ActD) was used as positive control for the translocation of HuR. Lamin A/C is a nuclear marker, while tubulin is a cytoplasmic marker. Results are expressed as the mean ± SEM of 5 independent experiments. **B.** COPD HLFs: there was an increase in HuR cytoplasmic localization in response to 2% CSE for 4 h (* $p < 0.05$). Results are expressed as the mean ± SEM of 3 independent experiments. Data between untreated and CSE-exposed cells were analyzed by a Mann–Whitney one-tailed t-test. **C.** Cytoplasmic HuR in non-smoker HLFs: HuR localization in non-smoker HLFs treated with 2% CSE was assessed by Imaging Flow Cytometry. There was an increase in HuR expression in response to 2% CSE for 4 h. ActD was used as a positive control for HuR translocation into the cytoplasm. A representative picture for cells is shown from 2 independent experiments. **D.** Cytoplasmic HuR in COPD HLFs: there was an increase in HuR expression in the cytoplasm of COPD HLFs exposed to 2% CSE for 4 h. A representative picture for cells is shown from one COPD subject.

Finally, we conducted knockdown experiments to evaluate if HuR regulates ACE2 expression in response to CSE. Verification of HuR knockdown is shown in Figure 3.9A. HuR knockdown had no effect on ACE2 protein or mRNA levels in the absence and presence of CSE exposure (Figure 3.9B and C). Thus, we show the differential expression of ELVAL1 (HuR) in lung cell populations and show that the regulation of ACE2 is unlikely to be mediated by HuR despite activation of HuR by cigarette smoke. Further insight into the molecular regulation of ACE2 is needed to facilitate the development of new medications to combat coronavirus infections.

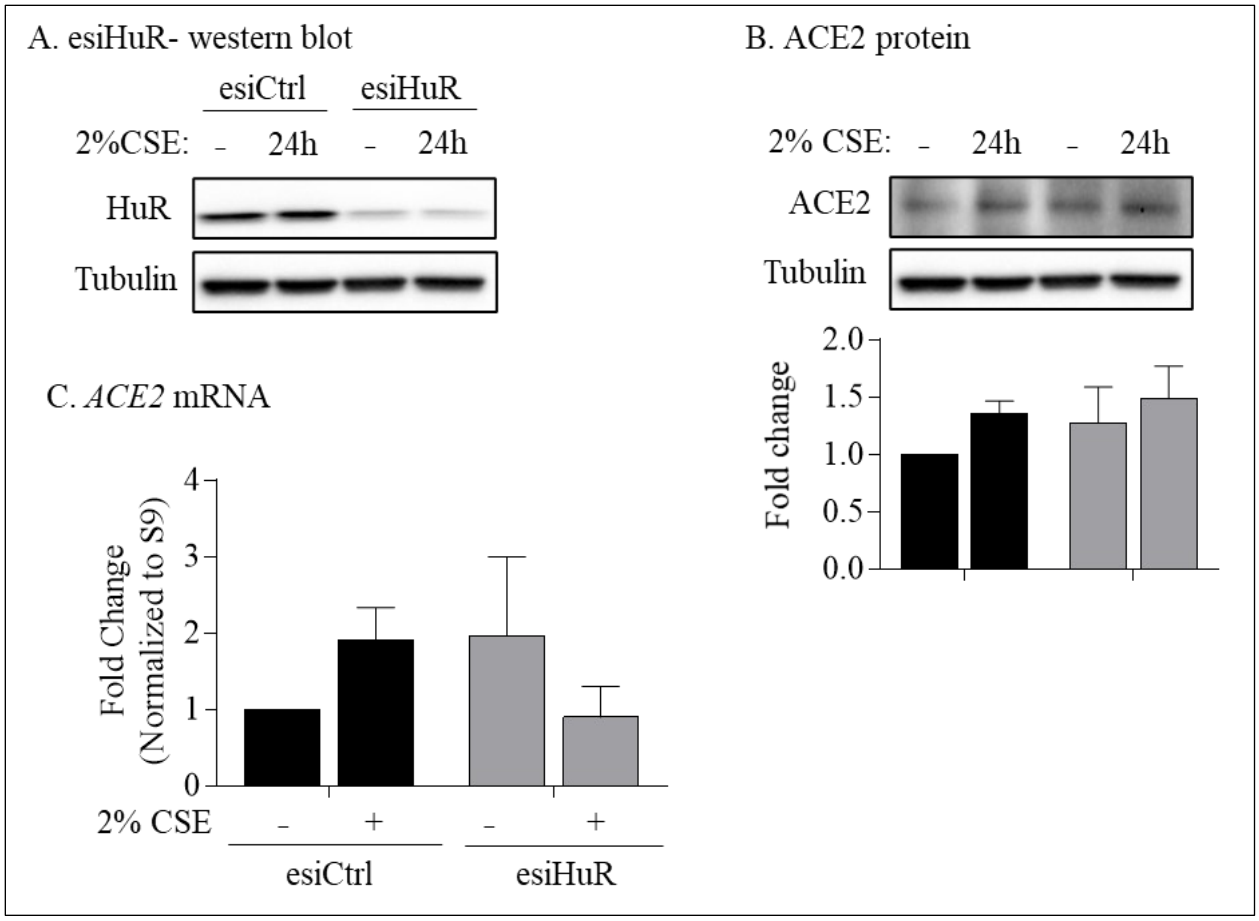

Figure 3.9. HuR silencing does not affect protein and mRNA expression of ACE2.

A. HuR protein—Western blot: transfection of non-smoker HLFs with esiHuR reduced the level of HuR protein by ~80%. **B.** ACE2 protein: there was no significant difference in ACE2 protein levels in esiHuR-transfected HLFs exposed to 2% CSE for 24 h compared to untreated esiHuR-transfected cells and to esiCtrl-transfected cells. Results are expressed as the mean ± SEM of 3 independent experiments (HLFs used from one non-smoker subject). **C.** *ACE2* mRNA: there was no significant difference in *ACE2* mRNA in esiHuR-transfected HLFs exposed to 2% CSE for 24 h compared to untreated esiHuR-transfected cells and to esiCtrl-transfected cells. Results are expressed as the mean ± SEM of 3 independent experiments (HLFs used from one non-smoker subject).

3.5. DISCUSSION

COPD is a major health problem with limited therapeutic options [1] that is primarily caused by cigarette smoke exposure [4]. COPD patients may be at risk of increased hospitalization and severe illness from COVID-19 caused by SARS-CoV-2 [5]. One possible reason behind increased susceptibility may be the upregulation of ACE2, the entry receptor for SARS-CoV-2 [6,7]. However, the mechanism(s) involved in the upregulation of ACE2 are poorly understood. Therefore, in this study, we investigated the role of HuR in the regulation of pulmonary ACE2. We also sought to comprehensively profile the expression of HuR/*ELAVL1* in the various cells of lungs from COPD and COVID-19 patients. Further, we predicted HuR would regulate expression of the ACE2 protein. Herein, we describe the differential regulation of *ELAVL1* in distinct populations of pulmonary cells and the extensive cytoplasmic localization of HuR in COPD lungs. We found that there was a significant positive correlation between *ELAVL1* and *ACE2* in COPD. While we speculate that the increased cytoplasmic HuR in COPD lungs drives features of disease pathology (e.g., inflammation), our data show that HuR is not likely to be involved in the regulation of ACE2 protein expression.

Our rationale for focusing on HuR is the fact that RBPs regulate mRNA post-transcriptional events of genes involved in various cellular mechanisms [43,44], including viral infection [45]. A recent study showed that SARS-CoV-2 RNA binds to 104 human proteins, including ribosomal proteins, translation factors, and RBPs [46]. Cellular nucleic acid-binding protein (CNBP) is one of the direct interactors with SARS-CoV-2 RNA. Another RBP that binds to SARS-CoV-2 RNA is la-related protein 1 (LARP1). In a LARP1 knockout cell line, intracellular viral RNA and the infectious virus production are elevated. In contrast, LARP1 overexpression

decreases viral RNA and the levels of infectious virus [46]. Furthermore, the alphavirus Sindbis virus, a single-stranded positive-sense RNA virus that contains multiple U-rich elements, recruits cellular HuR to stabilize its viral RNA to aid in the expression viral proteins and maintain infection. Sindbis virus infection also induces HuR cytoplasmic translocation where the viral RNAs accumulate [47]. HuR also associates with the U-rich elements of hepatitis C virus (HCV) RNA [48] and the late regulatory element (LRE) of human papillomaviruse 16 (HPV16), with HuR depletion reducing L1 capsid protein expression [49]. Because Sindbis virus has high affinity to HuR, it sequestrates HuR in the cytoplasm. Consequently, the alternative pre-mRNA polyadenylation and splicing of cellular pre-mRNAs as well as the stability of a subset of cellular mRNAs are dysregulated during Sindbis virus infection [50]. These studies provide rationale for investigating the function of RBPs in the context of viral infection, and they may be crucial to our understanding of infectivity, particularly in light of the ongoing COVID-19 pandemic.

We found that cytoplasmic localization of HuR is increased in lung structural cells, mainly epithelial cells and fibroblasts, in lung tissue from smoker and COPD subjects. These findings recapitulate those of a previous study showing cytoplasmic HuR is elevated in lung tissue from smoker and COPD patients [51] and suggests that smoking itself influences the cellular localization of HuR in the lung. We also found that macrophages from smoker and COPD subjects have higher cytoplasmic localization of HuR compared to macrophages from non-smokers. Macrophages are involved in the pathophysiology of COPD via the production of inflammatory mediators and proteases [52]. Alveolar macrophages are also involved in the pathogenesis of SARS-CoV-2 [53]. Matrix metalloproteinase-9 (MMP-9) is increased in COPD and by SARS-CoV-2 infection that may be involved in alveolar destruction [54,55]. HuR stabilizes MMP-9

mRNA and induces its protein expression [56]. Increased cytoplasmic expression of HuR also stabilizes tumor necrosis factor-α (TNF-α) and interlukin-6 (Il-6) mRNA in macrophages [57], two pro-inflammatory mediators that are also increased in COPD and SARS-CoV-2 infection [54,58]. HuR may also be involved in the pathogenesis of COVID-19 by its ability to increase inflammation, as SARS-CoV-2 infection induces TNF-α, IL-6, and CC-chemokine ligand 2 (CCL2) [58,59].

Although *ELAVL1* mRNA is significantly increased in COPD compared to smoker, the protein levels are similar between the two groups. This decoupling of protein and mRNA expression in COPD suggests that elevated mRNA levels in COPD might because of the increase in *ELAVL1* transcription and/or its mRNA stability. However, the regulation of *ELAVL1* at transcriptional and/or at post-transcriptional levels in smoker and COPD is not known yet. Other possible mechanism by which *ELAVL1* mRNA levels may rise in the absence of their translation is the sequestration of these transcripts in stress granules (SGs), which are cytoplasmic ribonucleoprotein complexes that assemble in response to stress and sequester mRNAs [60]. Currently, we do not know about SGs assembly during cigarette smoke exposure and in COPD.

Our notion that HuR could also control ACE2 expression was based in part on our recent report demonstrating increased ACE2 expression in COPD-derived lung fibroblasts, and that pulmonary ACE2 protein increases in response to chronic cigarette smoke exposure [9]. Lung fibroblasts provide structure and support to the lungs by synthesizing and maintaining an extracellular matrix (ECM) [61], and in the context of chronic inflammation, activation of

fibroblasts leads to the production of several cytokines and chemokines [62]. We found that CSE induced HuR translocation to the cytoplasm and that HuR binds to *ACE2* mRNA in lung fibroblasts from smoker, but silencing HuR had no effect on *ACE2* mRNA and protein. This is consistent with a previous observation that HuR binds to *PTGS2* mRNA in muscle cells treated with tumor necrosis factor alpha (TNF-α) and interferon gamma (IFN-γ). However, knockdown of HuR had no effect on PTGS2/COX-2 protein in these conditions [63]. Interestingly, independent study observed that HuR binds to *PTGS2* mRNA and HuR silencing decreases the expression of PTGS2/COX-2 in human colon carcinoma cells [64]. These data suggest that HuR does not directly regulate ACE2 expression in human lung fibroblasts with/without CSE, but it might regulate ACE2 expression in other conditions.

Furthermore, it is possible that ACE2 is regulated by RBPs other than HuR, such as the heterogeneous nuclear ribonucleoprotein F (hnRNP F). Overexpression of hnRNP F induces the transcription of renal *ACE2* gene, suppresses profibrotic genes (*TGF-β1*, *TGF-βrII*), and prevents renal fibrosis [65]. Another possibility is that ACE2 is regulated post-transcriptionally by miRNA, which are short noncoding RNAs that influence gene expression by controlling mRNA stability or by interfering with translation [66,67]. This is supported by the observation that in primary human cardiac myofibroblasts, miR-421 binds to *ACE2* to down-regulate protein levels [68]. Interestingly, miR-421 is downregulated in mouse lungs exposed to cigarette smoke [69]. This raises the possibility that the upregulation of pulmonary ACE2 protein in response to cigarette smoke and/or in the context of COPD could be due the downregulation of miR-421.

In addition to cellular localization, the cleavage of HuR may also affect cellular function. In this regard, we found significant differences in HuR protein cleavage, with cleaved HuR (CP-1) being observed in smoker and COPD HLFs but not in non-smoker HLFs. This suggests that smoking itself results in HuR cleavage. To this effect, in vitro administration of CSE induced the cleavage of HuR. Cleavage of HuR protein into two fragments (CP-1, 27 kDa, and CP-2, 8 kDa) occurs in response to lethal cellular damage [42,70]. These HuR fragments are involved in apoptosis through the regulation of proapoptotic mRNAs, such as caspase-9 (*CASP9*) [42,70,71]. Given that apoptotic cell death is increased in COPD and in response to cigarette smoke as well as in the SARS-CoV-2 infection [59,72,73], it is possible that cleaved HuR expression in smoker and COPD-derived cells is driving an apoptotic phenotype and consequent lung damage in these diseases. Thus, increased cleaved HuR (CP-1) in smokers and COPD subjects may exacerbate cell death associated with SARS-CoV-2 infection, and warrants further exploration.

In summary, our work is the first to investigate the possible link between HuR and ACE2, information that is important in light of the ongoing COVID-19 pandemic. Although our data do not support a role for HuR in controlling ACE2 expression in lung fibroblasts, our study enables investigators to focus on other possible pathways, such as miRNAs, that may regulate ACE2 in the lung. We should emphasize that our conclusion, regarding the lack of a critical role for HuR in the regulation of ACE2 expression, applies only to lung fibroblasts. Further studies should be dedicated to evaluating possible role for HuR in the regulation of ACE2 expression in pulmonary and airway epithelial cells, as these cells are the port of entry of SARS-CoV-2 into the respiratory system. It should also be noted that our study demonstrates that cytoplasmic HuR is elevated in COPD lungs and that cigarette smoke induces its cleavage, a finding that may implicate HuR in

the pathogenesis of both COPD and COVID-19 through the regulation of pro-inflammatory and pro-apoptotic genes that can damage the lungs. As such, our findings also point to HuR as a novel therapeutic target to combat a chronic lung disease with high morbidity and mortality, such as COPD. Further studies to mechanistically evaluate the contribution of HuR in the context of smoke-related pathologies are warranted.

Author Contributions

Conceptualization, N.A. and C.J.B.; data curation, N.A., Z.H. and J.D.; formal analysis, N.A., Z.H., J.D. and A.B.; funding acquisition, C.J.B.; investigation, N.A., S.N.H. and C.J.B.; methodology, N.A., J.D., I.-E.G. and S.D.M.; project administration, C.J.B.; resources, P.N. and I.-E.G.; supervision, D.H.E. and C.J.B.; visualization, N.A. and C.J.B.; writing—original draft, N.A. and Z.H.; writing—review and editing, J.D., P.N., A.B., D.H.E., I.-E.G., S.D.M., S.N.H. and C.J.B. All authors have read and agreed to the published version of the manuscript.

Institutional Review Board Statement

This study was approved by the Research Ethics Board of St. Joseph's Healthcare Hamilton.

Informed Consent Statement

Written informed consent has been obtained from the patient(s) to publish this paper.

Conflicts of Interest

The authors declare no conflict of interest.

3.6. REFERENCES

1. Lange, P.; Celli, B.; Agusti, A.; Boje Jensen, G.; Divo, M.; Faner, R.; Guerra, S.; Marott, J.L.; Martinez, F.D.; Martinez-Camblor, P.; et al. Lung-Function Trajectories Leading to Chronic Obstructive Pulmonary Disease. *N. Engl. J. Med.* **2015**, *373*, 111–122.
2. Report, W.H. Available online: **https://www.who.int/en/news-room/fact-sheets/detail/the-top-10-causes-of-death** (accessed on 20 December 2020).
3. Global Strategy for the Diagnosis. Global Initiative for Chronic Obstructive Lung Disease (GOLD). 2020. Available online: **https://goldcopd.org/** (accessed on 20 December 2020).
4. Athanazio, R. Airway disease: Similarities and differences between asthma, COPD and bronchiectasis. *Clinics* **2012**, *67*, 1335–1343.
5. Attaway, A.A.; Zein, J.; Hatipoglu, U.S. SARS-CoV-2 infection in the COPD population is associated with increased healthcare utilization: An analysis of Cleveland clinic's COVID-19 registry. *EClinicalMedicine* **2020**, *26*, 100515.
6. Zhou, P.; Yang, X.L.; Wang, X.G.; Hu, B.; Zhang, L.; Zhang, W.; Si, H.R.; Zhu, Y.; Li, B.; Huang, C.L.; et al. A pneumonia outbreak associated with a new coronavirus of probable bat origin. *Nature* **2020**, *579*, 270–273.
7. Hoffmann, M.; Kleine-Weber, H.; Schroeder, S.; Kruger, N.; Herrler, T.; Erichsen, S.; Schiergens, T.S.; Herrler, G.; Wu, N.H.; Nitsche, A.; et al. SARS-CoV-2 Cell Entry Depends on ACE2 and TMPRSS2 and Is Blocked by a Clinically Proven Protease Inhibitor. *Cell* **2020**, *181*, 271–280.e8.
8. Hamming, I.; Timens, W.; Bulthuis, M.L.; Lely, A.T.; Navis, G.; van Goor, H. Tissue distribution of ACE2 protein, the functional receptor for SARS coronavirus. A first step in understanding SARS pathogenesis. *J. Pathol.* **2004**, *203*, 631–637.
9. Aloufi, N.; Traboulsi, H.; Ding, J.; Fonseca, G.J.; Nair, P.; Huang, S.K.; Hussain, S.N.A.; Eidelman, D.H.; Baglole, C.J. Angiotensin-converting enzyme 2 expression in COPD and IPF fibroblasts: The forgotten cell in COVID-19. *Am. J. Physiol. Lung Cell. Mol. Physiol.* **2021**, *320*, L152–L157.
10. Leung, J.M.; Yang, C.X.; Tam, A.; Shaipanich, T.; Hackett, T.L.; Singhera, G.K.; Dorscheid, D.R.; Sin, D.D. ACE-2 expression in the small airway epithelia of smokers and COPD patients: Implications for COVID-19. *Eur. Respir. J.* **2020**, *55*, 2000688.
11. Brake, S.J.; Barnsley, K.; Lu, W.; McAlinden, K.D.; Eapen, M.S.; Sohal, S.S. Smoking Upregulates Angiotensin-Converting Enzyme-2 Receptor: A Potential Adhesion Site for Novel Coronavirus SARS-CoV-2 (COVID-19). *J. Clin. Med.* **2020**, *9*, 841.
12. Zhang, H.; Rostami, M.R.; Leopold, P.L.; Mezey, J.G.; O'Beirne, S.L.; Strulovici-Barel, Y.; Crystal, R.G. Expression of the SARS-CoV-2 ACE2 Receptor in the Human Airway Epithelium. *Am. J. Respir. Crit. Care Med.* **2020**, *202*, 219–229.
13. Lumbers, E.R.; Delforce, S.J.; Pringle, K.G.; Smith, G.R. The Lung, the Heart, the Novel Coronavirus, and the Renin-Angiotensin System; The Need for Clinical Trials. *Front. Med.* **2020**, *7*, 248.
14. Imai, Y.; Kuba, K.; Penninger, J.M. Angiotensin-converting enzyme 2 in acute respiratory distress syndrome. *Cell. Mol. Life Sci.* **2007**, *64*, 2006–2012.
15. Sparks, M.A.; Crowley, S.D.; Gurley, S.B.; Mirotsou, M.; Coffman, T.M. Classical Renin-Angiotensin system in kidney physiology. *Compr. Physiol.* **2014**, *4*, 1201–1228.
16. Lelis, D.F.; Freitas, D.F.; Machado, A.S.; Crespo, T.S.; Santos, S.H.S. Angiotensin-(1-7), Adipokines and Inflammation. *Metabolism* **2019**, *95*, 36–45.

17. Patel, V.B.; Zhong, J.C.; Grant, M.B.; Oudit, G.Y. Role of the ACE2/Angiotensin 1-7 Axis of the Renin-Angiotensin System in Heart Failure. *Circ. Res.* **2016**, *118*, 1313–1326.
18. Engin, A.B.; Engin, E.D.; Engin, A. Two important controversial risk factors in SARS-CoV-2 infection: Obesity and smoking. *Environ. Toxicol. Pharmacol.* **2020**, *78*, 103411.
19. Smith, J.C.; Sausville, E.L.; Girish, V.; Yuan, M.L.; Vasudevan, A.; John, K.M.; Sheltzer, J.M. Cigarette smoke exposure and inflammatory signaling increase the expression of the SARS-CoV-2 receptor ACE2 in the respiratory tract. *Dev. Cell.* **2020**, *53*, 514–529.
20. Jacobs, M.; Van Eeckhoutte, H.P.; Wijnant, S.R.A.; Janssens, W.; Joos, G.F.; Brusselle, G.G.; Bracke, K.R. Increased expression of ACE2, the SARS-CoV-2 entry receptor, in alveolar and bronchial epithelium of smokers and COPD subjects. *Eur. Respir. J.* **2020**, *56*, 2002378.
21. Shen, H.; Zhang, J.; Wang, C.; Jain, P.P.; Xiong, M.; Shi, X.; Lei, Y.; Chen, S.; Yin, Q.; Thistlethwaite, P.A.; et al. MDM2-Mediated Ubiquitination of Angiotensin-Converting Enzyme 2 Contributes to the Development of Pulmonary Arterial Hypertension. *Circulation* **2020**, *142*, 1190–1204.
22. Garcia-Maurino, S.M.; Rivero-Rodriguez, F.; Velazquez-Cruz, A.; Hernandez-Vellisca, M.; Diaz-Quintana, A.; De la Rosa, M.A.; Diaz-Moreno, I. RNA Binding Protein Regulation and Cross-Talk in the Control of AU-rich mRNA Fate. *Front. Mol. Biosci.* **2017**, *4*, 71.
23. Song, J.; Qu, H.; Hu, B.; Bi, C.; Li, M.; Wang, L.; Huang, X.; Zhang, M. Physiological cyclic stretch up-regulates angiotensin-converting enzyme 2 expression to reduce proliferation and migration of vascular smooth muscle cells. *Biosci. Rep.* **2020**, *40*, BSR20192012.
24. Srikantan, S.; Gorospe, M. HuR function in disease. *Front. Biosci. Landmark Ed.* **2012**, *17*, 189.
25. Grammatikakis, I.; Abdelmohsen, K.; Gorospe, M. Posttranslational control of HuR function. *Wiley Interdiscip. Rev. RNA* **2017**, *8*, e1372.
26. Izquierdo, J.M. Hu antigen R (HuR) functions as an alternative pre-mRNA splicing regulator of Fas apoptosis-promoting receptor on exon definition. *J. Biol. Chem.* **2008**, *283*, 19077–19084.
27. Brennan, C.M.; Steitz, J.A. HuR and mRNA stability. *Cell. Mol. Life Sci.* **2001**, *58*, 266–277.
28. Zago, M.; Sheridan, J.A.; Nair, P.; Rico de Souza, A.; Gallouzi, I.E.; Rousseau, S.; Di Marco, S.; Hamid, Q.; Eidelman, D.H.; Baglole, C.J. Aryl hydrocarbon receptor-dependent retention of nuclear HuR suppresses cigarette smoke-induced cyclooxygenase-2 expression independent of DNA-binding. *PLoS ONE* **2013**, *8*, e74953.
29. Adams, T.S.; Schupp, J.C.; Poli, S.; Ayaub, E.A.; Neumark, N.; Ahangari, F.; Chu, S.G.; Raby, B.A.; DeIuliis, G.; Januszyk, M.; et al. Single-cell RNA-seq reveals ectopic and aberrant lung-resident cell populations in idiopathic pulmonary fibrosis. *Sci. Adv.* **2020**, *6*, eaba1983.
30. Chua, R.L.; Lukassen, S.; Trump, S.; Hennig, B.P.; Wendisch, D.; Pott, F.; Debnath, O.; Thurmann, L.; Kurth, F.; Volker, M.T.; et al. COVID-19 severity correlates with airway epithelium-immune cell interactions identified by single-cell analysis. *Nat. Biotechnol.* **2020**, *38*, 970–979.
31. Wolf, F.A.; Angerer, P.; Theis, F.J. SCANPY: Large-scale single-cell gene expression data analysis. *Genome Biol.* **2018**, *19*, 15.

32. Guerrina, N.; Traboulsi, H.; Rico de Souza, A.; Bosse, Y.; Thatcher, T.H.; Robichaud, A.; Ding, J.; Li, P.Z.; Simon, L.; Pareek, S.; et al. Aryl hydrocarbon receptor deficiency causes the development of chronic obstructive pulmonary disease through the integration of multiple pathogenic mechanisms. *FASEB J.* **2021**, *35*, e21376.
33. Baglole, C.J.; Reddy, S.Y.; Pollock, S.J.; Feldon, S.E.; Sime, P.J.; Smith, T.J.; Phipps, R.P. Isolation and phenotypic characterization of lung fibroblasts. *Methods Mol. Med.* **2005**, *117*, 115–127.
34. Hecht, E.; Zago, M.; Sarill, M.; Rico de Souza, A.; Gomez, A.; Matthews, J.; Hamid, Q.; Eidelman, D.H.; Baglole, C.J. Aryl hydrocarbon receptor-dependent regulation of miR-196a expression controls lung fibroblast apoptosis but not proliferation. *Toxicol. Appl. Pharmacol.* **2014**, *280*, 511–525.
35. Keene, J.D.; Komisarow, J.M.; Friedersdorf, M.B. RIP-Chip: The isolation and identification of mRNAs, microRNAs and protein components of ribonucleoprotein complexes from cell extracts. *Nat. Protoc.* **2006**, *1*, 302–307.
36. Mubaid, S.; Ma, J.F.; Omer, A.; Ashour, K.; Lian, X.J.; Sanchez, B.J.; Robinson, S.; Cammas, A.; Dormoy-Raclet, V.; Di Marco, S.; et al. HuR counteracts miR-330 to promote STAT3 translation during inflammation-induced muscle wasting. *Proc. Natl. Acad. Sci. USA* **2019**, *116*, 17261–17270.
37. Hyman, R.W.; Davidson, N. Kinetics of the in vitro inhibition of transcription by actinomycin. *J. Mol. Biol.* **1970**, *50*, 421–438.
38. Guerrina, N.; Aloufi, N.; Shi, F.; Prasade, K.; Mehrotra, C.; Traboulsi, H.; Matthews, J.; Eidelman, D.H.; Hamid, Q.; Baglole, C.J. The aryl hydrocarbon receptor reduces LC3II expression and controls endoplasmic reticulum stress. *Am. J. Physiol. Lung Cell. Mol. Physiol.* **2021**, *320*, L339–L355.
39. Schneider-Poetsch, T.; Ju, J.; Eyler, D.E.; Dang, Y.; Bhat, S.; Merrick, W.C.; Green, R.; Shen, B.; Liu, J.O. Inhibition of eukaryotic translation elongation by cycloheximide and lactimidomycin. *Nat. Chem. Biol.* **2010**, *6*, 209–217.
40. Baglole, C.J.; Maggirwar, S.B.; Gasiewicz, T.A.; Thatcher, T.H.; Phipps, R.P.; Sime, P.J. The aryl hydrocarbon receptor attenuates tobacco smoke-induced cyclooxygenase-2 and prostaglandin production in lung fibroblasts through regulation of the NF-kappaB family member RelB. *J. Biol. Chem.* **2008**, *283*, 28944–28957.
41. Naderi, N.; Farias, R.; Abou Rjeili, M.; Mostafavi-Pour-Manshadi, S.M.; Krishnan, S.; Li, P.Z.; Baglole, C.J.; Bourbeau, J. Investigating the effect of pretreatment with azithromycin on inflammatory mediators in bronchial epithelial cells exposed to cigarette smoke. *Exp. Lung Res.* **2021**, *47*, 98–109.
42. Mazroui, R.; Di Marco, S.; Clair, E.; von Roretz, C.; Tenenbaum, S.A.; Keene, J.D.; Saleh, M.; Gallouzi, I.E. Caspase-mediated cleavage of HuR in the cytoplasm contributes to pp32/PHAP-I regulation of apoptosis. *J. Cell Biol.* **2008**, *180*, 113–127.
43. Corley, M.; Burns, M.C.; Yeo, G.W. How RNA-Binding Proteins Interact with RNA: Molecules and Mechanisms. *Mol. Cell* **2020**, *78*, 9–29.
44. Dreyfuss, G.; Kim, V.N.; Kataoka, N. Messenger-RNA-binding proteins and the messages they carry. *Nat. Rev. Mol. Cell. Biol.* **2002**, *3*, 195–205.
45. Garcia-Moreno, M.; Jarvelin, A.I.; Castello, A. Unconventional RNA-binding proteins step into the virus-host battlefront. *Wiley Interdiscip. Rev. RNA* **2018**, *9*, e1498.

46. Schmidt, N.; Lareau, C.A.; Keshishian, H.; Ganskih, S.; Schneider, C.; Hennig, T.; Melanson, R.; Werner, S.; Wei, Y.; Zimmer, M.; et al. The SARS-CoV-2 RNA-protein interactome in infected human cells. *Nat. Microbiol.* **2020**, *6*, 339–353.
47. Sokoloski, K.J.; Dickson, A.M.; Chaskey, E.L.; Garneau, N.L.; Wilusz, C.J.; Wilusz, J. Sindbis virus usurps the cellular HuR protein to stabilize its transcripts and promote productive infections in mammalian and mosquito cells. *Cell Host Microbe* **2010**, *8*, 196–207.
48. Spangberg, K.; Wiklund, L.; Schwartz, S. HuR, a protein implicated in oncogene and growth factor mRNA decay, binds to the 3′ ends of hepatitis C virus RNA of both polarities. *Virology* **2000**, *274*, 378–390.
49. Cumming, S.A.; Chuen-Im, T.; Zhang, J.; Graham, S.V. The RNA stability regulator HuR regulates L1 protein expression in vivo in differentiating cervical epithelial cells. *Virology* **2009**, *383*, 142–149.
50. Barnhart, M.D.; Moon, S.L.; Emch, A.W.; Wilusz, C.J.; Wilusz, J. Changes in cellular mRNA stability, splicing, and polyadenylation through HuR protein sequestration by a cytoplasmic RNA virus. *Cell Rep.* **2013**, *5*, 909–917.
51. Sun, J.; Gu, X.; Wu, N.; Zhang, P.; Liu, Y.; Jiang, S. Human antigen R enhances the epithelial-mesenchymal transition via regulation of ZEB-1 in the human airway epithelium. *Respir. Res.* **2018**, *19*, 109.
52. Vlahos, R.; Bozinovski, S. Role of alveolar macrophages in chronic obstructive pulmonary disease. *Front. Immunol.* **2014**, *5*, 435.
53. Lv, J.; Wang, Z.; Qu, Y.; Zhu, H.; Zhu, Q.; Tong, W.; Bao, L.; Lv, Q.; Cong, J.; Li, D.; et al. Distinct uptake, amplification, and release of SARS-CoV-2 by M1 and M2 alveolar macrophages. *Cell Discov.* **2021**, *7*, 24.
54. Barnes, P.J. Inflammatory mechanisms in patients with chronic obstructive pulmonary disease. *J. Allergy Clin. Immunol.* **2016**, *138*, 16–27.
55. Ueland, T.; Holter, J.C.; Holten, A.R.; Muller, K.E.; Lind, A.; Bekken, G.K.; Dudman, S.; Aukrust, P.; Dyrhol-Riise, A.M.; Heggelund, L. Distinct and early increase in circulating MMP-9 in COVID-19 patients with respiratory failure. *J. Infect.* **2020**, *81*, e41–e43.
56. Zhang, J.; Modi, Y.; Yarovinsky, T.; Yu, J.; Collinge, M.; Kyriakides, T.; Zhu, Y.; Sessa, W.C.; Pardi, R.; Bender, J.R. Macrophage beta2 integrin-mediated, HuR-dependent stabilization of angiogenic factor-encoding mRNAs in inflammatory angiogenesis. *Am. J. Pathol.* **2012**, *180*, 1751–1760.
57. Zhou, H.; Jarujaron, S.; Gurley, E.C.; Chen, L.; Ding, H.; Studer, E.; Pandak, W.M., Jr.; Hu, W.; Zou, T.; Wang, J.Y.; et al. HIV protease inhibitors increase TNF-alpha and IL-6 expression in macrophages: Involvement of the RNA-binding protein HuR. *Atherosclerosis* **2007**, *195*, e134–e143.
58. Merad, M.; Martin, J.C. Pathological inflammation in patients with COVID-19: A key role for monocytes and macrophages. *Nat. Rev. Immunol.* **2020**, *20*, 355–362.
59. Li, S.; Zhang, Y.; Guan, Z.; Li, H.; Ye, M.; Chen, X.; Shen, J.; Zhou, Y.; Shi, Z.L.; Zhou, P.; et al. SARS-CoV-2 triggers inflammatory responses and cell death through caspase-8 activation. *Signal. Transduct. Target Ther.* **2020**, *5*, 235.
60. Mahboubi, H.; Stochaj, U. Cytoplasmic stress granules: Dynamic modulators of cell signaling and disease. *Biochim. Biophys. Acta Mol. Basis Dis.* **2017**, *1863*, 884–895.
61. White, E.S. Lung extracellular matrix and fibroblast function. *Ann. Am. Thorac. Soc.* **2015**, *12* (Suppl. S1), S30–S33.

62. Buckley, C.D.; Pilling, D.; Lord, J.M.; Akbar, A.N.; Scheel-Toellner, D.; Salmon, M. Fibroblasts regulate the switch from acute resolving to chronic persistent inflammation. *Trends Immunol.* **2001**, *22*, 199–204.
63. Di Marco, S.; Mazroui, R.; Dallaire, P.; Chittur, S.; Tenenbaum, S.A.; Radzioch, D.; Marette, A.; Gallouzi, I.E. NF-kappa B-mediated MyoD decay during muscle wasting requires nitric oxide synthase mRNA stabilization, HuR protein, and nitric oxide release. *Mol. Cell. Biol.* **2005**, *25*, 6533–6545.
64. Doller, A.; Winkler, C.; Azrilian, I.; Schulz, S.; Hartmann, S.; Pfeilschifter, J.; Eberhardt, W. High-constitutive HuR phosphorylation at Ser 318 by PKC {delta} propagates tumor relevant functions in colon carcinoma cells. *Carcinogenesis* **2011**, *32*, 676–685.
65. Lo, C.S.; Shi, Y.; Chang, S.Y.; Abdo, S.; Chenier, I.; Filep, J.G.; Ingelfinger, J.R.; Zhang, S.L.; Chan, J.S. Overexpression of heterogeneous nuclear ribonucleoprotein F stimulates renal Ace-2 gene expression and prevents TGF-beta1-induced kidney injury in a mouse model of diabetes. *Diabetologia* **2015**, *58*, 2443–2454.
66. Kawamata, T.; Tomari, Y. Making RISC. *Trends Biochem. Sci.* **2010**, *35*, 368–376.
67. Fabian, M.R.; Sonenberg, N.; Filipowicz, W. Regulation of mRNA translation and stability by microRNAs. *Annu. Rev. Biochem.* **2010**, *79*, 351–379.
68. Lambert, D.W.; Lambert, L.A.; Clarke, N.E.; Hooper, N.M.; Porter, K.E.; Turner, A.J. Angiotensin-converting enzyme 2 is subject to post-transcriptional regulation by miR-421. *Clin. Sci.* **2014**, *127*, 243–249.
69. Izzotti, A.; Larghero, P.; Longobardi, M.; Cartiglia, C.; Camoirano, A.; Steele, V.E.; De Flora, S. Dose-responsiveness and persistence of microRNA expression alterations induced by cigarette smoke in mouse lung. *Mutat. Res.* **2011**, *717*, 9–16.
70. von Roretz, C.; Gallouzi, I.E. Protein kinase RNA/FADD/caspase-8 pathway mediates the proapoptotic activity of the RNA-binding protein human antigen R (HuR). *J. Biol. Chem.* **2010**, *285*, 16806–16813.
71. von Roretz, C.; Lian, X.J.; Macri, A.M.; Punjani, N.; Clair, E.; Drouin, O.; Dormoy-Raclet, V.; Ma, J.F.; Gallouzi, I.E. Apoptotic-induced cleavage shifts HuR from being a promoter of survival to an activator of caspase-mediated apoptosis. *Cell Death Differ.* **2013**, *20*, 154–168.
72. Chiappara, G.; Gjomarkaj, M.; Sciarrino, S.; Vitulo, P.; Pipitone, L.; Pace, E. Altered expression of p21, activated caspase-3, and PCNA in bronchiolar epithelium of smokers with and without chronic obstructive pulmonary disease. *Exp. Lung Res.* **2014**, *40*, 343–353.
73. Ahmed, A.; Thliveris, J.A.; Shaw, A.; Sowa, M.; Gilchrist, J.; Scott, J.E. Caspase 3 activity in isolated fetal rat lung fibroblasts and rat periodontal ligament fibroblasts: Cigarette smoke induced alterations. *Tob. Induc. Dis.* **2013**, *11*, 25.

PREFACE: CHAPTER IV

In Chapter III, we demonstrated that HuR/*ELAVL1* is expressed throughout the lungs, and its expression and cellular localization is altered in COPD. Here, there was elevated cytoplasmic HuR in cells within smoker and COPD lungs, suggesting its importance in lung disease pathogenesis. However, for HuR to be considered as a novel therapeutic target in COPD, further studies to mechanistically evaluate its contribution in the context of smoke-related pathologies, such as inflammation, is warranted.

Thus, in Chapter IV, we comprehensively explored HuR functions in HLFs using multi-omics approaches to show the importance of HuR in regulating numerous biological processes in response to CS, including inflammation. We have previously shown that lung fibroblasts produce COX-2 in response to CS [15, 59] and that the aryl hydrocarbon receptor (AhR) destabilizes *PTGS2* mRNA by sequestering HuR in the nucleus [290]. HuR can also directly regulates the expression of COX-2 and other inflammatory mediators [243, 298]. It is therefore the identification of these mechanisms could lead to elucidate HuR function in the pathogenesis of CS-related diseases, such as COPD.

CHAPTER IV

4. A multi-omics approach reveals fundamental roles for human antigen R in lung fibroblasts

Noof Aloufi[1,2,3,7], Mikal Hajjar[1,5], Gregory J. Fonseca[1,2,4], Parameswaran Nair[8], David H. Eidelman[1,2,4], and Carolyn J. Baglole[1,2,3,4,5,6*]

[1]Meakins-Christie Laboratories and [2]Translational Research in Respiratory Diseases Program at the Research Institute of the McGill University Health Centre, Departments of [3]Pathology, [4]Medicine, [5]Experimental Medicine and [6]Pharmacology and Therapeutics, McGill University; [7]Departments of Medical Laboratories Technology, Taibah University, Saudi Arabia; [8]Department of Medicine, McMaster University & St Joseph's Healthcare, Hamilton, Ontario, Canada

Correspondence and requests for materials should be addressed to:
*Carolyn J. Baglole
1001 Decarie Blvd (EM22248)
Montreal, Quebec H4A3J1
Telephone: (514) 934-1934 ext. 76109
E-mail: Carolyn.baglole@mcgill.ca

(This research has been prepared as a manuscript for submission, *In Progress*)

Keywords: HuR; fibroblast; inflammation; chronic obstructive pulmonary disease

Acknowledgement: This work was supported by the Canada Foundation for Innovation (CFI) and the Canadian Institutes for Health Research (CIHR). C.J.B. was supported by a salary award from the Fonds de recherche du Quebec-Sante (FRQ-S). N.A was supported by a scholarship from Taibah University, Saudi Arabia.

4.1. ABSTRACT

Human antigen R (HuR) is an RNA-binding protein that exerts post-transcriptional control over the expression of mRNA under physiological conditions and in response to various endogenous and exogenous stimuli. The lungs are an organ system constantly exposed to the external environment. In humans, the lungs contain over 400 million alveoli that covers an estimated surface area of up to 140m^2, with the quality of air greatly impacting our overall health. Exposure to noxious agents in inhaled air can include infectious organisms and air pollution caused by industries, traffic, common occupations, burning of biomass fuel and cigarette smoke (CS). CS remains the leading cause of preventable death worldwide and is the main risk factors for diseases such as lung cancer and chronic obstructive pulmonary disease (COPD). HuR is extensively expressed in the respiratory system and may control numerous pathological processes involved in chronic lung disease development. However, the molecular function of HuR in the lungs is largely unexplored. Herein, we comprehensively evaluated HuR functions in human lung fibroblasts (HLFs) using multi-omics approaches to show the importance of HuR in regulating numerous biological processes in response to CS, including pathways implicated in inflammation and oxidative stress. Thus, HuR plays fundamental roles in maintaining cellular homeostasis in the lungs in response to noxious stimuli, which suggests that therapeutic targeting of HuR may alleviate prevalent and deadly lung diseases.

4.2. INTRODUCTION

The respiratory system is comprised of airways that conduct air to and from the alveoli, the latter being the primary location for gas exchange [1]. There are over 40 types of cells within the respiratory system that contribute to lung structure and function. Among these cells are epithelial cells that line the respiratory tract, interstitial fibroblasts that provide structure, and immune cells, such as alveolar macrophages, that contribute to host defense. These cells not only maintain normal lung physiology but also respond to exogenous stimuli [2, 3]. The lungs are constantly exposed to the external environment, coming into contact with both inhaled pathogens as well as air pollution that is caused by industries, traffic, burning of biomass fuel and cigarette smoke (CS) [3, 4]. The World Health Organization (WHO) estimates that 9 out of 10 people worldwide breathe polluted air [5]; this includes CS, a prevalent respiratory toxicant, that today is still responsible for more than 8 million deaths each year worldwide [6]. Importantly, the carcinogenic and toxic components in CS are similar to that of air pollution [7]. Inhalational exposure to CS activates lung structural and resident immune cells to produce a myriad of inflammatory mediators that initiate a vicious cycle leading to chronic inflammation. Consequently, it is thought that this chronic inflammatory response underlies the development of lung diseases such as lung cancer and chronic obstructive pulmonary disease (COPD) [8-10]. Lung cancer and COPD exert significant morbidity and mortality worldwide and are complex diseases with perturbations in multiple cellular processes including differentiation, proliferation, cell survival, metabolism, and immune function [11-16]. However, the mechanisms through which inhaled toxicants, such as CS, lead to chronic lung disease remain poorly understood.

One potential protein whose dysregulation may alter these numerous cellular and physiological processes that occur in response to CS exposure is human antigen R (HuR) [17-21]. HuR, also known as embryonic lethal abnormal vision-like protein 1 (ELAVL1), is a ubiquitously expressed member in the ELAV family of RNA binding proteins (RBPs) [17, 18]. HuR is best known for its ability to associate with target mRNA within uridylate (U)- or adenylate-uridylate (AU)-rich elements (AREs) located at the 3'-untranslated region (UTR). This binding of HuR to mRNA influences pre-mRNA splicing, nucleocytoplasmic translocation, stability, and translation; the net effect of these underlies the ability of HuR to indirectly alter protein expression at the post-transcriptional level [18, 19, 22]. Under basal conditions, HuR is predominantly nuclear but is transported to the cytoplasm, along with bound mRNA, in response to various endogenous or exogenous stimuli, including CS [17-21]. Numerous mRNAs are regulated by HuR, and the protein products of these mRNA are involved in various cellular mechanisms, including cell proliferation, differentiation, inflammation, wound healing, cell survival, and senescence [17-19, 23-31]. Dysregulation of HuR expression is now well-described in many types of diseases including various cancers such as lung cancer, [24, 32-34]. In this context, HuR is implicated in the pathogenesis and the progression of lung cancer, such that high levels of HuR is associated with metastasis and poor survival [32]. Owing to the association between HuR and lung cancer, it has been suggested that targeting HuR could inhibit lung cancer cell proliferation, migration, and invasion [34]. Thus, HuR could be a novel and a promising therapeutic strategy to treat smoke-related diseases including lung cancer, but also COPD.

Interestingly, and in the context of COPD, we recently profiled HuR/ELAVL1 expression in the lungs via scRNA-seq analysis and found that HuR is present in multiple pulmonary cell

types. We also observed that mesenchymal cells (fibroblasts, myofibroblasts) had relatively high *ELAVL1* expression in COPD [21]. Lung fibroblasts provide structure to the lungs by synthesizing extracellular matrix (ECM) proteins and connecting type II pneumocytes to endothelial cells [35, 36], thereby playing a vital role in fibrotic lung diseases. In addition, their role in regulating immune responses is now being recognized [37]. Moreover, altered fibroblast function and phenotype can contribute to lung damage from CS [38-44]. However, the extent to which HuR controls perturbations in lung cell function- including fibroblasts- caused by CS is largely unexplored. Therefore, we used a combination of molecular silencing of HuR in human lung fibroblasts together with RNA-seq to investigate its role in controlling pathways implicated in the development of chronic lung diseases. Our results show that HuR controls the expression of hundreds of coding RNA that are linked to various pathological processes, including inflammation and oxidative stress, as well as a variety of signaling pathways that are activated in response to CS. As a key feature in the function of HuR is its ability to bind target mRNA, we also show that, under conditions of CS exposure, HuR binds to mRNA that are involved in mRNA maturation and post-translational modification of proteins. Surprisingly, we found that HuR suppresses the induction of two of its well-known targets- cyclooxygenase-2 (PTGS2/COX-2) and interleukin-8 (CXCL8/IL-8)- both at the basal level and in response to CS. COX-2 and IL-8 are among the inflammatory mediators that are increased by CS [41, 45, 46] and play an important role in the pathophysiology of airway diseases including COPD [47-49]. Together, these data highlight the importance of HuR in controlling fundamental cellular mechanisms whose dysregulation is linked to chronic lung disease development, supporting the utility of therapeutically targeting HuR for disease prevention.

4.3. METHODS

Chemicals

All chemicals were obtained from Sigma (St. Louis, MO) unless otherwise indicated. Actinomycin D (ActD) was obtained from Enzo Life Sciences.

Cell Culture

This study was approved by the Research Ethics Board of St Joseph's Healthcare Hamilton (00-1839). Primary human lung fibroblasts (HLFs) were isolated from cancer-free lung tissue by explant procedure [50]. Characterization of the fibroblasts is as previously described [50, 51]. Experiments were conducted with fibroblasts from three different individuals of non-smoker group (Normal; M/F = 1/2; age 68 ± 9 years) and within the passage five to nine.

Preparation of Cigarette Smoke Extract (CSE)

Research grade cigarettes (3R4F) with a filter were acquired from the Kentucky Tobacco Research Council (Lexington, KT). Each cigarette contains 0.73 mg of nicotine, 9.4 mg of tar, and 12.0 mg of CO as described by the manufacturer. CSE was produced as previously described [20, 45]. Briefly, CSE was prepared by bubbling smoke from a cigarette through 15 ml of serum-free MEM, sterile-filtering with a 0.45-μm filter (25-mm Acrodisc; Pall Corp., Ann Arbor, MI) and was used within 30 minutes of preparation. An optical density of 0.65 (320 nm) was regarded as 100% CSE [20, 45] which was diluted in serum-free MEM to the appropriate concentration.

HuR knock-down by siRNA

HLFs were seeded at 10x104 cells/cm2 and transfected with 60 nM of siRNA against HuR (siHuR, Santa Cruz, CA) or non-targeting control siRNA (siCtrl, Santa Cruz, CA) in accordance with manufacturer's instructions. Six hours after the transfection, 20% MEM was added on the cells. After 24 hours, the cells were treated with serum-free MEM for 18h, followed by exposure to 2% CSE. HLFs were also transfected with 60 pmol of endoribonuclease prepared siRNA (esiRNA) against ELAVL1 (MISSION® esiRNA, Sigma) or non-targeting control esiRNA (MISSION® esiRNA, Sigma) using Lipofectamine RNAiMAX transfection reagent (ThermoFisher) in accordance with manufacturer's instructions. One hour after the transfection, 10% MEM was added on the cells. After 24 hours, the cells were switched to serum-free MEM for 18h, followed by exposure to 2% CSE. Confirmation of HuR knock-down was done by western blot.

Library preparation for RNA-sequencing

siCtrl- and siHuR-transfected cells were cultured with serum-free MEM for 18 hours followed by exposure to 2% CSE for 24 hours. Then, total RNA was isolated using miRNeasy Kits (QIAzol based RNA purification, Qiagen). Sequencing libraries were prepared from polyA enriched mRNA as previously described [52]. Total RNA (0.446 µg; 8 µl) was incubated and PolyA enriched mRNA was fragmented in 0.5 µl of QIAseq FastSelect-rRNA HMR to remove rRNA (Qiagen) with 10x Superscript III RT buffer (Invitrogen), incubated at 95 °C for 9 min and immediately chilled on ice. The fragmented mRNA, 0.5 µl of Random primer (Invitrogen), 0.5 µl of Oligo dT primer (Invitrogen), 0.5 µl of SUPERase-In (Ambion) and 1 µl of dNTPs (10 mM)

were heated at 50 °C for 1 min. Then, 5.8 µL of water, 0.1 µl Actinomycin D (2 µg/µl), 1 µl of DTT (100 mM), 0.2 µl of 1% Tween-20 (Sigma) and 0.5 µl of Superscript III (Invitrogen) were added and incubated in a PCR machine under the following conditions: 25 °C for 10 min, 50 °C for 50 min. The product was then purified with 54 µl RNAClean XP beads and incubated on ice for 15 min. The beads were collected for 5 min on a magnet and the supernatant was discarded. The beads were washed twice with 75% ethanol and air-dried for 10 min. Then, the cDNA was eluted with 10 µl nuclease-free water. The RNA/cDNA double-stranded hybrid was then added to 1.5 µl of 10 X Blue Buffer (Enzymatics), 1 µl of PCR mix (10 mM dATP, dCTP, dGTP and dUTP), 0.1 µl dUTP (100nM), 0.2 µl of RNAse H (10 U/µl), 1 µl of DNA polymerase I (Enzymatics), 0.15 µl of 1% Tween-20 and 1.05 µl of nuclease-free water. The mixture was incubated at 16 °C for 2.5 h. The resulting dUTP-marked dsDNA was purified using 1 µl of Seradyn 3 EDAC Speedbeads (Thermo Fisher Scientific), diluted with 28 µl of 20% PEG8000/2.5M NaCl (final of 13% PEG), incubated at room temperature for 10 min, washed twice with 75% ethanol, air-dried for 10 min and eluted with 40 µl TE buffer (10 mM Tris-Cl EDTA, pH 8.5). The purified dsDNA (40 µl) underwent end repair by blunting. The mix (2.9 µl nuclease-free water, 0.5 µl of 1% Tween-20, 5 µl T4 ligase buffer, 1 µl dNTP mix (10mM), 0.3 µl T4 DNA polymerase, 0.06 µl Klenow and 0.3 µl T4 PNK) was added to 40 µl of dsDNA and incubated at 20 °C for 30 min. Next, a mixture of 1 µl of Seradyn 3 EDAC SpeedBeads (Thermo Fisher Scientific) and 93 µl of 20% PEG8000/2.5 M NaCl (13% final) was added and incubated for 10 min at room temperature. Magnetic beads were washed twice with 80% ethanol and air-dried for 10 min before elution in 15 µl TE buffer. dA-Tailing was performed by incubating DNA at 37 °C for 30 min in the mixture solution with 10.8 µl nuclease-free water, 0.3 µl 1% Tween-20, 3 µl 10 X Blue Buffer (Enzymatics), 0.6 µl dATP (10 mM, Thermo Fisher Scientific), 0.3 µl Klenow 3-5 Exo (Enzymatics). Then, 55.8 µl of 20%

PEG8000/2.5 M NaCl (13% final) was added and incubated for 10 min at room temperature. Magnetic beads were washed twice with 80% ethanol and air-dried for 10 min before elution in 15 µl TE buffer. For adapter ligation, each sample was mixed with 0.5 µl of a BIOO barcode adapter (BIOO Scientific, USA) with 15 µl Rapid Ligation Buffer (Enzymatics), 0.33 µl 1% Tween-20 and 0.5 µl T4 DNA ligase HC (Enzymatics) and incubated for 15 min at room temperature. Next, 7 µl of 20% PEG8000/2.5 M NaCl was added and incubated for 10 min at room temperature, washed twice with 80% ethanol, eluted with 20 µl TE buffer and 1 µl UDG and incubated at 37 °C for 30 min. Next, 10 µl from the eluted volume was further used for PCR amplification (16 cycles) with IGA primers (AATGATACGGCGACCACCGA) and IGB primers (CAAGCAGAAGACGGCATACGA) in a 1:1 ratio. Lastly, libraries were size selected using 10% PAGE/TBE gels, eluted and quantified with Qubit dsDNA HS Assay Kit (Thermo Fisher Scientific). Sequencing was performed on the Illumina NextSeq550. The reads were aligned. The Fastq files were obtained, and reads were mapped to the hg38 human genome using STAR. Transcript counts were obtained using HOMER analyze repeats and converted to fpkm normalized counts using HOMER. Differential expression analysis was analyzed using the edgeR package.

RNA Immunoprecipitation (RIP)

HLFs were grown to approximately 70-80% confluence and cultured with serum-free MEM for 18 hours followed by exposure to 2% CSE. Then, cells were collected in PBS and centrifuged at 1500 rpm, 4℃ for 5 minutes. The cell pellets were lysed (50 mM Tris PH 8; 0.5% Triton X100; 450 mM NaCl; Protease Inhibitor Cocktail; Phosphatase Inhibitor (Roche, US)), incubated for 15 min on ice and then centrifuged at 10,000 rpm, 4℃ for 15 min. The extracts were transferred into new tube and a buffer containing 50 mM Tris pH 8; 0.5% Triton X100; 10%

glycerol; Protease Inhibitor Cocktail; Phosphatase Inhibitor (Roche, US) [27, 53] was added. Protein concentration was measured by BCA Protein Assay Kit. Thirty-five µl of protein G SepharoseTM 4 fast glow beads (GE Healthcare) were pre-coated with 3 µg of IgG (Cell Signaling Technologies, CA) or 3 µg of anti-HuR (Santa Cruz Biotechnology) antibodies overnight on a rotator at 4°C. Beads were washed three times with buffer (50 mM Tris PH 8; 0.5% Triton X100; 150 mM NaCl) and incubated with cell extracts for 2 hours a 4°C [28]. Beads were washed three times to wash out unbound materials. RNA was then extracted using Genezol TriRNA pure kit (Geneaid RNA purification) according to manufacturer's instructions. For RNA sequencing, the RNA quality of the extracted RNA was assessed with the 2100 Bioanalyzer (Agilent Technologies) and all samples had a RIN above 9.5. Transcriptome libraries were generated using the KAPA RNA HyperPrep Kit with RiboErase (Roche) starting with 100ng of total RNA per sample. Sequencing was performed on the Illumina NextSeq500 75 cycles, obtaining around 60M single-end reads per sample. The reads were trimmed using fastp and then aligned using the STAR aligner. From the aligned reads, HTSeq was used to get the raw read counts. If there was a known batch effect, it was accounted for using the sva R package.

Functional annotation and pathway enrichment analysis

Commonly expressed up– and down–regulated differentially expressed genes (DEGs) between groups was selected using the Venn diagram (Venny, v2.1.0) [54]. For RNA-seq, the differentially regulated mRNA was selected using the following criteria: log2 fold change ≥ 2 for upregulated and ≤ -2 for downregulated genes and the adjusted p value ≤ 0.05. For the RIP-RNA-seq, the differentially regulated mRNA was selected using the following criteria: log2 fold change ≥ 1.5. To functionally annotate DEGs identified by the comparison groups, annotation, and

visualization of gene ontology (GO) biological processes and Kyoto Encyclopedia of Genes and Genomes (KEGG) pathways was performed on Metascape [55]. The overlap between DEG lists of GO terms were visualized by Circos plot on Metascape [55]. Molecular complex detection (MCODE) algorithm was used on Metascape to identify densely connected network of protein-protein interaction, where the MCODE complexes were colored according to their identities. All the data were performed on the latest version of Metascape database (last updated on 2022-01-01).

Quantitative RT-PCR (qRT-PCR)

Total RNA was isolated as described above and quantification conducted on a Nanodrop 1000 spectrophotometer (infinite M200 pro, TECAN, CA). Reverse transcription of RNA was carried out using iScript™ Reverse Transcription Supermix (Bio-Rad Laboratories, Mississauga, ON). Then, the mRNA levels of *ELAVL1*, *PTGS2*, *CXCL8* and *S9* were analyzed using this cDNA template and gene-specific primers (Table 4.1). Quantitative PCR (qPCR) was performed by addition of 1 µl cDNA and 0.5 µM primers with SsoFast™ EvaGreen® (Bio-Rad Laboratories, Mississauga, ON), and PCR amplification was performed using a CFX96 Real-Time PCR Detection System (Bio-Rad, CA). Thermal cycling was initiated at 95°C for 3 minutes and followed by 39 cycles denaturation at 95°C for 10 seconds and annealing at 59°C for 5 seconds. Gene expression was analyzed using the ΔΔCT method, and results are presented as fold-change normalized to housekeeping gene (S9). For RIP-qPCR, the extracted RNA was reverse transcribed and analyzed by qPCR. The RNA expression was normalized to S9 mRNA bound in a non-specific manner to IgG.

Table 4.1. Primer sequences used for qRT-PCR analysis.

Gene	Forward Primer Sequence	Reverse Primer Sequence
ELAVL1	AAC GCC TCC TCC GGC TGG TGC	GCG GTA GCC GTT CAG GCT GGC
PTGS2	TCA CAG GCT TCC ATT GAC CAG	CCG AGG CTT TTC TAC CAG A
CXCL8	GAT GTC AGT GCA TAA AGA CAT ACT CCA A	GCT CTC TTC CAT CAG AAA GCT TTA CAA TA
S9	CAG CTT CAT CTT GCC CTC A	CTG CTG ACG CTT GAT GAG AA

Western Blot

HLFs were grown to approximately 70-80% confluence and cultured with serum-free MEM for 18 hours before the treatment. Total cellular protein was extracted using RIPA lysis buffer (Thermo Scientific, Rockford) and Protease Inhibitor Cocktail (PIC, Roche, US). Ten to twenty μg of protein lysate were subjected to 10% SDS-PAGE gels and transferred onto Immuno-blot PVDF membranes (Bio-Rad Laboratories, Hercules, CA) as previously described [56]. Then, the membrane was blocked for one hour at room temperature in blocking solution (5% w/v of non-fat dry milk in 1x PBS/0.1% Tween-20). Antibodies against HuR (1:2000; Santa Cruz, CA), COX 2 (1:1000; Cell Signalling Technologies, CA), and β-Tubulin (1:50000; Sigma, CA) were used. The secondary antibodies goat anti-rabbit IgG, HRP-linked (1:10000, Cell Signaling Technologies, CA) and HRP-conjugated horse anti-mouse IgG (1:10000, Cell Signaling Technologies, CA) were used. Detection of protein levels was catalyzed by ClarityTM western ECL substrate (Bio-Rad Laboratories, Mississauga, ON) or AmershamTM western ECL substrate (GE Healthcare, Italy). Protein bands were visualized using a ChemiDoc™ MP Imaging System (Bio-Rad, CA). Densitometric analysis was performed using Image Lab™ Software Version 5 (Bio-Rad, CA). Protein expression was normalized to β-Tubulin and the data presented as fold-change relative to untreated condition.

Enzyme-linked immunosorbent assay (ELISA)

The concentration of interleukin-8 (IL-8) in the cell culture supernatant from was determined by ELISA (Human IL-8 ELISA Duo Set, R&D Systems, U.S) according to the manufacturer's instructions. The absorbance was read at 450 nm and 570 nm within fifteen minutes by infinite TECAN (M200 pro, TECAN, CA).

Determination of mRNA stability

SiCtrl and siHuR- transfected cells were prepared for treatment as described above. Then, cells were exposed to 2% CSE for 24 hours followed by the treatment of Actinomycin D (ActD; 2 μg/ml), an inhibitor of RNA synthesis [20, 57], for 1 hours or 3 hours. Total RNA was harvested, and qPCR was performed to determine the remaining levels of *PTGS2* and *CXCL8* mRNAs.

Statistical Analysis

Statistical analysis was performed using GraphPad Prism 9 (v. 9.02; La Jolla, CA). Statistical analysis was performed using two-way analysis of variance (ANOVA), followed by Tukey's or Sidak's multiple comparisons tests to evaluate differences between treatment groups of more than two. Results are presented as mean ± standard error of the mean (SEM) of the fold-changes compared to control cells. In all cases, a p value < 0.05 is considered statistically significant. The heatmaps of top mRNA were created using GraphPad Prism 9 (v. 9.02; La Jolla, CA).

4.4. RESULTS

Knockdown of HuR impacts mRNA expression that is associated with numerous biological pathways in primary lung fibroblasts

HuR regulates hundreds of RNA that are involved in diverse biological processes [17, 18, 58-62] but its role in lung fibroblasts is not well known. To first address the global transcriptional profile controlled by HuR in these primary lung cells, we transiently transfected HLFs with either HuR-specific siRNA (siH) or with control siRNA (siC), followed by treatment with 2% CSE; siH reduced HuR levels by approximately 50% (Figure 4.1A). Then, we profiled the transcriptome using RNA sequencing (RNA-Seq). We detected a total of 14,401 coding and noncoding genes (Supplementary Table S4.1). To understand the extent to which CSE induces gene transcription in HLFs, we first compared cells transfected with siC and either exposed to CSE or not, as these represent cells with constitutive HuR expression. This group is designated as siC-CSE and had 89 upregulated mRNA (Figure 4.1C). To then identify differences in mRNA based on HuR expression alone (*i.e.,* no CSE exposure), we compared DEG profiles in cells whereby HuR was knocked down but untreated; comparison was to the untreated siC cells; this comparison group was designated as ΔsiH. There were 161 upregulated mRNA (Figure 4.1C), suggesting that HuR regulates multiple genes at the basal level. Our next DEG comparison was in HuR knockdown cells exposed to CSE relative to siC cells exposed to CSE (ΔsiH-CSE); this resulted in the upregulation of 162 mRNA (Figure 4.1C). Finally, the overall effect of HuR knockdown and exposure to CSE was evaluated by comparing untreated siC cells with siH cells exposed to CSE (siC/siH-CSE); this comparison yielded the induction of 82 distinct mRNA (Figure 4.1C). These last two comparisons suggest that HuR controls the expression of genes in response to CSE. In addition to mRNA whose expression is distinct between the four experimental comparisons, there

were two common mRNA- *PTGS2* and *CXCL8*- amongst all four (Figure 4.1B). These two mRNA are well known to be upregulated in response to CSE in lung fibroblasts [41, 45, 46, 51]. Although *PTGS2* and *CXCL8* mRNA were upregulated in response to CSE, the largest fold-increase occurred upon HuR knockdown (Table 4.2). Thus, our data not only confirm that CSE induces the expression of *PTGS2* and *CXCL8* in HLFs but importantly, that HuR knockdown induced their expression even in the absence of CSE. These data suggest that HuR plays a direct regulatory role for these mRNA, further supporting that HuR supresses the expression of hundreds of mRNA both at the basal level and in response to CSE in primary HLFs.

While the previous data indicate that HuR suppresses the expression of numerous genes, including those linked to an inflammatory response, analysis of these data also showed that there was numerous mRNA whose expression was downregulated both at the basal level and in response to CSE upon HuR knockdown. Even in cells which express HuR and that were treated with or without CSE (siC-CSE), there were 194 downregulated mRNA (Figure 4.1D). Knockdown of HuR also downregulated the expression of 137 mRNA at the basal level (Figure 4.1D, ΔsiH), supporting that HuR is fundamentally necessary to control mRNA expression even in the absence of exogenous stimuli. In response to CSE, HuR silencing also downregulated 83 distinct mRNA (Figure 4.1D, ΔsiH-CSE). Finally, in response to CSE, HuR knockdown reduced 114 mRNA compared to cells expressing HuR at the basal level (Figure 4.1D, siC/siH-CSE). These observations suggest that HuR is also essential for promoting the expression of genes in cells exposed to CSE. The functions of the top upregulated and downregulated genes for each comparison group are shown in Table 4.2. Note that some of these genes have no described function whereas others have well known functions. The complete list of upregulated and

downregulated mRNA is shown in Supplementary Tables S4.2 and S4.3, respectively. Altogether, these data show that HuR controls the expression of numerous mRNA at the basal level and in response to CSE in primary lung cells.

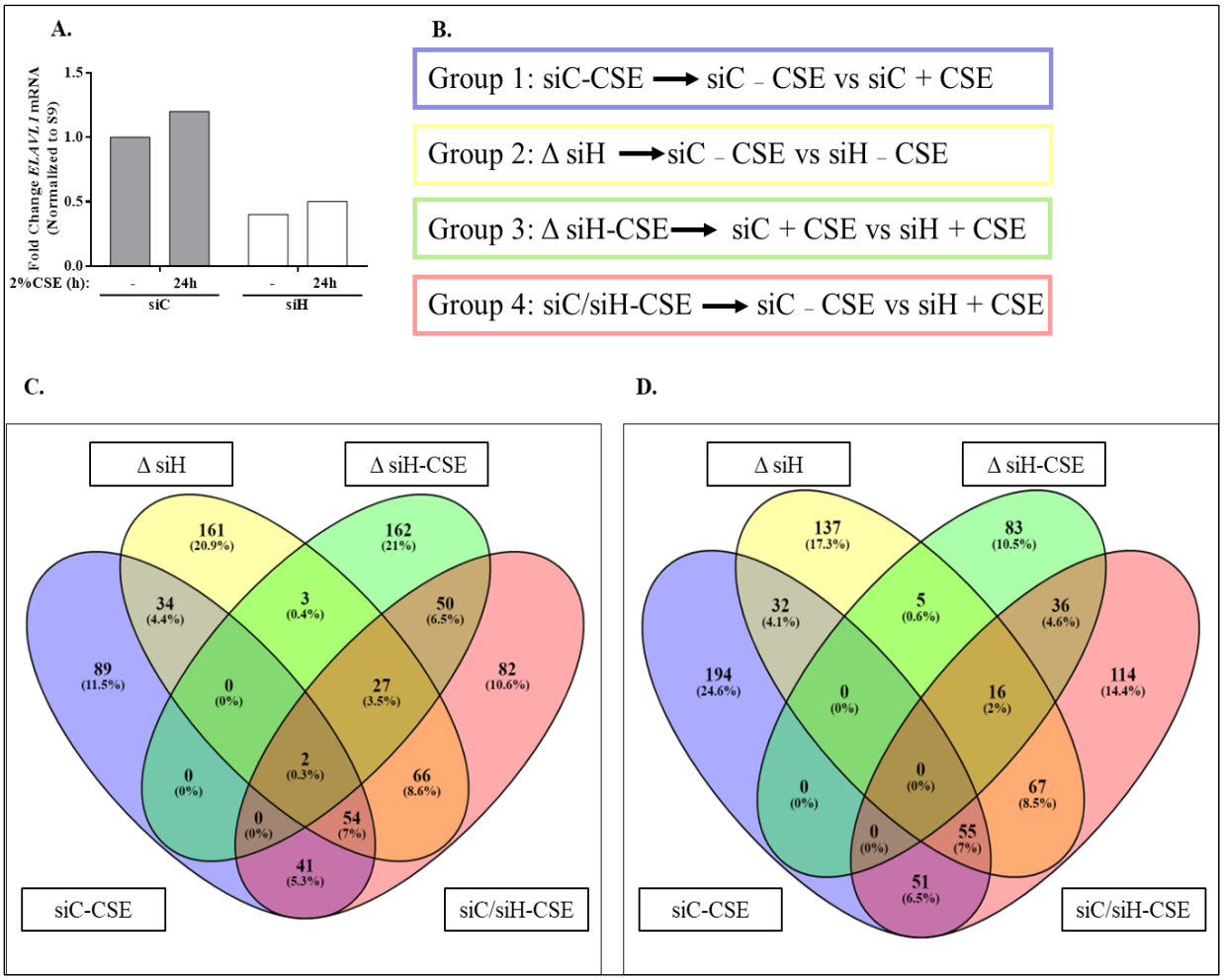

Figure 4.1. Identification of mRNAs in HLFs.

A. RT-qPCR was conducted to demonstrate the efficiency of HuR silencing. **B.** Nomenclature for the 4 comparison groups. **C.** Venn diagram indicating the number of the upregulated mRNA across the four key comparisons: siC-CSE, Δ siH, Δ siH-CSE and siC/siH-CSE, and the overlap between each set of genes. **D.** Venn diagram indicating the number of the downregulated mRNAs across four comparison groups and the overlap between each set of genes.

Table 4.2. Top genes differentially expressed by HuR silencing.

Ensembl	Gene	Name	Group	Log2 (Fold Change)	PANTHER Protein Class	Function
ENSG00000073756	*PTGS2*	Prostaglandin G/H synthase 2/ COX-2	siC-CSE, Δ siH, Δ siH-CSE, siC/siH-CSE	2.4, 2.5, 3.4, 5.8	Oxygenase	Prostaglandin metabolic process
ENSG00000169429	*CXCL8*	C-X-C Motif Chemokine Ligand 8/ IL-8	siC-CSE, Δ siH, Δ siH-CSE, siC/siH-CSE	2.2, 3.4, 3.8, 6.1	Chemokine	Chemotactic for leucocytes.
ENSG00000189195	*BTBD8*	BTB/POZ domain-containing protein 8	siC-CSE	8.5	N/A	N/A
ENSG00000173535	*TNFRSF10C*	TNF Receptor Superfamily Member 10c	Δ siH	9.4	Transmembrane signal receptor	Decoy receptors for the TNF-related apoptosis-inducing ligand (TRAIL), a member of the TNF family
ENSG00000160326	*SLC2A6*	Solute Carrier Family 2 Member 6	Δ siH-CSE	8.6	N/A	N/A

ENSG00000183850	*ZNF730*	Zinc Finger Protein 730	siC/siH-CSE	8.1	DNA-binding transcription factor	N/A
ENSG00000143858	*SYT2*	Synaptotagmin-2	siC-CSE	-9.6	Membrane trafficking regulatory protein	Regulation of ion transport
ENSG00000141086	*CTRL*	Chymotrypsin Like	Δ siH	-8.1	Serine protease	Proteolysis
ENSG00000114529	*C3orf52*	Chromosome 3 Open Reading Frame 52	Δ siH-CSE	-7.9	N/A	N/A
ENSG00000065717	*TLE2*	TLE Family Member 2, Transcriptional Corepressor	siC/siH-CSE	-8.2	Transcription cofactor	Transcription regulator complex

To further characterize the mRNA whose expression is upregulated in HLFs, DEGs were classified into GO biological process pathways. First, we generated a heatmap to show the top enriched clusters and their enrichment patterns across the four groups (Figure 4.2A). Pathways related to detoxification and response to reactive oxygen species (ROS) were enriched in siC-CSE group (Figure 4.2A), suggesting that CS controls the expression of genes implicated in these pathways. The expression of some genes in these two pathways were also changed with HuR knockdown; hence, these two pathways were also enriched in siC/siH-CSE group, indicating that HuR may play an important role in the regulation of detoxification and response to ROS. Furthermore, several pathways related to inflammation, such as inflammatory response, response to cytokines and cytokine-mediated signaling, were not enriched in siC-CSE group but were enriched in the ΔsiH, ΔsiH-CSE and siC/siH-CSE groups (Figure 4.2A). Together, this supports

the involvement of HuR in the regulation of inflammation, even in the absence of exogenous stimuli.

Next, we used a Circos plot to visualize the extent to which genes from the input lists (*i.e.,* siC-CSE, ΔsiH, ΔsiH-CSE and siC/siH-CSE) used in the GO analysis overlapped (Figure 4.2B). On the outside, each colored curve represents the identity of the gene list, while on the inside, each colored curve represents the gene list, whereby each gene of that list was assigned a spot on the curve. Note that the size of the outside curve represents the total number of genes in each list, whereby the shortest curve (red) is represented in siC-CSE group- which had the lowest number of total genes- whereas the longest curve (blue) occurred with the siC/siH-CSE comparison group and thus had the greatest number of genes. These data indicate that HuR impacts a greater number of genes compared to CSE alone. The inside curved, dark orange color represents the genes that are shared by multiple groups whereas the lighter orange portion of that same curve represents genes which were unique to that comparison group. Additionally, the purple lines link the same genes that are shared between the groups. In other words, the greater the number of purple links and the longer the dark orange curve, the greater the overlap among the comparison groups. For example, the siC/siH-CSE comparison group had the longest portion of the dark orange curve and therefore the greatest number of genes that were shared with the other three groups, while the ΔsiH and ΔsiH-CSE comparison groups had the greatest number of unique genes (light orange). Finally, the blue lines link the genes that fall under the same GO term, which means that blue links indicate the amount of functional overlap among the input gene lists.

Next, we selected pathways related to ROS and inflammation from Figure 4.2A because it is well known that these two pathways are involved in CS-induced lung damage [9, 10, 15, 41,

46]. We generated a heatmap to show the top genes from these two pathways and their expression across the four comparisons groups. For those genes involved in the response to ROS pathway (Figure 4.2C), many of these are known HuR targets, including *HMOX1*, *NQO1*, *SLC7A11*, *PTGS2* and *IL6*. However, many of the genes in this pathway have not been associated with HuR and thus are novel HuR targets; these genes included *AKR1C3*, *UCP3*, *RNF112*, *FXN*, *MAPT*, *APOD*, *TACR1*, *SRXN1*, *GPX2* and *CD36*. We also mapped the upregulated mRNA that belong to inflammation pathways, which included both known the HuR targets *PTGS2*, *CXCL8*, *CXCL2*, *IL6*, *IL7* and *IL12RB1* as well as novel HuR targets *CXCR6*, *IL15*, *CD14*, *CD36*, *PTGER3*, *LAG3*, *TNFSF13*, *MST1R*, *ERBB3* and *APOD* (Figure 4.2D). These data show for the first time that HuR controls the expression of genes involved in ROS and inflammation pathways in response to CS. Then, using KEGG analysis, our data show that some pathways, such as the cytokine-cytokine receptor interaction pathway, was enriched only in ΔsiH-CSE and siC/siH-CSE groups (Figure 4.3), indicating that genes involved in inflammation, that are part of numerous biological pathways, may be universally regulated by HuR. The genes that fell under each GO biological processes and KEGG pathways are listed in Supplementary Tables S4.4 and S4.5, respectively. Overall, these data indicate that HuR controls the expression of mRNA that are involved in numerous biological processes including inflammation, a key feature implicated in the pathogenesis of CS-related diseases.

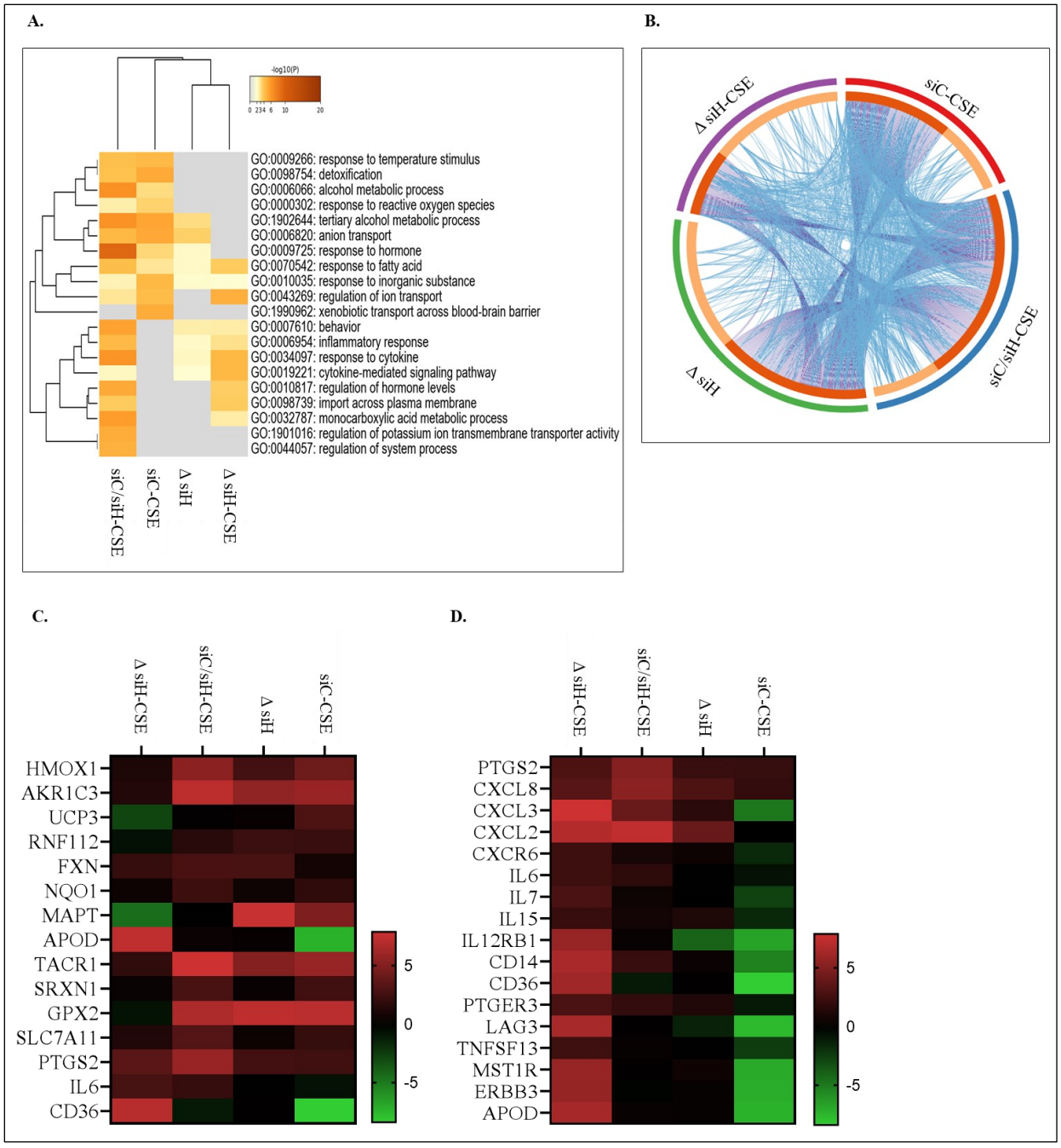

Figure 4.2. HuR regulates different genes involved in inflammation and oxidative stress in HLFs.

A. Heatmap of enriched GO terms across input gene lists for the comparison groups Δ siH, Δ siH-CSE, siC-CSE and siC/siH-CSE, colored by p-values. Gray color indicates a lack of significance. **B.** Circos plot shows overlap between gene lists from the comparison groups Δ siH, Δ siH-CSE, siC-CSE and siC/siH-CSE at the gene level (purple curves on the inside the circle) and at the shared term level (blue curves on the inside the circle) which link genes that belong to the same enriched ontology term. Genes that hit multiple lists are colored in dark orange, and genes unique

to a list are shown in light orange. **C.** Heatmap of mRNA involved in response to reactive oxygen species (GO:0000302) in Δ siH, Δ siH-CSE, siC-CSE and siC/siH-CSE comparison groups. The gradation from red to green represents the transition from large to small values of log2 fold change. **D.** Heatmap of mRNA involved in inflammation pathways (GO:0006954, GO:0019221 and GO:0034097) for the Δ siH, Δ siH-CSE, siC-CSE and siC/siH-CSE comparison groups. The gradation from red to green represents the transition from large to small values of log2 fold change.

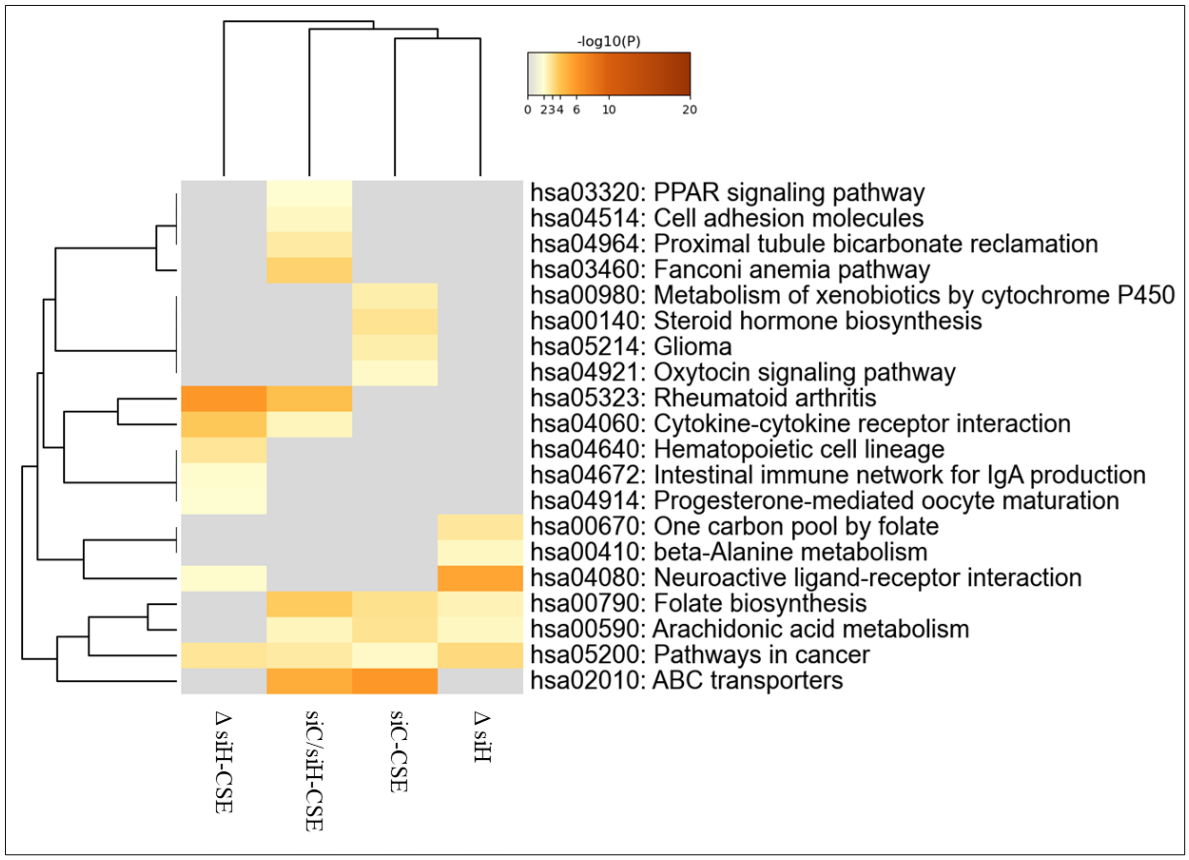

Figure 4.3. KEGG pathway analysis of upregulated mRNA.

Heatmap of enriched KEGG pathways across input gene lists for the comparison groups Δ siH, Δ siH-CSE, siC-CSE and siC/siH-CSE, colored by p-values. Gray color indicates a lack of significance.

While the above information pertained to those genes whose expression was upregulated, we also performed similar analysis for mRNA whose expression was downregulated in our

comparison groups. First, the heatmap generated from these downregulated genes shows the top enriched clusters and their enrichment patterns across the four groups (Figure 4.4A). Some pathways were enriched only in ΔsiH group (*i.e.,* independent of CSE); this included the activation of GTPase activity pathway (Figure 4.4A). However, several other pathways, including the regulation of ion transport, regulation of cytosolic calcium ion concentration, inflammatory response and positive regulation of MAPK cascade, were enriched in ΔsiH, ΔsiH-CSE and siC/siH-CSE groups (Figure 4.4A). This suggests that HuR is required for the expression of genes involved in these pathways- regardless of CSE exposure. Interestingly, peptidyl-serine phosphorylation and the positive regulation of cytosolic calcium ion concentration involved in phospholipase C-activating G protein-coupled signaling pathways were enriched only in ΔsiH-CSE comparison group (Figure 4.4A). This means that, in response to CSE, HuR promotes the expression of genes that may involved in protein phosphorylation and related signaling pathways.

Next, we used the Circos plot to show how genes from these gene lists (*i.e.,* derived from the siC-CSE, ΔsiH, ΔsiH-CSE and siC/siH-CSE comparison groups) in the GO analysis overlapped (Figure 4.4B). The shortest curve (purple), representing ΔsiH-CSE comparison group, had the lowest number of overall genes, while the longest curve (green), representing the siC/siH-CSE comparison group, had the greatest number of genes. This suggests that HuR controls a large number of genes in HLFs. Finally, this plot informs that the siC/siH-CSE comparison group, which has the longest dark orange curve, has the biggest number of genes that were shared with the other three comparison groups, while siC-CSE had the greatest number of unique genes (light orange).

We then generated a heatmap to show the top downregulated genes from the positive regulation of cytosolic calcium ion concentration involved in phospholipase C-activating G protein-coupled signaling pathway in Figure 4.4A as well as their expression across the four comparisons groups. We selected this pathway because it has been reported that CS controls the expression of G protein-coupled receptors (GPCRs) [63]. However, not much is known about the involvement of GPCRs in CS-induced lung damage or COPD pathogenesis. Overall, these genes are novel HuR targets and included *GPR55*, *GPR18*, *F2RL3*, *EDN1*, *PTN4R*, *STARD8*, *PLEKHG4B*. Of these, *GPR55* and *GPR18* mRNA were upregulated in siC-CSE group, showing for the first time that CSE increases their expression. Yet, in response to CSE, knockdown of HuR decreased the expression of *GPR55* and *GPR18* (Figure 4.4C), suggesting that HuR is important for the expression of these genes in response to smoke. Then, we assessed the downregulated genes associated with HuR silencing that are involved in the inflammatory response pathway from Figure 4.4A. The heatmap showed the expression of genes involved in this pathway, which included known HuR targets, such as *IL5*, and novel HuR targets, such as *IL17D*, *IL34*, *LTB4R*, *LIAS*, *HP*, *GGT5*, *AOC3*, *NLRC4*, *ALOX5AP* and *ADORA2A* (Figure 4.4D). Then, KEGG analysis revealed that the calcium signaling pathway was enriched in ΔsiH, ΔsiH-CSE and siC/siH-CSE comparison groups (Figure 4.5). The genes under each GO biological processes and KEGG pathways are listed in Supplementary Tables S4.6 and S4.7, respectively. In summary, our RNA-seq data showed that HuR controls genes linked to biological processes, particularly inflammation, at the basal level and in response to CSE.

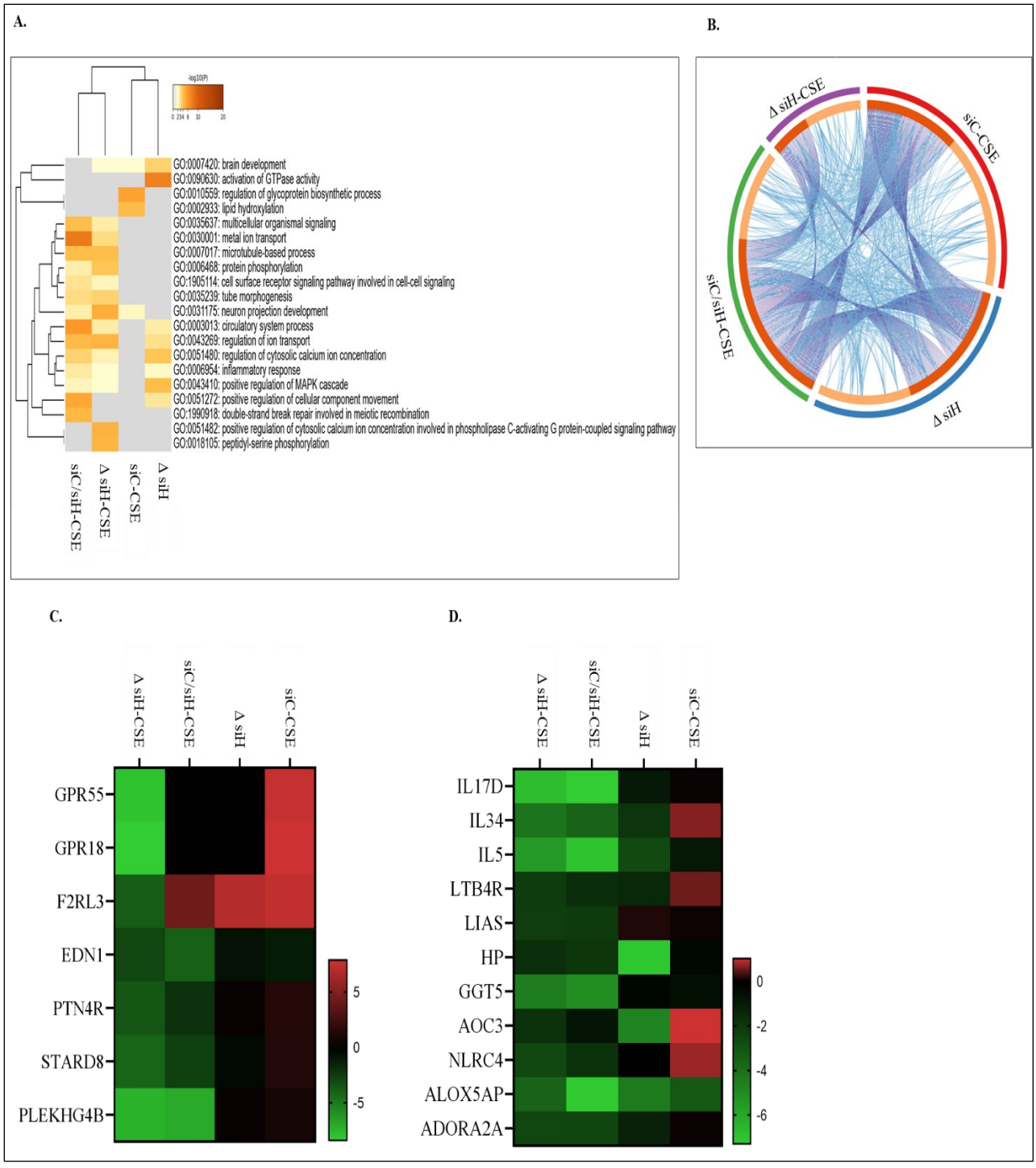

Figure 4.4. HuR induces the expression of mRNA involved in the regulation of cytosolic calcium and inflammatory response.

A. Heatmap of enriched GO terms across input gene lists for the comparison groups Δ siH, Δ siH-CSE, siC-CSE and siC/siH-CSE, colored by p-values. Gray color indicates a lack of significance. **B.** Circos plot shows overlap between gene lists from the comparison groups: Δ siH, Δ siH-CSE,

siC-CSE and siC/siH-CSE. **C.** Heatmap of mRNA involved in the regulation of cytosolic calcium ion concentration (GO:0051482) in Δ siH, Δ siH-CSE, siC-CSE and siC/siH-CSE comparison groups. The gradation from red to green represents the transition from large to small values of log2 fold change. **D.** Heatmap of mRNA involved in inflammatory response (GO:0006954) in Δ siH, Δ siH-CSE, siC-CSE and siC/siH-CSE comparison groups. The gradation from red to green represents the transition from large to small values of log2 fold change.

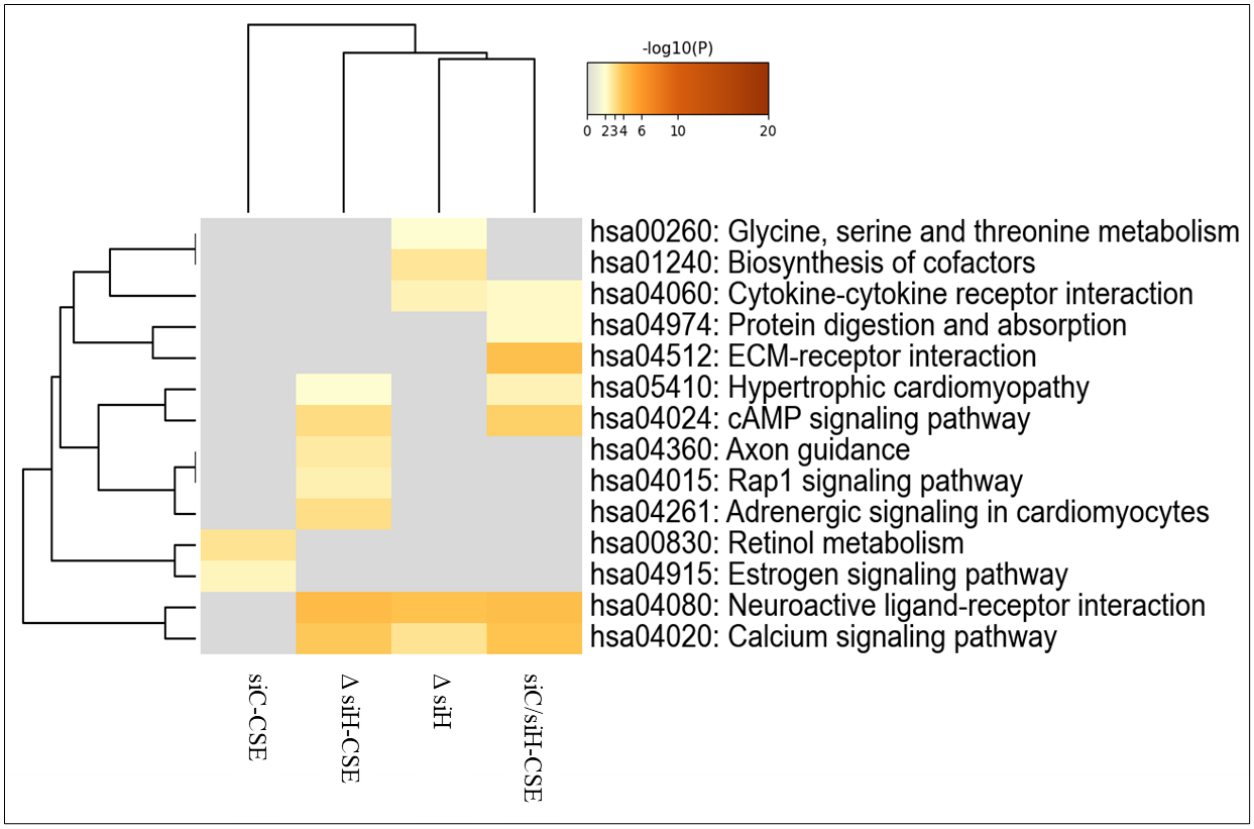

Figure 4.5. KEGG pathway analysis of the downregulated mRNA.

Heatmap of enriched KEGG pathways across input gene lists for the comparison groups Δ siH, Δ siH-CSE, siC-CSE and siC/siH-CSE, colored by p-values. Gray color indicates a lack of significance.

HuR physically associates with genes involved in multiple cellular pathways in primary lung fibroblasts

As we have shown above, HuR controls the expression of hundreds of mRNA. However, how HuR regulates the expression of these genes is not fully understood. One possibility is that HuR associates with target genes to control their cellular levels. In this regard, HuR is known for its ability to bind to target mRNA, which allows for that mRNA to be stabilized and subsequently translated into protein [17, 18, 58-62]. To assess HuR binding to mRNA, we immunoprecipitated HuR from primary HLFs and performed RNA-seq on the extracted RNA (RIP-Seq). Note the specificity of the IP, where the IgG (non-specific; control) antibody did not immunoprecipitate HuR as indicated by the absence of the band (Figure 4.6A). For the RIP-Seq analysis, we compared IP-HuR relative to IP-IgG at the basal level (ΔIP-HuR) and IP-HuR relative to IP-IgG in response to CSE (ΔIP-HuR-CSE). From these comparisons, we found that 618 genes were enriched in both ΔIP-HuR and ΔIP-HuR-CSE comparison groups, where 276 of these genes were common to both groups (Figure 4.6C). In other words, HuR binds to hundreds of genes in HLFs regardless of CSE exposure. These data also revealed that HuR associated with 35 genes at the basal level (Figure 4.6C, ΔIP-HuR) but in response to CSE, HuR bound to 307 genes (ΔIP-HuR-CSE).

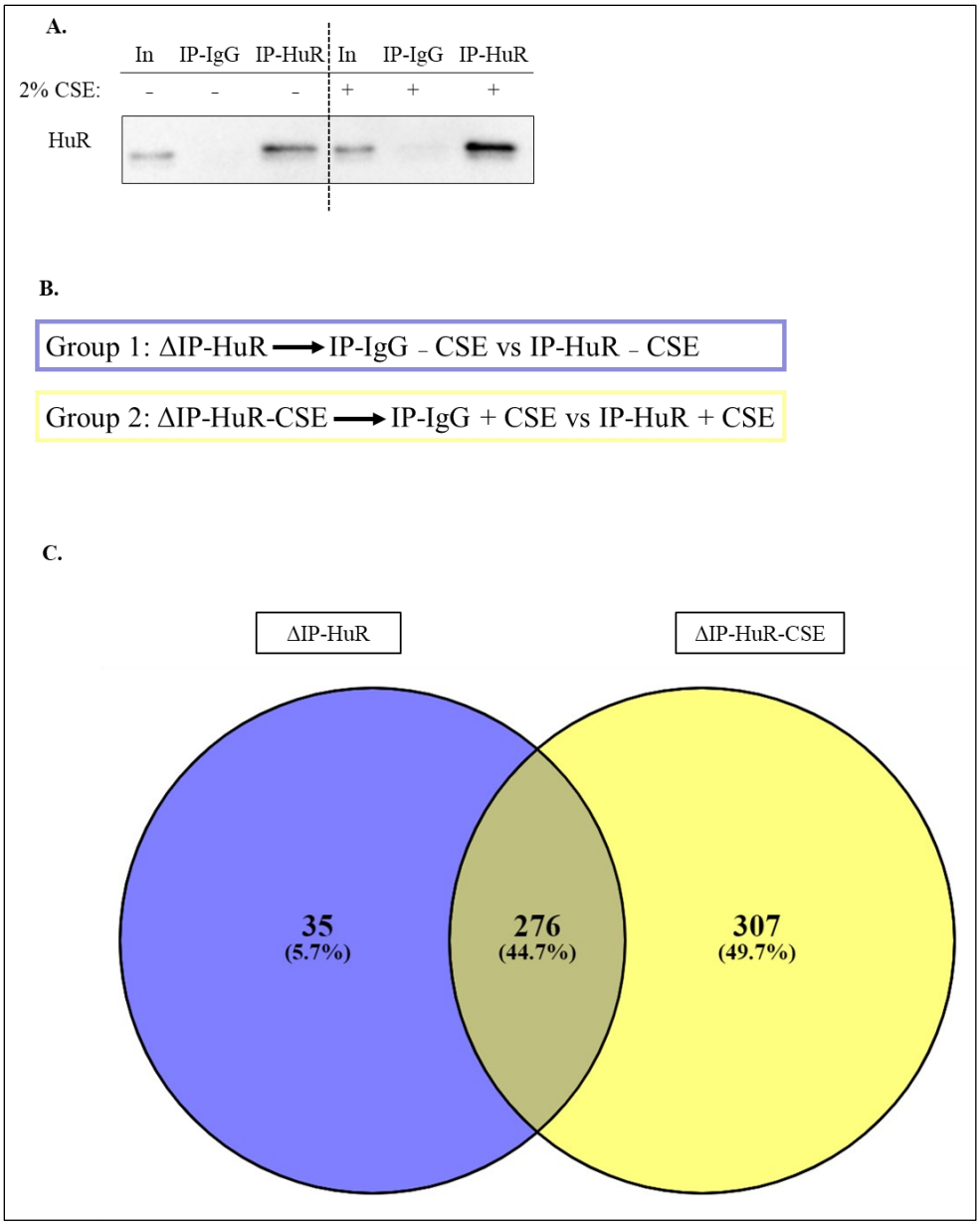

Figure 4.6. HuR binds to hundreds of genes in HLFs.

A. Representative western blot of HuR immunoprecipitation (IP) is shown. Input (In) refers to cell lysates. IgG refers to IP with control IgG antibody while HuR refers to the IP with anti-HuR IgG antibody. Note the presence of HuR protein in HuR but not in IgG. **B.** Nomenclature for the 2 comparison groups. **C.** Venn diagram indicating the number of genes across two key comparisons: ΔIP-HuR (Blue) and ΔIP-HuR-CSE (Yellow) and the overlap between each set of genes.

To further characterize the genes whose expression is enriched in ΔIP-HuR and ΔIP-HuR-CSE comparison groups, DEGs were classified into GO biological process pathways. The heatmap revealed the top enriched pathways in ΔIP-HuR and ΔIP-HuR-CSE groups (Figure 4.7A). Several pathways were enriched in both groups, such as the positive regulation of I-kappaB kinase/NF-kappaB signaling, cellular response to external stimuli and regulation of cellular response to stress, suggesting that HuR binds to genes within these pathways. Then, the overlap of genes between the two groups was visualized using a Circos plot (Figure 4.7B). The shortest curve (blue) within the ΔIP-HuR comparison group reveals that this group had the lowest number of genes, while the longest curve (red) within the ΔIP-HuR-CSE comparison group therefore had the greatest number of genes. This latter comparison group also had the greatest number of unique genes (light orange). These observations collectively suggest that HuR associates with more genes in the presence of CSE. Furthermore, KEGG analysis revealed that MAPK signaling, TNF signaling, and RNA degradation pathways were enriched in both groups (Figure 4.7C). The lists of genes in GO and KEGG pathways are shown in Supplementary Tables S4.8 and S4.9, respectively. These data suggest that HuR binds to hundreds of RNA that regulate several biological processes in HLFs both at the basal level and in response to CSE.

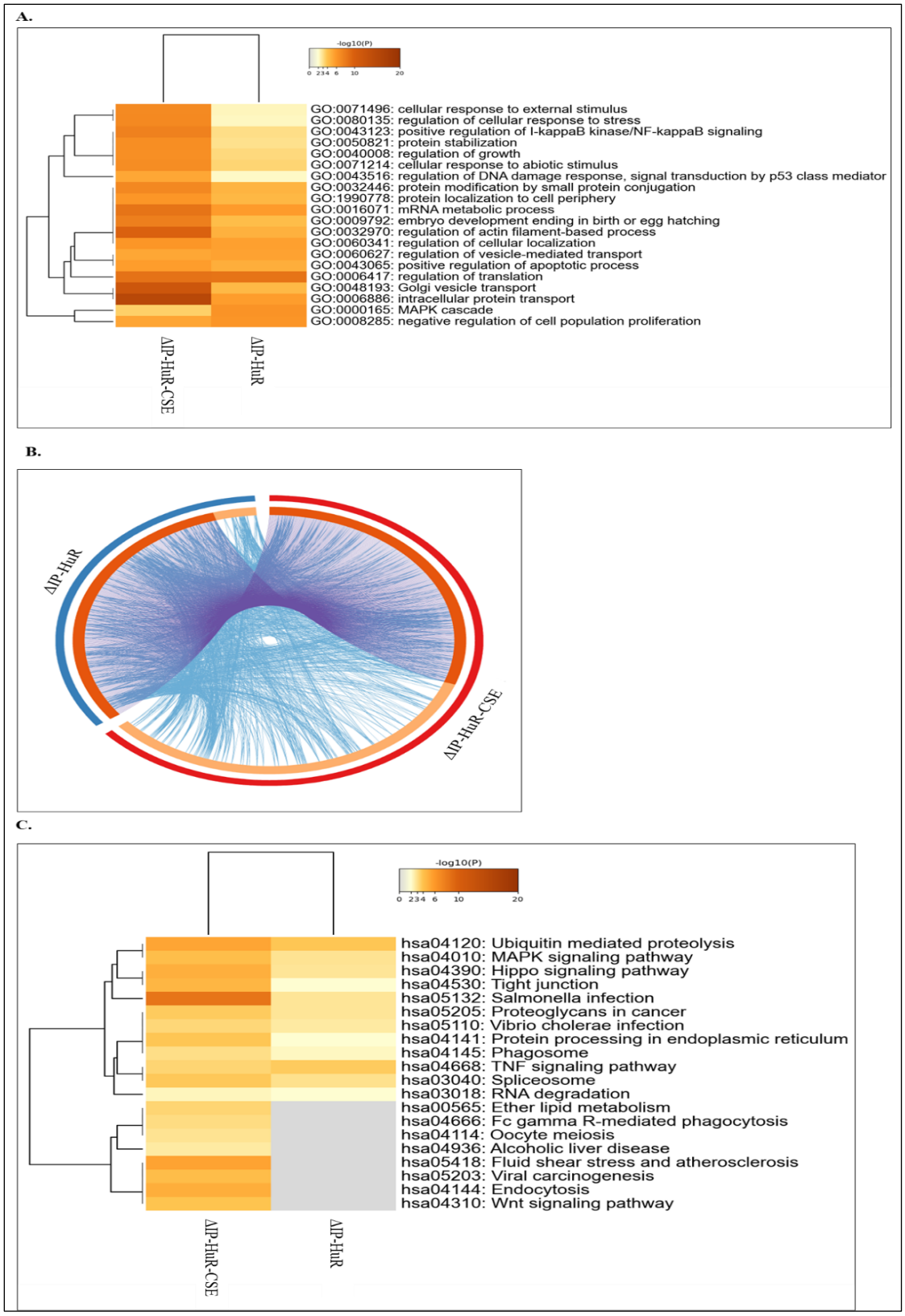

Figure 4.7. GO and KEGG pathway analysis of HuR-associated genes.

A. Heatmap of enriched GO terms across input gene lists between ΔIP-HuR and ΔIP-HuR-CSE, colored by p-values. Gray color indicates a lack of significance. **B.** Circos plot shows overlap between the gene lists from the 2 comparison groups: ΔIP-HuR and ΔIP-HuR-CSE. The plot shows that most of the genes were shared between the 2 comparison groups and the ΔIP-HuR-CSE group has the most unique genes. **C.** Heatmap of enriched KEGG pathways across input gene lists, ΔIP-HuR and ΔIP-HuR-CSE, colored by p-values. Gray color indicates a lack of significance.

Then, to describe the full repertoire of protein-protein interactions from the RIP-seq data, we assessed the interactome using the MCODE clustering algorithm on Metascape. The MCODE algorithm identifies proteins that are densely connected by automatically extracting protein complexes embedded in the large network. The MCODE analysis for our RIP-seq data demonstrated that genes were grouped into 8 MCODE complexes, which is assigned a unique color for each complex (Figure 4.8). The three most significantly enriched GO terms were combined to explain putative biological roles within each MCODE complex (Table 4.3). Because enriched GO terms for MCODE_6, 7 and 8 complexes were not available, their functions are not further defined. However, the enriched GO terms for the other 5 MCODE complexes are indicated in Table 4.3 and reveals that HuR binds to RNA which are largely involved in protein modifications, including protein phosphorylation, intracellular transport and translation, as well as genes involved in mRNA splicing.

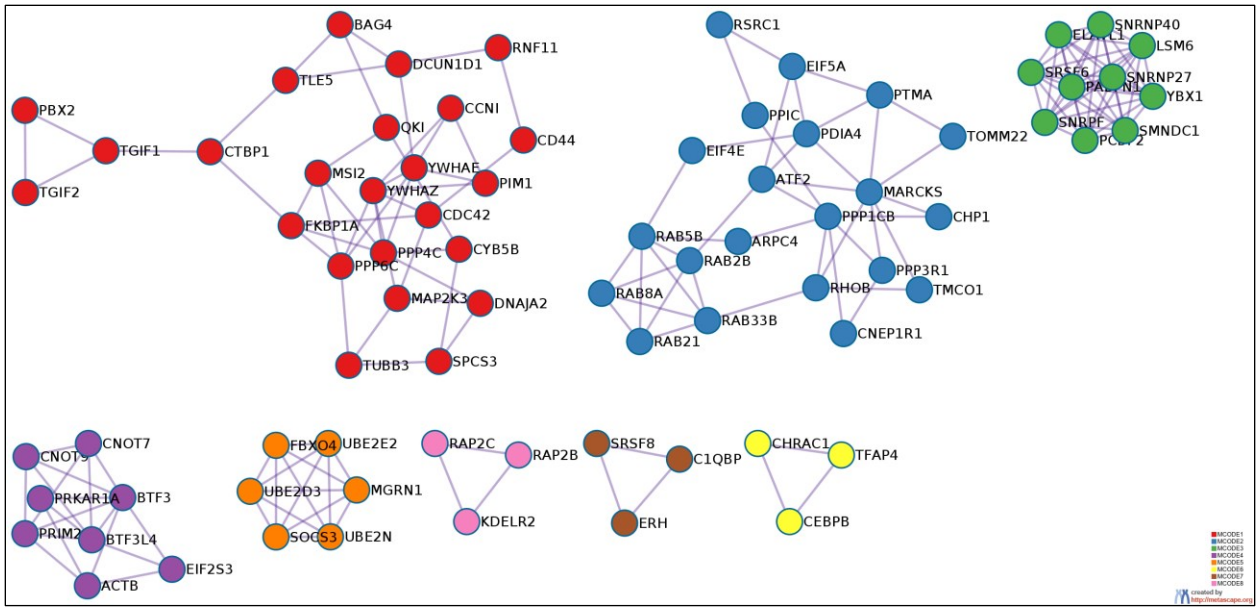

Figure 4.8. Protein-protein interaction network and MCODE components.

MCODE method was applied to identify closely related protein from protein-protein interaction network. The MCODE algorithm subclustered the network into 8 MCODE. The proteins from each MCODE have the same GO pathway. The detail of each MCODE is given in Table 4.3.

Table 4.3. GO enrichment analysis and MCODE network components.

Color	MCODE	GO	Description	Log10(P)
RED	MCODE_1	GO:0035305	negative regulation of dephosphorylation	-5.1
	MCODE_1	GO:0035303	regulation of dephosphorylation	-3.8
	MCODE_1	GO:0006468	protein phosphorylation	-3.7
BLUE	MCODE_2	GO:0006886	intracellular protein transport	-6.7
	MCODE_2	GO:0017157	regulation of exocytosis	-5.0
	MCODE_2	GO:0060627	regulation of vesicle-mediated transport	-4.6
GREEN	MCODE_3	GO:0016071	mRNA metabolic process	-14.3
	MCODE_3	GO:0006397	mRNA processing	-12.9
	MCODE_3	GO:0008380	RNA splicing	-11.2
PURPLE	MCODE_4	GO:0006417	regulation of translation	-3.7
	MCODE_4	GO:0034248	regulation of cellular amide metabolic process	-3.6
ORANGE	MCODE_5	GO:0016567	protein ubiquitination	-9.9
	MCODE_5	GO:0000209	protein polyubiquitination	-9.9
	MCODE_5	GO:0032446	protein modification by small protein conjugation	-9.7

HuR abrogates CS-induced COX-2 and IL-8 in primary lung fibroblasts

To further investigate the molecular function of HuR in HLFs, we next focused on the expression of COX-2 and IL-8 for several reasons. First, it is well established that HuR promotes the expression of these genes in many cell types [24, 32-34]. Second, CS is well described by us and other to induce the expression of COX-2 and IL-8 in various cell types including lung fibroblasts [41, 45, 46]. Finally, our data showed that HuR controls the expression of these two genes at the basal level and in response to CSE (Figure 4.2D). Thus, we utilized COX-2 and IL-8 to further evaluate how HuR is controlling their expression in primary lung cells. First, we confirmed the RNA-seq data using RT-qPCR in which HuR was silenced (siH). Here, there was a robust increase in the level of *PTGS2* and *CXCL8* mRNA in siH HLFs at the basal level and in response to CSE (Figure 4.9A and 4.9B), confirming that HuR prevents the induction of *PTGS2* and *CXCL8* in response to CSE.

We next evaluated the expression of COX-2 and IL-8 at the protein level upon knockdown of HuR (Figure 4.9C). In accordance with mRNA expression, there was also a significant increase in COX-2 protein when HuR expression was reduced (Figure 4.9D). Similarly, IL-8 was also significantly increased with HuR knockdown (Figure 4.9E). To be sure these results were not due to off-target effects of the siRNA, we utilized HuR-specific esiRNA (esiHuR) and corresponding control esiRNA (esiCtrl) (Figure 4.10A). Using these, we confirmed that COX-2 and IL-8 were significantly increased by HuR silencing following CSE exposure (Figure 4.10B and 4.10C). Hence, HuR suppresses CSE-induced COX-2 and IL-8 in HLFs.

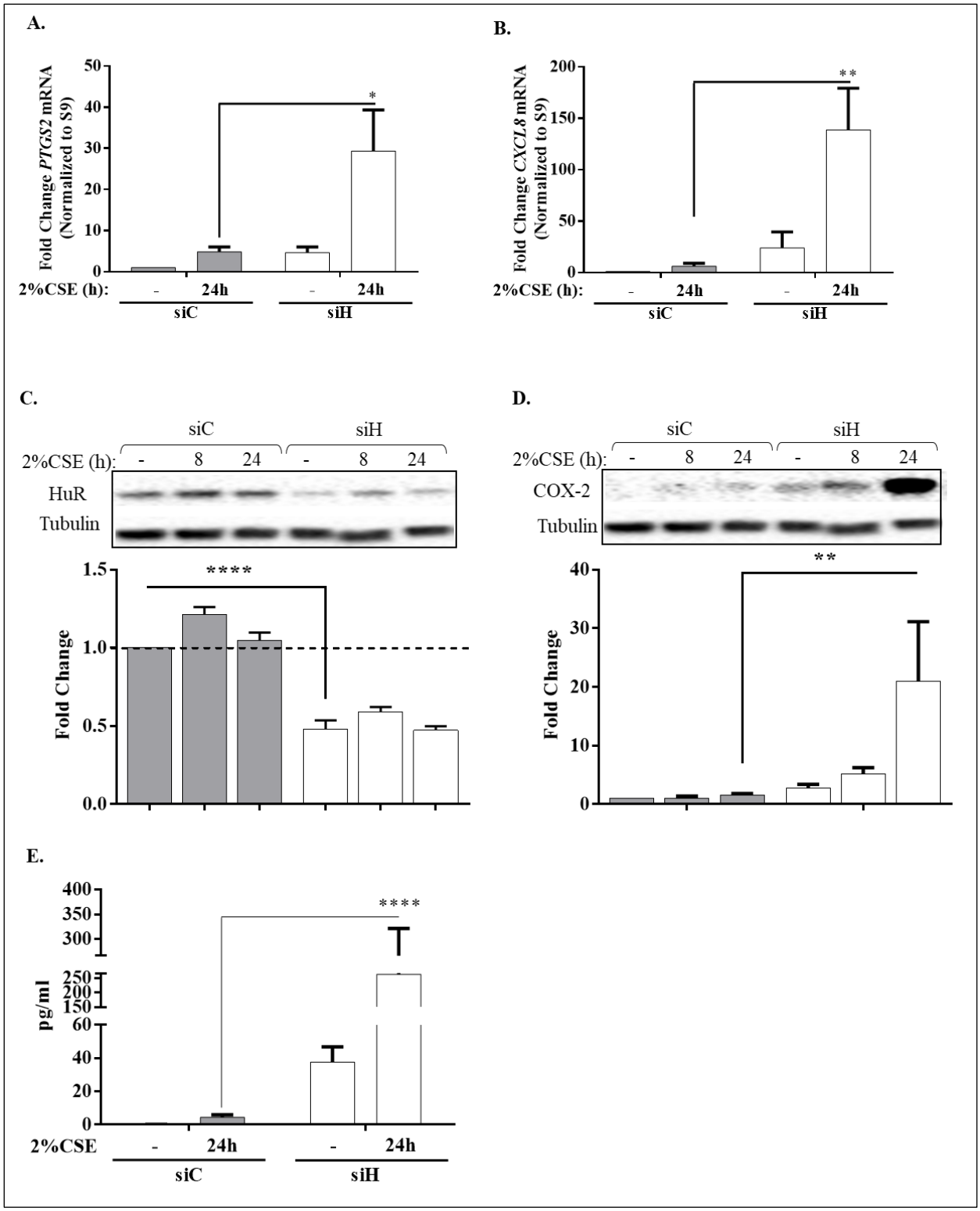

Figure 4.9. HuR silencing increases COX-2 and IL-8 expression in CSE-exposed HLFs.

A. There was an increase in the *PTGS2* mRNA in siHuR cells at the basal level and in response to 2% CSE for 24h. Results are expressed as the mean ± SEM of 5 independent experiments. **B.** There was an increase in the *CXCL8* mRNA in siHuR cells at the basal level and in response to 2% CSE for 24h. Results are expressed as the mean ± SEM of 4 independent experiments. **C.** Transfection of HLFs with siHuR reduced the level of HuR protein to ~50%. Results are expressed as the mean ± SEM of 5 independent experiments. **D.** There was significant increase in COX-2 protein levels in siHuR-transfected cells exposed to 2% CSE for 24h compared to siCtrl-transfected cells exposed to 2% CSE for 24h (***p= 0.0004). Results are expressed as the mean ± SEM of 5 independent experiments. **E.** There was significant increase in IL-8 protein levels in the cell culture supernatant from siHuR-transfected cells exposed to 2% CSE for 24h (****p=0.0001). Results are expressed as the mean ± SEM of 3 independent experiments.

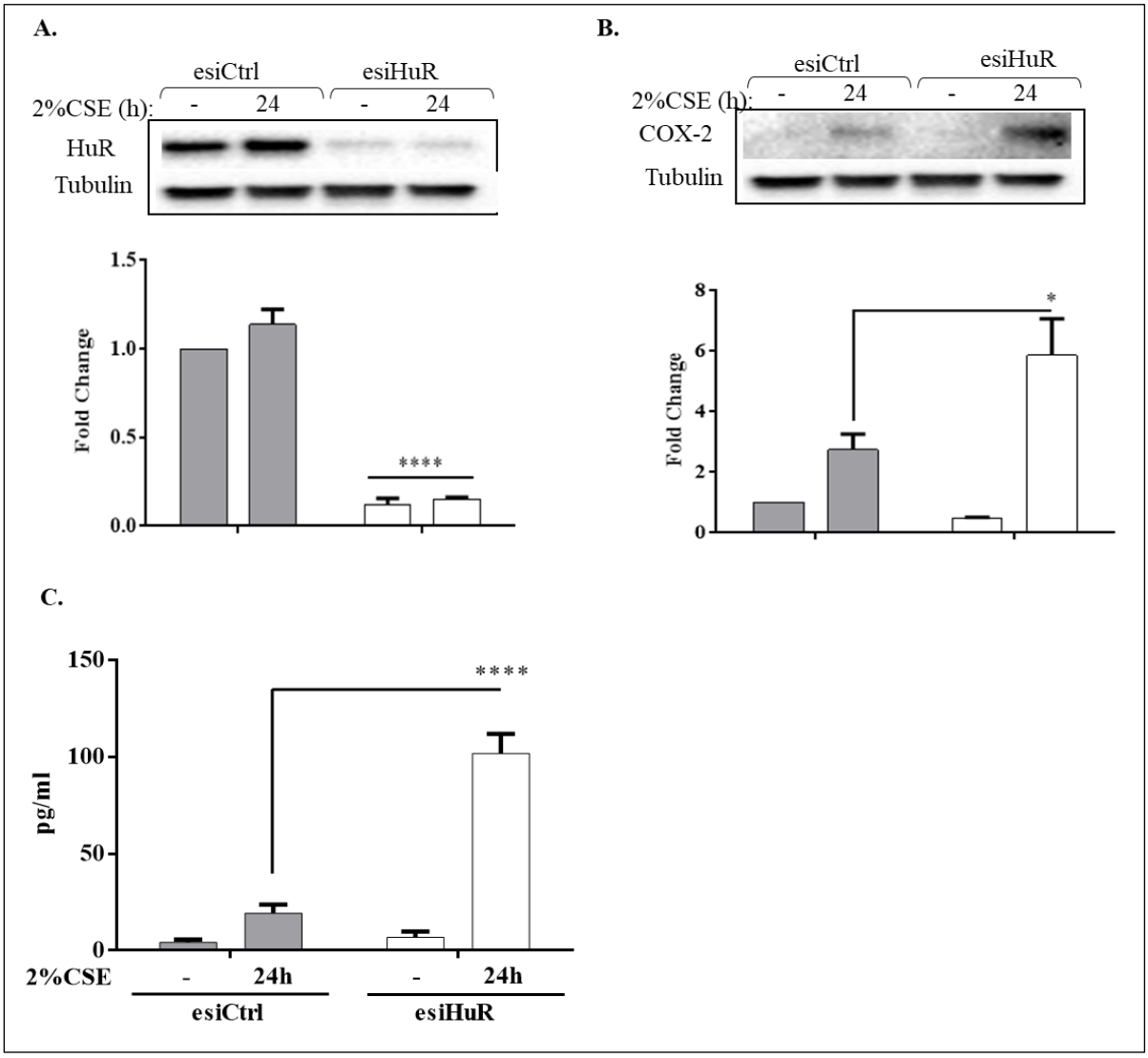

Figure 4.10. Validation of HuR suppression to CSE-induced COX-2 and IL-8 in HLFs.

A. The transfection of HLFs with esiHuR reduced the level of HuR protein to ~80%. Results are expressed as the mean ± SEM of 3 independent experiments. **B.** There was significant increase in COX-2 protein levels in esiHuR-transfected cells exposed to 2% CSE for 24h compared to siCtrl-transfected cells (*p= 0.01). Results are expressed as the mean ± SEM of 3 independent experiments. **C.** There was significant increase in IL-8 protein levels in the media from siHuR-transfected cells exposed to 2% CSE for 24h (****p=0.0001). Results are expressed as the mean ± SEM of 3 independent experiments.

HuR silencing stabilizes *PTGS2* and *CXCL8* mRNA in primary lung fibroblasts exposed to CSE.

HuR binds to target mRNA, thereby impacting their expression by regulating the stability of the transcript [18]. It is not known whether HuR associates with *PTGS2* and *CXCL8* mRNA in response to CS. To address this, we assessed HuR association with mRNA by immunoprecipitation of HuR followed by RT-qPCR analysis of *PTGS2* and *CXCL8* mRNA. Confirmation of successful HuR immunoprecipitation is in Figure 4.11A. In response to CSE, HuR strongly bound to *PTGS2* and *CXCL8* mRNA (Figure 4.11B and 4.11C). We also noticed that HuR associated with these two genes at the basal level. Thus, HuR binds to *PTGS2* and *CXCL8* mRNA in HLFs both at the basal level and in response to CSE. Then, we assessed if HuR controls the decay of *PTGS2* and *CXCL8* mRNA by performing ActD-chase experiments. We found that HuR knockdown increased the stability of *PTGS2* and *CXCL8* mRNA with CSE exposure (Figure 4.12A and 4.12B). Surprisingly, HuR abrogates CS-induced COX-2 and IL-8 expression by promoting the decay of their mRNA in HLFs. Altogether, these results support the importance of HuR in numerous cellular responses, including inflammation, in primary lung fibroblasts. Further insight into the molecular regulation of CS-induced inflammatory mediators, such as COX-2 and IL-8, is needed to understand the exact function of HuR in the context of CS-related diseases and further to facilitate the development of new target therapy.

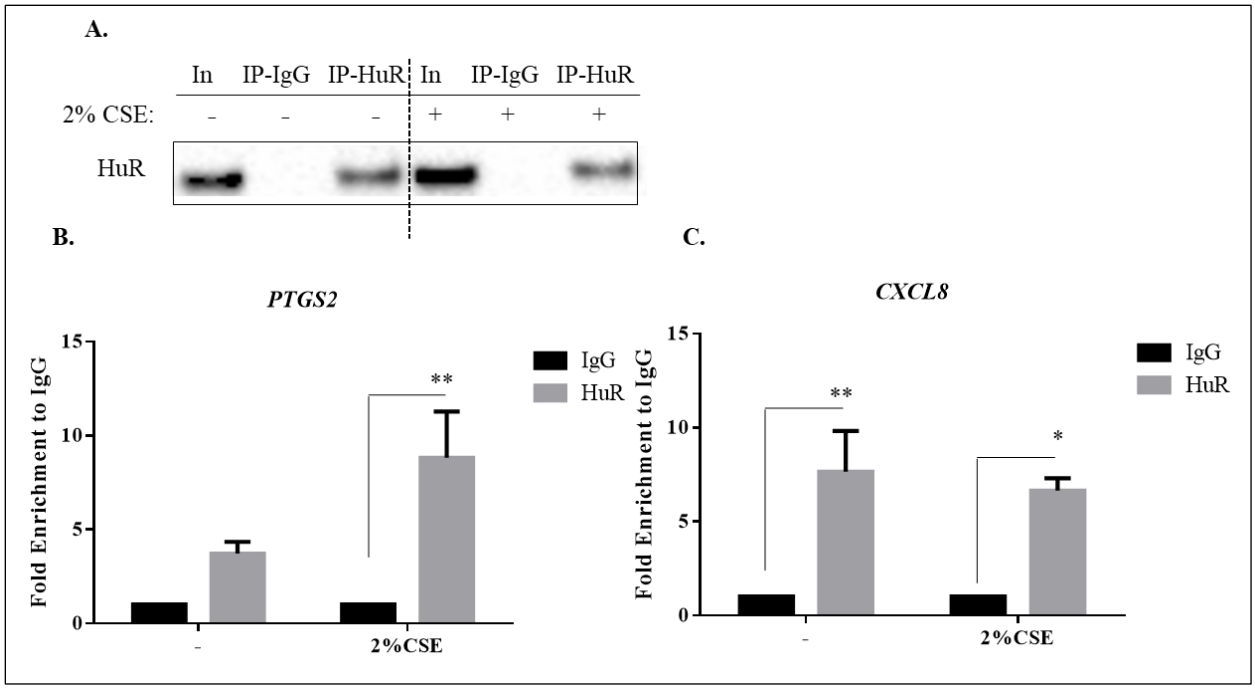

Figure 4.11. HuR binds to *PTGS2* and *CXCL8* mRNA in response to CSE.

A. Representative western blot (4 independent experiments) of IP-HuR is shown. Note the presence of HuR protein in IP-HuR but not in IP-IgG in both conditions. **B.** Enrichment of *PTGS2* mRNA in IP-HuR of HLFs at the basal level and in response to 2% CSE for 24h. Results are presented as the mean ± SEM of 4 independent experiments (** p = 0.01 compared to IgG). **C.** Enrichment of *CXCL8* mRNA in IP-HuR of HLFs at the basal level and in response to 2% CSE for 24h. Results are presented as the mean ± SEM of 3 independent experiments (* p = 0.01 and ** p = 0.006 compared to IgG).

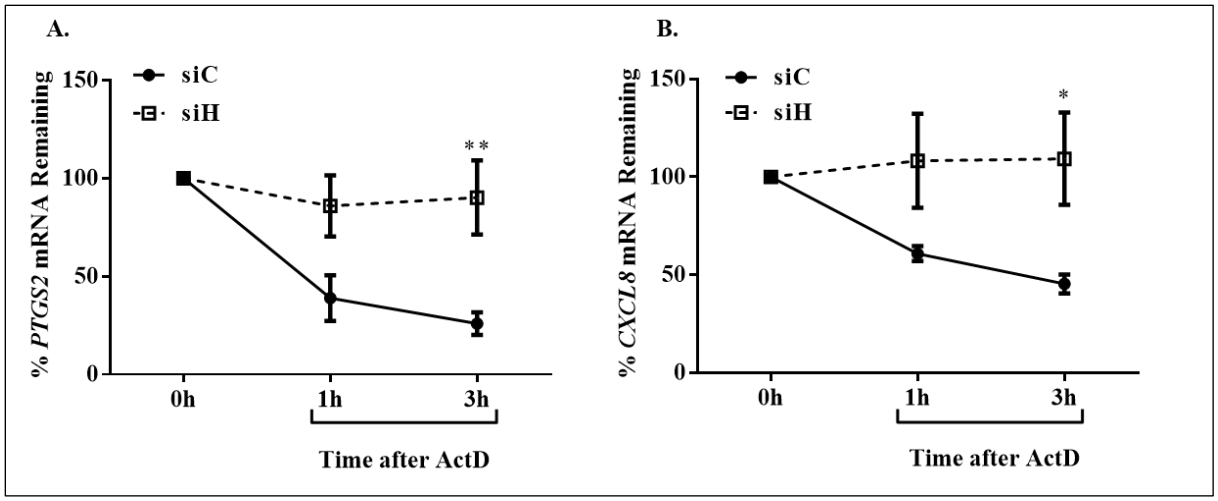

Figure 4.12. Knockdown of HuR stabilizes *PTGS2* and *CXCL8* mRNA in response to CSE.

A. siCtrl- and siHuR-transfected cells were treated with 2% CSE for 24h and then exposed to ActD (2 ug/ ml) for the indicated time point. *PTGS2* levels were set to equal 100% after CSE treatment for 24h and are expressed as percentage (%) of *PTGS2* mRNA remaining. In siHuR-transfected HLF, *PTGS2* mRNA was stable compared to siCtrl-transfected HLFs after exposure to ActD for 3h (** $p = 0.005$). Results are expressed as the mean ± SEM of 3 independent experiments. **B.** *CXCL8* mRNA was stable copmared to siCtrl-transfected HLF after exposure to ActD for 3h (* $p = 0.02$). Results are expressed as the mean ± SEM of 3 independent experiments.

4.5. DISCUSSION

Depending on the stimuli, HuR differently regulates the post-transcriptional modifications of target mRNAs; these modifications include mRNA stability [17, 19, 64]. To stabilize target mRNA, HuR translocates from the nucleus (where it normally resides) to the cytoplasm. HuR targets mRNA encoding proteins that are involved in numerous cellular processes including inflammation [17-21]. We recently found that HuR cytoplasmic localization is increased in the airway epithelium from smokers with or without COPD. We also observed that CSE induces HuR translocation to the cytoplasm in human lung fibroblasts, suggesting that smoke activates HuR [21]. However, HuR function in CS-induced lung inflammation still remains unclear. Therefore, in our current study, we sought to identify the role of HuR in lung fibroblasts in response to CSE using a multi-omics approach. We found that HuR reduces and induces genes involved in inflammation and calcium signaling pathways, respectively. HuR also binds to genes involved in the post-transcriptional regulations of mRNA. Mechanistically, we also reported that HuR repressed CS-induced COX-2 and IL-8 in lung fibroblasts by inducing the degradation of their mRNA.

Transcriptome analysis is a powerful tool that can be used to examine the quantity and sequences of RNA in a biological sample, which leads to the unbiased identification of genes. Consequently, this technique can help to elucidate the molecular regulatory mechanisms of these genes in cells upon administration of a stimuli such as CS. One of the main features of chronic CS exposure is the presence of inflammation, characterized in part by elevated levels of inflammatory mediators [41, 42]. Using an established *in vitro* system of CS exposure together with RNA-seq, we found that HuR can reduce and induce the expression of hundreds of genes implicated in

multiple cellular pathways. For instance, HuR supresses genes involved in the inflammatory response, including *PTGS2*, *CXCL8* and *CD36*. Surprisingly, this overall result is opposite to what has been found in previous studies. For example, it is well-established that HuR targets inflammatory genes, such as *PTGS2*, and can increase its expression in cancer cells [65-68]. A similar function of HuR was also observed in response to exogenous stimuli such as lipopolysaccharide (LPS) [67, 69, 70]. Here, we showed, for the first time, that HuR supresses the expression of these genes in lung fibroblasts exposed to CSE. One possible reason for the discrepancy between these results and ours may be due to differences in the disease state of the cells (cancer versus normal) and/or to the exogenous stimuli given the fact that we used primary HLFs derived from a non-smoker (without COPD) and utilized CSE as the stimuli. In light of this discrepancy, it would be advantageous to investigate HuR in HLFs from Smoker and COPD subjects, as HuR may function differently in diseased HLFs. However, our findings are not without precedence in the literature, as deletion of HuR *in vivo* enhances inflammation [71, 72]. It is noteworthy that HuR did promote the expression of other inflammatory genes, including *IL17D*. Moreover, we show for the first time that *IL17D* is expressed in lung fibroblasts and that its expression is regulated by HuR. Observations that IL-17D-deficient mice exhibit signs of more severe viral infection compared to wild type mice [73] suggests that IL-17D has an anti-inflammatory function and may protect the host against viral infection. However, the function of IL-17D in the lungs under CS exposure conditions needs to be elucidated. Altogether, HuR may act as both a repressor of pro-inflammatory genes and a promoter of genes that may have anti-inflammatory function in lung fibroblasts exposed to CSE.

HuR is well-described in the literature to promote the expression COX-2 [65, 68, 69, 74-76], an inducible enzyme that metabolizes arachidonic acid that has been released from the plasma membrane via phospholipase [77]. COX-2 synthesizes prostaglandins, including prostaglandin (PG) E2 [77]. HuR also induces the expression of IL-8 [78, 79], a chemokine that attracts immune cells to the site of the injury, particularly neutrophils and monocytes [47, 48]. However, when we knockdown HuR in lung fibroblasts, we observed an increase in COX-2 and IL-8 expression at the protein levels, findings that are therefore inconsistent with previous studies but in accordance with the mRNA expression discussed above. For example, knockdown HuR decreased IL-8 secretion in primary human bronchial epithelial cells exposed to CSE in combination with human rhinovirus (HRV) [79]. HRV infection is a common trigger of virus-associated COPD exacerbations that is correlated with persistent lung inflammation [80, 81]. Although HuR function in response to HRV alone is not clear, previous studies showed that HuR can participate in other viral infection [82]. For instance, Sindbis virus has high affinity for HuR and sequestrates HuR in cytoplasm; consequently, the expression of cellular mRNA is dysregulated during infection [83]. This finding reveals that HRV may induce HuR translocation to the cytoplasm to differentially regulate target genes. Mechanistically, we postulated that HuR would stabilize *PTGS2* and *CXCL8* mRNA in response to CSE as a means to increase their protein expression. However, we found that HuR promotes the decay of *PTGS2* and *CXCL8* mRNA upon exposure to CSE, and subsequently reduces their expression. Although HuR is well recognized for its ability to stabilize target mRNA, there are some studies have found that HuR induces the decay of target mRNA- results that are similar to ours. A possible mechanism for HuR to induce the decay of target genes is through the collaboration with microRNA (miRNA). miRNA pairs to the 3′ UTR of mRNA by partial sequence matching after being incorporated into the RNA-induced silencing complex (RISC). This leads to

direct post-transcriptional repression by inhibiting translation and/or inducing mRNA decay [84, 85]. HuR also pairs to the 3′ UTR of mRNA; hence miRNA and HuR may interact to further fine-tune post-transcriptional regulatory mechanisms. For example, HuR promotes the interaction of miRNA *let-7*- loaded RISC with the 3′ UTR of the proto-oncogene *MYC* mRNA to repress its expression [86]. Interestingly, overexpression of *let-7* miRNA reduces the expression of *PTGS2* and *CXCL8* [87, 88]. These finding suggest that HuR may collaborate with *let-7* miRNA to repress COX-2 and IL-8 in lung fibroblasts. Further, CS can differentially up- and down-regulate miRNA at the same time [89, 90], suggesting that HuR collaboration with miRNA to regulate the expression target genes may depend on the timing and level of select miRNA within the cell. For example, *let-7* miRNA is downregulated in response to chronic CS exposure and in COPD [90-92], and we previously found that COX-2 is elevated in COPD-derived lung fibroblasts [49]. Although a role for HuR and/or *let-7* interaction in COPD is not known yet, these data raise the possibility that the loss of *let-7* may switch HuR function from a destabilizer to a stabilizer of *PTGS2* mRNA in the context of CS and/or COPD.

HuR can also cooperate with other RBPs to bind target mRNA and regulate their expression. An example of this is the ability of HuR to promote the interaction of the RBP KH-type splicing regulatory protein (KSRP) with *Nucleophosmin* (NPM, also known as B23) mRNA leading to a decrease in its protein level [29]. KSRP can also destabilize *PTGS2* and *CXCL8* mRNA [93], a finding that suggests the possibility that HuR and KSRP may collaborate to destabilize *PTGS2* and *CXCL8* mRNA in lung fibroblasts. However, the function of HuR and/or KSRP in CS-induced diseases, including COPD, needs further investigation. One mechanism not explored in this study is the potential that HuR may be increasing the protein level and/or the

activity of other RBPs, which would change the expression of target mRNA. For example, HuR induces the protein expression of KSRP and T-cell intracellular antigen 1 (TIA-1) [94]. Thus, in addition to HuR cooperating with KSRP, HuR may also induce KSRP as a means to reduce target gene expression in lung fibroblast. Additionally, TIA-1 is a well known RBP that represses the expression of various mRNA, including *PTGS2* [95, 96]. TIA-1 is also involved in the pathogenesis of asthma because of its ability to decrease pulmonary inflammation [97]. These data raise the possibility that HuR may upregulate TIA-1 as a mechanism through which COX-2 expression is attenuated in lung fibroblasts. However, the function of HuR, KSRP and/or TIA-1 in CS-related diseases, including COPD, needs additional investigation.

Our data also suggests that HuR regulation of protein expression occurs at multiple levels within the cell. We found that HuR up- and down-regulates hundreds of genes; HuR also binds to hundreds of genes, suggesting action at the post-transcriptional level. This is supported by our observation that HuR associates with *PTGS2* and *CXCL8* mRNA and induces their mRNA degradation, which subsequently reduces their expression. This was not the case for all genes, where we found that HuR binds to numerous mRNA but does not control the mRNA level of these genes, suggesting differential response based on the particular gene itself. Another well known function of HuR is its ability to regulate protein translation. An example of this is HuR binding to *STAT3* mRNA and promoting its translation- but without affecting the mRNA level of *STAT3* [27]. HuR can also binds to the P53 (*TP53*) mRNA and induces its translation [98]. P53 is a tumor suppressor protein that controls the transcription of many genes involved in cell cycle arrest and DNA repair [98]. Here, we found that in response to CSE, HuR binds to *TP53* mRNA. However, HuR did not regulate its mRNA level, and we did not assess whether HuR alters the protein level

of *TP53* mRNA in our experimental system. Based on the above evidence, however, these data suggest that HuR may bind to target mRNA to control protein levels by either inducing or suppressing translation without changing the mRNA level.

To date, there are only a handful studies that have investigated HuR in the pathogenesis of COPD, a leading cause of chronic morbidity and mortality worldwide [99]. COPD is a lung disease characterized by both emphysema and chronic bronchitis [100]. Small airway disease is also a recognized feature of COPD, and is characterized by the presence of inflammation, fibrosis, and mucous plugging, all of which correlate with the severity of airflow obstruction [101]. We recently found that HuR cytoplasmic localization is higher in lung cells, including epithelial cells and fibroblasts, from smoker and COPD subjects as well as in lung fibroblasts exposed to CSE [21]. These findings raise the possibility that the expression and localization of HuR in important lung structural cells may predispose to the aberrant tissue damage in response to CS. In support of this, we found that lung fibroblasts express *IL34* and that HuR promotes its expression. IL-34 is a cytokine that binds to colony-stimulating factor (CSF)-1 receptor, which induces monocytes survival and growth, and their differentiation into macrophages [102]. Intriguingly, IL-34 increases the secretion of IL-10, an anti-inflammatory cytokine, in macrophages [103]. This data suggests that HuR may have an anti-inflammatory function in response to CS by promoting the expression of IL-34. Further, liver- and intestinal-derived fibroblasts express IL-34, which induces collagen production [104, 105]. We and others have also found that HuR induces the expression of COL I [28, 106, 107], which is associated with fibrosis formation. These data suggest that HuR may promote fibrosis via IL-34 in lung fibroblasts, and thus could be involved in fibrosis formation, a feature of small airway disease. Moreover, we found that HuR reduces *CD36*

expression in lung fibroblasts exposed to CSE. CD36 is a multi-ligand scavenger receptor that is expressed in various cell types, including fibroblasts [108]. CD36 induces COL I degradation [109]. These data indicate a possible mechanism by which HuR control over *CD36* may promote the expression of COL I by lung fibroblasts, leading to the development of fibrosis in COPD. CD36 is also required for the senescence-associated secretory phenotype, and is upregulated in senescent fibroblasts [108, 110]. It is also known that HuR silencing accelerates the senescent phenotype [30]. Although senescence is a hallmark in COPD [111, 112], and the function and regulation of CD36 by HuR in the context of COPD pathogenesis is not known, it could be that HuR may prevent cellular senescence, in part, through the downregulation of *CD36* expression.

In summary, using multi-omics approaches, our work is the first to elucidate the regulatory role of HuR in lung fibroblasts at the basal level and in response to CSE. We found that HuR demotes inflammation and oxidative stress and promotes calcium signaling pathways. HuR also binds to genes involved in the post-transcriptional regulation of mRNA. Mechanistically, we showed that HuR dampens the expression of COX-2 and IL-8 in lung fibroblasts exposed to CSE by inducing the decay of *PTGS2* and *CXCL8* mRNA (Figure 4.13). With a growing interest in understanding the molecular underpinnings of post-transcriptional gene regulation by HuR, our results raise awareness for the consideration of additional molecular investigation of HuR in lungs. The uncovering of these mechanisms may lead to the identification of novel target therapy of CS-related diseases, including COPD.

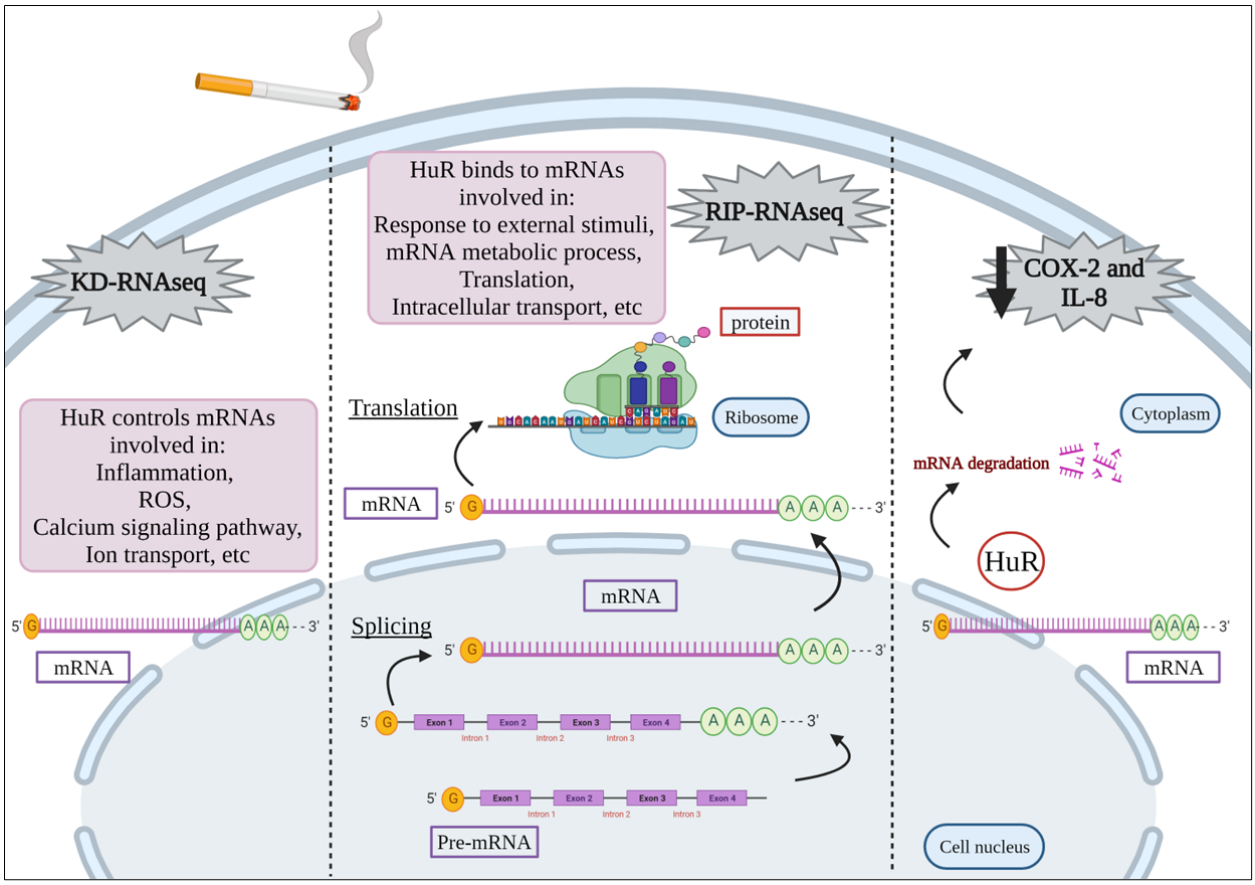

Figure 4.13. HuR function in lung fibroblasts exposed to CS.

Integrated analysis of HuR in lung fibroblasts indicates that HuR controls mRNA involved in numererous cellular pathways including Inflammation, ROS, Calcium signaling pathway, Ion transport, etc., and binds to mRNAs involved in the Response to external stimuli, mRNA metabolic process, Translation, Intracellular transport, etc. Notably, HuR decreases the expression of COX-2 and IL-8 by inducing mRNA degradation. KD-RNAseq; knockdown of HuR followed by RNA-seq.

4.6. SUPPLEMENTARY TABLES

Tables S4.: Supplementary tables from the RNA-seq data.

Table S4.1 D:\Supplementary 1.xlsx

Table S4.2 D:\Supplementary 2.xlsx

Table S4.3 D:\Supplementary 3.xlsx

Table S4.4 D:\Supplementary 4.xlsx

Table S4.5 D:\Supplementary 5.xlsx

Table S4.6 D:\Supplementary 6.xlsx

Table S4.7 D:\Supplementary 7.xlsx

Table S4.8 D:\Supplementary 8.xlsx

Table S4.9 D:\Supplementary 9.xlsx

4.7. REFERENCES

1. Haddad, M. and S. Sharma, Physiology, Lung, in StatPearls. 2022: Treasure Island (FL).

2. Franks, T.J., et al., Resident cellular components of the human lung: current knowledge and goals for research on cell phenotyping and function. Proc Am Thorac Soc, 2008. 5(7): p. 763-6.

3. Nicod, L.P., Lung defences: an overview. European Respiratory Review, 2005. 14: p. 45-50.

4. Kurt, O.K., J. Zhang, and K.E. Pinkerton, Pulmonary health effects of air pollution. Current opinion in pulmonary medicine, 2016. 22(2): p. 138-143.

5. WHO. Air pollution. 2021; Available from: https://www.who.int/health-topics/air-pollution#tab=tab_1.

6. WHO. 2020; Available from: https://www.who.int/news-room/fact-sheets/detail/tobacco.

7. Zhou, G., Tobacco, air pollution, environmental carcinogenesis, and thoughts on conquering strategies of lung cancer. Cancer Biol Med, 2019. 16(4): p. 700-713.

8. Bhalla, D.K., et al., Cigarette smoke, inflammation, and lung injury: a mechanistic perspective. J Toxicol Environ Health B Crit Rev, 2009. 12(1): p. 45-64.

9. Stampfli, M.R. and G.P. Anderson, How cigarette smoke skews immune responses to promote infection, lung disease and cancer. Nat Rev Immunol, 2009. 9(5): p. 377-84.

10. Lee, J., V. Taneja, and R. Vassallo, Cigarette smoking and inflammation: cellular and molecular mechanisms. J Dent Res, 2012. 91(2): p. 142-9.

11. WHO. COPD. 2021; Available from: https://www.who.int/news-room/fact-sheets/detail/chronic-obstructive-pulmonary-disease-(copd).

12. WHO. Cancer. 2021; Available from: https://www.who.int/news-room/fact-sheets/detail/cancer.

13. Fong, K.M., et al., Lung cancer. 9: Molecular biology of lung cancer: clinical implications. Thorax, 2003. 58(10): p. 892-900.

14. Bagdonas, E., et al., Novel aspects of pathogenesis and regeneration mechanisms in COPD. Int J Chron Obstruct Pulmon Dis, 2015. 10: p. 995-1013.

15. Baglole, C.J., et al., Differential induction of apoptosis by cigarette smoke extract in primary human lung fibroblast strains: implications for emphysema. Am J Physiol Lung Cell Mol Physiol, 2006. 291(1): p. L19-29.

16. Michaeloudes, C., et al., Dealing with Stress: Defective Metabolic Adaptation in Chronic Obstructive Pulmonary Disease Pathogenesis. Ann Am Thorac Soc, 2017. 14(Supplement_5): p. S374-S382.

17. Srikantan, S. and M. Gorospe, HuR function in disease. Frontiers in bioscience (Landmark edition), 2012. 17: p. 189.

18. Grammatikakis, I., K. Abdelmohsen, and M. Gorospe, Posttranslational control of HuR function. Wiley Interdiscip Rev RNA, 2017. 8(1).

19. Brennan, C.M. and J.A. Steitz, HuR and mRNA stability. Cell Mol Life Sci, 2001. 58(2): p. 266-77.

20. Zago, M., et al., Aryl Hydrocarbon Receptor-Dependent Retention of Nuclear HuR Suppresses Cigarette Smoke-Induced Cyclooxygenase-2 Expression Independent of DNA-Binding. PLoS One, 2013. 8(9): p. e74953.

21. Aloufi, N., et al., Role of Human Antigen R (HuR) in the Regulation of Pulmonary ACE2 Expression. Cells, 2021. 11(1).

22. Izquierdo, J.M., Hu antigen R (HuR) functions as an alternative pre-mRNA splicing regulator of Fas apoptosis-promoting receptor on exon definition. J Biol Chem, 2008. 283(27): p. 19077-84.

23. Dormoy-Raclet, V., et al., The RNA-binding protein HuR promotes cell migration and cell invasion by stabilizing the beta-actin mRNA in a U-rich-element-dependent manner. Mol Cell Biol, 2007. 27(15): p. 5365-80.

24. Wang, J., et al., Multiple functions of the RNA-binding protein HuR in cancer progression, treatment responses and prognosis. Int J Mol Sci, 2013. 14(5): p. 10015-41.

25. Nabors, L.B., et al., HuR, a RNA stability factor, is expressed in malignant brain tumors and binds to adenine- and uridine-rich elements within the 3' untranslated regions of cytokine and angiogenic factor mRNAs. Cancer Res, 2001. 61(5): p. 2154-61.

26. Abdelmohsen, K., et al., Posttranscriptional orchestration of an anti-apoptotic program by HuR. Cell Cycle, 2007. 6(11): p. 1288-92.

27. Mubaid, S., et al., HuR counteracts miR-330 to promote STAT3 translation during inflammation-induced muscle wasting. Proc Natl Acad Sci U S A, 2019. 116(35): p. 17261-17270.

28. Al-Habeeb, F., et al., Human antigen R promotes lung fibroblast differentiation to myofibroblasts and increases extracellular matrix production. J Cell Physiol, 2021. 236(10): p. 6836-6851.

29. Cammas, A., et al., Destabilization of nucleophosmin mRNA by the HuR/KSRP complex is required for muscle fibre formation. Nat Commun, 2014. 5: p. 4190.

30. Lee, J.H., et al., Loss of RNA-binding protein HuR facilitates cellular senescence through posttranscriptional regulation of TIN2 mRNA. Nucleic Acids Res, 2018. 46(8): p. 4271-4285.

31. Cui, Y.H., et al., Posttranscriptional regulation of MMP-9 by HuR contributes to IL-1beta-induced pterygium fibroblast migration and invasion. J Cell Physiol, 2020. 235(6): p. 5130-5140.

32. Giaginis, C., et al., Hu-antigen receptor (HuR) and cyclooxygenase-2 (COX-2) expression in human non-small-cell lung carcinoma: associations with clinicopathological parameters, tumor proliferative capacity and patients' survival. Tumour Biol, 2015. 36(1): p. 315-27.

33. Wang, J., et al., The expression of RNA-binding protein HuR in non-small cell lung cancer correlates with vascular endothelial growth factor-C expression and lymph node metastasis. Oncology, 2009. 76(6): p. 420-9.

34. Muralidharan, R., et al., HuR-targeted nanotherapy in combination with AMD3100 suppresses CXCR4 expression, cell growth, migration and invasion in lung cancer. Cancer Gene Ther, 2015. 22(12): p. 581-90.

35. Sirianni, F.E., F.S. Chu, and D.C. Walker, Human alveolar wall fibroblasts directly link epithelial type 2 cells to capillary endothelium. Am J Respir Crit Care Med, 2003. 168(12): p. 1532-7.

36. White, E.S., Lung extracellular matrix and fibroblast function. Ann Am Thorac Soc, 2015. 12 Suppl 1: p. S30-3.

37. Krausgruber, T., et al., Structural cells are key regulators of organ-specific immune responses. Nature, 2020. 583(7815): p. 296-302.

38. Togo, S., et al., Lung fibroblast repair functions in patients with chronic obstructive pulmonary disease are altered by multiple mechanisms. Am J Respir Crit Care Med, 2008. 178(3): p. 248-60.

39. Zhang, X., et al., Increased interleukin (IL)-8 and decreased IL-17 production in chronic obstructive pulmonary disease (COPD) provoked by cigarette smoke. Cytokine, 2011. 56(3): p. 717-25.

40. Zhang, J., et al., Pro-inflammatory phenotype of COPD fibroblasts not compatible with repair in COPD lung. J Cell Mol Med, 2012. 16(7): p. 1522-32.

41. Martey, C.A., et al., Cigarette smoke induces cyclooxygenase-2 and microsomal prostaglandin E2 synthase in human lung fibroblasts: implications for lung inflammation and cancer. Am J Physiol Lung Cell Mol Physiol, 2004. 287(5): p. L981-91.

42. Barnes, P.J., Inflammatory mechanisms in patients with chronic obstructive pulmonary disease. J Allergy Clin Immunol, 2016. 138(1): p. 16-27.

43. Barnes, P.J., S.D. Shapiro, and R.A. Pauwels, Chronic obstructive pulmonary disease: molecular and cellular mechanisms. Eur Respir J, 2003. 22(4): p. 672-88.

44. Vlahos, R. and S. Bozinovski, Role of alveolar macrophages in chronic obstructive pulmonary disease. Front Immunol, 2014. 5: p. 435.

45. Baglole, C.J., et al., The aryl hydrocarbon receptor attenuates tobacco smoke-induced cyclooxygenase-2 and prostaglandin production in lung fibroblasts through regulation of the NF-kappaB family member RelB. J Biol Chem, 2008. 283(43): p. 28944-57.

46. Li, C.J., et al., MAPK pathway mediates EGR-1-HSP70-dependent cigarette smoke-induced chemokine production. Am J Physiol Lung Cell Mol Physiol, 2007. 292(5): p. L1297-303.

47. Qazi, B.S., K. Tang, and A. Qazi, Recent advances in underlying pathologies provide insight into interleukin-8 expression-mediated inflammation and angiogenesis. Int J Inflam, 2011. 2011: p. 908468.

48. Moretto, N., et al., Cigarette smoke and its component acrolein augment IL-8/CXCL8 mRNA stability via p38 MAPK/MK2 signaling in human pulmonary cells. Am J Physiol Lung Cell Mol Physiol, 2012. 303(10): p. L929-38.

49. Zago, M., et al., Low levels of the AhR in chronic obstructive pulmonary disease (COPD)-derived lung cells increases COX-2 protein by altering mRNA stability. PloS one, 2017. 12(7): p. e0180881-e0180881.

50. Martey, C.A., et al., The aryl hydrocarbon receptor is a regulator of cigarette smoke induction of the cyclooxygenase and prostaglandin pathways in human lung fibroblasts. Am J Physiol Lung Cell Mol Physiol, 2005. 289(3): p. L391-9.

51. Sheridan, J.A., et al., Decreased expression of the NF-kappaB family member RelB in lung fibroblasts from Smokers with and without COPD potentiates cigarette smoke-induced COX-2 expression. Respir Res, 2015. 16: p. 54.

52. Fonseca, G.J., et al., Diverse motif ensembles specify non-redundant DNA binding activities of AP-1 family members in macrophages. Nat Commun, 2019. 10(1): p. 414.

53. Keene, J.D., J.M. Komisarow, and M.B. Friedersdorf, RIP-Chip: the isolation and identification of mRNAs, microRNAs and protein components of ribonucleoprotein complexes from cell extracts. Nat Protoc, 2006. 1(1): p. 302-7.

54. Oliveros, J.C. Venny. An interactive tool for comparing lists with Venn's diagrams. 2007-2015; Available from: https://bioinfogp.cnb.csic.es/tools/venny/index.html.

55. Zhou, Y., et al., Metascape provides a biologist-oriented resource for the analysis of systems-level datasets. Nat Commun, 2019. 10(1): p. 1523.

56. Hecht, E., et al., Aryl hydrocarbon receptor-dependent regulation of miR-196a expression controls lung fibroblast apoptosis but not proliferation. Toxicol Appl Pharmacol, 2014. 280(3): p. 511-25.

57. Hyman, R.W. and N. Davidson, Kinetics of the in vitro inhibition of transcription by actinomycin. J Mol Biol, 1970. 50(2): p. 421-38.

58. Meisner, N.C. and W. Filipowicz, Properties of the Regulatory RNA-Binding Protein HuR and its Role in Controlling miRNA Repression. Adv Exp Med Biol, 2011. 700: p. 106-23.

59. Kotta-Loizou, I., et al., Current Evidence and Future Perspectives on HuR and Breast Cancer Development, Prognosis, and Treatment. Neoplasia, 2016. 18(11): p. 674-688.

60. Srikantan, S. and M. Gorospe, HuR function in disease. Front Biosci (Landmark Ed), 2012. 17: p. 189-205.

61. Prechtel, A.T., et al., Expression of CD83 is regulated by HuR via a novel cis-active coding region RNA element. J Biol Chem, 2006. 281(16): p. 10912-25.

62. Yeh, C.H., et al., RNA-binding protein HuR interacts with thrombomodulin 5'untranslated region and represses internal ribosome entry site-mediated translation under IL-1 beta treatment. Mol Biol Cell, 2008. 19(9): p. 3812-22.

63. Koks, G., et al., Smoking-induced expression of the GPR15 gene indicates its potential role in chronic inflammatory pathologies. Am J Pathol, 2015. 185(11): p. 2898-906.

64. Aloufi, N., et al., Aberrant Post-Transcriptional Regulation of Protein Expression in the Development of Chronic Obstructive Pulmonary Disease. Int J Mol Sci, 2021. 22(21).

65. Doller, A., et al., High-constitutive HuR phosphorylation at Ser 318 by PKC{delta} propagates tumor relevant functions in colon carcinoma cells. Carcinogenesis, 2011. 32(5): p. 676-85.

66. Dixon, D.A., et al., Altered expression of the mRNA stability factor HuR promotes cyclooxygenase-2 expression in colon cancer cells. J Clin Invest, 2001. 108(11): p. 1657-65.

67. Nabors, L.B., et al., Tumor necrosis factor alpha induces angiogenic factor up-regulation in malignant glioma cells: a role for RNA stabilization and HuR. Cancer Res, 2003. 63(14): p. 4181-7.

68. Liao, W.L., et al., The RNA-binding protein HuR stabilizes cytosolic phospholipase A2alpha mRNA under interleukin-1beta treatment in non-small cell lung cancer A549 Cells. J Biol Chem, 2011. 286(41): p. 35499-35508.

69. Fernau, N.S., et al., Role of HuR and p38MAPK in ultraviolet B-induced post-transcriptional regulation of COX-2 expression in the human keratinocyte cell line HaCaT. The Journal of biological chemistry, 2010. 285(6): p. 3896-3904.

70. Ke, Y., et al., Erratum: PARP1 promotes gene expression at the post-transcriptional level by modulating the RNA-binding protein HuR. Nat Commun, 2017. 8: p. 15191.

71. Yiakouvaki, A., et al., Myeloid cell expression of the RNA-binding protein HuR protects mice from pathologic inflammation and colorectal carcinogenesis. J Clin Invest, 2012. 122(1): p. 48-61.

72. Siang, D.T.C., et al., The RNA-binding protein HuR is a negative regulator in adipogenesis. Nat Commun, 2020. 11(1): p. 213.

73. Saddawi-Konefka, R., et al., Nrf2 Induces IL-17D to Mediate Tumor and Virus Surveillance. Cell Rep, 2016. 16(9): p. 2348-58.

74. Doller, A., et al., Posttranslational modification of the AU-rich element binding protein HuR by protein kinase Cdelta elicits angiotensin II-induced stabilization and nuclear export of cyclooxygenase 2 mRNA. Mol Cell Biol, 2008. 28(8): p. 2608-25.

75. Doller, A., et al., Protein kinase C alpha-dependent phosphorylation of the mRNA-stabilizing factor HuR: implications for posttranscriptional regulation of cyclooxygenase-2. Mol Biol Cell, 2007. 18(6): p. 2137-48.

76. Fernau, N.S., et al., Role of HuR and p38MAPK in ultraviolet B-induced post-transcriptional regulation of COX-2 expression in the human keratinocyte cell line HaCaT. J Biol Chem, 2010. 285(6): p. 3896-904.

77. Sobolewski, C., et al., The role of cyclooxygenase-2 in cell proliferation and cell death in human malignancies. Int J Cell Biol, 2010. 2010: p. 215158.

78. Choi, H.J., et al., HuR/ELAVL1 RNA binding protein modulates interleukin-8 induction by muco-active ribotoxin deoxynivalenol. Toxicol Appl Pharmacol, 2009. 240(1): p. 46-54.

79. Hudy, M.H. and D. Proud, Cigarette smoke enhances human rhinovirus-induced CXCL8 production via HuR-mediated mRNA stabilization in human airway epithelial cells. Respir Res, 2013. 14: p. 88.

80. George, S.N., et al., Human rhinovirus infection during naturally occurring COPD exacerbations. Eur Respir J, 2014. 44(1): p. 87-96.

81. Owuor, N., et al., Rhinovirus and COPD airway epithelium. Pulm Crit Care Med, 2017. 2(3).

82. Garcia-Moreno, M., A.I. Jarvelin, and A. Castello, Unconventional RNA-binding proteins step into the virus-host battlefront. Wiley Interdiscip Rev RNA, 2018. 9(6): p. e1498.

83. Barnhart, M.D., et al., Changes in cellular mRNA stability, splicing, and polyadenylation through HuR protein sequestration by a cytoplasmic RNA virus. Cell Rep, 2013. 5(4): p. 909-17.

84. Kawamata, T. and Y. Tomari, Making RISC. Trends Biochem Sci, 2010. 35(7): p. 368-76.

85. Fabian, M.R., N. Sonenberg, and W. Filipowicz, Regulation of mRNA translation and stability by microRNAs. Annu Rev Biochem, 2010. 79: p. 351-79.

86. Kim, H.H., et al., HuR recruits let-7/RISC to repress c-Myc expression. Genes Dev, 2009. 23(15): p. 1743-8.

87. Teng, G.G., et al., Let-7b is involved in the inflammation and immune responses associated with Helicobacter pylori infection by targeting Toll-like receptor 4. PLoS One, 2013. 8(2): p. e56709.

88. Peng, C.Y., et al., Let-7c restores radiosensitivity and chemosensitivity and impairs stemness in oral cancer cells through inhibiting interleukin-8. J Oral Pathol Med, 2018. 47(6): p. 590-597.

89. Schembri, F., et al., MicroRNAs as modulators of smoking-induced gene expression changes in human airway epithelium. Proc Natl Acad Sci U S A, 2009. 106(7): p. 2319-24.

90. Izzotti, A., et al., Downregulation of microRNA expression in the lungs of rats exposed to cigarette smoke. FASEB J, 2009. 23(3): p. 806-12.

91. Van Pottelberge, G.R., et al., MicroRNA expression in induced sputum of smokers and patients with chronic obstructive pulmonary disease. Am J Respir Crit Care Med, 2011. 183(7): p. 898-906.

92. Izzotti, A., et al., Dose-responsiveness and persistence of microRNA expression alterations induced by cigarette smoke in mouse lung. Mutat Res, 2011. 717(1-2): p. 9-16.

93. Winzen, R., et al., Functional analysis of KSRP interaction with the AU-rich element of interleukin-8 and identification of inflammatory mRNA targets. Mol Cell Biol, 2007. 27(23): p. 8388-400.

94. Pullmann, R., Jr., et al., Analysis of turnover and translation regulatory RNA-binding protein expression through binding to cognate mRNAs. Mol Cell Biol, 2007. 27(18): p. 6265-78.

95. Dixon, D.A., et al., Regulation of cyclooxygenase-2 expression by the translational silencer TIA-1. J Exp Med, 2003. 198(3): p. 475-81.

96. Fernandez-Gomez, A. and J.M. Izquierdo, The Multifunctional Faces of T-Cell Intracellular Antigen 1 in Health and Disease. Int J Mol Sci, 2022. 23(3).

97. Simarro, M., et al., The translational repressor T-cell intracellular antigen-1 (TIA-1) is a key modulator of Th2 and Th17 responses driving pulmonary inflammation induced by exposure to house dust mite. Immunology letters, 2012. 146(1-2): p. 8-14.

98. Mazan-Mamczarz, K., et al., RNA-binding protein HuR enhances p53 translation in response to ultraviolet light irradiation. Proceedings of the National Academy of Sciences of the United States of America, 2003. 100(14): p. 8354-8359.

99. Vestbo, J., et al., Global strategy for the diagnosis, management, and prevention of chronic obstructive pulmonary disease: GOLD executive summary. Am J Respir Crit Care Med, 2013. 187(4): p. 347-65.

100. Pauwels, R.A. and K.F. Rabe, Burden and clinical features of chronic obstructive pulmonary disease (COPD). Lancet, 2004. 364(9434): p. 613-20.

101. Macnee, W., et al. , COPD: Pathogenesis and Natural History, in Murray and Nadel's Textbook of Respiratory Medicine. 2016. p. 751-766.e7.

102. Lelios, I., et al., Emerging roles of IL-34 in health and disease. J Exp Med, 2020. 217(3).

103. Boulakirba, S., et al., IL-34 and CSF-1 display an equivalent macrophage differentiation ability but a different polarization potential. Sci Rep, 2018. 8(1): p. 256.

104. Shoji, H., et al., Interleukin-34 as a fibroblast-derived marker of liver fibrosis in patients with non-alcoholic fatty liver disease. Scientific reports, 2016. 6: p. 28814-28814.

105. Franze, E., et al., Interleukin-34 Stimulates Gut Fibroblasts to Produce Collagen Synthesis. J Crohns Colitis, 2020. 14(10): p. 1436-1445.

106. Trivlidis, J., et al., HuR drives lung fibroblast differentiation but not metabolic reprogramming in response to TGF-beta and hypoxia. Respir Res, 2021. 22(1): p. 323.

107. Ge, J., et al., Essential Roles of RNA-binding Protein HuR in Activation of Hepatic Stellate Cells Induced by Transforming Growth Factor-beta1. Sci Rep, 2016. 6: p. 22141.

108. Heinzelmann, K., et al., Cell-surface phenotyping identifies CD36 and CD97 as novel markers of fibroblast quiescence in lung fibrosis. Am J Physiol Lung Cell Mol Physiol, 2018. 315(5): p. L682-L696.

109. Zhao, X., et al., Metabolic regulation of dermal fibroblasts contributes to skin extracellular matrix homeostasis and fibrosis. Nat Metab, 2019. 1(1): p. 147-157.

110. Chong, M., et al., CD36 initiates the secretory phenotype during the establishment of cellular senescence. EMBO Rep, 2018. 19(6).

111. Barnes, P.J., Senescence in COPD and Its Comorbidities. Annu Rev Physiol, 2017. 79: p. 517-539.

112. Antony, V.B. and V.J. Thannickal, Cellular Senescence in Chronic Obstructive Pulmonary Disease: Multifaceted and Multifunctional. Am J Respir Cell Mol Biol, 2018. 59(2): p. 135-136.

PREFACE: CHAPTER V

In the last two Chapters, we demonstrated the contribution of HuR in the context of CS-related pathologies, namely inflammation. Importantly, other inhalational toxicants may be also involved in the pathogenesis of lung diseases; this includes inhalation of cannabis smoke [296]. However, no standardized protocol for cannabis smoke extract currently exists. To understand the impact of cannabis smoke on biological and toxicological indices, the development of *in vitro* surrogates of cannabis smoke exposure is necessary. Therefore, in Chapter V, we optimized a standardized protocol to generate cannabis smoke extract (CaSE) in order to elucidate its effect on different mechanisms *in vitro*. Our standardized protocol can be then used to interrogate the extent to which HuR participates in cellular functions that altered by cannabis smoke, including inflammation.

CHAPTER V

5. Standardized cannabis smoke extract induces inflammation in human lung fibroblasts

Noof Aloufi[1,2,3,4], Yoon Namkung[5], Hussein Traboulsi[1,2,5], Emily Wilson[1,2,6], Stephane A. Laporte[5,6], Barbara L.F. Kaplan[7], Matthew Ross[7], Parameswaran Nair[8], David H. Eidelman[1,2,5], and Carolyn J. Baglole[1,2,3,5,6*]

[1]Meakins-Christie Laboratories and [2]Translational Research in Respiratory Diseases Program at the Research Institute of the McGill University Health Centre; Department of [3]Pathology, McGill University; [4]Department of Medical Laboratory Technology, Taibah University, Saudi Arabia; Departments of [5]Medicine and [6]Pharmacology and Therapeutics, McGill University; [7]Department of Comparative Biomedical Sciences, Mississippi State University, United States; [8]Department of Medicine, McMaster University & St Joseph's Healthcare, Hamilton, Ontario, Canada.

Correspondence and requests for materials should be addressed to:
*Carolyn J. Baglole
1001 Decarie Blvd (EM22248)
Montreal, Quebec H4A3J1
Telephone: (514) 934-1934 ext. 76109
E-mail: Carolyn.baglole@mcgill.ca

(This research was originally published in **Frontiers in Pharmacology** Aloufi, N., Namkung, Y., Traboulsi, H., Wilson, E. T., Laporte, S. A., Kaplan, B. L. F., Ross, M. K., Nair, P., Eidelman, D. H., & Baglole, C. J. (2022). Standardized Cannabis Smoke Extract Induces Inflammation in Human Lung Fibroblasts. *Front. Pharmacol.*, 13 [4].)

Keywords: fibroblast, inflammation, cannabis smoke, thc, cbd, lungs, CB1, BRET

Acknowledgement: This work was supported by the Canadian Institutes for Health Research Project Grants (168836 and 162273) and the Natural Sciences and Engineering Research Council of Canada (NSERC). CB was supported by a salary award from the Fonds de recherche du Quebec-Sante (FRQ-S). NA was supported by a scholarship from Taibah University, Saudi Arabia. HT was supported by a Réseau de recherche en santé réspiratoire du Québec (RSR) Scholarship and a Meakins-Christie Laboratories Collaborative Research Award. SL was supported by the Canadian Institutes of Health Research (PJT-162368 and PJT-173504).

5.1. ABSTRACT

Cannabis (marijuana) is the most commonly used illicit product in the world and is the second most smoked plant after tobacco. There has been a rapid increase in the number of countries legalizing cannabis for both recreational and medicinal purposes. Smoking cannabis in the form of a joint is the most common mode of cannabis consumption. Combustion of cannabis smoke generates many of the same chemicals as tobacco smoke. Although the impact of tobacco smoke on respiratory health is well-known, the consequence of cannabis smoke on the respiratory system and, in particular, the inflammatory response is unclear. Besides the combustion products present in cannabis smoke, cannabis also contains cannabinoids including Δ^9-tetrahydrocannabinol (Δ^9-THC) and cannabidiol (CBD). These compounds are hydrophobic and not present in aqueous solutions. In order to understand the impact of cannabis smoke on pathological mechanisms associated with adverse respiratory outcomes, the development of *in vitro* surrogates of cannabis smoke exposure is needed. Therefore, we developed a standardized protocol for the generation of cannabis smoke extract (CaSE) to investigate its effect on cellular mechanisms *in vitro*. First, we determined the concentration of Δ^9-THC, one of the major cannabinoids, by ELISA and found that addition of methanol to the cell culture media during generation of the aqueous smoke extract significantly increased the amount of Δ^9-THC. We also observed by LC-MS/MS that CaSE preparation with methanol contains CBD. Using a functional assay in cells for CB1 receptors, the major target of cannabinoids, we found that this CaSE contains Δ^9-THC which activates CB1 receptors. Finally, this standardized preparation of CaSE induces an inflammatory response in human lung fibroblasts. This study provides an optimized protocol for aqueous CaSE preparation containing biologically active cannabinoids that can be used for *in vitro* experimentation of cannabis smoke and its potential impact on various indices of pulmonary health.

5.2. INTRODUCTION

Cannabis has been used for medical purposes for thousands of years (Hillig, 2005; Rana, 2010; Atakan, 2012). Cannabis, commonly referred as marijuana, is a flowering plant belonging to the family Cannabaceae. There are three main subspecies of cannabis: *C. sativa*, *C. indica* and *C. ruderalis*, which are differentiated by key physical characteristics and production of cannabinoids (Hillig, 2005; Rana, 2010; Atakan, 2012). Cannabis produces more than 100 cannabinoids (Baron, 2018) that have many effects in the human body, including modulation of mood, memory and the immune response. One of the major cannabinoids is Δ^9-tetrahydrocannabinol (Δ^9-THC), which is responsible for the psychotropic effect of cannabis via activation of cannabinoid-1 (CB1) receptors in the brain (Mersiades et al., 2018). Cannabidiol (CBD), cannabigerol (CBG) and cannabichromene (CBC) are other cannabinoids currently under scientific investigation for their therapeutic potential. Of these, CBD has gained the most interest, particularly as an anti-inflammatory agent that lacks the psychoactive properties of Δ^9-THC (Rajan et al., 2016; Morales et al., 2017).

Δ^9-THC and CBD are produced in the trichomes of the female inflorescence as acidic precursors THCA and CBDA, respectively, that undergo decarboxylation when heated by consumption methods such as smoking (Tahir et al., 2021). According to the World Health Organization (WHO), approximately 15 million people (3% of world population) consume cannabis each year, making this the most widely-used illicit drug in the world. Currently, cannabis is the second most-smoked plant after tobacco (Baron, 2018; Brown, 2020; Campeny et al., 2020; Li et al., 2020), making inhalation of cannabis smoke the most common consumption method (Schuermeyer et al., 2014). Smoking cannabis provides the fastest Δ^9-THC delivery to the body,

resulting in rapid onset of psychoactive effects. Like tobacco smoke, cannabis smoke also contains carcinogens [e.g., polycyclic aromatic hydrocarbons (PAHs)] and other toxicants (e.g., carbon monoxide) (Moir et al., 2008; Maertens et al., 2009; Graves et al., 2020). A recent study showed that there are 4,350 and 2,575 compounds in tobacco and cannabis smoke, respectively. Of these, 69 were common in both and are known to have adverse health risks through carcinogenic, mutagenic, or other toxic mechanisms (Graves et al., 2020). Unlike tobacco smoke, where the adverse respiratory effects are well-established (Strzelak et al., 2018), there are significant gaps in our understanding of the impact of cannabis smoke on respiratory health. Based on a limited number of studies, there is evidence that cannabis smoking is associated with inflammation and chronic bronchitis (Yayan and Rasche, 2016; Urban and Hureaux, 2017). Cannabis smoke can also negatively affect physical (e.g., mucociliary clearance) and immunological respiratory defense mechanisms (Chatkin et al., 2017). Regular cannabis use may also increase risk for asthma and accelerate the decline in lung function (Chatkin et al., 2019). However, the net effects of cannabis smoke on respiratory health, and in particular inflammation, remain largely unknown and such findings are often complicated by concurrent tobacco use in human participants. Thus, there is a pressing need to understand the consequences of cannabis smoke on the inflammatory response.

Our understanding of the ill health effects of tobacco smoke were driven in part by preclinical models of exposure. There are now established *in vitro* and *in vivo* models that recapitulate many of the exposure parameters observed in humans. These models have been extensively used to evaluate the mechanistic impact of tobacco smoke exposure (Carp and Janoff, 1978; Aoshiba et al., 2001; Carnevali et al., 2003; Baglole et al., 2006; Damico et al., 2011; Zago et al., 2013; de Souza et al., 2014; Guerrina et al., 2021a; Rico de Souza et al., 2021). Of these,

cigarette smoke extract (CSE) is a widely-utilized *in vitro* surrogate for tobacco smoke exposure, and protocols for the generation of CSE are established and readily adaptable by many laboratories (Carp and Janoff, 1978; Martey et al., 2005; Baglole et al., 2006; Baglole et al., 2008b; Bertram et al., 2009; Damico et al., 2011). However, no such standardized protocol for cannabis smoke extract (CaSE) currently exists, greatly limiting investigation into the impact of cannabis smoke on biological and toxicological indices. Therefore, we developed a standardized protocol for the preparation of an aqueous cannabis smoke extract (CaSE) for *in vitro* evaluation. We used a legal cannabis source with a described composition and developed a protocol for standardization that allows for comparison between studies; this CaSE can be prepared and standardized using common laboratory equipment. Importantly, we confirmed that these CaSE preparations contain pharmacologically active Δ^9-THC using a signaling pathway downstream of the CB1 receptor: the Rho small G protein, with a Bioluminescence Resonance Energy Transfer (BRET) assay for this effector (Namkung et al., 2018). Finally, we used CaSE to show that key inflammatory markers are induced in human lung cells, suggesting that cannabis smoke is not harmless. With more countries legalizing cannabis for medical purposes, additional research is needed to better understand the cellular and molecular consequences of cannabis smoke exposure.

5.3. MATERIALS AND METHODS

Chemicals

All chemicals were obtained from Sigma (St. Louis, MO) unless otherwise indicated. Coelenterazine 400a was purchased from Nanolight™ Technology. 2-AG, Δ^9-THC and CBD are from Cayman Chemical (Ann Arbor, MI). The sp-hCB1 encoding plasmid (signal peptide human CB1) was a gift from Michel Bouvier, (University of Montreal).

Preparation of Cigarette Smoke Extract (CSE)

Research grade cigarettes (3R4F) with a filter were acquired from the Kentucky Tobacco Research Council (Lexington, KY). Research grade cigarettes (3R4F) contain 0.73 mg of nicotine, 9.4 mg of tar, and 12.0 mg of CO as described by the manufacturer. CSE was produced as previously described by us (Baglole et al., 2008a; Zago et al., 2013; Guerrina et al., 2021a; Guerrina et al., 2021b). Briefly, CSE was prepared by bubbling smoke from a cigarette through 10 ml of serum-free cell culture medium with the exception that some extracts were prepared with 30% methanol (MeOH). The CSE was then sterile-filtered with a 0.45-μm filter (25-mm Acrodisc; Pall Corp., Ann Arbor, MI). Standardization was done for each CSE preparation by spectrophotometer using an OD320 nm of 0.65 to represent 100% CSE as described (Baglole et al., 2006; Zago et al., 2013).

Preparation of Cannabis Smoke Extract

Cannabis was purchased from the Société québécoise du cannabis SQDC online store (Quebec, Canada). Whole flower cannabis that was selected for purchase contained varying cannabinoid profiles based on THC/CBD content. Those purchased were as follows: 1) Indica-THC dominant; contains 16–22% THC and 0–0.1% CBD (#688083002311). 2): Sativa-CBD dominant; contains 0.1–2% THC and 13–19% CBD (#694144000219) and 3) Hybrid-Balanced: contains 5–11% THC and 5–11% CBD (#688083002588). Cannabis joints (cigarettes) were hand-rolled by grinding the dried cannabis flower with a plastic grinder and packing the product into classic 1 1/4 size rolling paper (RAW®). Each cannabis cigarette contained 0.5 ± 0.05 g of cannabis. A slim unrefined cellulose filter (RAW®) was added to the end of the joint. Then, CaSE was produced as previously described for CSE (Baglole et al., 2008a; Zago et al., 2013; Guerrina et al., 2021b) where the smoke from the lit cannabis cigarette was bubbled through 10ml of serum-free cell culture Dulbecco's modified Eagle's medium (DMEM) with or without 30% methanol (MeOH) or 30% ethanol (EtOH). CaSE was then filtered using a 0.45-µm filter (25-mm Acrodisc; Pall Corp., Ann Arbor, MI). Because the tar components in tobacco and cannabis are similar (Tashkin, 2013), and chemical species of tobacco tar absorb light at 320 nm (Taylor et al., 2020), we standardized each CaSE preparation as previously described for CSE (Baglole et al., 2008a; Zago et al., 2013; Guerrina et al., 2021a; Guerrina et al., 2021b) to ensure consistency in CaSE preparations between experiments. Similar to CSE preparation described above, an optical density of 0.65 was considered to represent 100% CaSE. Then, the CaSE solution was diluted with serum-free MEM for further analysis. The pH of 2% CaSE and 5% CaSE was 7.3 ± 0.06 and 7.7 ± 0.08, respectively.

Enzyme-Linked Immunosorbent Assay

Δ^9-THC concentration in CaSE was analyzed by a direct competitive THC Forensic ELISA kit (NEOGEN®) according to manufacturer's instructions. The concentration of interleukin-8 (IL-8) in the cell culture supernatant was determined by ELISA (Human IL-8 ELISA Duo Set, R&D Systems, United States) according to the manufacturer's instructions. The absorbance was read at 450 and 570 nm within 15 minutes by infinite TECAN (M200 pro, TECAN, CA).

Cell Culture and Transfection

Human embryonic kidney (HEK) 293 cells were cultured in DMEM supplemented with 10% fetal bovine serum (FBS) and gentamicin (20 μg/ml). Cells were grown at 37°C in 5% CO2 and 90% humidity. HEK293 cells were seeded at a density of 1×10^6 cells per 100-mm dish and transfected the next day with 3 μg of sp-hCB1 with 120 ng of PKN-RBD-RlucII and 480 ng of rGFP-CAAX using PEI methods as described previously (Boussif et al., 1995; Namkung et al., 2018). Briefly, a total of 6 μg of DNA (adjusted with pcDNA3.1 zeo (+)) in 0.5 ml of PBS was mixed with 12 μl of PEI (25 kDa linear, 1 mg/ml) in 0.5 ml PBS and then incubated for 20 min at RT prior to applying to the cells. After 24 h, cells were detached and seeded onto poly-ornithine-coated 96-well white plates at a density of 25,000 cells per well for the BRET assays, which were performed 48 h after transfection.

Primary human lung fibroblasts (HLFs) were isolated from cancer-free lung tissue by explant procedure as described (Baglole et al., 2005). This study was approved by the Research Ethics Board of St. Joseph's Healthcare Hamilton and informed written consent was obtained from each patient. Experiments were conducted with fibroblasts from three different individuals of the

non-smoker group (Normal; M/F = 1/2; age 68 ± 9 years) and within passage six to nine. HLFs were cultured in 10% MEM and treated with THC dominant CaSE for 6 and 24 h.

Rho BRET Assay

BRET assay for detecting Rho activation was performed as previously described (Namkung et al., 2018). Briefly, cells in 96 well plates were washed once with 150 μl/well of Tyrode's buffer (140 mM NaCl, 2.7 mM KCl, 1 mM $CaCl_2$, 12 mM $NaHCO_3$, 5.6 mM D-glucose, 0.5 mM $MgCl_2$, 0.37 mM NaH_2PO_4, 25 mM HEPES, pH 7.4) and left in 80 μl/well of Tyrode's buffer. 2-AG, THC, and CBD were serially diluted in 15% MeOH in Tyrode's buffer. The final concentration of MeOH in the assay is 3.75%. For BRET assay, the cells were loaded with 10 μl of coelenterazine 400a (final concentrations of ~3.5 μM) and then the cells were stimulated with 30 μl of ligands or two-fold diluted CaSE in Tyrode's buffer for 4 min prior to BRET measurement. Thus, final concentrations of CaSE were 12.5% (8-fold dilution of original CaSE). BRET signals were measured using a Synergy2 (BioTek) microplate reader. The filter was set at 410/80 nm and 515/30 nm for detecting the RlucII Renilla luciferase (donor) and rGFP (acceptor) light emissions, respectively. The BRET ratio was determined by calculating the ratio of the light emitted by rGFP over the light emitted by the RlucII.

Liquid Chromatography with Tandem Mass Spectrometry

CaSE culture media samples were diluted 1:20 v/v by adding 10 μl to 190 μl of MeOH containing an internal standard CBD-d9 (10 pmol); 10 μl was subsequently analyzed by LC-MS/MS. In some cases, a 1:2 dilution was prepared by mixing 100 μl of CaSE culture medium

with 100 µl of methanol containing internal standard CBD-d9 (10 pmol). CBD was chromatographed on a Waters UPLC reversed phase column (100 × 2.1 mm i.d.) using a blend of water and acetonitrile containing 0.1% acetic acid with a flow rate of 0.2 ml/min. The eluate was directed into a Thermo Quantum Access Max triple-quadrupole mass spectrometer and the CBD and CBD-d9 detected by single-reaction monitoring. The peak area for CBD was normalized by the peak area for the internal standard (CBD-d9) and the ratio compared to an external calibration curve for CBD prepared in MeOH. The limit of quantitation for CBD was 10 nM.

Western Blot

HLFs were grown to approximately 70–80% confluence and cultured with serum-free MEM for 18 h before the treatment. Total cellular protein was extracted using RIPA lysis buffer (Thermo Scientific, Rockford) containing Protease Inhibitor Cocktail (PIC, Roche, United States). Ten to 20 µg of protein lysate were subjected to 10% SDS-PAGE gels and transferred onto Immuno-blot PVDF membranes (Bio-Rad Laboratories, Hercules, CA). Then, the membrane was blocked for 1 hour at room temperature in blocking solution (5% w/v of non-fat dry milk in 1x PBS/0.1% Tween-20). The primary antibodies, COX-2 (1:1,000; Cell Signaling Technology, CA) and β-Tubulin (1:50000; Sigma, CA) were added to the membranes and incubated overnight at 4°C or 1 h at room temperature. After several washes, membrane was incubated with secondary antibodies goat anti-rabbit IgG HRP-linked (1:10000, Cell Signaling Technology, CA) or HRP-conjugated horse anti-mouse IgG (1:10000, Cell Signaling Technology, CA). Detection of protein was done by enhanced chemiluminescence (ECL) and visualized using a ChemiDoc™ MP Imaging System (Bio-Rad, CA). Densitometric analysis was performed using Image Lab™

Software Version 5 (Bio-Rad, CA). Protein expression was normalized to β-tubulin and the data presented as the fold-change relative to the untreated condition.

Quantitative RT-PCR

Using the Aurum™ Total RNA Kit (Bio-Rad, CA), total RNA was isolated according to the manufacturer's instructions. Quantification of RNA was conducted on a Nanodrop 1,000 spectrophotometer. Reverse transcription of RNA was carried out using iScript™ Reverse Transcription Supermix (Bio-Rad, CA). Then, using this cDNA template, mRNA levels of *PTGS2*, *CXCL8* and *S9* (Table 5.1) were analyzed by quantitative PCR (qPCR) by using 1 µl of cDNA (10 ng/µl) and 0.5 µM primers with SsoFast™ EvaGreen® (Bio-Rad, CA). Sequences of gene-specific primers are listed in Table 1. PCR amplification was performed using a CFX96 Real-Time PCR Detection System (Bio-Rad, CA). Thermal cycling was initiated at 95°C for 3 min and followed by 39 cycles denaturation at 95°C for 10 s and annealing at 59°C for 5 s. Gene expression was analyzed using the ΔΔCT method, and results are presented as fold-change normalized to housekeeping gene (*S9*).

Table 5.1. Primer sequences used for qRT-PCR analysis.

Gene	Forward Primer Sequence	Reverse Primer Sequence
PTGS2	TCA CAG GCT TCC ATT GAC CAG	CCG AGG CTT TTC TAC CAG A
CXCL8	GAT GTC AGT GCA TAA AGA CAT ACT CCA A	GCT CTC TTC CAT CAG AAA GCT TTA CAA TA
S9	CAG CTT CAT CTT GCC CTC A	CTG CTG ACG CTT GAT GAG AA

Statistical Analysis

Using GraphPad Prism 6 (v. 6.02; La Jolla, CA), statistical analysis was performed using a one-way analysis of variance (ANOVA) followed by Dunn's multiple comparisons test to assess differences between treatments. Groups of two were analyzed by paired t-test. A two-way analysis of variance (ANOVA), followed by Tukey's multiple comparisons test was used to evaluate differences between groups and conditions of more than two. Results are presented as mean ± standard error of the mean (SEM) or as mean ± standard deviation (SD) of the fold-changes compared to control cells. Experimental readings were done in triplicate and averaged; statistical analysis was therefore done using averaged values from three to five independent experiments unless otherwise indicated. In all cases, a p value <0.05 is considered statistically significant. For Table 5.4 and Table 5.5, the standard THC concentration response curve was obtained from a nonlinear regression curve fitting in GraphPad Prism software. The mean, upper limits, and lower limits of the unknowns were interpolated from the fitted standard curve with a confidential interval of 95%.

5.4. RESULTS

Generation of Cannabis Smoke Extract Preparations That Contains Δ^9-THC and CBD

Like tobacco, cannabis smoke contains hundreds of combustion products. However, cannabis also contains cannabinoids that exert biological and pharmacological effects. Standardized preparations of aqueous cigarette smoke extract (CSE) are well-described in the literature and are used to understand the consequences of tobacco exposure (Carnevali et al., 2003; Baglole et al., 2006; Baglole et al., 2008b; Hecht et al., 2014); no such standardized extract for cannabis smoke exists. Moreover, CSE prepared in cell culture media or PBS contains water soluble gas and particle phases of cigarette smoke (Kim et al., 2018). While many of these same compounds would be captured from cannabis smoke, cannabis also contains cannabinoids which are hydrophobic (Huestis, 2007) and unlikely to be present in an aqueous extract suitable for *in vitro* testing. Therefore, we sought to develop a cannabis smoke extract (CaSE) that contains biologically active cannabinoids. First, we utilized a semi-quantitative THC Forensic ELISA kit for which we developed a standard curve using Δ^9-THC to allow for subsequent quantification. The standard curve was first prepared to calculate the relative concentration of Δ^9-THC relative to the absorbance. We diluted Δ^9-THC (in the ELISA buffer) from a starting concentration of 1 mg/ml to an upper limit of 4 μg/ml. The concentration of this Δ^9-THC standard curve therefore ranged from 0 μg/ml (buffer only)- 4 μg/ml (0–12.7 μM) (Figure 5.1) and was used for analysis with all CaSE preparations.

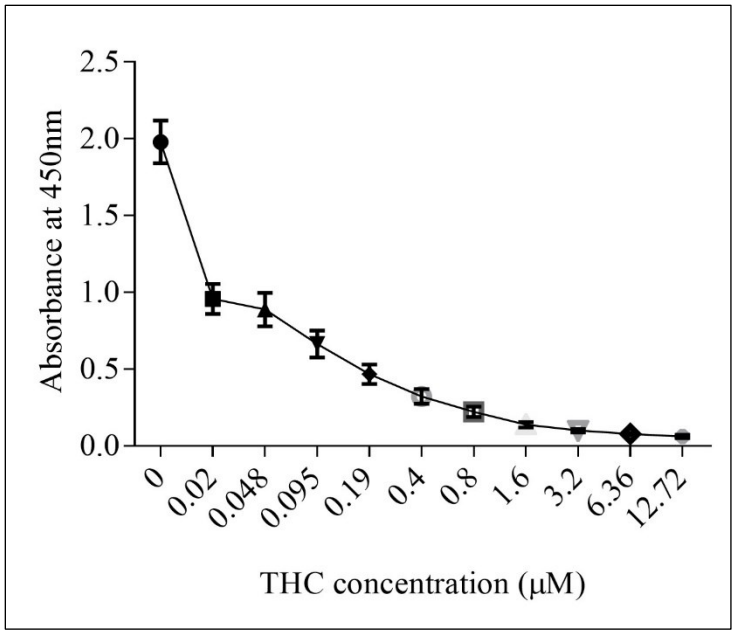

Figure 5.1. The standard curve for Δ^9-THC.

Δ^9-THC was diluted in ELISA buffer from a starting concentration of 1 mg/ml to an upper limit of 4 μg/ml. Then, the concentration of this Δ^9-THC standard curve was ranged from 0 μg/ml (buffer only)- 4 μg/ml (0–12.7 μM). Results are expressed as the mean ± SEM of two to four independent experiments.

Next, we evaluated Δ^9-THC level by ELISA and CBD level LC-MS/MS in various aqueous CaSE preparations. Given that cannabinoids are hydrophobic, we compared Δ^9-THC levels in CaSE prepared in standard cell culture media with and without MeOH. As additional controls, we also evaluated Δ^9-THC concentrations in CSE prepared from research grade cigarettes. As expected, cell culture media alone with 30% MeOH as well as CSE (with 30% MeOH) contained no Δ^9-THC or CBD (Table 5.2). We also measured Δ^9-THC and CBD concentrations in CaSE prepared from the different strains of cannabis with reported varying amounts of Δ^9-THC and CBD. Δ^9-THC levels in CaSE generated from the Δ^9-THC dominant and THC/CBD balanced strains with 10% MeOH were 0.62 ± 0.2 and 0.36 ± 0.02, respectively, and were therefore similar to the level in CaSE without MeOH. However, in CaSE generated from the Δ^9-THC dominant strain with 30% MeOH, there were significantly higher levels of Δ^9-THC compared to the CaSE

without MeOH (THC dominant CaSE; Table 5.2). CBD levels were below the limit of detection by LC-MS/MS. Here, the estimated Δ^9-THC concentration was 6.7 ± 0.29 μM in CaSE prepared in cell culture media with 30% MeOH. Preparation of CaSE from the balanced cannabis strain with 5–10% THC and 5–11% CBD also yielded significant Δ^9-THC levels only when CaSE was prepared in media containing 30% MeOH. Finally, CaSE prepared from the CBD dominant cannabis strain in media with 30% MeOH has less Δ^9-THC compared to CaSE prepared from the other two cannabis strains (Table 5.2). In CaSE generated from the balanced cannabis strain with 5–10% THC and 5–11% CBD, there were higher levels of CBD compared to the CaSE without MeOH (THC/CBD balanced CaSE; Table 5.2). CaSE prepared from the CBD dominant cannabis strain in media with 30% MeOH has higher CBD compared to CaSE prepared from the THC dominant strains. However, CBD levels are similar between CBD dominant and THC/CBD balanced strains (Table 5.2). We also generated CaSE from the Δ^9-THC dominant strain in media with 30% EtOH. We found that the Δ^9-THC level was slightly less in CaSE containing EtOH (5.7 ± 0.35 μM) comparing to CaSE with MeOH (6.7 ± 0.29 μM). These data show that preparation of CaSE in cell culture media with MeOH yields significantly higher concentrations of Δ^9-THC and CBD compared to CaSE prepared without MeOH. Thus, the remainder of experiments were conducted with CaSE prepared in media with 30% MeOH and is refereed to hereafter as CaSE.

Table 5.2. Estimated concentration of Δ^9-THC and CBD in CaSE.

Extract	THC Absorbance (ELISA)	Δ^9-THC (µM) (ELISA)	CBD (µM) (LC-MS/MS)
Media + 30% MeOH	1.662	0	<0.01
CSE+ 30% MeOH	1.398	0	<0.01
THC dominant CaSE	0.29± 0.02	0.67± 0.05	<0.01
THC dominant CaSE + 30% MeOH	0.08± 0.002	6.7± 0.29*	<0.01
THC/CBD balanced CaSE	0.4538± 0.037	0.34± 0.05	<0.01
THC/CBD balanced CaSE + 30% MeOH	0.087± 0.008	5.5± 0.46**	10.31± 9.125
CBD dominant CaSE+ 30% MeOH	0.16± 0.01	1.7± 0.4	7.733± 2.652

Results presented as average ± SEM.

*THC dominant CaSE+30% MeOH was significantly higher ($p < 0.03$) compared to THC dominant CaSE without MeOH.; **THC/CBD balanced CaSE+30% MeOH was significantly higher ($p < 0.008$) compared to THC/CBD balanced CaSE without MeOH. Results are expressed as the mean ± SEM of three to five independent extracts.

Standardization of Cannabis Smoke Extract Using OD_{320}

The tar components in tobacco and cannabis are similar (Tashkin, 2013), and chemical species of tobacco tar absorb light at 320 nm (Taylor et al., 2020). Thus, to ensure consistency in CaSE preparations between experiments, we standardized each CaSE preparation as previously described for CSE (Baglole et al., 2008a; Zago et al., 2013; Guerrina et al., 2021a; Guerrina et al.,

2021b). Nine extracts from THC dominant cannabis were prepared and two measurements were taken for fresh extracts and after thawing of the same extracts that had been frozen at −80°C for 16 weeks. The optical density (OD) at 320 was 0.7 ± 0.05 and 0.64 ± 0.05 for fresh and frozen extracts, respectively (Table 5.3). Given that an OD of 0.65 is used to represent 100% CaSE, the percentage of CaSE averaged to be 110% ± 8 and 99% ± 7.7 for fresh and frozen extracts, respectively. We also evaluated Δ^9-THC content by ELISA. The estimated Δ^9-THC concentration of fresh and frozen extracts was similar and was approximately 12 µM. These data suggest that storage of CaSE extracts up to 16 weeks at −80°C does not affect Δ^9-THC concentration and that an OD320 can be used to standardize aqueous CaSE to minimize batch-to-batch variability.

Table 5.3. Δ^9-THC absorbance (OD_{320}) and estimated concentration by ELISA.

Extract	OD_{320}	Percentage	THC EISA	Δ^9-THC (µM)
Fresh CaSE	0.7 ± 0.05	110% ± 8	0.06 ± 0.0005	12.4 ± 0.2
Frozen CaSE	0.64 ± 0.05	99% ± 7.7	0.066 ± 0.001	12.2 ± 0.2

Results presented as mean ± SEM of 9 independent extracts.

Cannabis Smoke Extract Activates CB1 Receptors

Δ^9-THC has high affinity to CB1 and CB2 receptors (Pertwee, 2010), which are G protein coupled receptors (GPCRs). CB1 couples to not only $G_{i/o}$ but also to the $G_{12/13}$ subfamily and activates the down-stream protein Rho (Inoue et al., 2019; Krishna Kumar et al., 2019; Avet et al., 2020). To determine whether there is sufficient Δ^9-THC in the CaSE preparations to activate CB1, we used a BRET-based Rho biosensor (Namkung et al., 2018). We transiently transfected HEK293

cells with signal-peptide-human CB1 (CB1) along with PKN-RBD-RLucII and rGFP-CAAX (Rho sensor) and stimulated the cells with Δ^9-THC, CBD and 2-arachidonoylglycerol (2-AG), an endogenous CB ligand (Figure 5.2). The BRET signal increased in response to Δ^9-THC and 2-AG but not to CBD (Figure 5.2A). Further, we observed that AM251, a CB1-specific antagonist, abolished the THC- and 2-AG- promoted BRET signals (Figure 5.2B). To verify the specificity of AM251 on CB1-mediated Rho activation, we examined the effect of AM251 on angiotensin II type 1 receptor (AT1R)-mediated Rho activation, which also couple to this pathway (Namkung et al., 2018). AM251 showed no effect on the basal BRET whereas AngII induced a BRET signal in HEK293 cells expressing AT1R along with Rho sensor (Figure 5.2C). These data show that Δ^9-THC- and 2-AG- promoted CB1 activation and signaling to the $G_{12/13}$-Rho pathway.

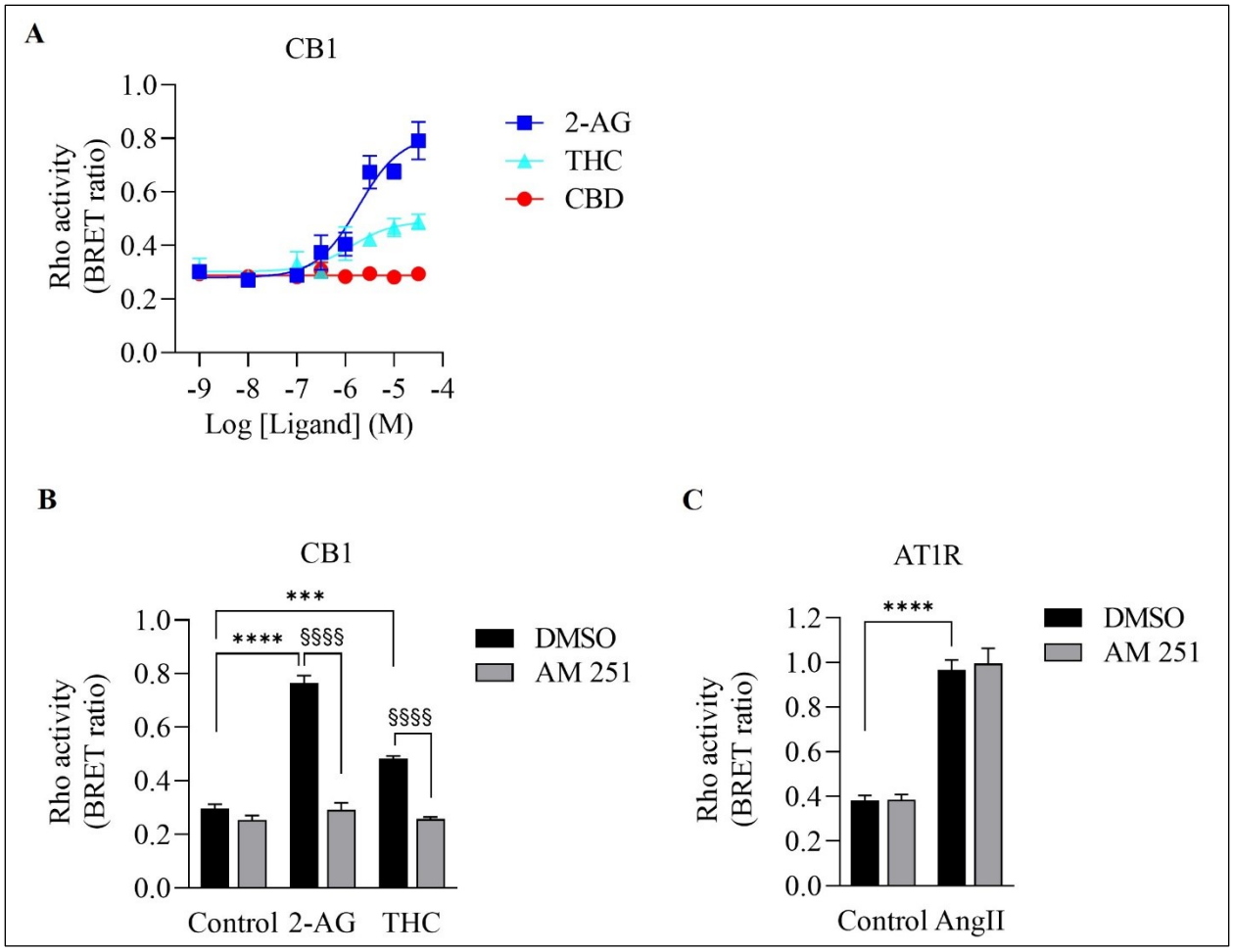

Figure 5.2. Validation of CB1-mediated Rho activation.

A. Concentration response curves of Rho activation in HEK293 cells expressing CB1, PKN-RBD-RLucII and rGFP-CAAX. Cells were stimulated with either 2-AG (blue square), THC (turquoise triangle) or CBD (red circle). CB1 was activated with 2-AG and Δ^9-THC but not with CBD. Data represent means ± SEM of four independent experiments performed in triplicate. **B.** Validation of CB1-mediated Rho activation by CB1 antagonist AM-251. Cells were stimulated with control, 2-AG (10 µM) or Δ^9-THC (THC, 10 µM) in the absence (vehicle, 0.1% DMSO (black bar)) or presence of 10 µM of AM-251 (grey bar). There was an increase in Rho activation in cells exposed to 2-AG (****$p < 0.0001$) and Δ^9-THC (***$p < 0.0002$). AM251 abolished 2-AG- and THC-induced CB1 activation (§§§§ $p < 0.0001$). **C.** Cells expressing AT1R, PKN-RBD-RLucII and rGFP-CAAX were stimulated with control or with 100 nM of AngII, agonist for AT1R, with 0.1% of DMSO (black bar) or 10 µM of AM-251 (grey bar). There was an increase in AT1R-mediated Rho activation in cells exposed to AngII (****$p < 0.0001$). There was no effect of AM251 on AT1R-mediated Rho activation. Data represent means ± SEM of three independent experiments.

We next vetted three different extracts prepared from THC-dominant or THC/CBD balanced cannabis prepared in media with or without 30% MeOH to verify that these CaSE

preparations contained biologically active Δ^9-THC; we utilized the same extracts as for the data presented in Table 5.2. First, the activation of CB1 in response to different concentrations of Δ^9-THC (0.3–25 μM) was assessed. There was a concentration-dependent activation of CB1 by Δ^9-THC (Figure 5.3). Furthermore, there was an increase in CB1 activation in cells treated with CaSE from THC dominant or THC/CBD balanced cannabis prepared in media with 30% MeOH (Figure 5.3). Extracts in media without 30% MeOH did not show BRET signals in our assay (data not shown). Based on CB1 activation by Δ^9-THC (Figure 5.3), we extrapolated that CaSE prepared from THC-dominant cannabis activates CB1 in concentrations equivalent to 5–7 μM of Δ^9-THC (Table 5.4). CaSE from THC/CBD balanced cannabis also activates the receptor, which is equivalent to 3–50 μM of Δ^9-THC (Table 5.4).

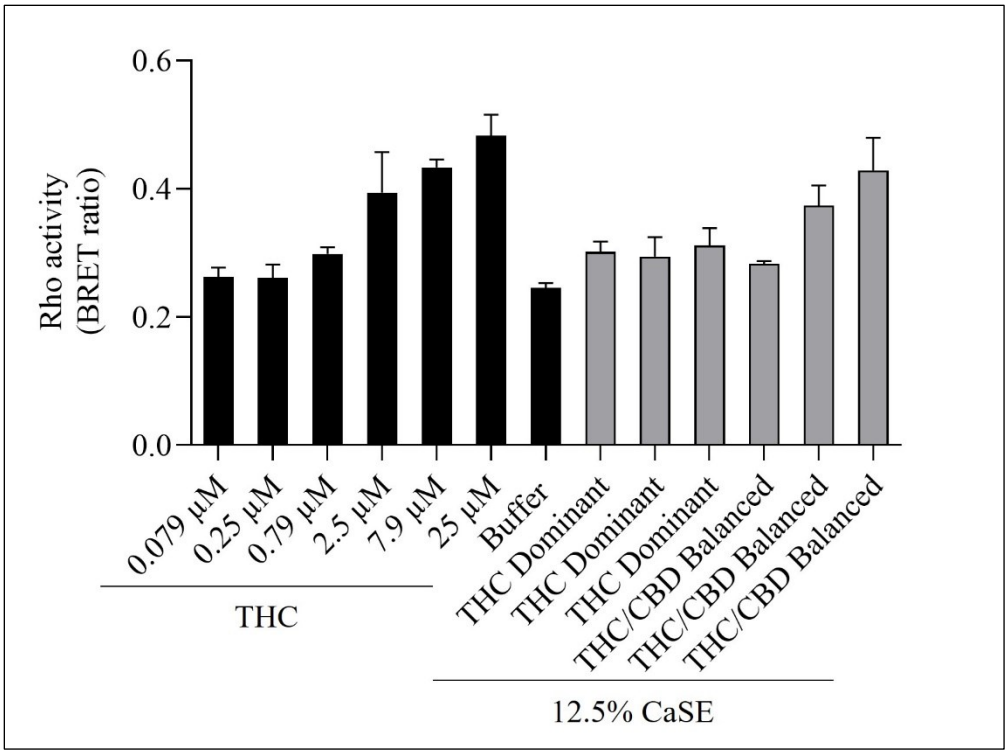

Figure 5.3. CaSE promotes Rho activation in CB1 expressing cells.

HEK293 cells expressing CB1 along with PKN-RBD-RLucII and rGFP-CAAX were stimulated with indicated concentrations of Δ^9-THC in buffer or 8-fold diluted CaSE (15 µl in total 120 µl assay volume, 12.5% CaSE) from Δ^9-THC dominant and THC/CBD balanced strains prepared in media with 30% MeOH. There was an increase in CB1 activation in a concentration-dependent manner by Δ^9-THC. There was an increase in the activation of CB1 in cells treated with CaSE from THC dominant or THC/CBD balanced cannabis. Buffer was 8-fold dilution of 30% MeOH/DMEM with Tyrode's buffer. Data represent means ± SD of triplicate (THC) and duplicate (CaSE) of a representative experiment. Similar results were obtained with 20 µl or 10 µl application of CaSE.

Table 5.4. Estimation of THC concentrations in 100% CaSE. THC concentrations in CaSE were estimated from interpolation of standard THC concentration response curve in Figure 5.3.

CaSE	THC conc. (μM)	95% CI
THC dominant	5.32	3.47-8.31
THC dominant	4.45	2.77-7.04
THC dominant	6.58	4.43-10.14
THC/CBD balanced	3.23	1.67-5.30
THC/CBD balanced	18.83	12.80-27.10
THC/CBD balanced	47.16	31.88-73.00

We then tested whether the receptor itself was affected by the MeOH and evaluated the specificity of the system by adding CSE prepared in media with 30% MeOH; we also included CaSE from all three cannabis strains (see Table 5.2). We found that there was no Rho activation with media containing 30% MeOH or CSE (Figure 5.4). CaSE from THC dominant, THC/CBD balanced, and CBD-dominant cannabis all activated Rho signaling (Figure 5.4), at levels that corresponded approximately to between 4–22 μM of Δ^9-THC present in the extracts (Table 5.5). Thus, CaSE, but not media containing MeOH or CSE, activates the CB1 receptor. Finally, we used the CB1 antagonist AM251 to confirm that CaSE is specific in its ability to activate CB1. AM251 inhibited THC-induced Rho activation. We also found that AM251 significantly inhibits CaSE-induced Rho activation for the CaSE prepared from the THC-dominant and THC/CBD balanced strains (Figure 5.5). Thus, CaSE induces Rho activation through CB1. Taken together, these data show that a standardized preparation of CaSE contains biologically active cannabinoids.

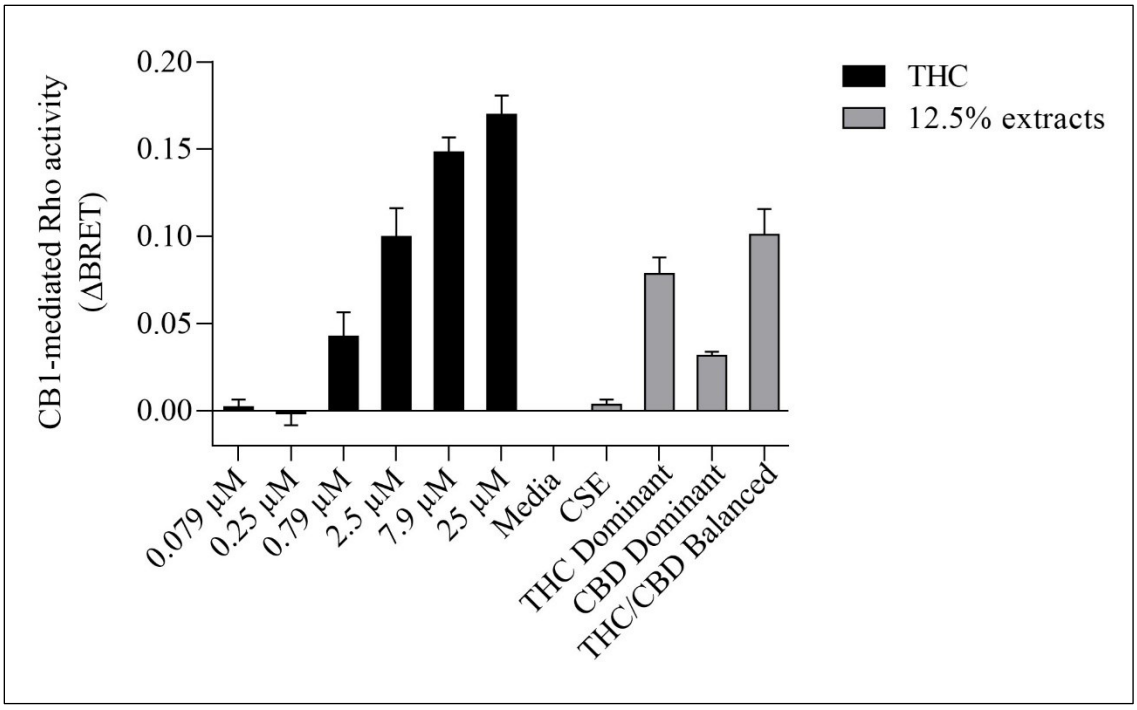

Figure 5.4. CaSE promotes Rho activation in CB1 expressing cells in comparison to Δ^9-THC.

HEK293 cells expressing CB1 along with Rho sensor were stimulated with indicated concentrations of Δ^9-THC in buffer or 8-fold diluted indicated extracts prepared in media with 30% MeOH: Media with only 30% MeOH, CaSE and CSE. There was an increase in CB1 activation in cells exposed to CaSE from THC dominant, THC/CBD balanced and CBD-dominant cannabis, but not Media with MeOH or CSE. Buffer was 8-fold dilution of 30% MeOH/DMEM with Tyrode's buffer. Data were expressed as a ligand-promoted BRET (ΔBRET) by subtracting BRET ratio in control media. Data represent mean ± SEM of three to five independent experiments.

Table 5.5. Estimation of THC concentration in 100% CaSE. THC concentrations in CaSE were estimated from interpolation of standard THC concentration response curve in Figure 5.4.

CaSE	Est. Concentration (µM)	95% CI
THC dominant	13.9	10.0-19.5
THC/CBD balanced	22.1	15.7 - 30.3
CBD dominant	4.5	3.0 - 6.7

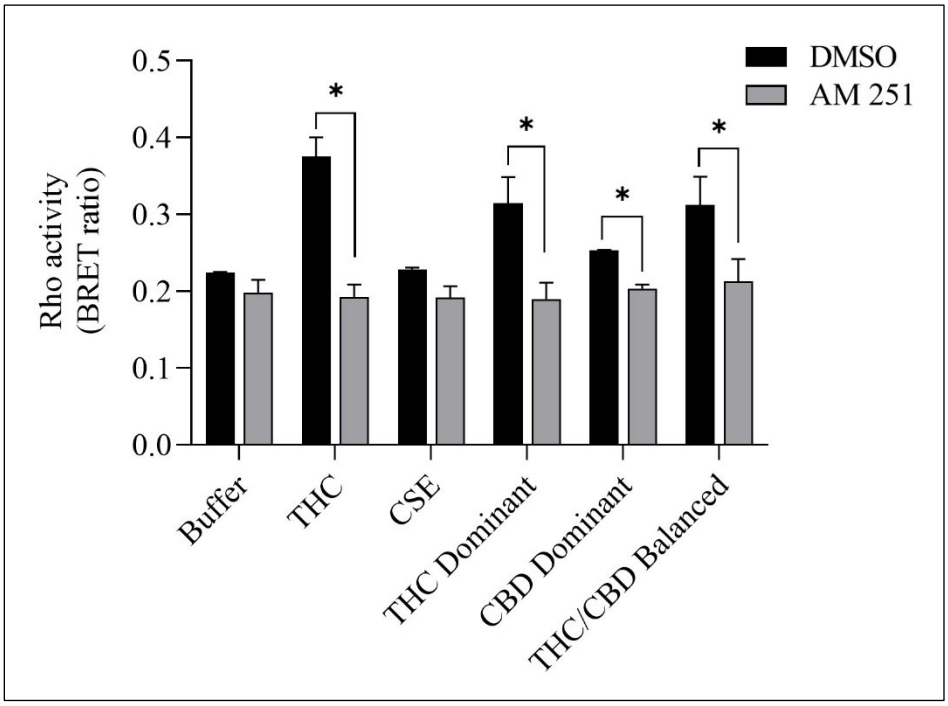

Figure 5.5. CaSE-induced Rho activation is mediated by CB1.

HEK293 cells expressing CB1 and Rho sensor were stimulated with Δ^9-THC (25 µM) or indicated CaSE (12.5%) in the absence (0.1% DMSO, black bar) or presence of AM 251 (10 µM) (grey bar). AM 251 abolished the Δ^9-THC- and CaSE-mediated Rho activation in CaSE prepared from THC dominant and THC/CBD balanced strains (*$p < 0.05$). CSE treatment did not increase Rho activity compared to buffer; AM 251 had no effect. Data represent mean ± SD from two independent experiments.

COX-2 and IL-8 Are Increased in HLFs Exposed to Cannabis Smoke Extract

COX-2 and IL-8 are among the proinflammatory mediators that are induced by tobacco smoke (Martey et al., 2004; Li et al., 2007). IL-8 is also elevated in serum from cannabis smokers (Bayazit et al., 2017). To explore whether we could replicate these findings, we characterized the effect of CaSE exposure on the expression of COX-2 and IL-8 at the mRNA and protein levels in primary HLFs. For these experiments, HLFs were treated with either 2% or 5% CaSE that was prepared from THC dominant cannabis. Selection of these concentrations was based on our

previous publications with CSE (Baglole et al., 2008a; Guerrina et al., 2021a). These concentrations of CaSE did not affect cell viability (data not shown). The concentration of Δ^9-THC in 2% CaSE was 0.18 ± 0.003 μM and in 5% CaSE was 0.45 ± 0.006 μM (n = 3). The mRNA for *PTGS2* did not increase with 6 h of CaSE (Figure 5.6A). However, there was a significant increase in *PTGS2* mRNA upon exposure to 5% CaSE for 24 h- but not 2% CaSE. Accordingly, there was a significant increase in COX-2 protein with 5% CaSE (Figure 5.6B). There was also a significant increase in *CXCL8* mRNA in response to 5% CaSE for 24 h (Figure 5.6C). At the protein level, IL-8 was also induced upon 5% CaSE treatment for 24 h (Figure 5.6D). These data indicate that a standardized CaSE preparation, containing biologically active cannabinoids, induces an inflammatory response in primary HLFs.

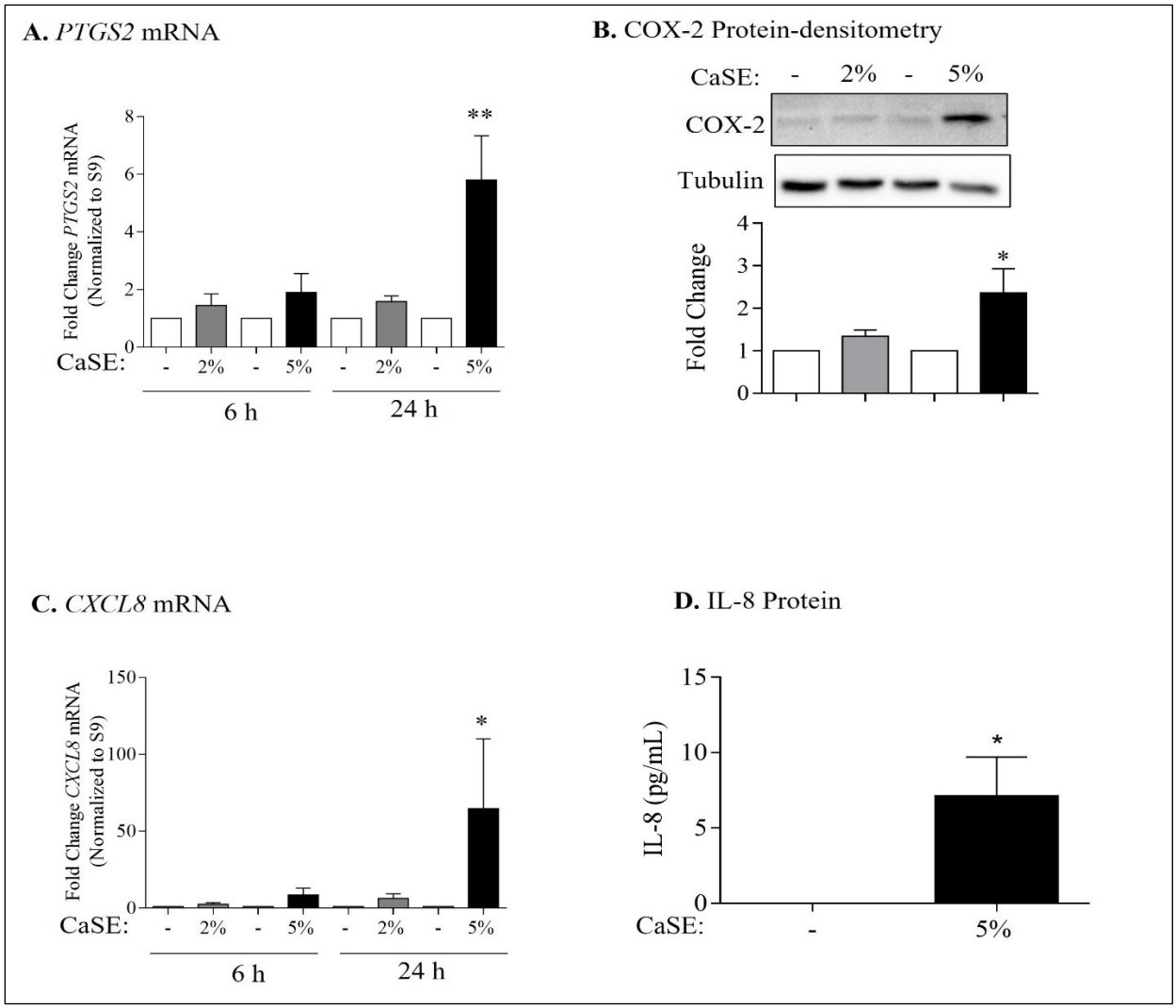

Figure 5.6. CaSE induces COX-2 and IL-8 expression in human lung fibroblasts.

A. *PTGS2* mRNA: there was a slight increase, but not statistically significant, in *PTGS2* mRNA in HLFs exposed to 2 and 5% CaSE for 6 h and in HLFs exposed to 2% CaSE for 24 h compared to corresponding control. There was significant increase in *PTGS2* mRNA in HLFs exposed to 5% CaSE for 24 h (**p = 0.009) compared to corresponding control. Results are expressed as the mean ± SEM of 4 independent experiments of HLFs used from 3 Normal subjects. **B.** COX-2 Protein-densitometry: there was significant increase in COX-2 protein levels in HLFs exposed to 5% CaSE for 24 h (*p = 0.04) compared to corresponding control. Results are expressed as the mean ± SEM of 3 independent experiments (HLFs used from 3 Normal subjects). **C.** *CXCL8* mRNA: there was a slight -but not statistically significant-increase in *CXCL8* mRNA in HLFs exposed to 2 and 5% CaSE for 6 h There was significant increase in *CXCL8* mRNA in HLFs exposed to 5% CaSE for 24 h (*p = 0.01) compared to corresponding control. Results are expressed as the mean ± SEM of 4 independent experiments (HLFs used from 3 Normal subjects). **D.** IL-8 Protein: there was an increase in IL-8 protein levels in the media from HLFs exposed to 5% CaSE for 24 h compared to corresponding control. Results are expressed as the mean ± SEM of 3 independent experiments (HLFs used from 3 Normal subjects).

5.5. DISCUSSION

Cannabis is the most commonly-smoked plant after tobacco (Baron, 2018; Brown, 2020; Campeny et al., 2020; Li et al., 2020). Recently, the personal use of cannabis has been approved in nine states of the United States as well as in Uruguay and Canada (Campeny et al., 2020). Cannabis smoke is often considered to be harmless compared to tobacco smoke (Sinclair et al., 2013). However, cannabis smoke contains many chemicals (toxicants, irritants, carcinogens, and fine particles) as does tobacco smoke (Moir et al., 2008; Manolis et al., 2019; Graves et al., 2020). The latest report from the Canadian Centre on Substance Use and Addiction (CCSA) highlights the risks of cannabis smoking to the heart and lungs as heavy users of cannabis can potentially develop cardiovascular and respiratory diseases (Canadian Centre on Substance Use and Addiction, 2020). Cannabis smoking is associated with a greater incidence of respiratory symptoms including sore throat, productive cough, and shortness of breath (Henderson et al., 1972). These symptoms are likely due to harmful impacts of cannabis smoke on the respiratory system. Indeed, there is evidence of goblet cell hyperplasia, squamous metaplasia, and inflammation in tracheobronchial specimens of cannabis smokers compared to non-smokers (Fligiel et al., 1997) as well as airway inflammatory changes in asymptomatic marijuana smokers compared to non-smokers (Roth et al., 1998). This is also supported by *in vivo* studies which showed that exposing mice to cannabis smoke alters the immune cell populations in the airways and lung tissue (Fantauzzi et al., 2021) and induces bronchial hyperreactivity, inflammation, and tissue destruction (Helyes et al., 2017). Thus, cannabis smoke may cause adverse respiratory features, and may increase the risk of developing lung diseases similar to tobacco smoke. However, the number of studies investigating the health effects of cannabis smoke exposure remains limited, and it is not well understood if there is a link between exposure to cannabis smoke and respiratory

disease development. Thus, there is a need for experimental models into order to investigate the impact of cannabis smoke on respiratory health.

Despite this need, there are no validated experimental models with which to perform detailed evaluations on the effect of cannabis smoke *in vitro*. We are only aware of one study utilizing a cannabis smoke extract for *in vitro* assessment (Aguiar et al., 2019). However, the cannabis smoke extract in that study was prepared without adding a solvent to capture the cannabinoids in the aqueous solution; the presence of Δ^9-THC or other cannabinoids was also not measured (Aguiar et al., 2019). Based on our results, an aqueous preparation of cannabis smoke-as in the study by Aguiar and colleagues-likely did not contain active cannabinoids. Therefore, we sought to develop a standardized protocol for the preparation of CaSE utilizing a protocol similar to that used in the generation of CSE (Baglole et al., 2008a; Zago et al., 2013; Guerrina et al., 2021a; Guerrina et al., 2021b) but one that contains cannabinoids. To achieve this, we made a modification to the preparation via the addition of MeOH to the cell culture media, as cannabinoids are hydrophobic (Huestis, 2007) and MeOH is a suitable solvent for the isolation of fat-soluble compounds (Rozanc et al., 2021). Thus, the addition of MeOH significantly increased the concentration of Δ^9-THC and CBD in the extract compared to negligible levels in CaSE prepared in culture media alone. One of the advantages of this standardized method is that it can be performed using common laboratory equipment, allowing for easy adaptation. Here, we followed the same standardization method for CSE by measuring the absorbance of CaSE at 320 nm, similar to what we have previously used for CSE (Martey et al., 2004; Baglole et al., 2008a; Zago et al., 2013; Zago et al., 2014). Because the tar components in tobacco and cannabis are similar (Tashkin, 2013) and the chemical species of tar in tobacco absorb light at 320 nm (Taylor et al., 2020),

standardization can be performed via spectroscopy, and confirmation of cannabinoid presence made by a commercial ELISA. One of the limitations of this study is that we measured only Δ^9-THC and CBD levels in CaSE, and thus cannot provide information on the presence or absence of additional cannabinoids or other compounds, including those could also affect the activity of the CB1 receptor. Another limitation that we did not assess whether MeOH affects the solubility of the chemical species found in the tar fraction. Nonetheless, this methodology allows for robust and reliable generation of a cannabis extract that contains biologically-active cannabinoids (Δ^9-THC and CBD) to allow for consistency between experiments and comparison between studies.

The detection of cannabinoids in CaSE is important as cannabinoids carry out a variety of physiological functions by engaging with receptors present in the body, including cannabinoids receptors (CBR) (Reggio, 2010). The first discovered CBRs are CB1 and CB2, which belong to the GPCR superfamily. CB1 is expressed predominantly in the central nervous system (CNS), particularly in the basal ganglia, hippocampus, cortex, and cerebellum; these CB1 receptors mediate the psychoactive effects from Δ^9-THC (Sim-Selley, 2003; Kawamura et al., 2006). Δ^9-THC also binds to CB2 receptors with similar binding affinity (Pertwee, 2010). CB2 receptors are present mainly on the surface of immune and hematopoietic cells (Graham et al., 2010). In the respiratory system, CB1 and CB2 receptors are both expressed on epithelial cells with alveolar type II cells displaying CB1 receptor and lung fibroblasts having CB2 receptor (Kicman et al., 2021). Although lung fibroblasts provide structure and support to the lungs by synthesizing and maintaining an extracellular matrix (ECM) (White, 2015), fibroblast activation also leads to the production of several cytokines and chemokines (Buckley et al., 2001; Davidson et al., 2021). The effects of CSE on lung fibroblasts is well-described by us and others (Carnevali et al., 2003; Martey

et al., 2004; Baglole et al., 2006; Baglole et al., 2008a; Baglole et al., 2008b), making these a relevant lung cell type. Herein, we observed that the CaSE-like CSE-induces an inflammatory response in primary lung fibroblasts, including induction of COX-2 and IL-8 levels by 5% CaSE derived from the THC dominant strain. By our estimation, this preparation contains ~0.45 μM of Δ^9-THC, which is similar to the plasma levels of THC in cannabis smokers (~ 1 μM) (Azorlosa et al., 1992). The ability of 5% CaSE to induce COX-2 and IL-8 expression occurred despite the presence of cannabinoids at physiologically-relevant concentrations. It could be that Δ^9-THC itself induced the inflammatory response; this would be in line with another publication whereby COX-2 is induced by Δ^9-THC in neurons and astroglial cells (Chen et al., 2013). It could also be that the cannabinoids present in the extract could not compensate for products of combustion-which promote an inflammatory response typified by the induction of COX-2 (Martey et al., 2004). Of note is the absence of CBD from extracts prepared from the THC dominant strain. CBD has anti-oxidative and anti-inflammatory properties (Atalay et al., 2019). Comparison of CaSE prepared from different cannabis strains (with varying THC/CBD ratios) may shed light on whether all CaSE preparations have the same inflammatory potential.

In order for Δ^9-THC and CBD to be biologically active, the acidic precursors THCA and CBDA need to undergo decarboxylation, a process that is facilitated by combustion. Our standardized CaSE indeed contained forms of cannabinoids that activated the CB1 receptor. As the CB1 receptor is coupled to $G_{i/o}$ and $G_{12/13}$ subfamilies and activates its down-stream Rho (Inoue et al., 2019; Krishna Kumar et al., 2019; Avet et al., 2020), we transfected cells with CB1 receptors along with Rho sensor to evaluate CB1 receptor activation. Here, it was only with CaSE prepared with MeOH that activated the CB1 receptor, with highest activation in extracts from the THC/CBD

balanced strain. This was surprising, given that CBD has relatively low affinity for the CB1 receptor (McPartland et al., 2015) and our result showed that pure CBD does not activate CB1. However, it is still possible that CBD may modulate the activity of the receptor (McPartland et al., 2015) or that CBD and/or other cannabinoids in the extract affects the binding of Δ^9-THC to the CB1 receptor. We also found that the estimated Δ^9-THC concentration in these extracts from the functional assay was 3–50 μM, which is higher than the estimated concentration from the ELISA (~5.5 μM). Nonetheless, the presence of biologically-active cannabinoids in this CaSE preparation further highlights its utility in evaluating the physiological and pathological implications of cannabis smoke.

A limitation of this study is that we did not assess additional signaling mechanisms that may account for the induction of inflammation of CaSE or the ability of CaSE to activate other receptors. For example, Δ^9-THC also binds to the CB2 receptor (Pertwee, 2010) with CB2 activation controlling inflammation and immune functions (Turcotte et al., 2016). Δ^9-THC can also activate the nuclear factor-κB (NF-κB) pathway (Do et al., 2004), a transcription factor that regulates genes involved inflammation, such as COX-2 and IL-8 (Ahn and Aggarwal, 2005). As lung fibroblasts express the CB2 receptor (Kicman et al., 2021), it may be that CaSE induces inflammation via the activation of CB2 receptor and/or NF-κB. However, Δ^9-THC can also activate other GPCRs such as GPR55 (Sharir and Abood, 2010) which is also expressed in the lung (Ryberg et al., 2007). Interestingly, agonist interaction with GPR55 can also activate NF-κB (Henstridge et al., 2010). However, direct regulation of cannabinoids on the activation of GPR55 still needs to be elucidated. Finally, one of the downstream signaling pathways of the CB1 receptor is p38 MAPK (Chen et al., 2013). It is well studied that cigarette smoke can also active p38 MAPK

to induce an inflammatory response (Moretto et al., 2012; Marumo et al., 2014). However, nothing is known about the effect of cannabis smoke on this- and other-signaling pathways in pulmonary cells, a deficit in knowledge that can be addressed by utilization of this standardized extract.

In this study, we sought to develop a protocol for the preparation of a cannabis smoke extract that could be used to investigate the effect of cannabis smoke *in vitro*. We successfully captured Δ^9-THC and CBD within an aqueous preparation (CaSE), which allowed us to recapitulate as closely as possible to what smokers are inhaling; this includes cannabinoids and combustion products. Our data also revealed that this CaSE activates CB1 receptors, further highlighting that it contains biologically active cannabinoids. Importantly, this extract can be prepared and standardized using common laboratory equipment. This CaSE can be used for further molecular investigation into the downstream mechanisms of cannabis smoke/cannabinoids that will ultimately improve our understanding about the effect of cannabis smoke on features of lung pathology.

Ethics Statement

The studies involving human participants were reviewed and approved by Research Ethics Board of St. Joseph's Healthcare Hamilton. The patients/participants provided their written informed consent to participate in this study.

Author Contributions

Data curation and/or analysis: NA, YN, MR; Funding acquisition: CB; Methodology: NA, YN, HT, EW, SL, BK, MR; Resources: PN, SL; Project administration: CB, SL; Supervision: CB, SL; Intellectual contributions: NA, CB, DE, SL, BK, MR; Manuscript writing, review and editing: NA, YN, HT, CB, DE, SL, BK, MR.

Conflict of Interest

The Rho BRET biosensor has been licensed to Domain Therapeutics for commercialization. It can be obtained for academic research with a standard academic material transfer agreement (MTA) from SL. The remaining authors declare that the research was conducted in the absence of any commercial or financial relationships that could be construed as a potential conflict of interest.

5.6. REFERENCES

Aguiar J. A., Huff R. D., Tse W., Stämpfli M. R., Mcconkey B. J., Doxey A. C., et al. (2019). Transcriptomic and Barrier Responses of Human Airway Epithelial Cells Exposed to Cannabis Smoke. Physiol. Rep. 7, e14249. 10.14814/phy2.14249

Ahn K. S., Aggarwal B. B. (2005). Transcription Factor NF-kappaB: a Sensor for Smoke and Stress Signals. Ann. N. Y Acad. Sci. 1056, 218–233. 10.1196/annals.1352.026

Aoshiba K., Tamaoki J., Nagai A. (2001). Acute Cigarette Smoke Exposure Induces Apoptosis of Alveolar Macrophages. Am. J. Physiol. Lung Cel. Mol. Physiol. 281, L1392–L1401. 10.1152/ajplung.2001.281.6.L1392

Atakan Z. (2012). Cannabis, a Complex Plant: Different Compounds and Different Effects on Individuals. Ther. Adv. Psychopharmacol. 2, 241–254. 10.1177/2045125312457586

Atalay S., Jarocka-Karpowicz I., Skrzydlewska E. (2019). Antioxidative and Anti-inflammatory Properties of Cannabidiol. Antioxidants (Basel) 9, 21. 10.3390/antiox9010021

Avet C., Mancini A., Breton B., Le Gouill C., Hauser A. S., Normand C., et al. (2020). Selectivity Landscape of 100 Therapeutically Relevant GPCR Profiled by an Effector Translocation-Based BRET Platform. bioRxiv. 10.1101/2020.04.20.052027

Azorlosa J. L., Heishman S. J., Stitzer M. L., Mahaffey J. M. (1992). Marijuana Smoking: Effect of Varying delta 9-Tetrahydrocannabinol Content and Number of Puffs. J. Pharmacol. Exp. Ther. 261, 114–122.

Baglole C. J., Reddy S. Y., Pollock S. J., Feldon S. E., Sime P. J., Smith T. J., et al. (2005). Isolation and Phenotypic Characterization of Lung Fibroblasts. Methods Mol. Med. 117, 115–127. 10.1385/1-59259-940-0:115

Baglole C. J., Bushinsky S. M., Garcia T. M., Kode A., Rahman I., Sime P. J., et al. (2006). Differential Induction of Apoptosis by Cigarette Smoke Extract in Primary Human Lung Fibroblast Strains: Implications for Emphysema. Am. J. Physiol. Lung Cel Mol Physiol 291, L19–L29. 10.1152/ajplung.00306.2005

Baglole C. J., Maggirwar S. B., Gasiewicz T. A., Thatcher T. H., Phipps R. P., Sime P. J. (2008a). The Aryl Hydrocarbon Receptor Attenuates Tobacco Smoke-Induced Cyclooxygenase-2 and Prostaglandin Production in Lung Fibroblasts through Regulation of the NF-kappaB Family Member RelB. J. Biol. Chem. 283, 28944–28957. 10.1074/jbc.M800685200 [PMC free article]

Baglole C. J., Sime P. J., Phipps R. P. (2008b). Cigarette Smoke-Induced Expression of Heme Oxygenase-1 in Human Lung Fibroblasts Is Regulated by Intracellular Glutathione. Am. J. Physiol. Lung Cel Mol. Physiol. 295, L624–L636. 10.1152/ajplung.90215.2008 [PMC free article]

Baron E. P. (2018). Medicinal Properties of Cannabinoids, Terpenes, and Flavonoids in Cannabis, and Benefits in Migraine, Headache, and Pain: An Update on Current Evidence and Cannabis Science. Headache 58, 1139–1186. 10.1111/head.13345

Bayazit H., Selek S., Karababa I. F., Cicek E., Aksoy N. (2017). Evaluation of Oxidant/Antioxidant Status and Cytokine Levels in Patients with Cannabis Use Disorder. Clin. Psychopharmacol. Neurosci. 15, 237–242. 10.9758/cpn.2017.15.3.237

Bertram K. M., Baglole C. J., Phipps R. P., Libby R. T. (2009). Molecular Regulation of Cigarette Smoke Induced-Oxidative Stress in Human Retinal Pigment Epithelial Cells: Implications for Age-Related Macular Degeneration. Am. J. Physiol. Cel. Physiol. 297, C1200–C1210. 10.1152/ajpcell.00126.2009

Boussif O., Lezoualc'h F., Zanta M. A., Mergny M. D., Scherman D., Demeneix B., et al. (1995). A Versatile Vector for Gene and Oligonucleotide Transfer into Cells in Culture and In Vivo: Polyethylenimine. Proc. Natl. Acad. Sci. U S A. 92, 7297–7301. 10.1073/pnas.92.16.7297

Brown J. D. (2020). Potential Adverse Drug Events with Tetrahydrocannabinol (THC) Due to Drug-Drug Interactions. J. Clin. Med. 9, 919. 10.3390/jcm9040919

Buckley C. D., Pilling D., Lord J. M., Akbar A. N., Scheel-Toellner D., Salmon M. (2001). Fibroblasts Regulate the Switch from Acute Resolving to Chronic Persistent Inflammation. Trends Immunol. 22, 199–204. 10.1016/s1471-4906(01)01863-4

Campeny E., Lopez-Pelayo H., Nutt D., Blithikioti C., Oliveras C., Nuno L., et al. (2020). The Blind Men and the Elephant: Systematic Review of Systematic Reviews of Cannabis Use Related Health Harms. Eur. Neuropsychopharmacol. 33, 1–15. 10.1016/j.euroneuro.2020.02.003

Canadian Centre on Substance Use and Addiction (2020). COVID-19 and Cannabis Smoking and Vaping: Four Things You Should Know. [Online]. Available at: https://ccsa.ca/covid-19-and-cannabis-smoking-and-vaping-four-things-you-should-know-report (Accessed October, 2021).

Carnevali S., Petruzzelli S., Longoni B., Vanacore R., Barale R., Cipollini M., et al. (2003). Cigarette Smoke Extract Induces Oxidative Stress and Apoptosis in Human Lung Fibroblasts. Am. J. Physiol. Lung Cel Mol. Physiol. 284, L955–L963. 10.1152/ajplung.00466.2001

Carp H., Janoff A. (1978). Possible Mechanisms of Emphysema in Smokers. In Vitro Suppression of Serum Elastase-Inhibitory Capacity by Fresh Cigarette Smoke and its Prevention by Antioxidants. Am. Rev. Respir. Dis. 118, 617–621. 10.1164/arrd.1978.118.3.617

Chatkin J. M., Zabert G., Zabert I., Chatkin G., Jiménez-Ruiz C. A., De Granda-Orive J. I., et al. (2017). Lung Disease Associated with Marijuana Use. Arch. Bronconeumol 53, 510–515. 10.1016/j.arbres.2017.03.019

Chatkin J. M., Zani-Silva L., Ferreira I., Zamel N. (2019). Cannabis-Associated Asthma and Allergies. Clin. Rev. Allergy Immunol. 56, 196–206. 10.1007/s12016-017-8644-1

Chen R., Zhang J., Fan N., Teng Z. Q., Wu Y., Yang H., et al. (2013). Δ9-THC-caused Synaptic and Memory Impairments Are Mediated through COX-2 Signaling. Cell 155, 1154–1165. 10.1016/j.cell.2013.10.042

Damico R., Simms T., Kim B. S., Tekeste Z., Amankwan H., Damarla M., et al. (2011). p53 Mediates Cigarette Smoke-Induced Apoptosis of Pulmonary Endothelial Cells: Inhibitory Effects of Macrophage Migration Inhibitor Factor. Am. J. Respir. Cel Mol Biol 44, 323–332. 10.1165/rcmb.2009-0379OC

Davidson S., Coles M., Thomas T., Kollias G., Ludewig B., Turley S., et al. (2021). Fibroblasts as Immune Regulators in Infection, Inflammation and Cancer. Nat. Rev. Immunol. 21, 704–717. 10.1038/s41577-021-00540-z

de Souza A. R., Zago M., Eidelman D. H., Hamid Q., Baglole C. J. (2014). Aryl Hydrocarbon Receptor (AhR) Attenuation of Subchronic Cigarette Smoke-Induced Pulmonary Neutrophilia Is Associated with Retention of Nuclear RelB and Suppression of Intercellular Adhesion Molecule-1 (ICAM-1). Toxicol. Sci. 140, 204–223. 10.1093/toxsci/kfu068

Do Y., Mckallip R. J., Nagarkatti M., Nagarkatti P. S. (2004). Activation through Cannabinoid Receptors 1 and 2 on Dendritic Cells Triggers NF-kappaB-dependent Apoptosis: Novel Role for Endogenous and Exogenous Cannabinoids in Immunoregulation. J. Immunol. 173, 2373–2382. 10.4049/jimmunol.173.4.2373

Fantauzzi M. F., Cass S. P., Mcgrath J. J. C., Thayaparan D., Wang P., Stampfli M. R., et al. (2021). Development and Validation of a Mouse Model of Contemporary Cannabis Smoke Exposure. ERJ Open Res. 7, 00107–02021. 10.1183/23120541.00107-2021 [PMC free article]

Fligiel S. E., Roth M. D., Kleerup E. C., Barsky S. H., Simmons M. S., Tashkin D. P. (1997). Tracheobronchial Histopathology in Habitual Smokers of Cocaine, Marijuana, And/or Tobacco. Chest 112, 319–326. 10.1378/chest.112.2.319

Graham E. S., Angel C. E., Schwarcz L. E., Dunbar P. R., Glass M. (2010). Detailed Characterisation of CB2 Receptor Protein Expression in Peripheral Blood Immune Cells from Healthy Human Volunteers Using Flow Cytometry. Int. J. Immunopathol. Pharmacol. 23, 25–34. 10.1177/039463201002300103

Graves B. M., Johnson T. J., Nishida R. T., Dias R. P., Savareear B., Harynuk J. J., et al. (2020). Comprehensive Characterization of Mainstream Marijuana and Tobacco Smoke. Sci. Rep. 10, 7160. 10.1038/s41598-020-63120-6

Guerrina N., Aloufi N., Shi F., Prasade K., Mehrotra C., Traboulsi H., et al. (2021a). The Aryl Hydrocarbon Receptor Reduces LC3II Expression and Controls Endoplasmic Reticulum Stress. Am. J. Physiol. Lung Cel Mol. Physiol. 320, L339–L355. 10.1152/ajplung.00122.2020

Guerrina N., Traboulsi H., Rico De Souza A., Bossé Y., Thatcher T. H., Robichaud A., et al. (2021b). Aryl Hydrocarbon Receptor Deficiency Causes the Development of Chronic Obstructive Pulmonary Disease through the Integration of Multiple Pathogenic Mechanisms. FASEB J. 35, e21376. 10.1096/fj.202002350R

Hecht E., Zago M., Sarill M., Rico De Souza A., Gomez A., Matthews J., et al. (2014). Aryl Hydrocarbon Receptor-dependent Regulation of miR-196a Expression Controls Lung Fibroblast Apoptosis but Not Proliferation. Toxicol. Appl. Pharmacol. 280, 511–525. 10.1016/j.taap.2014.08.023

Helyes Z., Kemény Á., Csekő K., Szőke É., Elekes K., Mester M., et al. (2017). Marijuana Smoke Induces Severe Pulmonary Hyperresponsiveness, Inflammation, and Emphysema in a Predictive Mouse Model Not via CB1 Receptor Activation. Am. J. Physiol. Lung Cel. Mol. Physiol. 313, L267–L277. 10.1152/ajplung.00354.2016

Henderson R. L., Tennant F. S., Guerry R. (1972). Respiratory Manifestations of Hashish Smoking. Arch. Otolaryngol. 95, 248–251. 10.1001/archotol.1972.00770080390012

Henstridge C. M., Balenga N. A., Schröder R., Kargl J. K., Platzer W., Martini L., et al. (2010). GPR55 Ligands Promote Receptor Coupling to Multiple Signalling Pathways. Br. J. Pharmacol. 160, 604–614. 10.1111/j.1476-5381.2009.00625.x

Hillig K. W. (2005). Genetic Evidence for Speciation in Cannabis (Cannabaceae). Genet. Resour. Crop Evol. 52, 161–180. 10.1007/s10722-003-4452-y [

Huestis M. A. (2007). Human Cannabinoid Pharmacokinetics. Chem. Biodivers 4, 1770–1804. 10.1002/cbdv.200790152

Inoue A., Raimondi F., Kadji F. M. N., Singh G., Kishi T., Uwamizu A., et al. (2019). Illuminating G-Protein-Coupling Selectivity of GPCRs. Cell 177, 1933–1947.e25. 10.1016/j.cell.2019.04.044

Kawamura Y., Fukaya M., Maejima T., Yoshida T., Miura E., Watanabe M., et al. (2006). The CB1 Cannabinoid Receptor Is the Major Cannabinoid Receptor at Excitatory Presynaptic Sites in the hippocampus and Cerebellum. J. Neurosci. 26, 2991–3001. 10.1523/JNEUROSCI.4872-05.2006

Kicman A., Pędzińska-Betiuk A., Kozłowska H. (2021). The Potential of Cannabinoids and Inhibitors of Endocannabinoid Degradation in Respiratory Diseases. Eur. J. Pharmacol. 911, 174560. 10.1016/j.ejphar.2021.174560

Kim Y. H., An Y. J., Jo S., Lee S. H., Lee S. J., Choi S. J., et al. (2018). Comparison of Volatile Organic Compounds between Cigarette Smoke Condensate (CSC) and Extract (CSE) Samples. Environ. Health Toxicol. 33, e2018012–2018010. 10.5620/eht.e2018012

Krishna Kumar K., Shalev-Benami M., Robertson M. J., Hu H., Banister S. D., Hollingsworth S. A., et al. (2019). Structure of a Signaling Cannabinoid Receptor 1-G Protein Complex. Cell 176, 448–458.e12. 10.1016/j.cell.2018.11.040 [

Li C. J., Ning W., Matthay M. A., Feghali-Bostwick C. A., Choi A. M. (2007). MAPK Pathway Mediates EGR-1-HSP70-dependent Cigarette Smoke-Induced Chemokine Production. Am. J. Physiol. Lung Cel Mol Physiol. 292, L1297–L1303. 10.1152/ajplung.00194.2006

Li H., Liu Y., Tian D., Tian L., Ju X., Qi L., et al. (2020). Overview of Cannabidiol (CBD) and its Analogues: Structures, Biological Activities, and Neuroprotective Mechanisms in Epilepsy and Alzheimer's Disease. Eur. J. Med. Chem. 192, 112163. 10.1016/j.ejmech.2020.112163

Maertens R. M., White P. A., Rickert W., Levasseur G., Douglas G. R., Bellier P. V., et al. (2009). The Genotoxicity of Mainstream and Sidestream Marijuana and Tobacco Smoke Condensates. Chem. Res. Toxicol. 22, 1406–1414. 10.1021/tx9000286

Manolis T. A., Manolis A. A., Manolis A. S. (2019). Cannabis Associated "High" Cardiovascular Morbidity and Mortality: Marijuana Smoke like Tobacco Smoke? A Déjà Vu/Déjà Vécu Story? Mrmc 19, 870–879. 10.2174/1389557518666181114113947

Martey C. A., Pollock S. J., Turner C. K., O'reilly K. M., Baglole C. J., Phipps R. P., et al. (2004). Cigarette Smoke Induces Cyclooxygenase-2 and Microsomal Prostaglandin E2 Synthase in

Human Lung Fibroblasts: Implications for Lung Inflammation and Cancer. Am. J. Physiol. Lung Cel Mol Physiol. 287, L981–L991. 10.1152/ajplung.00239.2003

Martey C. A., Baglole C. J., Gasiewicz T. A., Sime P. J., Phipps R. P. (2005). The Aryl Hydrocarbon Receptor Is a Regulator of Cigarette Smoke Induction of the Cyclooxygenase and Prostaglandin Pathways in Human Lung Fibroblasts. Am. J. Physiol. Lung Cel Mol Physiol. 289, L391–L399. 10.1152/ajplung.00062.2005

Marumo S., Hoshino Y., Kiyokawa H., Tanabe N., Sato A., Ogawa E., et al. (2014). p38 Mitogen-Activated Protein Kinase Determines the Susceptibility to Cigarette Smoke-Induced Emphysema in Mice. BMC Pulm. Med. 14, 79. 10.1186/1471-2466-14-79

McPartland J. M., Duncan M., Di Marzo V., Pertwee R. G. (2015). Are Cannabidiol and Δ(9) - tetrahydrocannabivarin Negative Modulators of the Endocannabinoid System? A Systematic Review. Br. J. Pharmacol. 172, 737–753. 10.1111/bph.12944

Mersiades A. J., Tognela A., Haber P. S., Stockler M., Lintzeris N., Simes J., et al. (2018). Oral Cannabinoid-Rich THC/CBD Cannabis Extract for Secondary Prevention of Chemotherapy-Induced Nausea and Vomiting: a Study Protocol for a Pilot and Definitive Randomised Double-Blind Placebo-Controlled Trial (CannabisCINV). BMJ Open 8, e020745. 10.1136/bmjopen-2017-020745

Moir D., Rickert W. S., Levasseur G., Larose Y., Maertens R., White P., et al. (2008). A Comparison of Mainstream and Sidestream Marijuana and Tobacco Cigarette Smoke Produced under Two Machine Smoking Conditions. Chem. Res. Toxicol. 21, 494–502. 10.1021/tx700275p

Morales P., Hurst D. P., Reggio P. H. (2017). Molecular Targets of the Phytocannabinoids: A Complex Picture. Prog. Chem. Org. Nat. Prod. 103, 103–131. 10.1007/978-3-319-45541-9_4

Moretto N., Bertolini S., Iadicicco C., Marchini G., Kaur M., Volpi G., et al. (2012). Cigarette Smoke and its Component Acrolein Augment IL-8/CXCL8 mRNA Stability via P38 MAPK/MK2 Signaling in Human Pulmonary Cells. Am. J. Physiol. Lung Cel. Mol. Physiol. 303, L929–L938. 10.1152/ajplung.00046.2012

Namkung Y., Legouill C., Kumar S., Cao Y., Teixeira L. B., Lukasheva V., et al. (2018). Functional Selectivity Profiling of the Angiotensin II Type 1 Receptor Using Pathway-wide BRET Signaling Sensors. Sci. Signal. 11, eaat1631. 10.1126/scisignal.aat1631

Pertwee R. G. (2010). Receptors and Channels Targeted by Synthetic Cannabinoid Receptor Agonists and Antagonists. Curr. Med. Chem. 17, 1360–1381. 10.2174/092986710790980050

Rajan T. S., Giacoppo S., Iori R., De Nicola G. R., Grassi G., Pollastro F., et al. (2016). Anti-inflammatory and Antioxidant Effects of a Combination of Cannabidiol and Moringin in LPS-Stimulated Macrophages. Fitoterapia 112, 104–115. 10.1016/j.fitote.2016.05.008

Rana A. C. N. (2010). Floral Biology and Pollination Biology of Cannabis Sativa L. Int. J. Plant Reprod. Biol. 2, 191–195.

Reggio P. H. (2010). Endocannabinoid Binding to the Cannabinoid Receptors: what Is Known and what Remains Unknown. Curr. Med. Chem. 17, 1468–1486. 10.2174/092986710790980005

Rico de Souza A., Traboulsi H., Wang X., Fritz J. H., Eidelman D. H., Baglole C. J. (2021). The Aryl Hydrocarbon Receptor Attenuates Acute Cigarette Smoke-Induced Airway Neutrophilia Independent of the Dioxin Response Element. Front. Immunol. 12, 630427. 10.3389/fimmu.2021.630427

Roth M. D., Arora A., Barsky S. H., Kleerup E. C., Simmons M., Tashkin D. P. (1998). Airway Inflammation in Young Marijuana and Tobacco Smokers. Am. J. Respir. Crit. Care Med. 157, 928–937. 10.1164/ajrccm.157.3.9701026

Rozanc J., Kotnik P., Milojevic M., Gradisnik L., Knez Hrncic M., Knez Z., et al. (2021). Different Cannabis Sativa Extraction Methods Result in Different Biological Activities against a Colon Cancer Cell Line and Healthy Colon Cells. Plants (Basel) 10, 566. 10.3390/plants10030566

Ryberg E., Larsson N., Sjögren S., Hjorth S., Hermansson N. O., Leonova J., et al. (2007). The Orphan Receptor GPR55 Is a Novel Cannabinoid Receptor. Br. J. Pharmacol. 152, 1092–1101. 10.1038/sj.bjp.0707460

Schuermeyer J., Salomonsen-Sautel S., Price R. K., Balan S., Thurstone C., Min S. J., et al. (2014). Temporal Trends in Marijuana Attitudes, Availability and Use in Colorado Compared to Non-medical Marijuana States: 2003-11. Drug Alcohol Depend 140, 145–155. 10.1016/j.drugalcdep.2014.04.016

Sharir H., Abood M. E. (2010). Pharmacological Characterization of GPR55, a Putative Cannabinoid Receptor. Pharmacol. Ther. 126, 301–313. 10.1016/j.pharmthera.2010.02.004

Sim-Selley L. J. (2003). Regulation of Cannabinoid CB1 Receptors in the central Nervous System by Chronic Cannabinoids. Crit. Rev. Neurobiol. 15, 91–119. 10.1615/critrevneurobiol.v15.i2.10

Sinclair C. F., Foushee H. R., Scarinci I., Carroll W. R. (2013). Perceptions of Harm to Health from Cigarettes, Blunts, and Marijuana Among Young Adult African American Men. J. Health Care Poor Underserved 24, 1266–1275. 10.1353/hpu.2013.0126

Strzelak A., Ratajczak A., Adamiec A., Feleszko W. (2018). Tobacco Smoke Induces and Alters Immune Responses in the Lung Triggering Inflammation, Allergy, Asthma and Other Lung Diseases: A Mechanistic Review. Int. J. Environ. Res. Public Health 15, 1033. 10.3390/ijerph15051033

Tahir M. N., Shahbazi F., Rondeau-Gagné S., Trant J. F. (2021). The Biosynthesis of the Cannabinoids. J. Cannabis Res. 3, 7. 10.1186/s42238-021-00062-4

Tashkin D. P. (2013). Effects of Marijuana Smoking on the Lung. Ann. Am. Thorac. Soc. 10, 239–247. 10.1513/AnnalsATS.201212-127FR

Taylor M., Santopietro S., Baxter A., East N., Breheny D., Thorne D., et al. (2020). In Vitro biological Assessment of the Stability of Cigarette Smoke Aqueous Aerosol Extracts. BMC Res. Notes 13, 492. 10.1186/s13104-020-05337-2

Turcotte C., Blanchet M. R., Laviolette M., Flamand N. (2016). The CB2 Receptor and its Role as a Regulator of Inflammation. Cell Mol Life Sci 73, 4449–4470. 10.1007/s00018-016-2300-4

Urban T., Hureaux J. (2017). Cannabis et poumon. Ce que l'on sait et tout ce que l'on ne sait pas. Rev. Pneumol Clin. 73, 283–289. 10.1016/j.pneumo.2017.08.013

White E. S. (2015). Lung Extracellular Matrix and Fibroblast Function. Ann. Am. Thorac. Soc. 12 Suppl 1 (Suppl. 1), S30–S33. 10.1513/AnnalsATS.201406-240MG

Yayan J., Rasche K. (2016). Damaging Effects of Cannabis Use on the Lungs. Adv. Exp. Med. Biol. 952, 31–34. 10.1007/5584_2016_71

Zago M., Sheridan J. A., Nair P., Rico De Souza A., Gallouzi I. E., Rousseau S., et al. (2013). Aryl Hydrocarbon Receptor-dependent Retention of Nuclear HuR Suppresses Cigarette Smoke-Induced Cyclooxygenase-2 Expression Independent of DNA-Binding. PLoS One 8, e74953. 10.1371/journal.pone.0074953

Zago M., Rico De Souza A., Hecht E., Rousseau S., Hamid Q., Eidelman D. H., et al. (2014). The NF-κB Family Member RelB Regulates microRNA miR-146a to Suppress Cigarette Smoke-Induced COX-2 Protein Expression in Lung Fibroblasts. Toxicol. Lett. 226, 107–116. 10.1016/j.toxlet.2014.01.020

6. GENERAL DISCUSSION

It is now well-established that smoking is harmful to human health. Smoke- either from tobacco or cannabis combustion- contains many toxicants and carcinogens. Although it is well recognized that cigarette smoke is a risk factor for numerous diseases with no cure and limited therapeutic options, such as COPD [25, 294, 295], the mechanisms involved in smoke-induced lung damage are still poorly understood. In this body of work, we focused on the mechanistic link between COPD, smoke exposure and the RNA-binding protein HuR. It is well known that HuR regulates target mRNA at the post-transcriptional level [241, 299]. These mRNA are involved in various cellular mechanisms, ranging from cell proliferation and adaptation to the stress response to differentiation, inflammation, apoptosis, and senescence [142, 242, 246, 254, 260, 268, 299-303]. Hence, we postulated that HuR would control cellular features associated with COPD pathogenesis. First, in Chapter II, we found that ACE2 expression, the entry receptor for SARS-CoV-2 [77], is increased in lung fibroblasts from smoker and COPD subjects. Then, we determined the expression and the localization of HuR in the lungs from smokers and COPD subjects in Chapter III. We also reported the effect of CS on the cytoplasmic translocation of HuR, a feature of its activation status, and thus predicted that HuR activation by smoke would regulate the expression of ACE2. Then, in Chapter IV, we delved deeper into the molecular function of HuR in numerous biological processes of lung fibroblasts and how these change in response to CS. Finally, in Chapter V, we developed a standardized cannabis smoke extract protocol that can now be used to interrogate the extent to which HuR participates in cellular functions altered by cannabis smoke, another type of inhalation exposure that may lead to adverse pulmonary outcomes. Therefore, these studies lay the foundation for which unraveling the detailed mechanisms of HuR

function could lead to the development of therapeutic strategies against environmental diseases including COPD.

6.1. Where does HuR bind?

HuR contains three RRMs which associate with the 3'UTR, 5'UTR or coding region of target mRNA to regulate their stability, translation, as well as intracellular trafficking [198, 200, 201, 203, 204]. In this context, we demonstrated that HuR binds to hundreds of mRNA in lung fibroblasts at the basal level and in response to CS (Chapter IV). However, a limitation of this finding is that the exact binding site(s) on these target mRNAs was not investigated. Understanding HuR binding sites could lead to the design of potent and specific HuR inhibitors to be used as novel therapies for various diseases. In this context, there are some studies that have identified small molecule inhibitors that prevent HuR from binding to its target mRNA in numerous models of cancer [194, 304, 305]. For instance, CMLD-2, a coumarin-derived compound, is a small molecule inhibitor that disrupts HuR binding to the ARE within 3'UTR of target mRNA that are involved in cancer [304]. Thus, CMLD-2 has antitumor activity in colorectal, pancreatic and lung cancer cells in part by inducing cell death [304, 306]. However, this inhibitor has not been investigated in normal primary cells that are exposed to external stimuli. Altogether, the availability of these HuR small molecule disruptors could be extremely valuable as novel therapies for HuR-regulated diseases.

6.2. What are the possible protein partners of HuR that control target mRNA stability?

Dynamic interactions between RBPs may fine-tune post-transcriptional modifications of common mRNA. In this context, HuR can either cooperate or compete with other RBPs to bind target mRNA and regulate their expression. To investigate protein partners that associate with HuR in lung fibroblasts, we immunoprecipitated HuR and performed protein profiling using LC-MS/MS. Here, we observed that HuR associates with several proteins both at the basal level and in response to CSE (Table A1 and A2). For example, these data show that HuR binds to the RBP HNRNPAB/hnRNP A/B, regardless of exposure to CSE. hnRNP A/B belongs to the ubiquitous hnRNP family of proteins that control transcription, alternative splicing, mRNA stability, as well as translocation of mRNA from nucleus to cytoplasm [307]. There are approximately 20 hnRNP proteins identified in human cells, designated hnRNP A1 to U. The members in hnRNP A/B subfamily include hnRNP A1, A2/B1 and A3, which share a high degree of sequence homology [307, 308]. Although it is known that HuR associates with other members of hnRNPs family, including hnRNP A1, C1/C2, L and D [309], our data that HuR binds to hnRNP A/B is a novel finding. hnRNP A/B proteins are upregulated in lung cancer [308], and may thus be a marker for early lung cancer detection [310]. Mechanistically, hnRNP A2/B1 promotes migration and reduces the expression of E-cadherin, an epithelial marker; hence, it is thought that hnRNP A/B induces EMT in lung cancer cells [311]. EMT also occurs in COPD, which is a process that may contribute to fibrosis formation around the small airways, leading to airflow obstruction [192]. These data may therefore suggest that hnRNP A/B expression may be involved in the pathogenesis of COPD by promoting EMT. To our knowledge, the expression and function of hnRNP A/B proteins in COPD are unknown. Additionally, given that EMT occurs in response to CS [192], and that HuR

promotes CSE-induced EMT in human bronchial epithelial cells [289], we speculate that HuR and hnRNP A/B association might regulate the expression of mRNA involved in this process.

6.3. Are there miRNA partners of HuR that control target mRNA in response to CSE?

miRNA are small non-coding RNA (~22 nucleotides) that control genes expression at the post-transcriptional level. miRNA pairs to the 3′ UTR of mRNA by partial sequence matching after being incorporated into the RISC. This leads to direct post-transcriptional repression by inhibiting translation and/or inducing mRNA decay [312, 313]. miRNA and HuR interact to further fine-tune post-transcriptional regulatory mechanisms. An example of this is the ability of HuR to promote the interaction of let-7- loaded RISC with the 3′UTR of the proto-oncogene *MYC* mRNA to repress its expression [253]. Thus, we propose that HuR could work cooperatively with miRNA as a mechanism to downregulate target mRNA. HuR has a strong binding affinity to AREs in 3'UTR of *PTGS2* and *CXCL8* mRNA, which consequently induces their stability and protein expression in cancer cells [246, 247, 300]. Nevertheless, we found that HuR binds to *PTGS2* and *CXCL8* mRNA and destabilizes these mRNA (Chapter IV); thus, HuR may in fact supress inflammation in lung fibroblasts exposed to CS. Despite not knowing where HuR binds to *PTGS2* and *CXCL8* mRNA in the context of smoke exposure, we speculate that HuR may bind to 3'UTR of these genes to reduce their stability via miRNA, and hence supress protein expression. Therefore, our assessment of miRNA enrichment using RIP-RNA-seq revealed that HuR associates with subset of miRNA in lung fibroblasts both at the basal level and upon exposure to CSE (Tables A3 and A4). One miRNA that associated with HuR in lung fibroblasts exposed to CSE was MIR4517, a miRNA predicted to target *PTGS2* mRNA. Additionally, MIR5706 is a miRNA that associates with HuR in lung fibroblasts exposed to CSE and is predicted to target

CXCL8 mRNA. These data suggest that HuR may cooperate with MIR4517 and MIR5706 to dampen *PTGS2* and *CXCL8* expression, respectively, in lung fibroblasts. The discovery of crosstalk between HuR and miRNA supports the cooperative possibility for their dynamic regulation of gene expression associated with cellular mechanisms whose dysregulation contributes to the pathogenesis of COPD development.

6.4. Does HuR regulate miRNA expression in lung fibroblasts?

The above section highlights that HuR interaction with miRNA may be a mechanism that regulates gene expression [302, 314]. However, HuR itself may also indirectly control the expression of miRNA. For example, HuR silencing induces the expression of miR-466i, which destabilizes granulocyte-macrophage colony-stimulating factor (*GM-CSF*) and *IL-17* mRNA, subsequently reduces their expression in Th17 cells [315]. In addition to this, HuR promotes MAX Interactor 1 (Mxi1) mRNA and protein expression, which suppresses the function of c-Myc, a transcription factor that regulates miRNA expression, resulting in inhibition in the expression of miR-466i [315]. Our data also supports that HuR may control the expression of miRNA in lung fibroblasts. We found that knockdown of HuR differentially changed the expression of several miRNA (Table A5 and A6). Thus, it is possible that HuR changes the expression of miRNA, resulting in indirect inhibition of target mRNA expression.

6.5. Is HuR involved in SGs assembly caused by CS?

SGs are cytoplasmic ribonucleoprotein complexes that assemble in response to stress and sequester mRNA for storage and translational silencing, consequently promoting cell survival and

minimizing stress-related damage [148]. SG formation is initiated by G3BP stress granule assembly factor 1 (G3BP) as well as by the RBPs TIA-1, TTP, TIAR and FMRP, which are involved in RNA metabolism. Another RBP, PABP1, connects different SG components and interacts with SG proteins [148, 150]. It has been reported that SGs assemble in response to different stimuli, such as NO [316]. Currently, we do not know whether SGs assemble under CS exposure, but is a possibility given that CS contains high concentrations of NO [317]. Interestingly, and of relevance to this project, HuR sequesters *PTGS2* mRNA in SGs in response to IL-1β, the result of which decreases COX-2 protein expression due to a delay in translation of its mRNA [149]. Based on the results presented herein, we speculate that CS may induce SG assembly and that a function of HuR may be to sequester mRNA within them, resulting in a delay in translation. This could explain why knockdown of HuR increased the level of COX-2 protein (Chapter IV). Thus, the role of HuR in SG assembly is an area of ongoing experimentation.

6.6. How does CS control HuR function?

Posttranslational modifications of HuR impact its function by regulating its subcellular localization as well as its ability to bind to target mRNA. Some established posttranslational modifications of HuR include its phosphorylation by protein kinases, such as p38 MAPK [144, 221, 230-233] as well as its methylation by CARM1 [237, 239]. In this study, we observed that HuR cytoplasmic localization is higher in the lung cells from Smoker and COPD subjects as well as in lung fibroblasts exposed to CSE (Chapter III). Although the mechanism through which CS induces HuR translocation to the cytoplasm and/or its binding to target mRNA is unknown, we propose that it may involve activation of p38 MAPK pathway because: 1) phospho-p38 is elevated in smoker and COPD lungs; 2) CS activates p38 [318-320] and 3) HuR phosphorylation by p38

MAPK alters its subcellular localization [232, 233]. These data suggest that CS-induced HuR shuttling may be mediated through p38 activation.

It could also be that CARM1 controls HuR function in response to CS. CARM1 is a methyltransferase enzyme that belongs to PRMTs family and regulates the transcription of genes involved in proliferation, differentiation and senescence [236, 321]. For example, CARM1 methylates HuR to regulate the expression of mRNA involved in proliferation, including cyclin A. In support of this, CARM1 silencing reduces HuR target mRNA, the effect of which prevented proliferation and accelerated cellular senescence [239]. It is noteworthy that CARM1 expression is decreased in bronchial epithelial cells from COPD patients and that CARM1 silencing in human airway epithelial cells leads to cellular senescence [321]. Senescence is a hallmark of aging, and COPD is regarded as a form of accelerated lung aging [322, 323]. Cellular senescence is a permanent state of cell cycle arrest but remains one that is metabolically active. Senescent cells display a senescence-associated secretory phenotype that includes release of proinflammatory cytokines and chemokines as well as MMPs [324], all of which are involved in COPD pathogenesis (Chapter I: Section 1.2.2). Based on these observations, we propose that loss of CARM1 leads to reduction in HuR methylation, which may accelerate cellular senescence in COPD. Interestingly, in Chapter IV, we observed that HuR reduces the expression of *IL6*, *CXCL8* and *CD36*, which are markers of a senescence-associated secretory phenotype [325], suggesting that CARM1 may methylate HuR to prevent cellular senescence. Altogether, understanding the posttranslational modifications underlying the dynamic control of HuR could help to develop novel therapeutic strategies targeting HuR in COPD.

6.7. Does HuR regulate cannabis smoke-induced inflammation?

It is well known that CS is a risk factor for COPD development. However, other inhalational toxicants may be involved in the pathogenesis of this disease; this includes inhalation of cannabis smoke [296]. Although cannabis is the second most-smoked plant after tobacco [10-13], the consequence of cannabis smoke on cellular and pathological mechanisms associated with COPD remains unclear, in part because of concurrent tobacco use by study participants. To therefore understand the impact of cannabis smoke on cellular and pathological mechanisms, the development of *in vitro* surrogates of cannabis smoke exposure is necessary- much like CSE that was utilized throughout this study as a surrogate for tobacco. Unfortunately, there are no optimized exposure protocols with which to conduct such assessments. Therefore, we developed and optimized a standardized protocol to generate CaSE in order to elucidate its effect on cellular mechanisms *in vitro* (Chapter V). We found that CaSE- similar to CSE- induces the expression of COX-2 and IL-8 in lung fibroblasts; however, the mechanism(s) underlying the CaSE-induced inflammation are not known. In our study, CaSE preparation contains cannabinoids, including Δ^9-THC (Chapter V). Δ^9-THC carries out a variety of physiological functions by engaging with receptors in the body particularly *CNR1*/CB1 and *CNR2*/CB2 [326]. These GPCRs are part of the endocannabinoid system (ECS). In fact, Δ^9-THC has high affinity to CB1 and CB2 [327-329]. In the respiratory system, CB1 and CB2 are expressed on epithelial cells, with alveolar type II cells displaying CB1 and lung fibroblasts having CB2 [330]. One of the downstream signaling pathways of the CB1 receptor is p38 MAPK [331]. Although as noted above, CS actives p38 MAPK to induce an inflammatory response [318, 319], nothing is known about the effect of cannabis smoke on this- or other-signaling pathways in pulmonary cells; this includes HuR. Therefore, we speculate that CaSE may activate CB1 and its downstream signaling p38; p38 may then

phosphorylate HuR and induce its translocation to the cytoplasm. Moreover, there are emerging links between HuR and components of the ECS. For instance, HuR binds to *CNR1* mRNA and promotes its expression in macrophages exposed to arachidonyl-2′-chloroethylamide (ACEA), a synthetic CB1 agonist [332]. Based on these data we could envision a pathway through which activation of p38 MAPK in response to CaSE may phosphorylate and activate HuR, which then would control *CNR1* expression to regulate downstream signaling pathways. Additionally, the effect of HuR knockdown on cannabis smoke-induced COX-2 and IL-8 is consider for future investigation. In Chapter IV, we found that HuR reduces CS-induced inflammation, including COX-2 and IL-8. Because CS and cannabis smoke share similarities in chemical compounds [48, 49, 333], we hypothesize that HuR may also control the inflammatory response to cannabis smoke, and will be an area of active investigation.

6.8. Is HuR a friend or foe?

The collective results in this thesis still beg the question as to whether HuR is beneficial or detrimental to lung health in response to CS. HuR targets mRNA that encode protein involved in physiological processes, including organ development and immune function, and as such, dysregulation of HuR is linked to the pathogenesis of numerous human diseases. Information of the fundamental importance for HuR comes from the observation that whole-body deletion of HuR is embryonic lethal [334, 335], suggesting HuR as a friend during organ development. Therefore, utilization of models with tissue and/or cell specific knockout of HuR have shed light into its functions in physiology and disease. For example, adipose-specific deletion of HuR revealed that HuR in fact protects against obesity [336]. Furthermore, and of relevance to this project, HuR is involved in lung branching morphogenesis by regulating the synthesis of fibroblast growth factor

10 (*FGF10*) mRNA, a growth factor that controls airway tree morphogenesis, by inducing its translation into protein [337]. In the context of COPD, recent findings connected *FGF10* genetic variants to structural airway abnormalities in COPD among smokers [338]. This suggests that mutations in *FGF10* gene can cause structural abnormalities leading to COPD following years of environmental exposures. Although the implication of HuR in the regulation of *FGF10* genetic variants is not investigated, we speculate that HuR may regulate *FGF10* expression in smokers who are susceptible to developing COPD. In our RNA-seq data (Chapter IV), we found that HuR did not associate with *FGF10* mRNA, and that HuR knockdown did not change *FGF10* expression in response to CS. However, HuR may control the protein level of FGF10 based on the knowledge that HuR regulates the translation of *FGF10* mRNA in response to FGF9, an epithelia-derived inducer of FGF10 expression [337]. Altogether, the requirement of HuR for lung branching highlights its role in the lung development, and that HuR dysregulation may contribute to the airway abnormalities associated with the development of COPD. This suggests that HuR could be a friend during the development of COPD.

Dysregulation of HuR is also implicated in many cancers such as lung cancer [17, 277, 339, 340]. High HuR expression in lung cancer tissue is associated with metastasis and poor survival [277, 340]. Perhaps unsurprisingly, HuR controls many aspects of cancer pathogenesis, including apoptosis, proliferation, angiogenesis, and invasion [267, 301]. In this regard, HuR is acting as a foe. Hence, it is proposed that targeting HuR could be a promising therapeutic strategy to treat cancer. HuR also plays a key role in the pathogenesis of other diseases, such as IPF [260, 341-343]. We have recently shown that cytoplasmic HuR is increased in the lungs of IPF patients and mice exposed to bleomycin and thoracic radiation, two well characterized lung fibrosis models [260]. We and others have also found that HuR promotes the differentiation of lung fibroblasts to

myofibroblasts and induces the production of ECM in response to TGF- β [260, 261, 343]. Because of these findings, it could be that HuR controls fibrosis formation around the small airways in COPD, believed to be a major region of airflow limitation. Altogether, these studies highlight HuR as a foe in different pathologies.

Another lung disease we speculated that HuR might act as a foe is COVID-19, particularly as it relates to susceptibility in certain populations. Recently, it was reported that COPD patients have an increased risk for severe illness from COVID-19 because of the upregulation of ACE2 [77]. Although our study showed that HuR does not control the expression of ACE2 in lung fibroblasts (Chapter III), our experimental approach revealed that HuR reduces inflammation in response to CS (Chapter IV). This finding is consistent with previous reports showing that myeloid deletion of HuR induces the sensitivity of the mice to systemic inflammation [344, 345]. Further, we profiled *ELAVL1* expression in nasopharyngeal/bronchial cells from COVID-19 patients via scRNA-seq analysis. We observed that the expression of *ELAVL1* is significantly lower in critical COVID-19 patients than in moderate and control patients (Chapter III). These data suggest that the loss of HuR may be involved in the pathogenesis of COVID-19 by its ability to dampen inflammation, as SARS-CoV-2 infection induces pro-inflammatory mediators, including IL-8 and IL-6 [346]. Interestingly, these data raise the possibility that HuR may act as a friend during cellular response to external stimuli, such as viral infection and CS exposure.

6.9. Future Directions and Conclusion

The goal of this study was to investigate the role of HuR in pathological features involved in COPD development. First, in Chapter II, we found that the expression of ACE2, the entry receptor for SARS-CoV-2 [77], is increased in lung fibroblasts from Smoker and COPD subjects.

Then, in Chapter III, we identified that cytoplasmic localization of HuR in the lungs from Smokers and COPD subjects is increased. Using our *in vitro* model, we also showed that CS directly induces the cytoplasmic shuttling of HuR, a feature of its activation status, and thus predicted that HuR activation by smoke would regulate the expression of ACE2- this was not the case. However, we believe that additional studies should be devoted to evaluating HuR regulation of ACE2 expression in pulmonary epithelial cells, which are the port of entry of SARS-CoV-2 into the respiratory system.

Then, in Chapter IV, we delved deeper into how the molecular function of HuR changed in response to CS using multi-omics approaches. We found that HuR controlled numerous biological processes in response to cigarette smoke, including pathways involved in inflammation and oxidative stress, in part by its ability to bind to target mRNA. Mechanistically, we demonstrated that HuR abrogates CS-induced COX-2 and IL-8 through destabilization of their mRNA. As recommended above, this finding should be addressed in other lung cell types such as epithelial cells and macrophages, as HuR cytoplasmic expression was increased in these two cells in the lungs from Smokers and COPD subjects (Chapter III). Thus, we believe that HuR may control CS-induced inflammation in multiple lung cell types.

Our findings alone cannot definitively prove that HuR controls pathological responses in the lungs that caused by CS because our *in vitro* studies focused solely on lung fibroblasts. Further, in the context of chronic inflammation, activation of fibroblasts leads to the production of several cytokines and chemokines [347]. Indeed, our results clearly show that HuR controls multiple cellular mechanisms both at the basal level and in response to CS. Therefore, it would be interesting to study the role of HuR in lung physiology and in CS-induced lung damage *in vivo*. Based on our finding that HuR cleavage is elevated in lung fibroblasts from smoker and COPD

subjects as well as in response to CS (chapter III), we speculate that acute smoke exposure (3 days) and chronic smoke exposure (6 months) may induce HuR cleavage. The products of HuR cleavage promote apoptosis [223], and mutation of the cleavage site A226 delays apoptotic cell death [224]. Altogether, we believe that HuR cleavage may exaggerate CS-induced lung damage.

There are over 40 types of cells within the lungs that contribute to lung structure and function [65]. For this reason, as well as issues of embryonic lethality in the whole body knockout mouse, it would be advantageous to conditionally-knockout HuR in specific cell types, such epithelial cells or fibroblasts, in the mouse lung. Our lab has in fact optimized the conditional deletion of HuR in lung fibroblasts using the fibroblast-specific (*Col1α2*) gene promoter to generate the *Col1α*2Cre-transgenic mice. By breeding *Elavl1*$^{flox/flox}$ mice with *Col1α*2Cre mice, we have generated conditional fibroblast-specific HuR-deficient mice that is inducible with tamoxifen administration. Although the objective of generating these conditional knockout mice is to evaluate the role of HuR in lung fibrosis, we could expose these mice to CS and assess for changes in lung inflammation. Because in this thesis we showed that in the absence of HuR inflammatory mediators are upregulated in lung fibroblasts exposed to CS, we speculate that HuR would control recruitment of immune cells to the lungs, including neutrophils and monocytes, because of the increase in inflammatory mediators, such as IL-6 and CXCL2. Investigating the dysregulated mechanisms *in vivo* will provide a more in-depth understanding of the role of HuR in lung pathophysiology.

Based on the data within this collective body of work, we propose that HuR may be a double-edged sword in lung health and disease for the following reasons. First, we found that HuR abrogates CS-induced inflammation in lung fibroblasts by destabilizing *PTGS2* mRNA. Second, we previously demonstrated that knockout of AhR in lung fibroblasts exposed to CS induces HuR

translocation to the cytoplasm, hence stabilizing *PTGS2* mRNA [290]. Interestingly, we found that AhR expression is reduced in lung tissue from COPD subjects [348], and that COX-2 expression is elevated in COPD-derived lung fibroblasts which correlates with reduced levels of AhR [349]. These data suggest that the loss of AhR may induce HuR to stabilize *PTGS2* mRNA. Altogether, we speculate that HuR may shift its function from being a promoter of *PTGS2* mRNA decay to a promoter of *PTGS2* mRNA stability in lung fibroblasts exposed to CS through AhR expression. Finally, our belief that further studies investigating mechanisms regulated by HuR (Figure 6.1) will open the door to new therapies targeting HuR for deadly diseases with no cure, such as COPD.

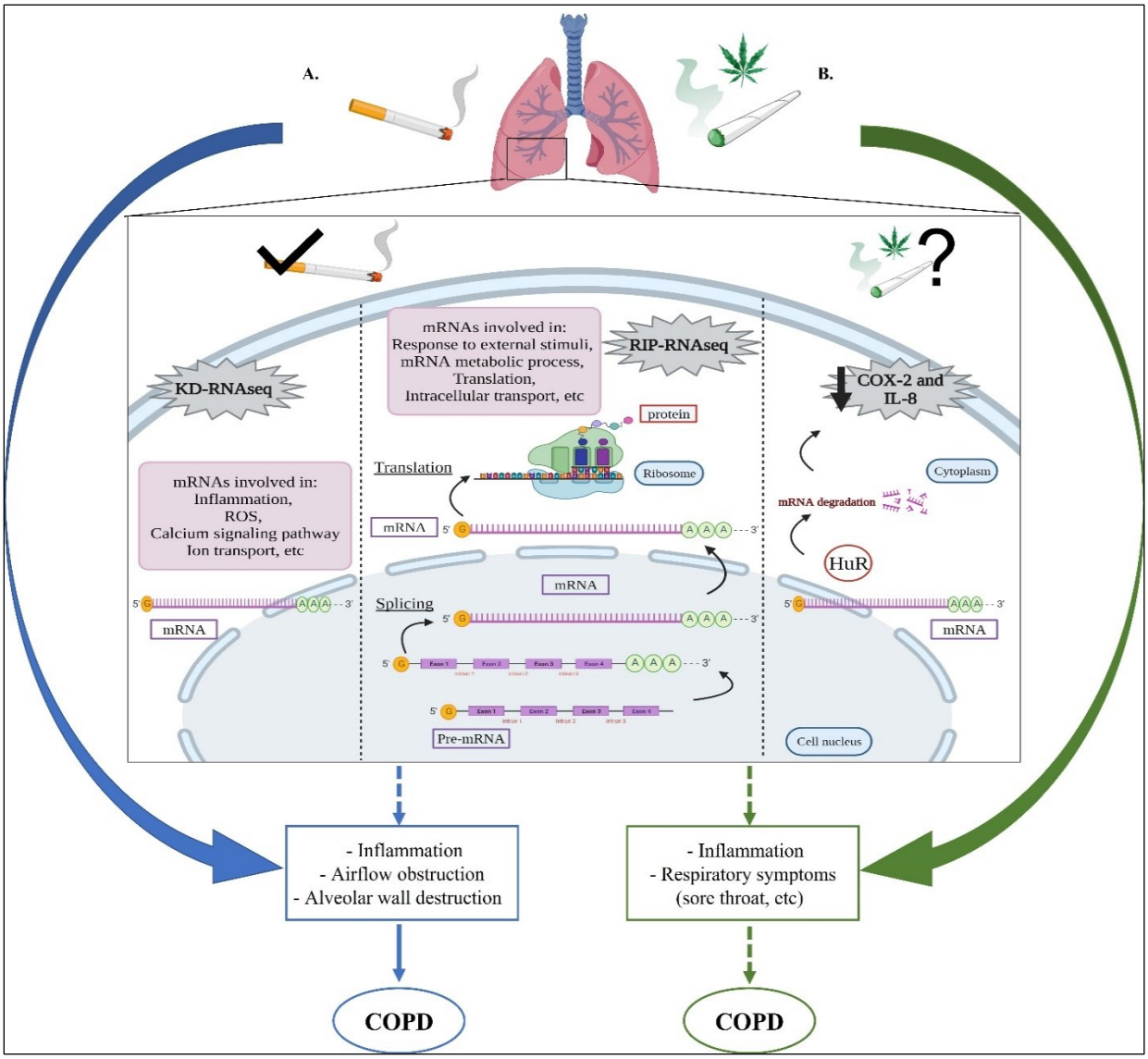

Figure 6.1. Mechanisms regulated by HuR in lung cells exposed to external stimuli.

A. Upon exposure to CS, lung cells produce inflammatory mediators and releases proteases. This cascade of events can lead to chronic pulmonary inflammation, airflow obstruction, and alveolar wall destruction (emphysema) that is involved in COPD pathogenesis. At the cellular level, integrated analysis of HuR in lung fibroblasts indicates that HuR controls mRNA involved in inflammation, ROS, calcium signaling, ion transport, etc., and binds to mRNA involved in the response to external stimuli, mRNA metabolic process, translation, intracellular transport, etc. HuR also reduces the expression of COX-2 and IL-8 protein by inducing the decay of their mRNA. All these processes may be involved in COPD pathogenesis. **B.** Cannabis smoke may cause pulmonary inflammation and respiratory symptoms including sore throat, productive cough and shortness of breath. However, the involvement of these pathological features in COPD development, and whether HuR controls these features still need to be elucidated. KD-RNAseq; knockdown of HuR followed by RNA-seq. Created with BioRender.com.

7. APPENDIX

Table A1. Proteins associated with HuR in lung fibroblasts at the basal level (ΔIP-HuR). LFQ (label-free quantification) ratios.

Gene Name	Protein Name	ΔIP-HuR (LFQ ratios)	PANTHER protein class	Function
EIF3F	Eukaryotic translation initiation factor 3 subunit F	2.5	Translation initiation factor	Translation
RCN1	Reticulocalbin-1	2.2	Calmodulin-related	Calcium ion binding
HNRNPAB	Heterogeneous nuclear ribonucleoprotein A/B	2.1	RNA metabolism protein	RNA binding
COPA	Coatomer subunit alpha;Xenin;Proxenin	2.0	Vesicle coat protein	Intracellular protein transport
HNRNPDL	Heterogeneous nuclear ribonucleoprotein D-like	2.0	RNA metabolism protein	RNA binding
CALU	Calumenin	2.0	Calmodulin-related	Calcium ion binding

Table A2. Proteins associated with HuR in lung fibroblasts exposed to CSE (ΔIP-HuR-CSE).

Gene Name	Protein Name	ΔIP-HuR-CSE (LFQ ratios)	PANTHER protein class	Function
RTN4	Reticulon-4	3.6	NA	NA
CANX	Calnexin	3.5	Chaperone	Protein folding
ITGB1	Integrin beta-1	3.3	Integrin	Cell adhesion
EIF3F	Eukaryotic translation initiation factor 3 subunit F	2.8	Translation initiation factor	Translation
EHD2	EH domain-containing protein 2	2.6	Membrane traffic protein	Protein localization
CYB5R3	Cytochrome B5 Reductase 3; NADH-cytochrome b5 reductase 3;	2.6	Reductase	Catalytic activity
PSMC4	26S protease regulatory subunit 6B	2.5	Protease	Proteasome-mediated ubiquitin-dependent protein catabolic process
HNRNPAB	Heterogeneous nuclear ribonucleoprotein A/B	2.4	RNA metabolism protein	RNA binding
DDOST	Dolichyl-diphosphooligosaccharide --protein glycosyltransferase 48 kDa subunit	2.3	Glycosyltransferase	Metabolic process
P4HB	Protein disulfide-isomerase	2.2	Chaperone	Protein folding
RPN2	Dolichyl-diphosphooligosaccharide --protein glycosyltransferase subunit 2	2.1	Glycosyltransferase	Metabolic process
CALR	Calreticulin	2.1	Chaperone	Protein folding
ATP5A1	ATP synthase subunit alpha, mitochondrial	2.1	NA	NA
HIST2H2AC; HIST2H2AA3	Histone H2A type 2-C; Histone H2A type 2-A	2.1	NA	NA

ATP5B	ATP synthase subunit beta, mitochondrial	2.1	NA	NA
PSMD11	26S proteasome non-ATPase regulatory subunit 11	2.0	NA	NA
TUBA1A	Tubulin alpha-1A chain	2.0	Tubulin	Microtubule cytoskeleton organization
PSMC5	26S protease regulatory subunit 8	2.0	Protease	Proteasome-mediated ubiquitin-dependent protein catabolic process
DYNC1I2	Cytoplasmic dynein 1 intermediate chain 2	2.0	Microtubule or microtubule-binding cytoskeletal protein	Transport along microtubule

Table A3. miRNA associated with HuR in lung fibroblasts at the basal level (ΔIP-HuR).

miRNA	ΔIP-HuR (log2 fold change)
MIR8072	4.27500705
MIRLET7B	3.01970191
MIR421	2.71588199
MIR221	2.6825733
MIR4800	2.34846671
MIR663A	2.24184018
MIR3190	2.15055968
MIR4683	1.78659636
MIR762	1.78659636
MIR7845	1.54596837

Table A4. miRNAs associated with HuR in lung fibroblasts exposed to CSE (ΔIP-HuR-CSE).

miRNA	ΔIP-HuR-CSE (log2 fold change)
MIR4517	3.14567746
MIR1306	3.12432814
MIR3198-2	3.02325535
MIR3655	2.81352469
MIR29C	2.52985083
MIR3662	2.43028527
MIR491	2.42760617
MIR34A	2.39854938
MIR590	2.32768736
MIR331	2.15380534
MIR5706	2.1473067
MIR3605	1.87970577
MIR4683	1.87184365
MIR30E	1.82374936
MIR4653	1.76977174
MIRLET7G	1.67355642
MIR542	1.58976349
MIR589	1.51601515

Table A5. miRNA differentially expressed with HuR silencing in lung fibroblasts at the basal level (ΔsiH).

miRNA	ΔsiH (log2 fold change)
MIR5047	8.214622
MIR9718	7.292987
MIR4258	7.142006
MIR4721	7.060144
MIR6809	7.060144
MIR711	6.973357
MIR4683	6.973357
MIR5193	6.973357
MIR10397	4.568847
MIR4751	-2.94454
MIR34A	-2.89936
MIR6716	-3.24478
MIR1271	-7.05013
MIR649	-7.63146
MIR4714	-7.63146

Table A6. miRNAs differentially expressed with HuR silencing in lung fibroblasts exposed to CSE (ΔsiH-CSE).

miRNA	ΔsiH-CSE (log2 fold change)
MIR3614	7.076787
MIR6864	7.006932
MIR555	6.687806
MIR10393	2.577937
MIR4687	-2.1155
MIR6869	-3.03775
MIR6892	-3.37917
MIR4709	-7.43067

8. REFERENCES

1. Aloufi, N., et al., *Aberrant Post-Transcriptional Regulation of Protein Expression in the Development of Chronic Obstructive Pulmonary Disease.* Int J Mol Sci, 2021. **22**(21).
2. Aloufi, N., et al., *Angiotensin-converting enzyme 2 expression in COPD and IPF fibroblasts: the forgotten cell in COVID-19.* Am J Physiol Lung Cell Mol Physiol, 2021. **320**(1): p. L152-L157.
3. Aloufi, N., et al., *Role of Human Antigen R (HuR) in the Regulation of Pulmonary ACE2 Expression.* Cells, 2021. **11**(1).
4. Aloufi, N., et al., *Standardized Cannabis Smoke Extract Induces Inflammation in Human Lung Fibroblasts.* 2022. **13**.
5. Orphanides, G. and D. Reinberg, *A unified theory of gene expression.* Cell, 2002. **108**(4): p. 439-51.
6. Keene, J.D., *RNA regulons: coordination of post-transcriptional events.* Nat Rev Genet, 2007. **8**(7): p. 533-43.
7. He, R.Z., D.X. Luo, and Y.Y. Mo, *Emerging roles of lncRNAs in the post-transcriptional regulation in cancer.* Genes Dis, 2019. **6**(1): p. 6-15.
8. Corley, M., M.C. Burns, and G.W. Yeo, *How RNA-Binding Proteins Interact with RNA: Molecules and Mechanisms.* Mol Cell, 2020. **78**(1): p. 9-29.
9. Tan, W.C., et al., *Characteristics of COPD in never-smokers and ever-smokers in the general population: results from the CanCOLD study.* Thorax, 2015. **70**(9): p. 822-9.
10. Baron, E.P., *Medicinal Properties of Cannabinoids, Terpenes, and Flavonoids in Cannabis, and Benefits in Migraine, Headache, and Pain: An Update on Current Evidence and Cannabis Science.* Headache, 2018. **58**(7): p. 1139-1186.
11. Li, H., et al., *Overview of cannabidiol (CBD) and its analogues: Structures, biological activities, and neuroprotective mechanisms in epilepsy and Alzheimer's disease.* Eur J Med Chem, 2020. **192**: p. 112163.
12. Brown, J.D., *Potential Adverse Drug Events with Tetrahydrocannabinol (THC) Due to Drug-Drug Interactions.* J Clin Med, 2020. **9**(4).
13. Campeny, E., et al., *The blind men and the elephant: Systematic review of systematic reviews of cannabis use related health harms.* Eur Neuropsychopharmacol, 2020.
14. Stampfli, M.R. and G.P. Anderson, *How cigarette smoke skews immune responses to promote infection, lung disease and cancer.* Nat Rev Immunol, 2009. **9**(5): p. 377-84.
15. Martey, C.A., et al., *Cigarette smoke induces cyclooxygenase-2 and microsomal prostaglandin E2 synthase in human lung fibroblasts: implications for lung inflammation and cancer.* Am J Physiol Lung Cell Mol Physiol, 2004. **287**(5): p. L981-91.
16. Li, C.J., et al., *MAPK pathway mediates EGR-1-HSP70-dependent cigarette smoke-induced chemokine production.* Am J Physiol Lung Cell Mol Physiol, 2007. **292**(5): p. L1297-303.
17. Bhalla, D.K., et al., *Cigarette smoke, inflammation, and lung injury: a mechanistic perspective.* J Toxicol Environ Health B Crit Rev, 2009. **12**(1): p. 45-64.
18. Kosmider, B., et al., *Human alveolar epithelial cell injury induced by cigarette smoke.* PLoS One, 2011. **6**(12): p. e26059.

19. Baglole, C.J., et al., *Differential induction of apoptosis by cigarette smoke extract in primary human lung fibroblast strains: implications for emphysema.* Am J Physiol Lung Cell Mol Physiol, 2006. **291**(1): p. L19-29.
20. Vestbo, J., et al., *Global strategy for the diagnosis, management, and prevention of chronic obstructive pulmonary disease: GOLD executive summary.* Am J Respir Crit Care Med, 2013. **187**(4): p. 347-65.
21. Report, W.H.; Available from: https://www.who.int/en/news-room/fact-sheets/detail/the-top-10-causes-of-death.
22. *Global Strategy for the Diagnosis, Management and Prevention of COPD, Global Initiative for Chronic Obstructive Lung Disease (GOLD)* 2020.
23. Pauwels, R.A. and K.F. Rabe, *Burden and clinical features of chronic obstructive pulmonary disease (COPD).* Lancet, 2004. **364**(9434): p. 613-20.
24. Macnee, W., et al. , *COPD: Pathogenesis and Natural History*, in *Murray and Nadel's Textbook of Respiratory Medicine*. 2016. p. 751-766.e7.
25. Decramer, M., W. Janssens, and M. Miravitlles, *Chronic obstructive pulmonary disease.* Lancet, 2012. **379**(9823): p. 1341-51.
26. Athanazio, R., *Airway disease: similarities and differences between asthma, COPD and bronchiectasis.* Clinics, 2012. **67.11** p. 1335-1343.
27. WHO. 2020; Available from: https://www.who.int/news-room/fact-sheets/detail/tobacco.
28. FDA. *Chemicals in Cigarettes: From Plant to Product to Puff*. 2020; Available from: https://www.fda.gov/tobacco-products/products-ingredients-components/chemicals-cigarettes-plant-product-puff.
29. Fowles, J. and E. Dybing, *Application of toxicological risk assessment principles to the chemical constituents of cigarette smoke.* Tob Control, 2003. **12**(4): p. 424-30.
30. King, P.T., *Inflammation in chronic obstructive pulmonary disease and its role in cardiovascular disease and lung cancer.* Clin Transl Med, 2015. **4**(1): p. 68.
31. van Durme, Y., et al., *Prevalence, incidence, and lifetime risk for the development of COPD in the elderly: the Rotterdam study.* Chest, 2009. **135**(2): p. 368-377.
32. Eisner, M.D., et al., *An official American Thoracic Society public policy statement: Novel risk factors and the global burden of chronic obstructive pulmonary disease.* Am J Respir Crit Care Med, 2010. **182**(5): p. 693-718.
33. WHO. *Air pollution*. 2021; Available from: https://www.who.int/health-topics/air-pollution#tab=tab_1.
34. Losacco, C. and A. Perillo, *Particulate matter air pollution and respiratory impact on humans and animals.* Environ Sci Pollut Res Int, 2018. **25**(34): p. 33901-33910.
35. Glencross, D.A., et al., *Air pollution and its effects on the immune system.* Free Radic Biol Med, 2020. **151**: p. 56-68.
36. WHO. *WHO global air quality guidelines*. 2021; Available from: https://www.who.int/publications/i/item/9789240034228.
37. Traboulsi, H., et al., *Inhalation Toxicology of Vaping Products and Implications for Pulmonary Health.* Int J Mol Sci, 2020. **21**(10).
38. Herrington, J.S. and C. Myers, *Electronic cigarette solutions and resultant aerosol profiles.* J Chromatogr A, 2015. **1418**: p. 192-199.
39. Jerzynski, T., et al., *Estimation of the global number of e-cigarette users in 2020.* Harm Reduct J, 2021. **18**(1): p. 109.

40. Osei, A.D., et al., *Association Between E-Cigarette Use and Chronic Obstructive Pulmonary Disease by Smoking Status: Behavioral Risk Factor Surveillance System 2016 and 2017.* Am J Prev Med, 2020. **58**(3): p. 336-342.
41. Garcia-Arcos, I., et al., *Chronic electronic cigarette exposure in mice induces features of COPD in a nicotine-dependent manner.* Thorax, 2016. **71**(12): p. 1119-1129.
42. Scott, A., et al., *Pro-inflammatory effects of e-cigarette vapour condensate on human alveolar macrophages.* Thorax, 2018. **73**(12): p. 1161-1169.
43. Rana, A.C., N. , *Floral Biology and Pollination Biology of Cannabis sativa L.* The International Journal of Plant Reproductive Biology, 2010. **2**: p. 191-195.
44. Hillig, K.W., *Genetic evidence for speciation in Cannabis (Cannabaceae).* Genetic Resources and Crop Evolution 2005. **52**(161-180.).
45. Atakan, Z., *Cannabis, a complex plant: different compounds and different effects on individuals.* Ther Adv Psychopharmacol, 2012. **2**(6): p. 241-54.
46. Mersiades, A.J., et al., *Oral cannabinoid-rich THC/CBD cannabis extract for secondary prevention of chemotherapy-induced nausea and vomiting: a study protocol for a pilot and definitive randomised double-blind placebo-controlled trial (CannabisCINV).* BMJ Open, 2018. **8**(9): p. e020745.
47. organisation, w.h. *Management of substance abuse*. Available from: https://www.who.int/substance_abuse/facts/cannabis/en/.
48. Moir, D., et al., *A comparison of mainstream and sidestream marijuana and tobacco cigarette smoke produced under two machine smoking conditions.* Chem Res Toxicol, 2008. **21**(2): p. 494-502.
49. Graves, B.M., et al., *Comprehensive characterization of mainstream marijuana and tobacco smoke.* Sci Rep, 2020. **10**(1): p. 7160.
50. Henderson, R.L., F.S. Tennant, and R. Guerry, *Respiratory manifestations of hashish smoking.* Arch Otolaryngol, 1972. **95**(3): p. 248-51.
51. Fligiel, S.E., et al., *Tracheobronchial histopathology in habitual smokers of cocaine, marijuana, and/or tobacco.* Chest, 1997. **112**(2): p. 319-26.
52. Roth, M.D., et al., *Airway inflammation in young marijuana and tobacco smokers.* Am J Respir Crit Care Med, 1998. **157**(3 Pt 1): p. 928-37.
53. Maertens, R.M., et al., *A global toxicogenomic analysis investigating the mechanistic differences between tobacco and marijuana smoke condensates in vitro.* Toxicology, 2013. **308**: p. 60-73.
54. Aguiar, J.A., et al., *Transcriptomic and barrier responses of human airway epithelial cells exposed to cannabis smoke.* Physiol Rep, 2019. **7**(20): p. e14249.
55. Barnes, P.J., *Inflammatory mechanisms in patients with chronic obstructive pulmonary disease.* J Allergy Clin Immunol, 2016. **138**(1): p. 16-27.
56. Sethi, S., et al., *Inflammation in COPD: implications for management.* Am J Med, 2012. **125**(12): p. 1162-70.
57. Donnelly, L.E. and P.J. Barnes, *Chemokine receptors as therapeutic targets in chronic obstructive pulmonary disease.* Trends Pharmacol Sci, 2006. **27**(10): p. 546-53.
58. Frankenberger, M., et al., *Chemokine expression by small sputum macrophages in COPD.* Mol Med, 2011. **17**(7-8): p. 762-70.
59. Sheridan, J.A., et al., *Decreased expression of the NF-kappaB family member RelB in lung fibroblasts from Smokers with and without COPD potentiates cigarette smoke-induced COX-2 expression.* Respir Res, 2015. **16**: p. 54.

60. Chen, Y., et al., *Enhanced levels of prostaglandin E2 and matrix metalloproteinase-2 correlate with the severity of airflow limitation in stable COPD.* Respirology, 2008. **13**(7): p. 1014-21.
61. Bagdonas, E., et al., *Novel aspects of pathogenesis and regeneration mechanisms in COPD.* Int J Chron Obstruct Pulmon Dis, 2015. **10**: p. 995-1013.
62. Barnes, P.J., S.D. Shapiro, and R.A. Pauwels, *Chronic obstructive pulmonary disease: molecular and cellular mechanisms.* Eur Respir J, 2003. **22**(4): p. 672-88.
63. Owen, C.A., *Roles for proteinases in the pathogenesis of chronic obstructive pulmonary disease.* Int J Chron Obstruct Pulmon Dis, 2008. **3**(2): p. 253-68.
64. Hoenderdos, K. and A. Condliffe, *The neutrophil in chronic obstructive pulmonary disease.* Am J Respir Cell Mol Biol, 2013. **48**(5): p. 531-9.
65. Franks, T.J., et al., *Resident cellular components of the human lung: current knowledge and goals for research on cell phenotyping and function.* Proc Am Thorac Soc, 2008. **5**(7): p. 763-6.
66. Barnes, P.J., *Cellular and molecular mechanisms of chronic obstructive pulmonary disease.* Clin Chest Med, 2014. **35**(1): p. 71-86.
67. Worrell, J.C. and M.K.L. MacLeod, *Stromal-immune cell crosstalk fundamentally alters the lung microenvironment following tissue insult.* Immunology, 2021. **163**(3): p. 239-249.
68. Sirianni, F.E., F.S. Chu, and D.C. Walker, *Human alveolar wall fibroblasts directly link epithelial type 2 cells to capillary endothelium.* Am J Respir Crit Care Med, 2003. **168**(12): p. 1532-7.
69. Burns, A.R., C.W. Smith, and D.C. Walker, *Unique structural features that influence neutrophil emigration into the lung.* Physiol Rev, 2003. **83**(2): p. 309-36.
70. Green, C.E. and A.M. Turner, *The role of the endothelium in asthma and chronic obstructive pulmonary disease (COPD).* Respir Res, 2017. **18**(1): p. 20.
71. Vlahos, R. and S. Bozinovski, *Role of alveolar macrophages in chronic obstructive pulmonary disease.* Front Immunol, 2014. **5**: p. 435.
72. Kapellos, T.S., et al., *Dysregulated Functions of Lung Macrophage Populations in COPD.* J Immunol Res, 2018. **2018**: p. 2349045.
73. Riise, G.C., et al., *Circulating cell adhesion molecules in bronchial lavage and serum in COPD patients with chronic bronchitis.* Eur Respir J, 1994. **7**(9): p. 1673-7.
74. Jasper, A.E., et al., *Understanding the role of neutrophils in chronic inflammatory airway disease.* F1000Res, 2019. **8**.
75. Grumelli, S., et al., *An immune basis for lung parenchymal destruction in chronic obstructive pulmonary disease and emphysema.* PLoS Med, 2004. **1**(1): p. e8.
76. Freeman, C.M. and J.L. Curtis, *Lung Dendritic Cells: Shaping Immune Responses throughout Chronic Obstructive Pulmonary Disease Progression.* Am J Respir Cell Mol Biol, 2017. **56**(2): p. 152-159.
77. Attaway, A.A., J. Zein, and U.S. Hatipoglu, *SARS-CoV-2 infection in the COPD population is associated with increased healthcare utilization: An analysis of Cleveland clinic's COVID-19 registry.* EClinicalMedicine, 2020. **26**: p. 100515.
78. Hoffmann, M., et al., *SARS-CoV-2 Cell Entry Depends on ACE2 and TMPRSS2 and Is Blocked by a Clinically Proven Protease Inhibitor.* Cell, 2020. **181**(2): p. 271-280 e8.
79. Hu, B., et al., *Characteristics of SARS-CoV-2 and COVID-19.* Nat Rev Microbiol, 2021. **19**(3): p. 141-154.

80. Leung, J.M., et al., *ACE-2 expression in the small airway epithelia of smokers and COPD patients: implications for COVID-19.* Eur Respir J, 2020. **55**(5).
81. Jacobs, M., et al., *Increased expression of ACE2, the SARS-CoV-2 entry receptor, in alveolar and bronchial epithelium of smokers and COPD subjects.* Eur Respir J, 2020. **56**(2).
82. Balkissoon, R., et al., *Chronic obstructive pulmonary disease: a concise review.* Med Clin North Am, 2011. **95**(6): p. 1125-41.
83. Billington, C.K., et al., *cAMP regulation of airway smooth muscle function.* Pulm Pharmacol Ther, 2013. **26**(1): p. 112-20.
84. Malerba, M., et al., *Investigational beta-2 adrenergic agonists for the treatment of chronic obstructive pulmonary disease.* Expert Opin Investig Drugs, 2017. **26**(3): p. 319-329.
85. Khorasani, N., et al., *Reversal of corticosteroid insensitivity by p38 MAPK inhibition in peripheral blood mononuclear cells from COPD.* Int J Chron Obstruct Pulmon Dis, 2015. **10**: p. 283-91.
86. Ahn, K.S. and B.B. Aggarwal, *Transcription factor NF-kappaB: a sensor for smoke and stress signals.* Ann N Y Acad Sci, 2005. **1056**: p. 218-33.
87. Di Stefano, A., et al., *Increased expression of nuclear factor-kappaB in bronchial biopsies from smokers and patients with COPD.* Eur Respir J, 2002. **20**(3): p. 556-63.
88. Edwards, M.R., et al., *Targeting the NF-kappaB pathway in asthma and chronic obstructive pulmonary disease.* Pharmacol Ther, 2009. **121**(1): p. 1-13.
89. Wang, C., et al., *Progress in the mechanism and targeted drug therapy for COPD.* Signal Transduct Target Ther, 2020. **5**(1): p. 248.
90. Barnes, P.J., *Transcription factors in airway diseases.* Lab Invest, 2006. **86**(9): p. 867-72.
91. Caramori, G., P. Casolari, and I. Adcock, *Role of transcription factors in the pathogenesis of asthma and COPD.* Cell Commun Adhes, 2013. **20**(1-2): p. 21-40.
92. Khabar, K.S., *Post-transcriptional control during chronic inflammation and cancer: a focus on AU-rich elements.* Cell Mol Life Sci, 2010. **67**(17): p. 2937-55.
93. Dreyfuss, G., V.N. Kim, and N. Kataoka, *Messenger-RNA-binding proteins and the messages they carry.* Nat Rev Mol Cell Biol, 2002. **3**(3): p. 195-205.
94. Burd, C.G. and G. Dreyfuss, *Conserved structures and diversity of functions of RNA-binding proteins.* Science, 1994. **265**(5172): p. 615-21.
95. Glisovic, T., et al., *RNA-binding proteins and post-transcriptional gene regulation.* FEBS Lett, 2008. **582**(14): p. 1977-86.
96. Lunde, B.M., C. Moore, and G. Varani, *RNA-binding proteins: modular design for efficient function.* Nat Rev Mol Cell Biol, 2007. **8**(6): p. 479-90.
97. Lorković, Z.J., *RNA binding proteins*. Molecular biology intelligence unit. 2012, Austin, Tex.: Landes Bioscience. 162 p.
98. Auweter, S.D., F.C. Oberstrass, and F.H. Allain, *Sequence-specific binding of single-stranded RNA: is there a code for recognition?* Nucleic Acids Res, 2006. **34**(17): p. 4943-59.
99. Richter, J.D. and X. Zhao, *The molecular biology of FMRP: new insights into fragile X syndrome.* Nat Rev Neurosci, 2021. **22**(4): p. 209-222.
100. Takagaki, Y., et al., *The human 64-kDa polyadenylylation factor contains a ribonucleoprotein-type RNA binding domain and unusual auxiliary motifs.* Proc Natl Acad Sci U S A, 1992. **89**(4): p. 1403-7.

101. Shimberg, G.D., et al., *Cleavage and polyadenylation specificity factor 30: An RNA-binding zinc-finger protein with an unexpected 2Fe-2S cluster.* Proc Natl Acad Sci U S A, 2016. **113**(17): p. 4700-5.
102. Neve, J., et al., *Cleavage and polyadenylation: Ending the message expands gene regulation.* RNA Biol, 2017. **14**(7): p. 865-890.
103. Minvielle-Sebastia, L. and W. Keller, *mRNA polyadenylation and its coupling to other RNA processing reactions and to transcription.* Curr Opin Cell Biol, 1999. **11**(3): p. 352-7.
104. Dettwiler, S., et al., *Distinct sequence motifs within the 68-kDa subunit of cleavage factor Im mediate RNA binding, protein-protein interactions, and subcellular localization.* J Biol Chem, 2004. **279**(34): p. 35788-97.
105. Wahle, E., *A novel poly(A)-binding protein acts as a specificity factor in the second phase of messenger RNA polyadenylation.* Cell, 1991. **66**(4): p. 759-68.
106. Bienroth, S., W. Keller, and E. Wahle, *Assembly of a processive messenger RNA polyadenylation complex.* EMBO J, 1993. **12**(2): p. 585-94.
107. Staley, J.P. and C. Guthrie, *Mechanical devices of the spliceosome: motors, clocks, springs, and things.* Cell, 1998. **92**(3): p. 315-26.
108. Zahler, A.M., et al., *SR proteins: a conserved family of pre-mRNA splicing factors.* Genes Dev, 1992. **6**(5): p. 837-47.
109. Will, C.L. and R. Luhrmann, *Spliceosome structure and function.* Cold Spring Harb Perspect Biol, 2011. **3**(7).
110. Johnson, J.M., et al., *Genome-wide survey of human alternative pre-mRNA splicing with exon junction microarrays.* Science, 2003. **302**(5653): p. 2141-4.
111. Pan, Q., et al., *Deep surveying of alternative splicing complexity in the human transcriptome by high-throughput sequencing.* Nat Genet, 2008. **40**(12): p. 1413-5.
112. Wang, E.T., et al., *Alternative isoform regulation in human tissue transcriptomes.* Nature, 2008. **456**(7221): p. 470-6.
113. Wang, Z. and C.B. Burge, *Splicing regulation: from a parts list of regulatory elements to an integrated splicing code.* RNA, 2008. **14**(5): p. 802-13.
114. Huelga, S.C., et al., *Integrative genome-wide analysis reveals cooperative regulation of alternative splicing by hnRNP proteins.* Cell Rep, 2012. **1**(2): p. 167-78.
115. Bass, B.L., *RNA editing and hypermutation by adenosine deamination.* Trends Biochem Sci, 1997. **22**(5): p. 157-62.
116. Schaub, M. and W. Keller, *RNA editing by adenosine deaminases generates RNA and protein diversity.* Biochimie, 2002. **84**(8): p. 791-803.
117. Valente, L. and K. Nishikura, *ADAR gene family and A-to-I RNA editing: diverse roles in posttranscriptional gene regulation.* Prog Nucleic Acid Res Mol Biol, 2005. **79**: p. 299-338.
118. Athanasiadis, A., A. Rich, and S. Maas, *Widespread A-to-I RNA editing of Alu-containing mRNAs in the human transcriptome.* PLoS Biol, 2004. **2**(12): p. e391.
119. Keller, W., J. Wolf, and A. Gerber, *Editing of messenger RNA precursors and of tRNAs by adenosine to inosine conversion.* FEBS Lett, 1999. **452**(1-2): p. 71-6.
120. Gerber, A.P. and W. Keller, *RNA editing by base deamination: more enzymes, more targets, new mysteries.* Trends Biochem Sci, 2001. **26**(6): p. 376-84.
121. Bass, B.L., *RNA editing by adenosine deaminases that act on RNA.* Annu Rev Biochem, 2002. **71**: p. 817-46.

122. Bass, B.L., et al., *A standardized nomenclature for adenosine deaminases that act on RNA.* RNA, 1997. **3**(9): p. 947-9.
123. Chen, C.X., et al., *A third member of the RNA-specific adenosine deaminase gene family, ADAR3, contains both single- and double-stranded RNA binding domains.* RNA, 2000. **6**(5): p. 755-67.
124. Levanon, E.Y., et al., *Systematic identification of abundant A-to-I editing sites in the human transcriptome.* Nat Biotechnol, 2004. **22**(8): p. 1001-5.
125. Kim, D.D., et al., *Widespread RNA editing of embedded alu elements in the human transcriptome.* Genome Res, 2004. **14**(9): p. 1719-25.
126. Schoenberg, D.R. and L.E. Maquat, *Regulation of cytoplasmic mRNA decay.* Nat Rev Genet, 2012. **13**(4): p. 246-59.
127. Blackshear, P.J., *Tristetraprolin and other CCCH tandem zinc-finger proteins in the regulation of mRNA turnover.* Biochem Soc Trans, 2002. **30**(Pt 6): p. 945-52.
128. Carballo, E., W.S. Lai, and P.J. Blackshear, *Feedback inhibition of macrophage tumor necrosis factor-alpha production by tristetraprolin.* Science, 1998. **281**(5379): p. 1001-5.
129. Lai, W.S., et al., *Evidence that tristetraprolin binds to AU-rich elements and promotes the deadenylation and destabilization of tumor necrosis factor alpha mRNA.* Mol Cell Biol, 1999. **19**(6): p. 4311-23.
130. Kratochvill, F., et al., *Tristetraprolin-driven regulatory circuit controls quality and timing of mRNA decay in inflammation.* Mol Syst Biol, 2011. **7**: p. 560.
131. Sauer, I., et al., *Interferons limit inflammatory responses by induction of tristetraprolin.* Blood, 2006. **107**(12): p. 4790-7.
132. Ogilvie, R.L., et al., *Tristetraprolin down-regulates IL-2 gene expression through AU-rich element-mediated mRNA decay.* J Immunol, 2005. **174**(2): p. 953-61.
133. Phillips, K., et al., *Arthritis suppressor genes TIA-1 and TTP dampen the expression of tumor necrosis factor alpha, cyclooxygenase 2, and inflammatory arthritis.* Proc Natl Acad Sci U S A, 2004. **101**(7): p. 2011-6.
134. Winzen, R., et al., *Functional analysis of KSRP interaction with the AU-rich element of interleukin-8 and identification of inflammatory mRNA targets.* Mol Cell Biol, 2007. **27**(23): p. 8388-400.
135. Leppek, K., et al., *Roquin promotes constitutive mRNA decay via a conserved class of stem-loop recognition motifs.* Cell, 2013. **153**(4): p. 869-81.
136. Paschoud, S., et al., *Destabilization of interleukin-6 mRNA requires a putative RNA stem-loop structure, an AU-rich element, and the RNA-binding protein AUF1.* Mol Cell Biol, 2006. **26**(22): p. 8228-41.
137. Gratacos, F.M. and G. Brewer, *The role of AUF1 in regulated mRNA decay.* Wiley Interdiscip Rev RNA, 2010. **1**(3): p. 457-73.
138. White, E.J., G. Brewer, and G.M. Wilson, *Post-transcriptional control of gene expression by AUF1: mechanisms, physiological targets, and regulation.* Biochim Biophys Acta, 2013. **1829**(6-7): p. 680-8.
139. Wang, W., et al., *HuR regulates cyclin A and cyclin B1 mRNA stability during cell proliferation.* EMBO J, 2000. **19**(10): p. 2340-50.
140. Figueroa, A., et al., *Role of HuR in skeletal myogenesis through coordinate regulation of muscle differentiation genes.* Mol Cell Biol, 2003. **23**(14): p. 4991-5004.
141. van der Giessen, K., et al., *RNAi-mediated HuR depletion leads to the inhibition of muscle cell differentiation.* J Biol Chem, 2003. **278**(47): p. 47119-28.

142. Dormoy-Raclet, V., et al., *The RNA-binding protein HuR promotes cell migration and cell invasion by stabilizing the beta-actin mRNA in a U-rich-element-dependent manner.* Mol Cell Biol, 2007. **27**(15): p. 5365-80.
143. Ishimaru, D., et al., *Regulation of Bcl-2 expression by HuR in HL60 leukemia cells and A431 carcinoma cells.* Mol Cancer Res, 2009. **7**(8): p. 1354-66.
144. Doller, A., et al., *Protein kinase C alpha-dependent phosphorylation of the mRNA-stabilizing factor HuR: implications for posttranscriptional regulation of cyclooxygenase-2.* Mol Biol Cell, 2007. **18**(6): p. 2137-48.
145. Fan, J., et al., *Chemokine transcripts as targets of the RNA-binding protein HuR in human airway epithelium.* J Immunol, 2011. **186**(4): p. 2482-94.
146. Bai, D., et al., *A conserved TGFbeta1/HuR feedback circuit regulates the fibrogenic response in fibroblasts.* Cell Signal, 2012. **24**(7): p. 1426-32.
147. Adjibade, P. and R. Mazroui, *Control of mRNA turnover: implication of cytoplasmic RNA granules.* Semin Cell Dev Biol, 2014. **34**: p. 15-23.
148. Mahboubi, H. and U. Stochaj, *Cytoplasmic stress granules: Dynamic modulators of cell signaling and disease.* Biochim Biophys Acta Mol Basis Dis, 2017. **1863**(4): p. 884-895.
149. Ansari, M.Y. and T.M. Haqqi, *Interleukin-1beta induced Stress Granules Sequester COX-2 mRNA and Regulates its Stability and Translation in Human OA Chondrocytes.* Sci Rep, 2016. **6**: p. 27611.
150. Kedersha, N., P. Ivanov, and P. Anderson, *Stress granules and cell signaling: more than just a passing phase?* Trends Biochem Sci, 2013. **38**(10): p. 494-506.
151. Jain, S. and R. Parker, *The discovery and analysis of P Bodies.* Adv Exp Med Biol, 2013. **768**: p. 23-43.
152. Glasmacher, E., et al., *Roquin binds inducible costimulator mRNA and effectors of mRNA decay to induce microRNA-independent post-transcriptional repression.* Nat Immunol, 2010. **11**(8): p. 725-33.
153. Kahvejian, A., et al., *Mammalian poly(A)-binding protein is a eukaryotic translation initiation factor, which acts via multiple mechanisms.* Genes Dev, 2005. **19**(1): p. 104-13.
154. Dixon, D.A., et al., *Regulation of cyclooxygenase-2 expression by the translational silencer TIA-1.* J Exp Med, 2003. **198**(3): p. 475-81.
155. Wang, I.X., et al., *ADAR regulates RNA editing, transcript stability, and gene expression.* Cell Rep, 2013. **5**(3): p. 849-60.
156. Stellos, K., et al., *Adenosine-to-inosine RNA editing controls cathepsin S expression in atherosclerosis by enabling HuR-mediated post-transcriptional regulation.* Nat Med, 2016. **22**(10): p. 1140-1150.
157. Brown, R., et al., *Cathepsin S: investigating an old player in lung disease pathogenesis, comorbidities, and potential therapeutics.* Respir Res, 2020. **21**(1): p. 111.
158. Wigington, C.P., et al., *Post-transcriptional regulation of programmed cell death 4 (PDCD4) mRNA by the RNA-binding proteins human antigen R (HuR) and T-cell intracellular antigen 1 (TIA1).* J Biol Chem, 2015. **290**(6): p. 3468-87.
159. Zhang, X., et al., *Translation repression via modulation of the cytoplasmic poly(A)-binding protein in the inflammatory response.* Elife, 2017. **6**.
160. Bhattacharya, S., et al., *Molecular biomarkers for quantitative and discrete COPD phenotypes.* Am J Respir Cell Mol Biol, 2009. **40**(3): p. 359-67.
161. DeMeo, D.L., et al., *Integration of genomic and genetic approaches implicates IREB2 as a COPD susceptibility gene.* Am J Hum Genet, 2009. **85**(4): p. 493-502.

162. Qiu, W., et al., *Genetics of sputum gene expression in chronic obstructive pulmonary disease.* PLoS One, 2011. **6**(9): p. e24395.
163. Hardin, M., et al., *CHRNA3/5, IREB2, and ADCY2 are associated with severe chronic obstructive pulmonary disease in Poland.* Am J Respir Cell Mol Biol, 2012. **47**(2): p. 203-8.
164. Cloonan, S.M., et al., *Mitochondrial iron chelation ameliorates cigarette smoke-induced bronchitis and emphysema in mice.* Nat Med, 2016. **22**(2): p. 163-74.
165. Ghio, A.J., et al., *Particulate matter in cigarette smoke alters iron homeostasis to produce a biological effect.* Am J Respir Crit Care Med, 2008. **178**(11): p. 1130-8.
166. Philippot, Q., et al., *Increased iron sequestration in alveolar macrophages in chronic obstructive pulmonary disease.* PLoS One, 2014. **9**(5): p. e96285.
167. Ricciardi, L., et al., *Differential expression of RNA-binding proteins in bronchial epithelium of stable COPD patients.* Int J Chron Obstruct Pulmon Dis, 2018. **13**: p. 3173-3190.
168. Hogg, J.C. and W. Timens, *The pathology of chronic obstructive pulmonary disease.* Annu Rev Pathol, 2009. **4**: p. 435-59.
169. Thomson, E.M., et al., *Overexpression of tumor necrosis factor-alpha in the lungs alters immune response, matrix remodeling, and repair and maintenance pathways.* Am J Pathol, 2012. **180**(4): p. 1413-30.
170. Taylor, G.A., et al., *A pathogenetic role for TNF alpha in the syndrome of cachexia, arthritis, and autoimmunity resulting from tristetraprolin (TTP) deficiency.* Immunity, 1996. **4**(5): p. 445-54.
171. Prabhala, P. and A.J. Ammit, *Tristetraprolin and its role in regulation of airway inflammation.* Mol Pharmacol, 2015. **87**(4): p. 629-38.
172. Mino, T. and O. Takeuchi, *Post-transcriptional regulation of cytokine mRNA controls the initiation and resolution of inflammation.* Biotechnol Genet Eng Rev, 2013. **29**: p. 49-60.
173. Smoak, K. and J.A. Cidlowski, *Glucocorticoids regulate tristetraprolin synthesis and posttranscriptionally regulate tumor necrosis factor alpha inflammatory signaling.* Mol Cell Biol, 2006. **26**(23): p. 9126-35.
174. Ishmael, F.T., et al., *Role of the RNA-binding protein tristetraprolin in glucocorticoid-mediated gene regulation.* J Immunol, 2008. **180**(12): p. 8342-53.
175. Lu, J.Y., N. Sadri, and R.J. Schneider, *Endotoxic shock in AUF1 knockout mice mediated by failure to degrade proinflammatory cytokine mRNAs.* Genes Dev, 2006. **20**(22): p. 3174-84.
176. Sadri, N. and R.J. Schneider, *Auf1/Hnrnpd-deficient mice develop pruritic inflammatory skin disease.* J Invest Dermatol, 2009. **129**(3): p. 657-70.
177. Morissette, M.C., J. Parent, and J. Milot, *Alveolar epithelial and endothelial cell apoptosis in emphysema: what we know and what we need to know.* Int J Chron Obstruct Pulmon Dis, 2009. **4**: p. 19-31.
178. Aoshiba, K., N. Yokohori, and A. Nagai, *Alveolar wall apoptosis causes lung destruction and emphysematous changes.* Am J Respir Cell Mol Biol, 2003. **28**(5): p. 555-62.
179. Kasahara, Y., et al., *Inhibition of VEGF receptors causes lung cell apoptosis and emphysema.* J Clin Invest, 2000. **106**(11): p. 1311-9.
180. Kasahara, Y., et al., *Endothelial cell death and decreased expression of vascular endothelial growth factor and vascular endothelial growth factor receptor 2 in emphysema.* Am J Respir Crit Care Med, 2001. **163**(3 Pt 1): p. 737-44.

181. Kanazawa, H., et al., *Simultaneous assessment of hepatocyte growth factor and vascular endothelial growth factor in epithelial lining fluid from patients with COPD.* Chest, 2014. **146**(5): p. 1159-1165.
182. Essafi-Benkhadir, K., et al., *Tristetraprolin inhibits Ras-dependent tumor vascularization by inducing vascular endothelial growth factor mRNA degradation.* Mol Biol Cell, 2007. **18**(11): p. 4648-58.
183. Shih, S.C. and K.P. Claffey, *Regulation of human vascular endothelial growth factor mRNA stability in hypoxia by heterogeneous nuclear ribonucleoprotein L.* J Biol Chem, 1999. **274**(3): p. 1359-65.
184. Heiner, M., et al., *HnRNP L-mediated regulation of mammalian alternative splicing by interference with splice site recognition.* RNA Biol, 2010. **7**(1): p. 56-64.
185. Gaudreau, M.C., et al., *Heterogeneous Nuclear Ribonucleoprotein L is required for the survival and functional integrity of murine hematopoietic stem cells.* Sci Rep, 2016. **6**: p. 27379.
186. Van Tubergen, E.A., et al., *Inactivation or loss of TTP promotes invasion in head and neck cancer via transcript stabilization and secretion of MMP9, MMP2, and IL-6.* Clin Cancer Res, 2013. **19**(5): p. 1169-79.
187. Angeloni, D., *Molecular analysis of deletions in human chromosome 3p21 and the role of resident cancer genes in disease.* Brief Funct Genomic Proteomic, 2007. **6**(1): p. 19-39.
188. Timmer, T., et al., *A comparison of genomic structures and expression patterns of two closely related flanking genes in a critical lung cancer region at 3p21.3.* Eur J Hum Genet, 1999. **7**(4): p. 478-86.
189. Jamsai, D., et al., *In vivo evidence that RBM5 is a tumour suppressor in the lung.* Sci Rep, 2017. **7**(1): p. 16323.
190. Hao, Y.Q., et al., *RNA-binding motif protein 5 negatively regulates the activity of Wnt/beta-catenin signaling in cigarette smoke-induced alveolar epithelial injury.* Oncol Rep, 2015. **33**(5): p. 2438-44.
191. Carlier, F.M., et al., *Canonical WNT pathway is activated in the airway epithelium in chronic obstructive pulmonary disease.* EBioMedicine, 2020. **61**: p. 103034.
192. Milara, J., et al., *Epithelial to mesenchymal transition is increased in patients with COPD and induced by cigarette smoke.* Thorax, 2013. **68**(5): p. 410-20.
193. Meisner, N.C., et al., *Identification and mechanistic characterization of low-molecular-weight inhibitors for HuR.* Nat Chem Biol, 2007. **3**(8): p. 508-15.
194. Blanco, F.F., et al., *Impact of HuR inhibition by the small molecule MS-444 on colorectal cancer cell tumorigenesis.* Oncotarget, 2016. **7**(45): p. 74043-74058.
195. Antic, D. and J.D. Keene, *Embryonic lethal abnormal visual RNA-binding proteins involved in growth, differentiation, and posttranscriptional gene expression.* Am J Hum Genet, 1997. **61**(2): p. 273-8.
196. Dalmau, J., et al., *Detection of the anti-Hu antibody in the serum of patients with small cell lung cancer--a quantitative western blot analysis.* Ann Neurol, 1990. **27**(5): p. 544-52.
197. Szabo, A., et al., *HuD, a paraneoplastic encephalomyelitis antigen, contains RNA-binding domains and is homologous to Elav and Sex-lethal.* Cell, 1991. **67**(2): p. 325-33.
198. Ma, W.J., et al., *Cloning and characterization of HuR, a ubiquitously expressed Elav-like protein.* J Biol Chem, 1996. **271**(14): p. 8144-51.
199. Ma, W.J. and H. Furneaux, *Localization of the human HuR gene to chromosome 19p13.2.* Hum Genet, 1997. **99**(1): p. 32-3.

200. Fan, X.C. and J.A. Steitz, *HNS, a nuclear-cytoplasmic shuttling sequence in HuR.* Proc Natl Acad Sci U S A, 1998. **95**(26): p. 15293-8.
201. Ripin, N., et al., *Molecular basis for AU-rich element recognition and dimerization by the HuR C-terminal RRM.* Proc Natl Acad Sci U S A, 2019. **116**(8): p. 2935-2944.
202. Ma, W.J., S. Chung, and H. Furneaux, *The Elav-like proteins bind to AU-rich elements and to the poly(A) tail of mRNA.* Nucleic Acids Res, 1997. **25**(18): p. 3564-9.
203. Fan, X.C. and J.A. Steitz, *Overexpression of HuR, a nuclear-cytoplasmic shuttling protein, increases the in vivo stability of ARE-containing mRNAs.* EMBO J, 1998. **17**(12): p. 3448-60.
204. Brennan, C.M., I.E. Gallouzi, and J.A. Steitz, *Protein ligands to HuR modulate its interaction with target mRNAs in vivo.* J Cell Biol, 2000. **151**(1): p. 1-14.
205. Gallouzi, I.E. and J.A. Steitz, *Delineation of mRNA export pathways by the use of cell-permeable peptides.* Science, 2001. **294**(5548): p. 1895-901.
206. Rebane, A., A. Aab, and J.A. Steitz, *Transportins 1 and 2 are redundant nuclear import factors for hnRNP A1 and HuR.* RNA, 2004. **10**(4): p. 590-9.
207. Wang, W., et al., *AMP-activated protein kinase-regulated phosphorylation and acetylation of importin alpha1: involvement in the nuclear import of RNA-binding protein HuR.* J Biol Chem, 2004. **279**(46): p. 48376-88.
208. Kang, M.J., et al., *NF-kappaB activates transcription of the RNA-binding factor HuR, via PI3K-AKT signaling, to promote gastric tumorigenesis.* Gastroenterology, 2008. **135**(6): p. 2030-42, 2042 e1-3.
209. Jeyaraj, S.C., et al., *Transcriptional control of human antigen R by bone morphogenetic protein.* J Biol Chem, 2010. **285**(7): p. 4432-40.
210. Pullmann, R., Jr., et al., *Analysis of turnover and translation regulatory RNA-binding protein expression through binding to cognate mRNAs.* Mol Cell Biol, 2007. **27**(18): p. 6265-78.
211. Al-Ahmadi, W., et al., *Alternative polyadenylation variants of the RNA binding protein, HuR: abundance, role of AU-rich elements and auto-Regulation.* Nucleic Acids Res, 2009. **37**(11): p. 3612-24.
212. Yi, J., et al., *Reduced nuclear export of HuR mRNA by HuR is linked to the loss of HuR in replicative senescence.* Nucleic Acids Res, 2010. **38**(5): p. 1547-58.
213. Guo, X., Y. Wu, and R.S. Hartley, *MicroRNA-125a represses cell growth by targeting HuR in breast cancer.* RNA Biol, 2009. **6**(5): p. 575-83.
214. Abdelmohsen, K., et al., *miR-519 suppresses tumor growth by reducing HuR levels.* Cell Cycle, 2010. **9**(7): p. 1354-9.
215. Guo, J., et al., *MiR-291b-3p induces apoptosis in liver cell line NCTC1469 by reducing the level of RNA-binding protein HuR.* Cell Physiol Biochem, 2014. **33**(3): p. 810-22.
216. Roff, A.N., et al., *MicroRNA-570-3p regulates HuR and cytokine expression in airway epithelial cells.* Am J Clin Exp Immunol, 2014. **3**(2): p. 68-83.
217. Kliza, K. and K. Husnjak, *Resolving the Complexity of Ubiquitin Networks.* Front Mol Biosci, 2020. **7**: p. 21.
218. Abdelmohsen, K., et al., *Ubiquitin-mediated proteolysis of HuR by heat shock.* EMBO J, 2009. **28**(9): p. 1271-82.
219. Lucchesi, C., M.S. Sheikh, and Y. Huang, *Negative regulation of RNA-binding protein HuR by tumor-suppressor ECRG2.* Oncogene, 2016. **35**(20): p. 2565-73.

220. Guha, A., et al., *Integrated Regulation of HuR by Translation Repression and Protein Degradation Determines Pulsatile Expression of p53 Under DNA Damage.* iScience, 2019. **15**: p. 342-359.
221. Chu, P.C., et al., *The mRNA-stabilizing factor HuR protein is targeted by beta-TrCP protein for degradation in response to glycolysis inhibition.* J Biol Chem, 2012. **287**(52): p. 43639-50.
222. Zhou, H.L., et al., *The p97-UBXD8 complex destabilizes mRNA by promoting release of ubiquitinated HuR from mRNP.* Genes Dev, 2013. **27**(9): p. 1046-58.
223. von Roretz, C. and I.E. Gallouzi, *Protein kinase RNA/FADD/caspase-8 pathway mediates the proapoptotic activity of the RNA-binding protein human antigen R (HuR).* J Biol Chem, 2010. **285**(22): p. 16806-13.
224. Mazroui, R., et al., *Caspase-mediated cleavage of HuR in the cytoplasm contributes to pp32/PHAP-I regulation of apoptosis.* J Cell Biol, 2008. **180**(1): p. 113-27.
225. Talwar, S., et al., *Inhibition of caspases protects mice from radiation-induced oral mucositis and abolishes the cleavage of RNA-binding protein HuR.* J Biol Chem, 2014. **289**(6): p. 3487-500.
226. Janakiraman, H., et al., *Repression of caspase-3 and RNA-binding protein HuR cleavage by cyclooxygenase-2 promotes drug resistance in oral squamous cell carcinoma.* Oncogene, 2017. **36**(22): p. 3137-3148.
227. von Roretz, C., et al., *Apoptotic-induced cleavage shifts HuR from being a promoter of survival to an activator of caspase-mediated apoptosis.* Cell Death Differ, 2013. **20**(1): p. 154-68.
228. Beauchamp, P., et al., *The cleavage of HuR interferes with its transportin-2-mediated nuclear import and promotes muscle fiber formation.* Cell Death Differ, 2010. **17**(10): p. 1588-99.
229. Ardito, F., et al., *The crucial role of protein phosphorylation in cell signaling and its use as targeted therapy (Review).* Int J Mol Med, 2017. **40**(2): p. 271-280.
230. Kim, H.H., et al., *Nuclear HuR accumulation through phosphorylation by Cdk1.* Genes Dev, 2008. **22**(13): p. 1804-15.
231. Doller, A., et al., *Posttranslational modification of the AU-rich element binding protein HuR by protein kinase Cdelta elicits angiotensin II-induced stabilization and nuclear export of cyclooxygenase 2 mRNA.* Mol Cell Biol, 2008. **28**(8): p. 2608-25.
232. Lafarga, V., et al., *p38 Mitogen-activated protein kinase- and HuR-dependent stabilization of p21(Cip1) mRNA mediates the G(1)/S checkpoint.* Mol Cell Biol, 2009. **29**(16): p. 4341-51.
233. Liao, W.L., et al., *The RNA-binding protein HuR stabilizes cytosolic phospholipase A2alpha mRNA under interleukin-1beta treatment in non-small cell lung cancer A549 Cells.* J Biol Chem, 2011. **286**(41): p. 35499-35508.
234. Leslie, C.C., *Cytosolic phospholipase A(2): physiological function and role in disease.* J Lipid Res, 2015. **56**(8): p. 1386-402.
235. Sobolewski, C., et al., *The role of cyclooxygenase-2 in cell proliferation and cell death in human malignancies.* Int J Cell Biol, 2010. **2010**: p. 215158.
236. Bedford, M.T. and S.G. Clarke, *Protein arginine methylation in mammals: who, what, and why.* Mol Cell, 2009. **33**(1): p. 1-13.

237. Li, H., et al., *Lipopolysaccharide-induced methylation of HuR, an mRNA-stabilizing protein, by CARM1. Coactivator-associated arginine methyltransferase.* J Biol Chem, 2002. **277**(47): p. 44623-30.
238. Dean, J.L., et al., *The 3' untranslated region of tumor necrosis factor alpha mRNA is a target of the mRNA-stabilizing factor HuR.* Mol Cell Biol, 2001. **21**(3): p. 721-30.
239. Pang, L., et al., *Loss of CARM1 is linked to reduced HuR function in replicative senescence.* BMC Mol Biol, 2013. **14**: p. 15.
240. Zhu, H., et al., *Hu proteins regulate polyadenylation by blocking sites containing U-rich sequences.* J Biol Chem, 2007. **282**(4): p. 2203-10.
241. Izquierdo, J.M., *Hu antigen R (HuR) functions as an alternative pre-mRNA splicing regulator of Fas apoptosis-promoting receptor on exon definition.* J Biol Chem, 2008. **283**(27): p. 19077-84.
242. Brennan, C.M. and J.A. Steitz, *HuR and mRNA stability.* Cell Mol Life Sci, 2001. **58**(2): p. 266-77.
243. Srikantan, S. and M. Gorospe, *HuR function in disease.* Front Biosci (Landmark Ed), 2012. **17**: p. 189-205.
244. Lal, A., et al., *Concurrent versus individual binding of HuR and AUF1 to common labile target mRNAs.* EMBO J, 2004. **23**(15): p. 3092-102.
245. Guo, X. and R.S. Hartley, *HuR contributes to cyclin E1 deregulation in MCF-7 breast cancer cells.* Cancer Res, 2006. **66**(16): p. 7948-56.
246. Nabors, L.B., et al., *HuR, a RNA stability factor, is expressed in malignant brain tumors and binds to adenine- and uridine-rich elements within the 3' untranslated regions of cytokine and angiogenic factor mRNAs.* Cancer Res, 2001. **61**(5): p. 2154-61.
247. Kurosu, T., et al., *HuR keeps an angiogenic switch on by stabilising mRNA of VEGF and COX-2 in tumour endothelium.* Br J Cancer, 2011. **104**(5): p. 819-29.
248. Nabors, L.B., et al., *Tumor necrosis factor alpha induces angiogenic factor up-regulation in malignant glioma cells: a role for RNA stabilization and HuR.* Cancer Res, 2003. **63**(14): p. 4181-7.
249. Dixon, D.A., et al., *Altered expression of the mRNA stability factor HuR promotes cyclooxygenase-2 expression in colon cancer cells.* J Clin Invest, 2001. **108**(11): p. 1657-65.
250. Doller, A., et al., *High-constitutive HuR phosphorylation at Ser 318 by PKC{delta} propagates tumor relevant functions in colon carcinoma cells.* Carcinogenesis, 2011. **32**(5): p. 676-85.
251. Wang, N., et al., *A HuR/TGF-beta1 feedback circuit regulates airway remodeling in airway smooth muscle cells.* Respir Res, 2016. **17**(1): p. 117.
252. Choi, H.J., et al., *HuR/ELAVL1 RNA binding protein modulates interleukin-8 induction by muco-active ribotoxin deoxynivalenol.* Toxicol Appl Pharmacol, 2009. **240**(1): p. 46-54.
253. Kim, H.H., et al., *HuR recruits let-7/RISC to repress c-Myc expression.* Genes Dev, 2009. **23**(15): p. 1743-8.
254. Cammas, A., et al., *Destabilization of nucleophosmin mRNA by the HuR/KSRP complex is required for muscle fibre formation.* Nat Commun, 2014. **5**: p. 4190.
255. Lal, A., et al., *Antiapoptotic function of RNA-binding protein HuR effected through prothymosin alpha.* EMBO J, 2005. **24**(10): p. 1852-62.
256. Prechtel, A.T., et al., *Expression of CD83 is regulated by HuR via a novel cis-active coding region RNA element.* J Biol Chem, 2006. **281**(16): p. 10912-25.

257. Yeh, C.H., et al., *RNA-binding protein HuR interacts with thrombomodulin 5'untranslated region and represses internal ribosome entry site-mediated translation under IL-1 beta treatment.* Mol Biol Cell, 2008. **19**(9): p. 3812-22.
258. Galban, S., et al., *RNA-binding proteins HuR and PTB promote the translation of hypoxia-inducible factor 1alpha.* Mol Cell Biol, 2008. **28**(1): p. 93-107.
259. Levy, N.S., et al., *Hypoxic stabilization of vascular endothelial growth factor mRNA by the RNA-binding protein HuR.* J Biol Chem, 1998. **273**(11): p. 6417-23.
260. Al-Habeeb, F., et al., *Human antigen R promotes lung fibroblast differentiation to myofibroblasts and increases extracellular matrix production.* J Cell Physiol, 2021. **236**(10): p. 6836-6851.
261. Trivlidis, J., et al., *HuR drives lung fibroblast differentiation but not metabolic reprogramming in response to TGF-beta and hypoxia.* Respir Res, 2021. **22**(1): p. 323.
262. Sasaki, Y., et al., *NOX4 Regulates CCR2 and CCL2 mRNA Stability in Alcoholic Liver Disease.* Sci Rep, 2017. **7**: p. 46144.
263. Atasoy, U., et al., *Regulation of eotaxin gene expression by TNF-alpha and IL-4 through mRNA stabilization: involvement of the RNA-binding protein HuR.* J Immunol, 2003. **171**(8): p. 4369-78.
264. Yarovinsky, T.O., et al., *Early exposure to IL-4 stabilizes IL-4 mRNA in CD4+ T cells via RNA-binding protein HuR.* J Immunol, 2006. **177**(7): p. 4426-35.
265. Casolaro, V., et al., *Posttranscriptional regulation of IL-13 in T cells: role of the RNA-binding protein HuR.* J Allergy Clin Immunol, 2008. **121**(4): p. 853-9 e4.
266. Huwiler, A., et al., *ATP potentiates interleukin-1 beta-induced MMP-9 expression in mesangial cells via recruitment of the ELAV protein HuR.* J Biol Chem, 2003. **278**(51): p. 51758-69.
267. Abdelmohsen, K. and M. Gorospe, *Posttranscriptional regulation of cancer traits by HuR.* Wiley Interdiscip Rev RNA, 2010. **1**(2): p. 214-29.
268. Wang, J., et al., *Multiple functions of the RNA-binding protein HuR in cancer progression, treatment responses and prognosis.* Int J Mol Sci, 2013. **14**(5): p. 10015-41.
269. Kotta-Loizou, I., et al., *Current Evidence and Future Perspectives on HuR and Breast Cancer Development, Prognosis, and Treatment.* Neoplasia, 2016. **18**(11): p. 674-688.
270. Lopez de Silanes, I., et al., *Role of the RNA-binding protein HuR in colon carcinogenesis.* Oncogene, 2003. **22**(46): p. 7146-54.
271. Yoo, P.S., et al., *Tissue microarray analysis of 560 patients with colorectal adenocarcinoma: high expression of HuR predicts poor survival.* Ann Surg Oncol, 2009. **16**(1): p. 200-7.
272. Denkert, C., et al., *Overexpression of the embryonic-lethal abnormal vision-like protein HuR in ovarian carcinoma is a prognostic factor and is associated with increased cyclooxygenase 2 expression.* Cancer Res, 2004. **64**(1): p. 189-95.
273. WHO. *Cancer fact sheets*. 2020; Available from: https://gco.iarc.fr/today/fact-sheets-cancers.
274. Bade, B.C. and C.S. Dela Cruz, *Lung Cancer 2020: Epidemiology, Etiology, and Prevention.* Clin Chest Med, 2020. **41**(1): p. 1-24.
275. Malhotra, J., et al., *Risk factors for lung cancer worldwide.* Eur Respir J, 2016. **48**(3): p. 889-902.
276. Fong, K.M., et al., *Lung cancer. 9: Molecular biology of lung cancer: clinical implications.* Thorax, 2003. **58**(10): p. 892-900.

277. Giaginis, C., et al., *Hu-antigen receptor (HuR) and cyclooxygenase-2 (COX-2) expression in human non-small-cell lung carcinoma: associations with clinicopathological parameters, tumor proliferative capacity and patients' survival.* Tumour Biol, 2015. **36**(1): p. 315-27.
278. Wang, J., et al., *The expression of RNA-binding protein HuR in non-small cell lung cancer correlates with vascular endothelial growth factor-C expression and lymph node metastasis.* Oncology, 2009. **76**(6): p. 420-9.
279. Muralidharan, R., et al., *HuR-targeted nanotherapy in combination with AMD3100 suppresses CXCR4 expression, cell growth, migration and invasion in lung cancer.* Cancer Gene Ther, 2015. **22**(12): p. 581-90.
280. Muralidharan, R., et al., *HuR-targeted small molecule inhibitor exhibits cytotoxicity towards human lung cancer cells.* Sci Rep, 2017. **7**(1): p. 9694.
281. Maher, T.M., et al., *Global incidence and prevalence of idiopathic pulmonary fibrosis.* Respir Res, 2021. **22**(1): p. 197.
282. Morganstein, T., et al., *Involvement of the ACE2/Ang-(1-7)/MasR Axis in Pulmonary Fibrosis: Implications for COVID-19.* Int J Mol Sci, 2021. **22**(23).
283. WHO. *Asthma*. 2020; Available from: https://www.who.int/news-room/fact-sheets/detail/asthma.
284. Patel, S.J. and S.J. Teach, *Asthma.* Pediatr Rev, 2019. **40**(11): p. 549-567.
285. Castillo, J.R., S.P. Peters, and W.W. Busse, *Asthma Exacerbations: Pathogenesis, Prevention, and Treatment.* J Allergy Clin Immunol Pract, 2017. **5**(4): p. 918-927.
286. Mims, J.W., *Asthma: definitions and pathophysiology.* Int Forum Allergy Rhinol, 2015. **5 Suppl 1**: p. S2-6.
287. Cukic, V., et al., *Asthma and Chronic Obstructive Pulmonary Disease (COPD) - Differences and Similarities.* Mater Sociomed, 2012. **24**(2): p. 100-5.
288. Herjan, T., J. Xiao, and M. Dziendziel Kolanek, *RNA-Binding Protein HuR Promotes Airway Inflammation in a House Dust Mite-Induced Allergic Asthma Model.* Journal of interferon & cytokine research : the official journal of the International Society for Interferon and Cytokine Research, 2022. **42**(1): p. 29-38.
289. Sun, J., et al., *Human antigen R enhances the epithelial-mesenchymal transition via regulation of ZEB-1 in the human airway epithelium.* Respir Res, 2018. **19**(1): p. 109.
290. Zago, M., et al., *Aryl Hydrocarbon Receptor-Dependent Retention of Nuclear HuR Suppresses Cigarette Smoke-Induced Cyclooxygenase-2 Expression Independent of DNA-Binding.* PLoS One, 2013. **8**(9): p. e74953.
291. Hudy, M.H. and D. Proud, *Cigarette smoke enhances human rhinovirus-induced CXCL8 production via HuR-mediated mRNA stabilization in human airway epithelial cells.* Respir Res, 2013. **14**: p. 88.
292. Akool el, S., et al., *Nitric oxide increases the decay of matrix metalloproteinase 9 mRNA by inhibiting the expression of mRNA-stabilizing factor HuR.* Mol Cell Biol, 2003. **23**(14): p. 4901-16.
293. Krishnamurthy, P., et al., *IL-10 inhibits inflammation and attenuates left ventricular remodeling after myocardial infarction via activation of STAT3 and suppression of HuR.* Circ Res, 2009. **104**(2): p. e9-18.
294. Engin, A.B., E.D. Engin, and A. Engin, *Two important controversial risk factors in SARS-CoV-2 infection: Obesity and smoking.* Environ Toxicol Pharmacol, 2020. **78**: p. 103411.

295. Smith, J.C., et al., *Cigarette smoke exposure and inflammatory signaling increase the expression of the SARS-CoV-2 receptor ACE2 in the respiratory tract.* Dev Cell, 2020.
296. Campeny, E., et al., *The blind men and the elephant: Systematic review of systematic reviews of cannabis use related health harms.* Eur Neuropsychopharmacol, 2020. **33**: p. 1-35.
297. Shen, H., et al., *MDM2-Mediated Ubiquitination of Angiotensin-Converting Enzyme 2 Contributes to the Development of Pulmonary Arterial Hypertension.* Circulation, 2020. **142**(12): p. 1190-1204.
298. Zhou, H., et al., *HIV protease inhibitors increase TNF-alpha and IL-6 expression in macrophages: involvement of the RNA-binding protein HuR.* Atherosclerosis, 2007. **195**(1): p. e134-43.
299. Grammatikakis, I., K. Abdelmohsen, and M. Gorospe, *Posttranslational control of HuR function.* Wiley Interdiscip Rev RNA, 2017. **8**(1).
300. Srikantan, S. and M. Gorospe, *HuR function in disease.* Frontiers in bioscience (Landmark edition), 2012. **17**(1): p. 189-205.
301. Abdelmohsen, K., et al., *Posttranscriptional orchestration of an anti-apoptotic program by HuR.* Cell Cycle, 2007. **6**(11): p. 1288-92.
302. Mubaid, S., et al., *HuR counteracts miR-330 to promote STAT3 translation during inflammation-induced muscle wasting.* Proc Natl Acad Sci U S A, 2019. **116**(35): p. 17261-17270.
303. Lee, J.H., et al., *Loss of RNA-binding protein HuR facilitates cellular senescence through posttranscriptional regulation of TIN2 mRNA.* Nucleic Acids Res, 2018. **46**(8): p. 4271-4285.
304. Wu, X., et al., *Identification and validation of novel small molecule disruptors of HuR-mRNA interaction.* ACS chemical biology, 2015. **10**(6): p. 1476-1484.
305. Schultz, C.W., et al., *Understanding and targeting the disease-related RNA binding protein human antigen R (HuR).* Wiley interdisciplinary reviews. RNA, 2020. **11**(3): p. e1581-e1581.
306. Muralidharan, R., et al., *HuR-targeted small molecule inhibitor exhibits cytotoxicity towards human lung cancer cells.* Scientific reports, 2017. **7**(1): p. 9694-9694.
307. Thibault, P.A., et al., *hnRNP A/B Proteins: An Encyclopedic Assessment of Their Roles in Homeostasis and Disease.* Biology (Basel), 2021. **10**(8).
308. Boukakis, G., et al., *Deregulated expression of hnRNP A/B proteins in human non-small cell lung cancer: parallel assessment of protein and mRNA levels in paired tumour/non-tumour tissues.* BMC cancer, 2010. **10**: p. 434-434.
309. Papadopoulou, C., et al., *HuR-hnRNP interactions and the effect of cellular stress.* Mol Cell Biochem, 2013. **372**(1-2): p. 137-47.
310. Zhou, J., et al., *Expression of early lung cancer detection marker: hnRNP-A2/B1 and its relation to microsatellite alteration in non-small cell lung cancer.* Lung Cancer, 2001. **34**(3): p. 341-50.
311. Tauler, J., et al., *hnRNP A2/B1 modulates epithelial-mesenchymal transition in lung cancer cell lines.* Cancer Res, 2010. **70**(18): p. 7137-47.
312. Kawamata, T. and Y. Tomari, *Making RISC.* Trends Biochem Sci, 2010. **35**(7): p. 368-76.
313. Fabian, M.R., N. Sonenberg, and W. Filipowicz, *Regulation of mRNA translation and stability by microRNAs.* Annu Rev Biochem, 2010. **79**: p. 351-79.

314. Srikantan, S., K. Tominaga, and M. Gorospe, *Functional interplay between RNA-binding protein HuR and microRNAs.* Curr Protein Pept Sci, 2012. **13**(4): p. 372-9.
315. Chen, J., et al., *Interaction of RNA-binding protein HuR and miR-466i regulates GM-CSF expression.* Sci Rep, 2017. **7**(1): p. 17233.
316. Aulas, A., et al., *Nitric oxide triggers the assembly of "type II" stress granules linked to decreased cell viability.* Cell Death Dis, 2018. **9**(11): p. 1129.
317. Chambers, D.C., W.S. Tunnicliffe, and J.G. Ayres, *Acute inhalation of cigarette smoke increases lower respiratory tract nitric oxide concentrations.* Thorax, 1998. **53**(8): p. 677-9.
318. Moretto, N., et al., *Cigarette smoke and its component acrolein augment IL-8/CXCL8 mRNA stability via p38 MAPK/MK2 signaling in human pulmonary cells.* Am J Physiol Lung Cell Mol Physiol, 2012. **303**(10): p. L929-38.
319. Marumo, S., et al., *p38 mitogen-activated protein kinase determines the susceptibility to cigarette smoke-induced emphysema in mice.* BMC Pulm Med, 2014. **14**: p. 79.
320. Gaffey, K., et al., *Increased phosphorylated p38 mitogen-activated protein kinase in COPD lungs.* Eur Respir J, 2013. **42**(1): p. 28-41.
321. Sarker, R.S.J., et al., *CARM1 regulates senescence during airway epithelial cell injury in COPD pathogenesis.* Am J Physiol Lung Cell Mol Physiol, 2019. **317**(5): p. L602-L614.
322. Barnes, P.J., *Senescence in COPD and Its Comorbidities.* Annu Rev Physiol, 2017. **79**: p. 517-539.
323. Antony, V.B. and V.J. Thannickal, *Cellular Senescence in Chronic Obstructive Pulmonary Disease: Multifaceted and Multifunctional.* Am J Respir Cell Mol Biol, 2018. **59**(2): p. 135-136.
324. Hernandez-Segura, A., J. Nehme, and M. Demaria, *Hallmarks of Cellular Senescence.* Trends Cell Biol, 2018. **28**(6): p. 436-453.
325. Chong, M., et al., *CD36 initiates the secretory phenotype during the establishment of cellular senescence.* EMBO Rep, 2018. **19**(6).
326. Reggio, P.H., *Endocannabinoid binding to the cannabinoid receptors: what is known and what remains unknown.* Curr Med Chem, 2010. **17**(14): p. 1468-86.
327. Pertwee, R.G., *Receptors and channels targeted by synthetic cannabinoid receptor agonists and antagonists.* Curr Med Chem, 2010. **17**(14): p. 1360-81.
328. Sim-Selley, L.J., *Regulation of cannabinoid CB1 receptors in the central nervous system by chronic cannabinoids.* Crit Rev Neurobiol, 2003. **15**(2): p. 91-119.
329. Kawamura, Y., et al., *The CB1 cannabinoid receptor is the major cannabinoid receptor at excitatory presynaptic sites in the hippocampus and cerebellum.* J Neurosci, 2006. **26**(11): p. 2991-3001.
330. Kicman, A., A. Pedzinska-Betiuk, and H. Kozlowska, *The potential of cannabinoids and inhibitors of endocannabinoid degradation in respiratory diseases.* Eur J Pharmacol, 2021. **911**: p. 174560.
331. Chen, R., et al., *Delta9-THC-caused synaptic and memory impairments are mediated through COX-2 signaling.* Cell, 2013. **155**(5): p. 1154-1165.
332. Chang, N., et al., *Both HuR and miR-29s regulate expression of CB1 involved in infiltration of bone marrow monocyte/macrophage in chronic liver injury.* J Cell Physiol, 2020. **235**(3): p. 2532-2544.
333. Maertens, R.M., et al., *The genotoxicity of mainstream and sidestream marijuana and tobacco smoke condensates.* Chem Res Toxicol, 2009. **22**(8): p. 1406-14.

334. Katsanou, V., et al., *The RNA-binding protein Elavl1/HuR is essential for placental branching morphogenesis and embryonic development.* Mol Cell Biol, 2009. **29**(10): p. 2762-76.
335. Ghosh, M., et al., *Essential role of the RNA-binding protein HuR in progenitor cell survival in mice.* J Clin Invest, 2009. **119**(12): p. 3530-43.
336. Li, J., et al., *Adipose HuR protects against diet-induced obesity and insulin resistance.* Nat Commun, 2019. **10**(1): p. 2375.
337. Sgantzis, N., et al., *HuR controls lung branching morphogenesis and mesenchymal FGF networks.* Dev Biol, 2011. **354**(2): p. 267-79.
338. Smith, B.M., et al., *Human airway branch variation and chronic obstructive pulmonary disease.* Proc Natl Acad Sci U S A, 2018. **115**(5): p. E974-E981.
339. Kim, G.Y., S.J. Lim, and Y.W. Kim, *Expression of HuR, COX-2, and survivin in lung cancers; cytoplasmic HuR stabilizes cyclooxygenase-2 in squamous cell carcinomas.* Mod Pathol, 2011. **24**(10): p. 1336-47.
340. Wang, J., et al., *Cytoplasmic HuR expression correlates with angiogenesis, lymphangiogenesis, and poor outcome in lung cancer.* Med Oncol, 2011. **28 Suppl 1**: p. S577-85.
341. Li, H., et al., *Integrated Bioinformatics Analysis Identifies ELAVL1 and APP as Candidate Crucial Genes for Crohn's Disease.* J Immunol Res, 2020. **2020**: p. 3067273.
342. Green, L.C., et al., *Human antigen R as a therapeutic target in pathological cardiac hypertrophy.* JCI Insight, 2019. **4**(4).
343. Ge, J., et al., *Essential Roles of RNA-binding Protein HuR in Activation of Hepatic Stellate Cells Induced by Transforming Growth Factor-beta1.* Sci Rep, 2016. **6**: p. 22141.
344. Yiakouvaki, A., et al., *Myeloid cell expression of the RNA-binding protein HuR protects mice from pathologic inflammation and colorectal carcinogenesis.* J Clin Invest, 2012. **122**(1): p. 48-61.
345. Katsanou, V., et al., *HuR as a negative posttranscriptional modulator in inflammation.* Mol Cell, 2005. **19**(6): p. 777-89.
346. Merad, M. and J.C. Martin, *Pathological inflammation in patients with COVID-19: a key role for monocytes and macrophages.* Nature reviews. Immunology, 2020. **20**(6): p. 355-362.
347. Krausgruber, T., et al., *Structural cells are key regulators of organ-specific immune responses.* Nature, 2020. **583**(7815): p. 296-302.
348. Guerrina, N., et al., *Aryl hydrocarbon receptor deficiency causes the development of chronic obstructive pulmonary disease through the integration of multiple pathogenic mechanisms.* FASEB J, 2021. **35**(3): p. e21376.
349. Zago, M., et al., *Low levels of the AhR in chronic obstructive pulmonary disease (COPD)-derived lung cells increases COX-2 protein by altering mRNA stability.* PloS one, 2017. **12**(7): p. e0180881-e0180881.